Hydropower Development in the Brazilian Amazon

Submitted in partial fulfillment of the requirements for

the degree of

Doctor of Philosophy

in

Engineering and Public Policy

Felipe Aguiar Marcondes de Faria

B.S., Civil Engineering, University of São Paulo
M.S., Water Resources Engineering, University of São Paulo

Carnegie Mellon University
Pittsburgh, PA
August, 2016

DEDICATION

To my wife, Heloisa, and my parents, Nelson and Viviane.

ACKNOWLEDGMENTS

I would like to thank the crucial support and commitment from my advisor, Paulina Jaramillo, during those four years. I also thank the thesis committee Paulina Jaramillo (Chair), Alex Davis, Inês Lima Azevedo, and Sergio Pacca. I would also like to acknowledge the key contributions that the papers' co-authors made during the dissertation development. Paulina Jaramillo, Alex Davis, Edson Severnini, Nathan Barros, Henrique Sawakuchi, and Jeffrey Richey, all provided critical inputs and assistance for my research.

I am also thankful for the funding support provided from the Conselho Nacional de Desenvolvimento Científico - CNPQ (process:202484/2011-4), the RenewElec Project, and the Engineering and Public Policy department from Carnegie Mellon University.

I thank Raphael Chabar, Mario Pereira Veiga, Rafael Kelman, Silvio Binato, Luiz Carlos da Costa, Bernardo Bezerra, Celso Dalla'Orto, and Martha Carvalho from PSR (SDDP developer) for the appreciated support and suggestions during the modeling of the Brazilian electric system. I also thank CPFL Renováveis and Rafael Ribas for providing real data about Brazilian wind parks, and Dan Kirk-Davidoff and Steve Rose for crucial inputs for modeling wind generation using reanalysis data.

ABSTRACT
Hydropower development in the Brazilian Amazon

Brazil plans to meet the majority of its growing electricity demand with new hydropower plants located in the Amazon basin. The government's energy policy forecasts the construction of 55 GW of installed capacity by 2028, with total investments in the range of 100 and 200 billion reais (30 to 60 billion dollars), and the creation 9,000 km^2 of artificial reservoirs. However, the construction and operation of large hydropower plants may affect the environment, the local economy, and the population surrounding those projects. Considering the magnitude of the investments and the potential impacts for the Amazon basin, it is crucial to apply policy analysis techniques to support informed decisions about whether the construction of large hydropower plants in the Amazon is the best alternative to supply the additional electricity that Brazil needs, taking into account economic, social, and environmental costs and benefits. Here, I apply three different quantitative policy analysis techniques to assess three major questions related to the construction of hydropower plants in the Amazon region. First, I study the greenhouse gas emissions from hydropower reservoirs in the Amazon. Second, I explore the local socio-economic impacts of building hydropower plants. Finally, I investigate alternative electricity sources that could replace Amazon hydropower reservoirs by modeling the Brazilian electricity network under five capacity expansion scenarios.

TABLE OF CONTENTS

LIST OF TABLES

Table | Page

LIST OF FIGURES

Figure Page

1. INTRODUCTION

Since the middle of the 20^{th} century, Brazil has been supplying most of its growing electricity demand by building large hydropower plants. Currently, hydropower plants larger than 30 MW comprise 61% of the total installed capacity (145 GW), and the latest Brazilian government energy plans indicate that an additional 55 GW of hydropower plants will be required to satisfy the electricity demand by 2028. Fossil fuel power plants comprise 28% of the total installed capacity in 2015. Approximately 80% of such new hydropower capacity is expected to be sited over the Amazon basin. The Amazon basin is the focus of the recent hydropower development because the region encloses the last frontier of rivers with abundant hydropower resources that have not been developed yet. The hydropower development policy in the Amazon will require investments that range from 100 to 200 billion reais (30 to 60 billion dollars) and will lead to the creation of around 9,000 km^2 of artificial reservoirs over the Amazon.

Figure 1-1 describes the spatial distribution of hydropower plant sites that have been registered in the Brazilian electric agency from 2000 to 2012 and includes hydropower plants recently built, under construction, or at designing/licensing stages. The hydropower development in the Brazilian Amazon is a sensitive issue because building reservoirs over the Amazon forest could have several environmental, social, and economic impacts. The consequences of creating artificial reservoirs over rivers and lands have been discussed throughout the scientific literature and include: flooding of agricultural land; loss of terrestrial and aquatic ecosystems; fish migration interruption; change in the biogeochemical cycles affecting nutrient balance, oxygen levels, thermal conditions and sediment flow patterns; greenhouse gas emission associated with the degradation of the biomass within the reservoirs; the dissemination of waterborne diseases by producing a favorable environment for vectors; loss of cultural / historical heritages; population resettlement; and changes in economic activities and social cohesion.

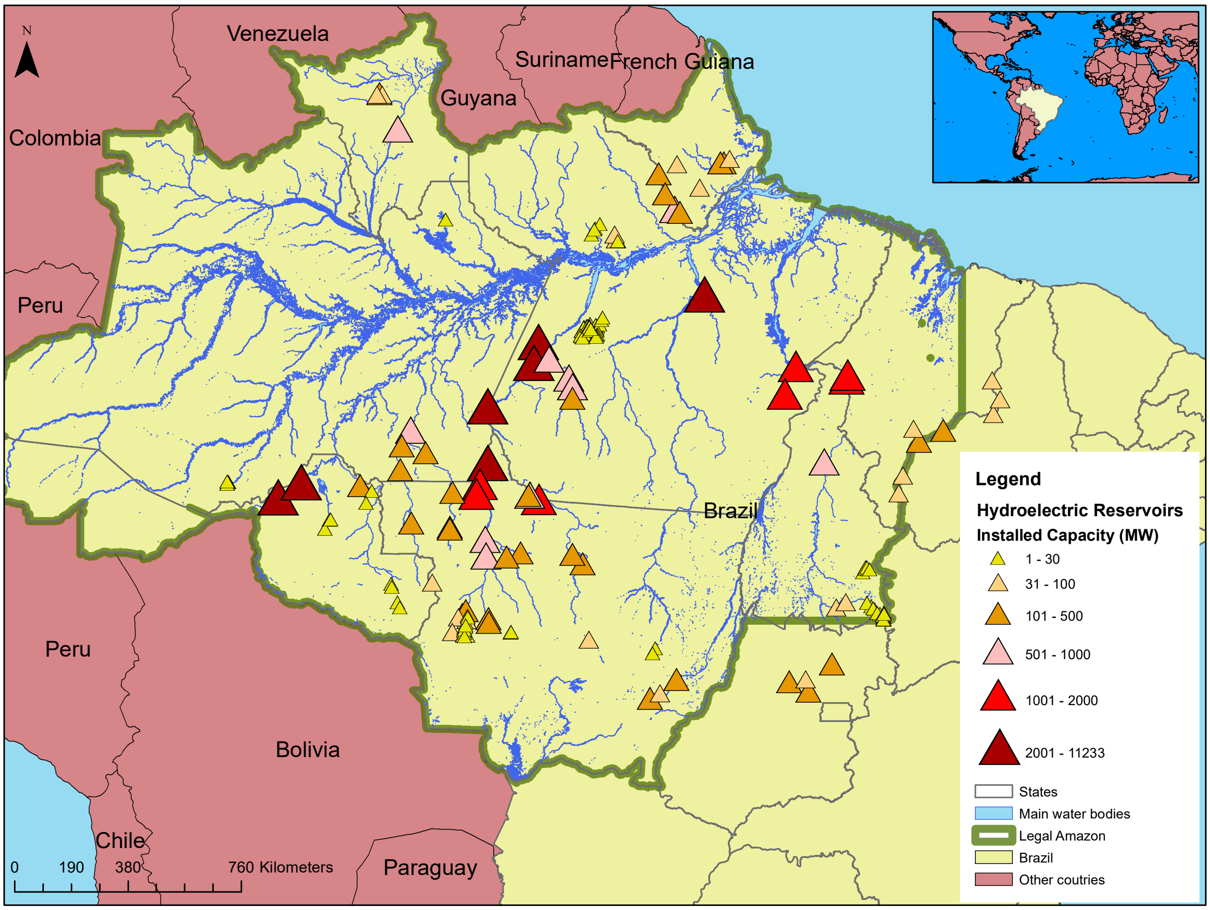

Figure 1-1: Spatial distribution of hydropower plants in the Legal Amazon. The figure includes hydropower plants in operation, under construction or earlier designing/licensing stages registered in the Brazilian electric agency between 2000 and 2012.

Despite the important environmental, social, and economic impacts from hydropower development, there are still several questions that should be studied about whether developing so many artificial reservoirs over the Amazon is the most cost-effective option to satisfy the future electricity demand in Brazil. In this dissertation, I applied quantitative policy analysis methods to answer three major questions related to the hydropower development policy in the Amazon.

In Chapter 2, I investigate the level of greenhouse gas emissions from recent and future Amazon hydropower plant reservoirs. Under the climate mitigation change efforts, this is a key question because the literature showed that reservoirs built over tropical and forest regions have the potential to produce greenhouse gas emissions of the same order of magnitude than fossil fuel power plants. Carbon dioxide and methane emissions from hydropower result from the oxic/anoxic decomposition of the flooded organic matter (OM) from different sources within the reservoir. In Chapter 2, I develop a method based on a Monte Carlo simulation to predict future emissions from Amazon reservoirs and I apply the method on eighteen new and planned hydropower plants.

In Chapter 3, I study the local economic and social impacts of constructing and operating hydropower plants in Brazil. According to recent environmental impact studies produced to support the licensing processes from Amazon hydropower plants, hydropower development will contribute to the boost the economic activity of counties surrounding the reservoir and thus improving social welfare. Here, I explore whether the positive economic and social impact predicted to the Amazon projects occurred in past projects. I apply econometric and statistical techniques to compare counties that built hydropower between 1991 and 2010 with control counties that had plans to build the power plants but the construction did not materialized.

The Brazilian government official energy plans do not assess alternatives to the construction of Amazon hydropower plants. The government plans assume that large hydropower plants present the most cost-effective alternative to fulfill most of the future electricity requirements. In Chapter 4, I explore alternatives to the construction of hydropower plants in the Amazon by creating alternative electricity expansion plans where wind and natural gas power plants replaces the new hydropower capacity. I employ a dispatch optimization tool to simulate the Brazilian integrated electric system, and compare the technical, economic, and environmental characteristics of the baseline scenario, which is heavily based on Amazon hydropower, against the alternative plans.

The forest biome of Amazonia is one of Earth's greatest biological treasures and a major component of the Earth system. The Amazon is also home of thousands of Brazilian Indians tribes and traditional river-dweller communities, embracing a rich cultural and historical heritage. My research has the main objective to employ quantitative policy analysis techniques to improve the stakeholders' knowledge about the positive and negative impacts from building hydropower in the Amazon, and thus support decision-making. Given the increase in electricity demand in developing countries, the Brazilian context provides important insights for policymaking in the developing world.

2. ESTIMATING GREENHOUSE GAS EMISSIONS FROM FUTURE AMAZONIAN HYDROELECTRIC RESERVOIRS

This chapter is based on research that appears in the journal Environmental Research Letters, as:
de Faria, F. A. M., Jaramillo, P., Sawakuchi, H. O., Richey, J. E., & Barros, N. (2015). Estimating greenhouse gas emissions from future Amazonian hydroelectric reservoirs. *Environmental Research Letters*, *10*(12), 1–13. doi:10.1088/1748-9326/10/12/124019

2.1 Introduction

The Brazilian energy plan states that, by 2022, 85% of new hydropower generation capacity (40 gigawatts) will come from hydroelectric power plants, set to be located in the Amazon region[1]. Supporters of this expansion claim that, among other benefits, hydropower is a low carbon source of electricity[2]. However, this idea has come under scrutiny, particularly for tropical forests reservoirs[3-7]. Specific hydropower reservoirs in the Amazon were reported to emit greenhouse gases (GHG) of the same order of magnitude as thermal power plants[8-10].

One of the major issues that contribute to the controversy about GHG emissions from hydropower is the lack of established method to estimate future emissions. While there are estimates of carbon (C) emissions from specific hydropower reservoirs in tropical forests and their effect on the regional and global C budget[4,8,9,11], previous work did not present methods to evaluate future emissions. Moreover, although the literature about the C balance in reservoirs has advanced considerably in the last decades, predicting the C budget for future reservoirs is still challenging because of the difficulty in representing the spatial and temporal variability of the C fluxes[12,13]. Given the high number of dams planned in the Amazon region and in other countries like China, it is imperative to develop models to estimate the C balance of large hydropower projects in order to support decision-making before the dam construction[14].

The GHG flux rates into the atmosphere from a tropical reservoir depend on a complex combination of physicochemical, meteorological, and reservoir features[3-5,7-9,11,15,16]. Part of the difficulty of quantifying the C balance spatial and temporal variability of future reservoirs resides in an incomplete understanding of the physical, chemical, and biological processes involved in the production, consumption, and C outgas from reservoirs[14]. For example, GHG production rate and C fate from flooded trunks is still undetermined[17].

Under this context of high uncertainty related to the C balance modeling, this chapter presents a set of models, based on a Monte Carlo simulation structure, to explore the GHG emissions in tropical forested reservoirs. We investigate the GHG emission from new Amazon reservoirs using two approaches: top-down (TD) and bottom-up (BU). The TD approach is based on carbon dioxide (CO_2) and methane (CH_4) flux data measured in reservoirs and rivers located in the Amazon region. The BU approach relies on a degradation model based on the available carbon stock within the reservoir area. We then compare our results to the GHG emissions that would occur with other electricity generation sources.

2.2 Data and Methods

2.2.1 GHG emissions from reservoirs and modeling overview

CO_2 and CH_4 emissions from hydropower result from the oxic/anoxic decomposition of the flooded organic matter (OM) from different sources within the reservoir (e.g. vegetation and soils, macrophytes, and algae produced in the reservoirs) and from outside the reservoir (e.g. sedimentary OM input from the upstream river basin)[8,17,18]. CO_2 is formed by bacterial respiration of OM in the soils, sediments, and water column but is also imported from upstream and lateral sources, such as drawdown zones[17]. Further, CO_2 in freshwaters is produced by respiration and decomposition and assimilated by aquatic primary production[19]. CH_4 is produced in the reservoir's anaerobic zones by methanogenic bacteria, and can then be oxidized into CO_2 by methanotrophic bacteria in both the soils' aerobic zones[17,20] and the water column[21,22].

After production, CO_2 and CH_4 are released into the atmosphere through four major pathways:

1. **Diffusion in the reservoir area,** which is the flux that occurs in the air-water interface of the reservoir due to the difference in gas concentrations at this layer[23].
2. **Ebullition in the reservoir area** that results from the quick release of GHG from sediment pore waters supersaturated with CH_4[24].
3. **Outlet degassing** that results from pressure and temperature changes that occur on discharge flows just after low-level outlets, such as turbines and spillways[8,9,11].
4. **Diffusion and ebullition downstream of the dam**, which occur in the river area below the dam and are associated with the high concentrations of GHG from the reservoir hypolimnion[8,11].

The net GHG emissions in a river basin resulting from the creation of a reservoir should account for the balance between emissions and sinks in all parts of the watershed affected by the reservoir before and after the impoundment[5,9,16,25]. To estimate net GHG emissions for the first 100 years of operation we employed two approaches.

First, the TD approach relies on GHG flux data measured in tropical Amazonian reservoirs (Balbina, Petit Saut, Tucuruí, Samuel, and Santo Antônio) and rivers, which were used to model the various emission components: diffusion and bubbling from the reservoir, outlet degassing, diffusion and ebullition from downstream, and the natural river. Therefore, this model directly accounts for the major emission pathways into the atmosphere, and the difference between emissions before and after the reservoir flooding defines the net reservoir emissions.

Second, the BU approach is based on the potential emissions derived from the degradation of the flooded OM in the reservoir area, accounting for GHG production rates and CH_4 oxidation in the water column. Brazilian environmental rules require vegetation clearing of the flooded area before filling the reservoir[26]. However, biomass regrowth and inefficient clearing may increase the flooded C stock. In the BU approach, the net reservoir emissions are defined as the difference between 1) the CO_2 and CH_4 production from the degradation of the flooded C stocks (soils and remaining foliage), and 2) the CH_4 consumption and CO_2 production in the freshwater system by CH_4 oxidation. The BU model also accounts for the emissions from the vegetation that is cleared, which decays within the time horizon of this analysis.

In our framework, we assigned probability distributions for each of the uncertain variables in the models. Based on independent sampling from these distributions, each simulation corresponds to the computation of a model outcome. We applied the models to new Amazon hydropower reservoirs, repeating each simulation 10,000 times.

2.2.2 Residence time, stratification, and GHG emissions

Reservoir stratification occurs as a result of thermal differentials in the water column that prevent vertical water mixing. The reservoir stratification with an anoxic bottom layer creates the conditions for CH_4 accumulation in the hypolimnion[3,8]. Old Amazonian reservoirs (Balbina, Samuel, Petit Saut and Tucuruí), where the GHG flux data that are the basis for the TD model were measured, stratify for long periods (several months) with intervals of complete mixing. The biogeochemical cycles in these reservoirs are strongly related to the decomposition of vegetation and anoxic conditions in the hypolimnion[27].

Previous work has described the stratification process and its relation to residence time (RT), which is defined by the time that a molecule of water remains in the reservoir (see Appendix A, section 6.1.1.3). Typical lake stratification occurs in reservoirs with high RT (>100 days)[28,29]. This trend is consistent with the conditions at the Petit Saut reservoir, where there is a high positive correlation between RT, CH_4 concentrations, and emissions[8,30]. Further, the high levels of CH_4 concentrations in the hypolimnions are highly correlated with outlet degassing and downstream emissions[15]. The main channel of reservoirs with low RT (<10 days), on the other hand, have characteristics that resemble a river zone: a completely mixed water column, with homogenous flow rate and temperature distribution[28,29]. This trend is consistent with the conditions in Santo Antônio reservoir[31]. However, tributary and bay zones in low RT reservoirs may present different conditions and stratify because of lower water flows in these areas[31]. Moreover, CH_4 oxidation efficiency also depends on the characteristics of the water column, such as light penetration[32], turbulence[22], and reservoir depth[21]. Therefore, GHG fluxes in new Amazonian reservoirs will depend on their stratification level.

2.2.3 New Amazonian hydroelectric reservoirs

We assessed CO_2 and CH_4 emissions of 18 reservoirs recently built, under construction, or planned in 8 rivers in the Amazon basin, corresponding to a total of 5,900 km^2 of reservoir area and a total installed capacity of 40 GW (Table 2-1). The design characteristics of the hydropower plants come from engineering reports provided by the Brazilian Electric Agency (Agência Nacional de Energia Elétrica – ANEEL). For each reservoir, we then cross-referenced the spatial location data of the reservoir shape with high-resolution maps of land surface, permanent water bodies, and forest biomass density in order to estimate the reservoir and river areas, and the biomass C stock in the reservoir area[33,34]. Appendix A (see section 6.2) provides a detailed explanation of the method used to estimate the reservoir and river areas.

Table 2-1: Characteristics of hydroelectric reservoirs included in this study. Table S8 in the Appendix A present the detailed data source from ANEEL for each project.

Hydroelectric Power Plant	River	Power (MW)	Capacity Factor	Reservoir Area: (km^2)	Reservoir Operation	Volume ($x10^6$ m^3)	Mean Flow (m^3/s)	Mean Depth (m)	Power Density (MW/km^2)	Water Type*
Belo Monte	Xingu	11233	0.41	516	run-of-river	4570	7800	9	21.8	Clear
Bem Querer	Branco	708	0.55	559	run-of-river	2530	3000	5	1.3	Clear
Cachoeira do Caí	Jamanxim	802	0.51	420	storage	3420	1940	8	1.9	Clear
Cachoeira do Caldeirão	Araguari	219	0.56	48	run-of-river	231	930	5	4.6	Clear
Cachoeira dos Patos	Jamanxim	528	0.32	117	storage	696	1330	6	4.5	Clear
Colíder	Teles Pires	300	0.56	172	run-of-river	1520	943	9	1.7	Clear
Ferreira Gomes	Araguari	252	0.60	18	run-of-river	137	963	8	14.2	Clear
Jamanxim	Jamanxim	881	0.53	74	storage	1000	1370	13	11.8	Clear
Jatobá	Tapajós	2338	0.55	646	run-of-river	4010	10400	6	3.6	Clear
Jirau	Madeira	3750	0.58	303	run-of-river	2750	17900	9	12.4	White
Marabá	Tocantins	1850	0.63	1,024	run-of-river	5350	10300	5	1.8	Clear
Salto Augusto de Baixo	Juruena	1461	0.54	125	run-of-river	362	4120	3	11.7	Clear
Santo Antônio	Madeira	3150	0.65	271	run-of-river	2080	18200	8	11.6	White
São Luís do Tapajos	Tapajós	6133	0.52	722	storage	7550	11900	10	8.5	Clear
São Manoel	Teles Pires	746	0.49	64	run-of-river	577	2260	9	11.7	Clear
Sao Simão Alto	Juruena	3509	0.55	284	run-of-river	3820	4190	13	12.4	Clear
Sinop	Teles Pires	461	0.43	330	storage	3070	894	8	1.4	Clear
Teles Pires	Teles Pires	1820	0.54	152	run-of-river	905	2410	6	12.0	Clear

The water type classification is based on the map elaborated by Junk et. al (2011)

2.2.4 Model details

Two stages characterize the C emissions from hydroelectric reservoirs. During the first stage, decomposition of easily degradable biomass in the flooded area (like soil micro fauna and green parts of the vegetation) drives a sharp increase in emissions during the first few years. During the second phase, emissions tend to be slower as the system reaches a steady state[3,5,12,18].

To account for the influence of water column conditions on reservoirs emissions, we developed separate TD models for stratified reservoirs (high RT) and well-mixed reservoirs (low RT) in our database. To assess the stratification level of each reservoir, we performed an analysis of the Densimetric Froude number, which is a more accurate criterion for the development of stratification compared to the RT alone[29] (see Appendix A, section 6.1.1.3, for more details). We classified the characteristics of each reservoir according to their operating characteristics, RT, and propensity to stratify. Based on this analysis, which we described in more detail in the Appendix A, we find that Cachoeira dos Patos, Cachoeira do Caí, Sinop, and Jamanxim are reservoirs with high RT and long periods of stratification, and they are assumed to behave similarly to the older reservoirs from which C flux data have been collected. All the other reservoirs in our database have well-mixed water columns with low RT throughout the year, and the main channel will thus resemble the emissions of natural rivers. Tributaries and bays in these low RT reservoirs, however, stratify and thus result in emissions that are similar to those of the high RT reservoirs.

The BU model, on the other hand, relies on a degradation model based on the flooded and cleared C stock in the reservoir area. Table 2-2 provides a summary of the models' variables and major assumptions.

Table 2-2: Summary of the modeling assumptions.

	Uncertain Variables	Major Assumptions
Bottom up		
	• Flooded carbon stock in the soils and foliage • Carbon stock from cleared biomass • CO_2/CH_4 Production • CH_4 Oxidation • CO_2 Production from CH_4 oxidation (Bacteria Efficiency Growth)	We assumed a uniform distribution that varies from 8 to 16 Gg C/km^2 for 0-20 cm layer to define the carbon stock in the soils[35]. We also assumed that an inefficient biomass clearing contributes to an additional flooded carbon stock from foliage that varies from 0.6 to 6.4 C/km^2 [36]. We explored a CH_4 oxidation fraction range that varies from 45% to 95% of the methane production[11,20,22,37]
Top-down		
High RT	• Reservoir Diffusion and Ebullition • Outlet Degassing • Downstream Diffusion and Bubbling • Natural Emissions	Based on emissions fluxes from classical "old" reservoirs of Tucuruí, Petit Saut, Samuel, and Balbina, which have high RT and present long periods of stratification throughout the year[8,10,11,15,38].
Low RT	• Reservoir Diffusion and Bubbling • Natural Emissions • Degassing/Downstream (parametrically)	We divided the reservoir area in two regions: • The main channel zone has well-mixed water columns and limnological characteristics similar to river zones. Therefore, the probability distributions adopted for the reservoir fluxes in this model rely on the fluxes data from large natural rivers in the Amazon. • The bays and tributaries zones have stratified conditions and probability distributions used are based on the emissions fluxes from classical "old" reservoirs. Degassing/downstream emissions in these reservoirs are based on Santo Antônio reservoir data[31]. We treated this pathway parametrically because only one estimate is available. See the Appendix A for details.

Bottom-up approach. We present a mass balance to estimate net reservoir emission using CO_2 and CH_4 production rates derived from incubation of soils and foliage from the Petit Saut reservoir[17]. The initial flooded C stock is defined by the multiplication of the flooded area (discounting the natural river area) and the soil/foliage OM C density. Additionally, we account for the fate of the cleared biomass C stock for each reservoir based on above the ground biomass distribution map[34]. We assumed that C of the cleared biomass decays in a period of 30 years and is released to the atmosphere as CO_2 (See Appendix A, section 6.4.2, for a more detailed discussion about the fate of cleared biomass).

We calculated GHG production using monthly times steps and production rates sampled from distributions based on the mean and standard deviation of GHG potential production rates obtained from soil/foliage incubation from Petit Saut reservoir[17]. We assumed that CH_4 production rates are the same for both low and high RT models because most of the organic C in the saturated soil/water layers is expected to be in similar anoxic environments. CH_4 oxidation is treated as a fraction of the CH_4 produced from soils/foliage (See Table 2-2). CH_4 oxidation results in CO_2 production and we assume that bacterial growth efficiency has a triangular distribution that ranges from 10% to 80% with the most probable value at 50%.

Top-down approach. In the top-down approach, we divided the GHG emissions in two systems: the river system (before flooding) and the reservoir system (after flooding). Using reservoir shape data, we identified the beginning of the reservoir at the upstream side (upstream limit) and extended the model boundary to cover C fluxes that occur up to a 40-kilometer river distance downstream the dam (downstream limit).

The river system represents the environment before the construction of the reservoir; in other words, the model accounts for the natural fluxes in Amazonian rivers. Rivers and wetlands in the Amazon are natural C sources as they transport, respire, and outgas C originating from organic matter from upland and flooded forests. For this study, we performed a meta-analysis of published CO_2 and CH_4 fluxes in Amazon rivers[39-44] and classified the measurements by spatial location, water-chemistry type, and river size. Based on this database, we fitted statistical distributions to represent the variability of GHG fluxes in large Amazon Rivers (width greater than 100 meters) according to water type: *black water* is associated with a high content of humic compounds; *white water* is associated with a high content of suspended sediment; and *clear wat*er is characterized by the lack of turbidity caused by sediments and a dark color caused by humic compounds[45,46].

The reservoir system characterizes the environment after the construction of the dam and consists of reservoir surface, degassing, and downstream fluxes. The differences in the fluxes into the atmosphere between the reservoir system and the river system define the reservoirs' net GHG emissions. We estimated CO_2 and CH_4 emissions for both systems. Using available data (described in Table 2-3), we fit several distribution functions to represent the flux rates' uncertainty and variability for each of the modeled pathways. Appendix A (section 6.3) provides detailed information about these distributions and data points.

The flux data we used in this study was collected years after the reservoirs started operations, so we assumed that our sample represents the behavior of the reservoir system in a steady state. We also assumed that natural rivers are in a steady state of emissions. We then chose the best distribution for each flux rate through the calculation of the Bayesian Information Criterion and Akaike Information Criterion[47]. We multiplied the specific flux and the associated surface area to define the total annual fluxes of CO_2 and CH_4 for each emissions pathway. Based on the emissions profile measured at Petit Saut in the first ten years of operation, we then modeled the first pulse of emissions by applying a multiplier factor to the steady state emissions for the reservoir system (three times for the first three years, and two times for the fourth and fifth years). Finally, we converted CH_4 emissions to the equivalent CO_2 emissions using the 20 and 100 year CH_4 global warming potential of 86 and 34, respectively[27,48]. Appendix A includes the detailed mathematical formulation of the models.

Table 2-3: Summary of flux data (n = data points). Details of each data point are described in Appendix A (section 6.3)

Emission Source	mg CH_4 m^{-2} d^{-1}			mg CO_2 m^{-2} d^{-1}			References
	Mean	Range	n	Mean	Range	n	
Rivers							
White	10	0-160	214	20,000	680-54,000	26	**A**
Clear	70	2-650	165	5,900	-760-24,000	42	**A**
Black	10	0-53	73	22,000	5,700-48,000	27	**A**
Reservoirs							
Reservoir	50	0-210	20	8,000	1,500-43,000	15	**B**
Degassing	220	50-900	9	70	50-90	6	**C**
Downstream	1,100	190-1,800	7	35,000	18,000-66,000	7	**C**

A) (Rasera et al. 2008, Alin et al. 2011; Ellis et al. 2012; Salimon et al. 2012; Rasera et al. 2013; Sawakuchi et al. 2014), **B**) (Delmas, Galy-Lacaux & Richard 2001; Fearnside 2002;Abril et al. 2005; Lima 2005; Guérin et al. 2006; Santos et al. 2006; Kemenes, Forsberg & Melack 2007; 2011), **C**) (Guérin et al. 2006; Kemenes, Forsberg & Melack 2007; 2011)

2.3. Results and Discussion

Figure 2-1 presents the summary of the mean and 95% confidence interval (CI) of net GHG emissions over 100 years that result from 10,000 simulations for each modeling approach for each assessed reservoir. The simulations reveal a high variability of fluxes across the dams as a consequence of the site-specific characteristics of each project (reservoir area, river areas, and water type), as well as modeling assumptions. Mean net GHG emissions for all reservoirs over 100 years vary from 90 Tg of C (CI: 80 – 100) in the BU approach to 340 Tg of C (CI: 210 – 520) in the TD approach.

The emission results from the BU model shown in Figure 2-1 are based on the initial soils and biomass C stock in the reservoir area. They represent lower bound estimates because C inputs from upstream and primary production in the reservoir are not included. Compared to the emissions from soils only, flooded foliage contributes to an average increase in CH_4 and CO_2 emissions of 33% and 28%, respectively. This result demonstrates the importance of the enforcement and improvement of vegetation clearing as a GHG emissions mitigation measure, as discussed in more detail in the Appendix A (section 6.4.2).

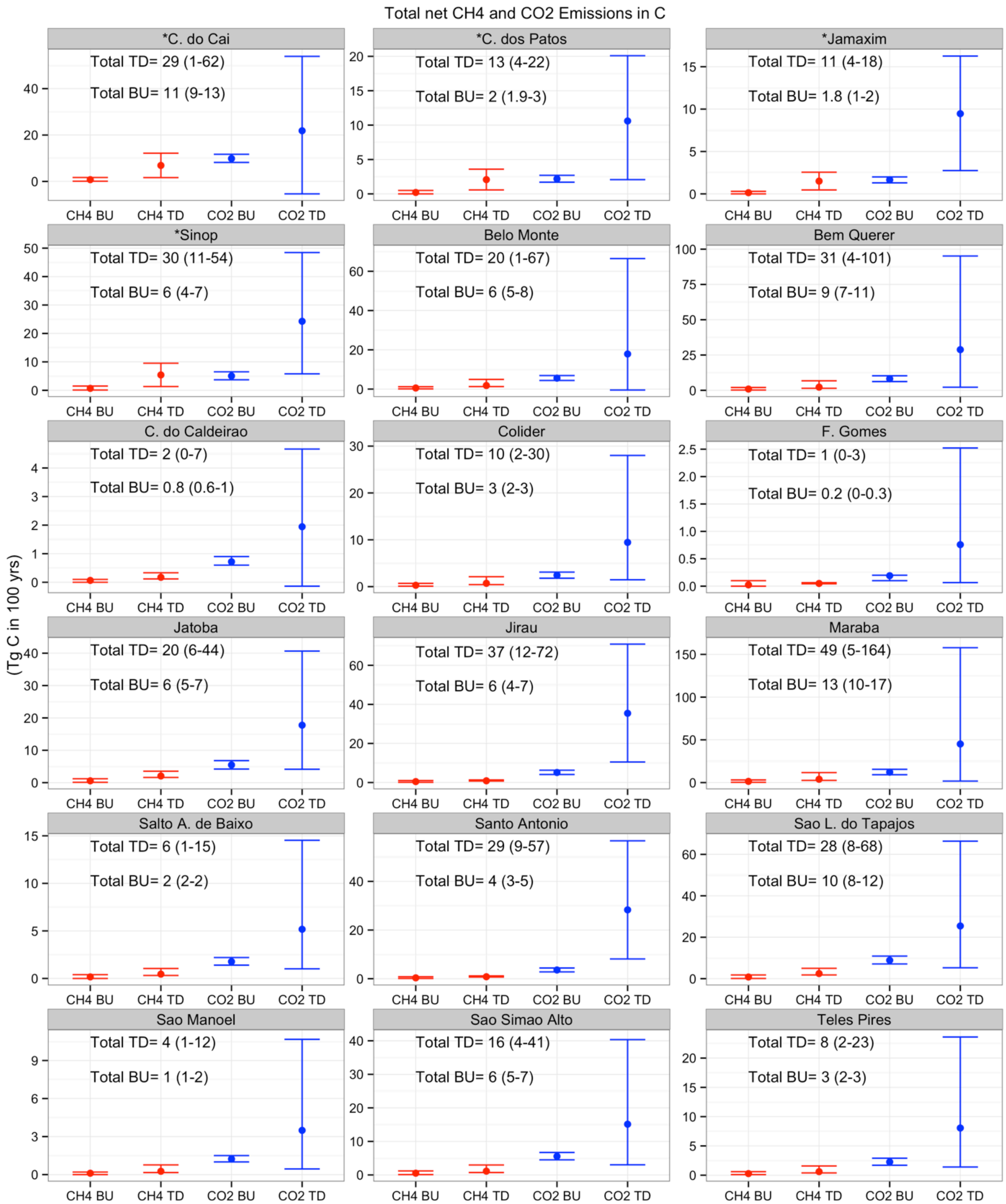

Figure 2-1: Simulation results summary for CH_4 (red) and CO_2 (blue) emissions. These values are in Tera grams (Tg) of Carbon, so they do not include the GWP values for CH_4. Mean net GHG emission over 100 years (circle) and 95% confidence intervals (error bars). Black numbers represent net reservoir emissions: mean and 95% confidence intervals in parenthesis. (*) Indicate high residence time reservoirs (first and second rows). Note that the scale of the y-axis is not consistent across all panels.

2.3.1 Low residence time reservoirs

In the case of the low RT reservoirs, Figure 2-1 shows that mean net GHG emissions over 100 years from the BU model range from 0.1 (CI: 0 – 0.2) Tg of C in Ferreira Gomes to 14 (CI: 10 – 17) Tg of C in Marabá. Mean TD estimates vary from 1 (CI: 0 – 3) Tg of C in Ferreira Gomes to 49 (CI: 5 – 160) Tg of C in Marabá. The BU method is based on a decreasing degradation function for the OM in the soils, residual foliage, and cleared vegetation (fixed initial C stock), while the TD model accounts for fluxes derived from freshwater systems. The TD fluxes were measured in the air-water interface and, thus, also account for other C inputs (e.g. upstream and lateral C inputs, and OM from primary production)[8,17,49]. As a result, the mean results in the TD approach are on average 4 times higher than the mean results in the BU approach. Both approaches, however, result in estimates within the same order of magnitude. Average CH_4 emissions have the same order of magnitude for both approaches, but the uncertainty from the TD method is higher due to the characteristics of the statistical distributions adjusted in this model, which are right-skewed and have a long tail. Figure S12 in the Appendix A highlights the contribution of each pathway to the total C budget.

2.3.2 High residence time reservoirs

For high RT reservoirs, the BU approach indicates that the mean net GHG emissions over 100 years vary from 1.8 (CI: 1– 2) Tg of C in Jamanxim to 11 (CI: 9 – 13) Tg of C in Cachoeira do Caí (Figure 2-1). The mean results in the TD model are one order of magnitude higher compared to the BU outcomes and vary from 11 (CI: 4 – 18) Tg of C in Jamanxim to 30 (CI: 11 – 54) Tg of C in Sinop. Again, this difference is a result of the distinctive methods employed for each approach. The BU model relies on a decreasing degradation function and provides a lower bound estimate that only accounts for the initial C stock in the reservoir area. In contrast, the TD approach relies on flux data measured in reservoirs where the above the ground biomass was not cleared. Thus, the TD approach accounts for fluxes into the atmosphere that derive from all inputs, including below and above-the-ground C stocks, as well as C imports from upstream and reservoir primary production.

New reservoirs in Brazil can only be filled after vegetation clearing[26,31], which did not occur in Petit Saut, Balbina, Tucuruí and Samuel. As a result, while the BU estimates are downward biased (underestimates), the TD approach is upward biased (overestimates) for high RT reservoirs. At this time, we are unable to assess the size of this bias, because we cannot distinguish between flooded, terrestrial, and aquatic inputs and their specific contribution to GHG emissions. This also justifies the use of two modeling approaches; merging them would leads to the risk of double counting. We propose, however, that the BU and TD results provide a range of plausible emissions from these reservoirs.

Figure 2-2 breaks down the contribution of each emission pathway to the net emissions (mean) for the TD approach in high RT reservoirs. For these reservoirs, the gross fluxes from the reservoir system (Figures 2-2A, 2-2C and 2-2E, after flooding) and the natural river system (Figures 2-2B, 2-2D and 2-2F, before flooding). In terms of C mass (Figures 2-2A and 2-2B), CO_2 emissions from the reservoir, downstream emissions, and CO_2 fluxes from the natural river are the largest contributors to C fluxes. On the other hand, when including the 20-year and 100-year GWP as a metric for climate impacts, Figure 2-2C and 2E show that CH_4 emissions account for most of the total Tera grams of CO_2 equivalents. In the mean scenario, natural emissions before the impoundment account for 5% to 30% of the reservoir system emissions (comparing

Figure 2-2A and 2-2B), highlighting the importance of accounting for this natural emission pathway in the net C balance of Amazonian reservoirs.

Figure S12 in Appendix A (section 6.4) shows similar results for the low RT reservoirs. While the magnitude of emissions varies significantly across reservoirs, Figure S12 highlights the same trends observed for high RT reservoirs in Figure 2-2: CH_4 emissions after the impoundment and natural emissions are critical components of the net C balance of these reservoirs. The main advantage of low RT reservoirs compared to high RT is the lack of stratification in the main channel. As a consequence, low RT reservoirs have lower average emissions from the reservoirs' surface in the main channel itself, as well as lower degassing/downstream fluxes. However, the major driver for high total GHG emissions is the size of the reservoir area. For example, Marabá is a low RT reservoir but resulted in the highest total GHG emissions over 100 years, because this reservoir has the greatest reservoir area from our database.

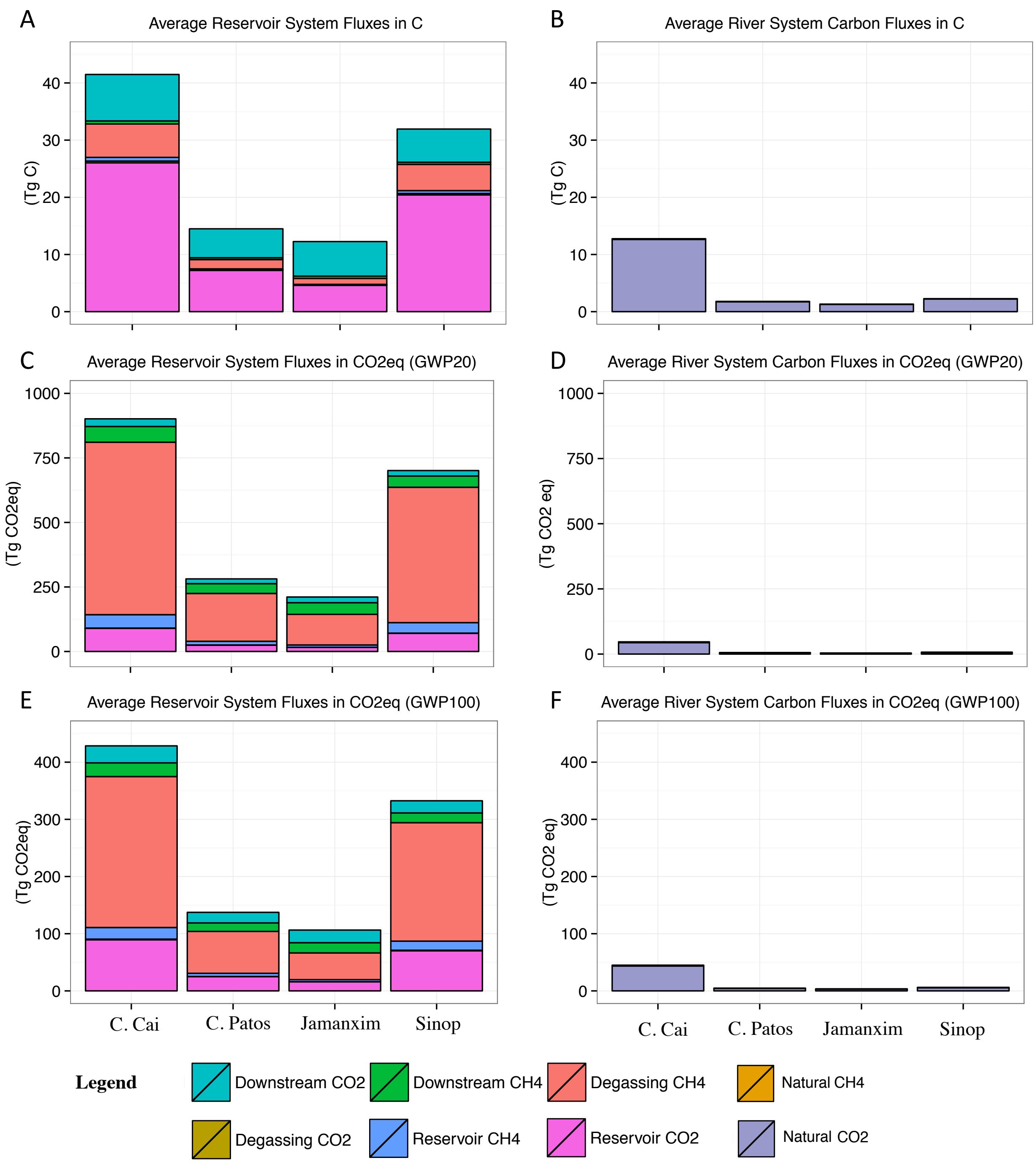

Figure 2-2: Top-down approach mean results for the four high residence time reservoirs in a hundred years by emission pathway. A- Reservoir system in C. B- River System (Natural Emissions) in C. C - Reservoir system in CO_2eq using the 20-year global warming potential (GWP) value for CH_4. D - River System in CO_2eq using the 20-year GWP value for CH_4. E - Reservoir system in CO_2eq using the 100-year GWP value for CH_4. F - River System in CO_2eq using the 100-year GWP value for CH_4.

2.3.3 Emission factors: hydropower in the Amazon versus other sources of electricity

To compare our results from hydropower plants in the Amazonian basin with other electricity generation sources, we calculated the emission factor for each reservoir in units of kg CO_2eq MWh^{-1} (Figure 2-3). As before, the results include the 20-year and 100-year GWP for CH_4. We used a meta-analysis from the Intergovernmental Panel on Climate Change (IPCC) with life cycle assessment studies as a reference to compare our results with other sources of electricity[50]. This literature indicates that the median emission factors for natural gas, oil, and coal-based power plants are 470, 840, and 1,000 kg CO_2-eq MWh^{-1}, respectively[50]. In the case of renewables, the median emission factors are 4, 12, and 46 kg CO_2-eq MWh^{-1} for hydropower, solar (photovoltaic) and wind, respectively. This comparison is not meant to be a recommendation about the source of energy Brazil should pursue, as such recommendation requires much more detailed analysis about the entire power system that is beyond the scope of this chapter.

Figure 2-3 shows that six of the reservoirs (Cachoeira do Caí, Cachoeira dos Patos, Sinop, Bem Querer, Colider and Marabá) have a significant number of simulations that result in emission factors that are comparable to those of thermal power plants. The simulation results confirm that using life cycle emission estimates from hydropower currently available in the IPCC report to aid decision-making may result in unintended consequences[51].

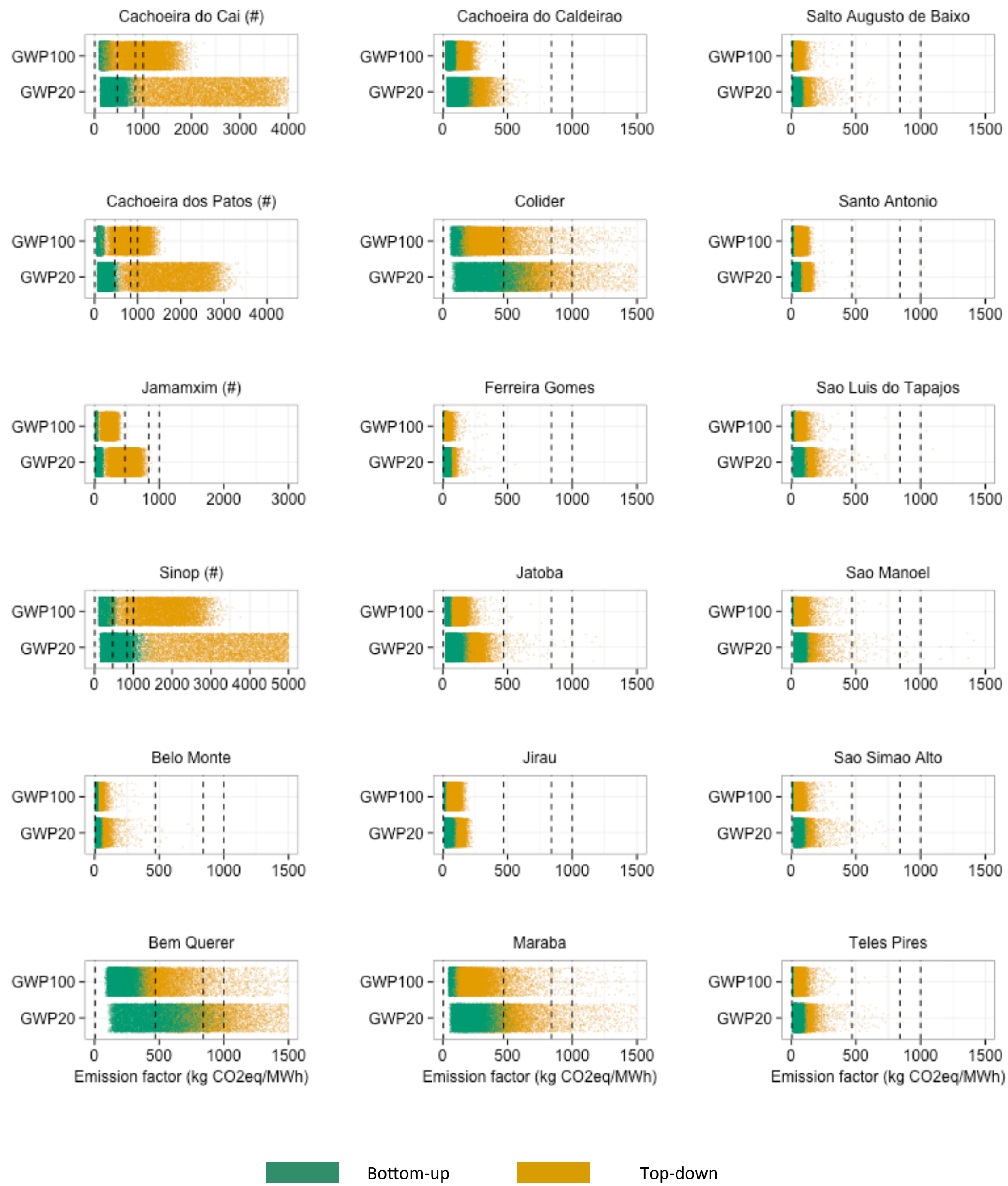

Figure 2-3: Average emission factors simulation results over 100-years (kg CO_2eq MWh^{-1}). Results are presented for two methane global warming potential (GWP). GWP20 represent the emission factors assuming GWP equal 86. GWP100 represent the emission factors assuming GWP equal 34.The x-axis plots each of the 10,000 simulation points against a random number generated within a fixed range in the y-axis. Black vertical dashed lines represent median power plant emission factors: hydropower (4), natural gas (470), oil (840) and coal (1,000) [50]. (#) Indicates high residence time reservoirs.

It is noteworthy that Figure 2-3 shows that high RT reservoirs have higher simulated emission factors compared to thermal power plants. Even though we concluded that the TD approach overestimates GHG emissions for new high RT reservoirs, combined with the lower bound estimates from the BU approach, we can gather useful information to understand the potential range of GHG emissions in new reservoirs. For example, the results indicate that Jamanxim reservoir likely has a lower emission factor than thermal power plants, because of the dominance of simulation results below the natural gas power plants reference value. In contrast, most of the simulated emission factors for Cachoeira dos Patos, Cachoeira do Caí, and Sinop are higher than those for thermal power plants.

Moreover, it is worth highlighting that because of the higher GWP for CH_4 over 20 years, the simulation results using this GWP are higher and suggest the hydropower emissions could have serious climate impacts in the short-term. Appendix A presents the emission factor simulation results by reservoir age. During the first three years of operation, all new hydropower plants in the Amazon have at least some emission factor outcomes above or at the natural gas generation level (See Tables S22 and S23 in the Appendix A). While GWP can serve as a proxy for climate impacts, recent studies suggest it can be an imperfect metric for policy analysis[52-55]. In this study, for example, using GWP implicitly assumes that the emissions over the entire life of these projects (100 years) occur as a pulse emission in year 0. Thus, the values in this study do not account for the timing of emissions. Hence, this study should not be the basis for statements about the global climate impacts of large reservoirs, such as the effect on global temperatures. The results in this study, however, present an account of C emissions that could later be used to model such climate impacts, and future work will expand on this area of research.

Focusing on low RT reservoirs, the reservoirs of Bem Querer, Colider and Marabá have a high number of simulations that suggest these reservoirs have emissions factors larger than those of thermal power plants. In the case of the 20-year results, the emission factors from the BU simulations are also high, consistent with the TD results. Further, Ferreira Gomes is the only reservoir with emission factors that are similar to those of solar and wind projects. In summary, Figure 2-3 shows that a robust treatment of the uncertainty, which is possible by the application of the Monte Carlo simulation structure and the clear statement of model assumptions, provides valuable information about each reservoir that can be used to support decision-making in most cases.

Another relevant difference worth noting between some of the old and new hydropower reservoirs in the Amazon is the relationship between flooded area and installed capacity (power density in MW km^{-2}). There is a strong negative correlation between the hydropower plant emission factors and its power density[5]. Reported emission factors for the old tropical reservoirs of Balbina, Tucuruí, Petit Saut, and Samuel are higher than those of fossil fuel power plants, with mean emission factors of 2,200, 480, 1,300, and 2,200 kg CO_2eq per MWh, respectively[5]. The power densities of Balbina, Tucuruí, Petit Saut, and Samuel reservoirs are 0.1, 2.9, 0.4 and 0.4 MW km^{-2}, respectively. In contrast to these old reservoirs, 13 of the new projects studied in this study have power densities greater than 3.5 MW/km^2 (See Table 2-1). Not surprisingly, the reservoirs with the lower energy densities are also the projects with higher emissions factors in our estimates (See Figure S13 and S14 in the Appendix A). Additionally, three out of the five storage power plants in our database are in the highest emission factor group because the additional volume for water storage often requires more reservoir area, which leads to lower energy densities and higher emission factors. Appendix A presents a sensitivity analysis about the effect of the reservoir area in our estimates for storage reservoir.

2.4 Implications and Uncertainty

Our results suggest that GHG emissions from hydroelectric reservoirs vary significantly across the different projects; these emissions could be higher than currently assumed and, under specific conditions, could even be comparable to those of fossil-based power plants. Most of the reservoir simulations resulted in lower emission factors when compared to those of thermal power plants, but higher when compared to those of solar or wind projects. It is important to note that this comparison is based on the accounting of emissions over the life of the projects and is not meant to be an assessment of the actual climate impacts from these energy projects, which would require either the use of more detailed climate metrics than GWP or a climate model.

Nevertheless, the comparison of emission factors between hydropower plants in the Amazon and other sources of electricity suggests that the climate impacts from large scale development of Amazonian hydropower can be greater than has been suggested in the life cycle literature. Over a hundred years, the 18 new reservoirs in the Amazon would lead to a average total emissions that vary from 9 Tg of CH_4 and 81 Tg of CO_2 (BU approach) to 21 Tg of CH_4 and 310 Tg of CO_2 (TD approach). As a point of comparison, emissions from the U.S. natural gas energy system totaled 10 Tg of CH_4 and 35 Tg of CO_2 in 2013 (EPA 2014). As the global community moves to mitigate global GHG emissions, the potential emissions from Amazonian reservoirs should be considered in the context of emissions from other alternatives.

The Brazilian government is currently evaluating whether to keep investing in low RT reservoirs due to the advantages of adding storage capacity to the electric system. The results in this chapter suggest that the adoption of high energy density reservoirs contributes to reduce overall GHG emissions for hydropower plants. Thus, the proposal to shift towards construction of storage reservoirs with larger areas and higher RT could result in increased emissions from Amazonian projects. Furthermore, our results suggest that the current policy that requires vegetation clearing before reservoir flooding supports a significant reduction in GHG emissions from these projects and should be improved.

Moreover, climate change and deforestation in the Amazon are factors that may affect atmospheric and surface conditions in the future, which would affect GHG emissions from reservoirs. Studies suggest that one of the impacts from land use change and climate will be changes in Amazon precipitation patterns[56]. Shifts in the regional climate patterns can influence reservoir emissions by changing the heat balance and surface mixed layer dynamics of hydroelectric reservoirs[57]. Any changes in precipitation and wind patterns can also affect emissions, as they are important factors to define gas exchange flux variability [8]. Because of the uncertainty and the lack of knowledge in modeling the correlation between climate patterns and GHG emissions from reservoirs, we are unable to quantify the magnitude of future climate and land use change in our estimates.

The challenge of evaluating net GHG emissions due to reservoir creation is complex because of high spatial and temporal variability and the multiple factors that can interfere in the production, consumption, and emissions of GHGs in tropical reservoirs. The scarcity of data, as well as the gaps in the knowledge about the physical, chemical, and biological processes involved, contribute to the difficulty in estimating the C budget of future reservoirs. Nevertheless, given the large number of hydropower dams that are planned in the Brazilian Amazon region, it is essential to use the available scientific information to develop methods to evaluate the potential GHG emissions from hydroelectric projects. While the uncertainties of our models are high, the simulations explore a vast range of GHG emission scenarios for each hydropower reservoir and provide information that is useful to support decision-making.

References

1. MMEEPE Plano Decenal de Expansão de Energia 2022. 1–410 (2013).

2. MMEEPE Plano Decenal de Expansão de Energia. 1–434 (2014).

3. Louis, V. L. S., Kelly, C. A., Duchemin, É., Rudd, J. W. M. & Rosenberg, D. M. Reservoir Surfaces as Sources of Greenhouse Gases to the Atmosphere: A Global Estimate. Bioscience 50, 766–775 (2000).

4. Barros, N. et al. Carbon emission from hydroelectric reservoirs linked to reservoir age and latitude. Nature Geoscience 4, 593–596 (2011).

5. Demarty, M. & Bastien, J. GHG emissions from hydroelectric reservoirs in tropical and equatorial regions: Review of 20 years of CH4 emission measurements. Energy Policy 39, 4197–4206 (2011).

6. Wehrli, B. Climate science: Renewable but not carbon-free. Nature Geoscience 4, 585–586 (2011).

7. Fearnside, P. M. & Pueyo, S. Greenhouse-gas emissions from tropical dams. Nature Climate Change 2, 382–384 (2012).

8. Abril, G. et al. Carbon dioxide and methane emissions and the carbon budget of a 10-year old tropical reservoir (Petit Saut, French Guiana). Global Biogeochem. Cycles 19, 1–16 (2005).

9. Kemenes, A., Forsberg, B. R. & Melack, J. M. CO2 emissions from a tropical hydroelectric reservoir (Balbina, Brazil). J. Geophys. Res. 116, G03004 (2011).

10. Santos, dos, M. A., Rosa, L. P., Sikar, B., Sikar, E. & Santos, dos, E. O. Gross greenhouse gas fluxes from hydro-power reservoir compared to thermo-power plants. Energy Policy 34, 481–488 (2006).

11. Kemenes, A., Forsberg, B. R. & Melack, J. M. Methane release below a tropical hydroelectric dam. Geophys. Res. Lett. 34, L12809 (2007).

12. Galy-Lacaux, C., Delmas, R., Kouadio, G., Richard, S. & Gosse, P. Long-term greenhouse gas emissions from hydroelectric reservoirsin tropical forest regions. Global Biogeochem. Cycles 13, 503–517 (1999).

13. Roland, F. et al. Variability of carbon dioxide flux from tropical (Cerrado) hydroelectric reservoirs. Aquatic Sciences 72, 283–293 (2010).

14. Hu, Y. & Cheng, H. The urgency of assessing the greenhouse gas budgets of hydroelectric reservoirs in China. Nature Climate Change 3, 708–712 (2013).

15. Guérin, F. et al. Methane and carbon dioxide emissions from tropical reservoirs: Significance of downstream rivers. Geophys. Res. Lett. 33, L21407 (2006).

16. Goldenfum, J. A. Challenges and Solutions for Assessing the Impact of Freshwater Reservoirs on Natural GHG Emissions. Ecohydrology&Hydrobiology 12, 115–122 (2012).

17. Guérin, F., Abril, G., de Junet, A. & Bonnet, M.-P. Anaerobic decomposition of tropical soils and plant material: Implication for the CO2 and CH4 budget of the Petit Saut Reservoir. Applied Geochemistry 23, 2272–2283 (2008).

18. Rosa, L. P., Santos, dos, M. A., Matvienko, B., Santos, dos, E. O. & Sikar, E. Greenhouse Gas Emissions From Hydroelectric Reservoirs in Tropical Regions. Climatic Change 66, 9–21 (2004).

19. Cole, J. J. et al. Plumbing the global carbon cycle: integrating inland waters into the terrestrial carbon budget. Ecosystems 10, 172–185 (2007).

20. Bastviken, D. Methane. Encyclopedia of Inland Waters 783–805 (2009).doi:10.1016/B978-012370626-3.00117-4

21. Lima, I. B. T. Biogeochemical distinction of methane releases from two Amazon hydroreservoirs. Chemosphere 59, 1697–1702 (2005).

22. Guérin, F. & Abril, G. Significance of pelagic aerobic methane oxidation in the methane and carbon budget of a tropical reservoir. J. Geophys. Res. 112, G03006 (2007).

23. Cole, J. J. & Caraco, N. F. Atmospheric exchange of carbon dioxide in a low-wind oligotrophic lake measured by the addition of SF6. Limnol. Oceangr. 43, 647–656 (1998).

24. DelSontro, T. et al. Spatial heterogeneity of methane ebullition in a large tropical reservoir. Environ. Sci. Technol. 45, 9866–9873 (2011).

25. Teodoru, C. R. et al. The net carbon footprint of a newly created boreal hydroelectric reservoir. Global Biogeochem. Cycles 26, GB2016 (2012).

26. Kubistcheck, J. Lei no 3.824, de 23 de novembro de 1960. 1–1 (Brazil, 1960).

27. Tundisi, J. G., Matsumura-Tundisi, T. & Calijuri, M. C. Limnology and Management of Reservoirs in Brazil. Comparative Reservoir Limnology and Water Quality Management 77, 22–55 (1993).

28. StrašKraba, M. Limnological basis for modeling reservoir ecosystems. Geophysical Monograph Series - Man-made Lakes: Their Problems and Environmental Effects 17, 517–535 (1973).

29. Straškraba, M., Tundisi, J. G. & Duncan, A. State-of-the-Art of Reservoir Limnology and Water Quality Management. Comparative Reservoir Limnology and Water Quality Management 77, 213–288 (1993).

30. Delmas, R., Galy-Lacaux, C. & Richard, S. Emissions of greenhouse gases from the Tropical hydroelectric reservoir of Petit Saut (French Guiana) compared with emissions from thermal alternatives. Global Biogeochem. Cycles 15, 993–1003 (2001).

31. Fearnside, P. M. Tropical hydropower in the clean development mechanism: Brazil's Santo Antônio dam as an example of the need for change. Climatic Change 131, 575–589 (2015).

32. Dumestre, J. F. & Guézennec, J. Influence of light intensity on methanotrophic bacterial activity in Petit Saut Reservoir, French Guiana. Applied and Environmental Microbiology 65, 534–539 (1999).

33. Hansen, M. C. et al. High-Resolution Global Maps of 21st-Century Forest Cover Change. Science 342, 850–853 (2013).

34. Saatchi, S. S., Houghton, R. A., Alves, D. & Nelson, B. LBA-ECO LC-15 Amazon Basin Aboveground Live Biomass Distribution Map: 1990-2000. (2008).doi:10.3334/ORNLDAAC/908

35. Cerri, C. E. P. et al. Predicted soil organic carbon stocks and changes in the Brazilian Amazon between 2000 and 2030. Agriculture, Ecosystems & Environment 122, 58–72 (2007).

36. Malhi, Y., Baldocchi, D. D. & Jarvis, P. G. The carbon balance of tropical, temperate and boreal forests. Plant, Cell and Environment (22, 715–740 (1999).

37. Angelis, M. A. & Scranton, M. I. Fate of methane in the Hudson River and estuary. Global Biogeochem. Cycles 7, 509–523 (1993).

38. Fearnside, P. M. Greenhouse gas emissions from a hydroelectric reservoir (Brazil Tucurui Dam) and the energy policy implications. Water, Air, & Soil Pollution 133, 69–96 (2002).

39. Rasera, M. de F. F. L. et al. Estimating the Surface Area of Small Rivers in the Southwestern Amazon and Their Role in CO 2Outgassing. Earth Interact. 12, 1–16 (2008).

40. Rasera, M. de F. F. L., krusche, A. V., Richey, J. E., Ballester, M. V. R. & Victoria, R. L. Spatial and temporal variability of pCO2 and CO2 efflux in seven Amazonian Rivers. Biogeochemistry 116, 241–259 (2013).

41. Ellis, E. E. et al. Factors controlling water-column respiration in rivers of the central and southwestern Amazon Basin. Limnol. Oceangr. 57, 527–540 (2012).

42. Alin, S. R. et al. Physical controls on carbon dioxide transfer velocity and flux in low-gradient river systems and implications for regional carbon budgets. J. Geophys. Res. 116, G01009 (2011).

43. Salimon, C., Santos Sousa, E., Alin, S. R., Krusche, A. V. & Ballester, M. V. Seasonal variation in dissolved carbon concentrations and fluxes in the upper Purus River, southwestern Amazon. Biogeochemistry 114, 245–254 (2012).

44. Sawakuchi, H. O. et al. Methane emissions from Amazonian Rivers and their contribution to the global methane budget. Global Change Biology 20, (2014).

45. Furch, K. Water chemistry of the Amazon basin: The distribution of chemical elements among freshwaters. 56, 167–199 (Monographiae Biologicae: Dordrecht, 1984).

46. Junk, W. J. et al. A Classification of Major Naturally-Occurring Amazonian Lowland Wetlands. Wetlands 31, 623–640 (2011).

47. Kuha, J. AIC and BIC: Comparisons of Assumptions and Performance. Sociological Methods & Research 33, 188–229 (2004).

48. IPCC Climate Change 2013. The Physical Science Basis. Working Group I Contribution to the Fifth Assessment Report of the Intergovernmental Panel on Climate Change. (Groupe d'experts intergouvernemental sur l'evolution du climat/Intergovernmental Panel on Climate Change-IPCC, C/O World Meteorological Organization, 7bis Avenue de la Paix, CP 2300 CH-1211 Geneva 2 (Switzerland): 2013).

49. Richey, J. E., Melack, J. M., Aufdenkampe, A. K. & Hess, V. M. B. L. L. Outgassing From Amazonian Rivers and Wetlands as a Large Tropical Source of Atmospheric CO2. Nature 416, 1–5 (2002).

50. Moomaw, W. et al. IPCC special report on renewable energy sources and climate change mitigation. (2011).

51. Fearnside, P. M. Emissions from tropical hydropower and the IPCC. Environmental Science and Policy 50, 225–239 (2015).

52. Kendall, A. Climate change mitigation: Deposing global warming potentials. Nature Climate Change 4, 331–332 (2014).

53. Peters, G. P., Aamaas, B., T Lund, M., Solli, C. & Fuglestvedt, J. S. Alternative 'Global Warming' Metrics in Life Cycle Assessment: A Case Study with Existing Transportation Data. Environ. Sci. Technol. 45, 8633–8641 (2011).

54. Shine, K. P. The global warming potential—the need for an interdisciplinary retrial. Climatic Change 96, 467–472 (2009).

55. Shine, K. P., Fuglestvedt, J. S., Hailemariam, K. & Stuber, N. Alternatives to the global warming potential for comparing climate impacts of emissions of greenhouse gases. Climatic Change 68, 281–302 (2005).

56. Malhi, Y., Roberts, J. T., Betts, R. A., Killeen, T. J. & Li, W. Climate change, deforestation, and the fate of the Amazon. Science 319, 1–5 (2008).

57. Curtarelli, M. P. et al. Influence of summertime mesoscale convective systems on the heat balance and surface mixed layer dynamics of a large Amazonian hydroelectric reservoir. J. Geophys. Res. Oceans 119, 8472–8494 (2014).

3. HYDROPOWER DEVELOPMENT AND SOCIO-ECONOMIC INDICATORS IN BRAZIL (1991-2010)

This chapter is based on research by *Felipe A. M. de Faria*[+], *Alex Davis*[+], *Edson Severnini*[ʻ] and *Paulina Jaramillo*[+] that is currently under review in the Proceedings of the National Academy of Sciences

[+]Department of Engineering & Public Policy, Carnegie Mellon University, [ʻ]Heinz College, Carnegie Mellon University

3.1 Introduction

The recent development of large hydropower plants in countries like China and Brazil has stimulated debate about the economic[1], social[2,3], and environmental[4,5] effects of these projects. Hydropower is regarded as an important electricity generation option because it provides electricity efficiently, reliably[6], and at a relatively low cost[7]. Additionally, hydropower has the potential to provide important ancillary services to the electric system[8], as well as non-energy services like flood control and irrigation services[9]. The construction of hydropower plants, like other energy projects, requires substantial investment and employs a significant number of people, with the potential to increase economic activity and tax revenues in surrounding regions[10-12] - an argument often used to muster support for these projects.

On the other hand, hydropower development has negative socio-economic and environmental impacts. For example, the influx of workers seeking jobs stresses local infrastructure (e.g., hospitals and housing)[13], and can lead to socially undesirable outcomes, such as increases in sexually transmitted diseases[14], crime, and drug use[15]. The resettlement of those who live in the reservoir areas and the encroachment by outsiders[16] may also lead to deterioration of social cohesion[2,9,14,17]. Moreover, energy projects increase the local demand for services (e.g., road repairs due to heavy truck traffic)[11]. Hydropower reservoirs also have negative environmental impacts, as they change the biogeochemical cycles of ecosystems by interrupting the river course, changing the nutrient balance, and shifting oxygen, thermal and sediment flow patterns[18,19]. Further, the fragmentation of the river ecosystem affects migration of aquatic species, and the flooding of large areas harm local biodiversity[9].

Despite the important socio-economic impacts of hydropower development, there are few studies examining these issues locally in developing countries[3,20,21]. In addition, available studies are limited to qualitative evaluations of just one or two projects. As a result, there are unanswered questions about impacts associated with hydropower. For instance, what happens to county-level economic activity during dam construction and operation? Do socio-economic conditions after the construction of a hydropower plant improve?

Using publicly available data we investigate the relationship between the hydropower development and the socio-economic conditions in Brazilian counties from 1991 to 2010. We find that counties that built hydropower plants had a gross domestic product (GDP) that was, on average, 10% (95% CI: 4% to 16%) greater per year during peak construction than counties with hydropower projects planned but not yet built (control group). After completion of plant construction, that difference diminished, and 14 years after construction starts, the average difference was just 3% (95% CI: -1% to 7%). We find a similar temporary increase for tax revenues**.** Furthermore, we find little evidence that social indicators (e.g. average income, life expectancy, educational level, access to piped water, access to public electricity, teenage pregnancy levels, and HIV cases) in counties that built hydropower plants differ from those that had plans to build plants that never materialized.

3.2 Data

To explore the socio-economic impacts from hydropower development, we use data from Brazilian counties. Brazil offers a unique setting for this study because of the significant number of counties affected by reservoirs. Currently, the country has 203 large (> 30 Megawatts of installed capacity) hydropower plants in operation, and 10 under construction[22]. Figure 3-1 shows the spatial distribution of hydropower plants built in Brazil between 1991 and 2010.

Despite the financial incentives available to support hydropower development in Brazil, many areas with hydropower potential do not succeed in developing their hydropower resources. We employ those counties where there were plans to build plants that never materialized as our counterfactual control group. Appendix B (section 7.2) includes a description of the hydropower projects used to define the control group, which are also included in Figure 3-1.

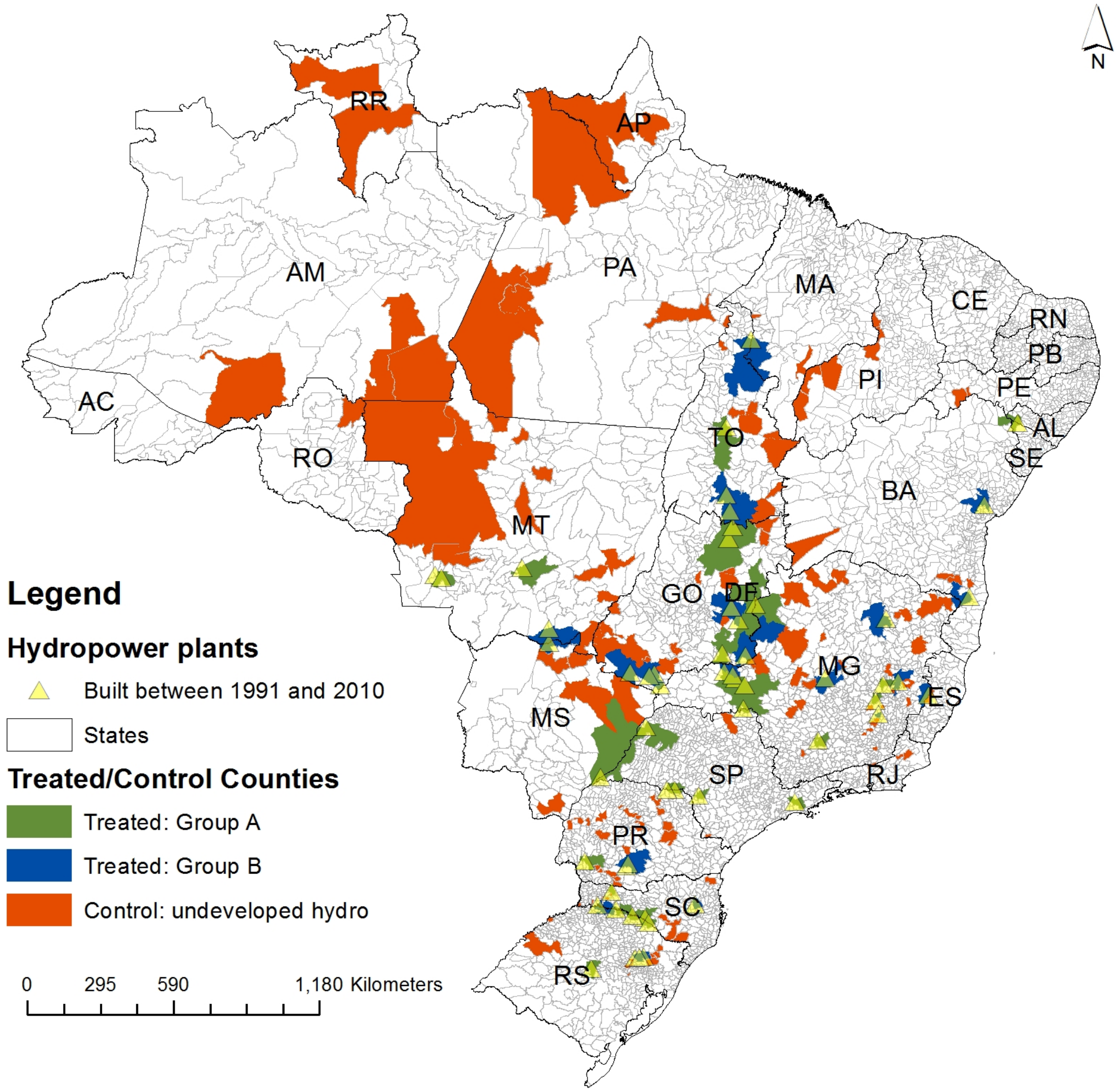

Figure 3-1: Spatial distribution of hydropower plants in Brazil and affected counties. Treated group A represents counties with hydropower plants built between 1991 and 2000. Treated group B represents counties with hydropower plants built between 2000 and 2010. The map presents all counties with undeveloped hydropower projects by 2010, but the control group includes only the counties that are located within a distance of 200 km from the treated counties.

To evaluate the effect of hydropower development on local economies, we gathered population, gross domestic product (GDP), and public revenue data for 5,565 Brazilian counties from 1991 to 2010. We also collected data from electric sector agency, Agência Nacional de Energia Elétrica (ANEEL), to identify the counties that have hydropower plants within their borders[37]. Population and GDP data came from the *Instituto Brasileiro de Geografia e Estatística*[38].

While the National Treasure Secretary is the primary source of public budget data in Brazil[39], we collected this information from the *Instituto de Pesquisa Economica Aplicada* (IPEA)[40]. We used the IPEA database because this institution was the only source providing annual data from 1991 to 1998. Furthermore, IPEA performed a reanalysis of the National Treasure Secretary dataset where the data was adjusted for currency changes, and also standardized according to counties created from 1991 to 2010. Thus, our final budget data includes annual budget information between 1991 and 2010.

Data for human development indicators, for each county, came from the Human Development Brazilian Atlas[33]. The Atlas database relies on the micro-date from the 1991, 2000, and 2010's Brazilian censuses. We use 3 indices available in this database (*Income, Longevity,* and *Education)* to characterize the socio-economic dimensions of each county. Equations (1), (2) and (3) define the three dependent variables for each county *i*:

$$Longevity_i = \frac{Life\ expectancy_i - min\{Life\ expectancy\}}{max\{Life\ expectancy\} - min\ \{Life\ expectancy\}} \quad (1)$$

where life expectancy at birth is measured in years. The minimum and maximum life expectancy values adopted by IPEA are 25 and 85 years old, respectively.

$$Education_i = \frac{(A_i + 2 * \frac{B_i + C_i + D_i + E_i}{4})}{3} \quad (2)$$

where A is the percentage of adults (18 and older) with primary education*;* B is the percentage of children between 5 and 6 years old in school; C is the percentage of children between 11 to 13 years in the final years of primary school; D is the percentage of children between 15 and 17 years old who completed primary school; and E is the percentage of young adults between 18 and 20 years old with a high school degree.

$$Income_i = \frac{\ln(Income\ per\ capita_i) - \ln(\min\ reference\ value)}{\ln(\max\ reference\ value) - \ln(\min\ reference\ value)} \qquad (3)$$

where *Income per capita* is the county's average income, and the maximum and minimum reference values adopted by IPEA are 4,033 and 8 reais (real values based on August 2010), respectively. Data on access to energy and electricity (% of serviced households) and teenage pregnancy rates (% of women pregnant between 12 and 17 years old) also come from the Atlas. HIV cases came from the health system database: DATASUS[41].

3.3 Method

The construction of hydropower plants in Brazil is expected to positively affect the counties surrounding hydropower reservoirs. Brazilian environmental law requires the development of an environmental impact assessment (EIA) to evaluate the social and environmental viability of large infrastructure projects, such as hydropower plants. A review of recent Amazon hydroelectric EIAs indicates that there is an expectation that hydro dams will improve economic activity and social welfare in surrounding regions. Hydropower development may increase local economic activity because of the high influx of workers and investments within a short period of time. Furthermore, according to the EIA from recent projects, the long-term drivers of improved economic conditions are 1) the water resources financial compensation (WRFC), and 2) an increase in tax revenues [23-26]. The WRFC is a legal mechanism that requires hydro dam owners to pay a fee for the water used to produce electricity. The resources are allocated to counties proportionally according to the share of the reservoir area in each county. Appendix B provides detailed information about the WRFC system.

Local economic activity

In this study we assess the economic effects of hydropower development by comparing counties that built plants between 1991 and 2010 (treated) with counties that had plans to build hydropower but had not yet begun construction by 2010 (controls). Table 3-1 summarizes the characteristics of the treatment and control groups. We focus on two outcomes related to economic activity: GDP and public revenue. Information on annual GDP by sector (agriculture, industry, and services) is available from 1999 to 2010. Annual public revenue information includes the annual public income for a county, which is available from 1991 to 2010. We also break down tax revenue information by its main subaccounts: local services tax (ISS), state transfers (ICMS), and federal government transfers (FPM). Appendix B includes details about the public revenue breakdown.

Table 3-1: County sample statistics (T= treatment and C=controls)

	Group	Mean	Standard deviation	Median	10th percentile	90th percentile	n
Gross domestic product (1999)							
Total GDP (x 1000 reais)	T	429	3,562	51	14	402	212
	C	179	544	52	12	329	111
Industry GDP (x 1000 reais)	T	64	221	5	1	150	212
	C	45	198	5	1	52	111
Services GDP (x 1000 reais)	T	308	3,121	24	8	196	212
	C	91	275	26	7	135	111
Agriculture GDP (x 1000 reais)	T	20	29	10	2	50	212
	C	25	36	15	3	52	111
Public Revenues (1991)							
Public Revenue (reais)	T	421	885	168	47	839	212
	C	482	1,338	204	67	788	111
Services Tax – ISS (reais)	T	23	74	1	0	54	212
	C	16	84	1	0	20	111
State transfer – ICMS (reais)	T	168	480	48	0	289	212
	C	182	546	63	1	350	111
Federal Transfer - FPM (reais)	T	114	113	84	3	210	212
	C	121	121	93	41	207	111

We use an event-study approach[27-30] to examine the relationship between hydropower plant construction and local economic activity. In this approach, counties treated earlier (those who got hydropower earlier in our period of analysis) are compared with counties treated later and with control counties. They are compared before hydropower plants are constructed and after these projects begin operation. By comparing all treated and control counties with themselves across time, we eliminate any time-invariant differences between groups. By comparing counties treated earlier versus later, we eliminate any common factors related to the timing of the event (beginning of construction), assuming the underlying forces leading to hydropower development at any point in time are similar for all treated locations. Finally, by comparing all treated and control counties with each other, we eliminate any effects that occur over time, assuming these effects apply to all treated and control counties equally[27]. Table 3-1 shows that treated and control groups are similar for some indicators (e.g. agriculture GDP) but differ for others (e.g. services GDP). To account for those differences, we include control covariates in the regression models.

Hydropower plant construction happens at different times in different counties. The event study framework exploits two of the major strengths of our database – the long period of time and the presence of many counties – in order to obtain a detailed picture of the economic activity patterns across both time and space[27]. The event-study technique can control for county-specific trends in the socio-economic indicators and recover the dynamics of the effect of hydropower development[29,30]. Equation (4) describes the mathematical formulation of the econometric model 1:

$$Model1: EconomicIndicator_{it} = \sum_y \beta_y D_{it}^y + \phi_t + \alpha_i + \gamma_k X_{k,it} + \epsilon_{it} \quad (4)$$

where $EconomicIndicator_{it}$ is the log of GDP (total, industry, services, or agriculture) or public revenue (total public revenue, ISS, ICMS, and FPM) indicators in county *i* in year *t*. We control for county fixed effects, α_i, and year fixed effects, ϕ_t. We also include a list of control variables defined by the matrix X_k, which attempts to account for heterogeneous characteristics across Brazilian counties. γ_k is a vector of the control variables coefficients. First, we include the state GDP to account for the spatial correlation between counties from the same state. Second, we include yearly average temperature and precipitation to control for exogenous time-varying attributes of each county. Third, we include the amount of Itaipu royalties per capita received by each county. Hydropower plants located in the Parana River basin can receive additional funds from Itaipu (the second largest power plants in the world) because they regulate the downstream water flows to Itaipu allowing the optimization of the energy production. Thus, this variable is required because the royalties are correlated with the dependent variable and event-time dummies. e_{it} is the error term.

The D_{it}^{y} are "event-time" dummies that equal one when hydropower construction is y periods away in a given treated county. Formally, we have:

$$D_{it}^{y} = I[t - e_c = y] \tag{5}$$

where I[.] is an indicator function for the expression in brackets being true, and e_c is the year that construction of a hydropower plant starts in county i[29,30]. Therefore, the b_y coefficients in equation (4) represent the time track of the economic indicator relative to the construction starting date, controlling for observed and unobserved heterogeneity. As a result, if hydro dams are randomly assigned to the counties, the restriction $\beta_y = 0$ should hold for all $y < 0$. In other words, the hydropower plant construction should not be, on average, preceded by trends in the counties' economic indicators. We normalize $\beta_{-1} = 0$ because not all the b_y can be identified due to collinearity between the D's and county fixed effects. Finally, we impose end point restrictions:

$$\beta_y = \begin{cases} \acute{\beta}, if y \geq 15 \\ \underline{\beta}, if y \leq -5 \end{cases} \tag{6}$$

which indicate that any dynamics wear off after 15 years[29]. This constraint helps to reduce part of the collinearity between the year and event-time dummies. Because the sample is unbalanced in event time, these endpoint coefficients give unequal weight to counties affected by hydropower early or late in the sample[29]. For this reason, we focus the analysis on the event-time coefficients falling between three years before construction and 14 years after construction, and where the Year 0 is the first year of construction.

The event-study approach relies on the assumption that the characteristics of the counties with plans to develop hydropower projects that do not materialize are similar to those counties that actually had hydropower constructed earlier or later in our period of analysis (random process assumption) conditional on observables. If this assumption is met, we can remove biases associated with siting decisions (e.g., natural advantages[30,42], profit maximization[43]) and the timing of construction (e.g., construction prices and technology advancements). Fortunately, we were able to test and confirm this assumption within this framework by looking at the behavior of the outcome variable prior to hydropower development. If the assumption is reasonable then there should be no observable differences in the event-study coefficients before construction begins, as is the case in our sample. The Results section demonstrates that this assumption is valid for our analysis.

Socio-economic indicators

To evaluate the post-construction impacts from hydropower development on local socio-economic conditions, we employed data for each Brazilian county from the Human Development Brazilian Atlas, a database that contains information about population, household characteristics, and human development indices based on census information[33]. We selected three of the major indices from this database to characterize the socio-economic dimensions of each county in 1991, 2000, and 2010. First, the Income Index (*Income*) measures the average purchasing power based on the average income of each county. Second, the Longevity Index (*Longevity*) is a synthesis of living, health, and sanitation conditions, and it relies on life expectancy at birth. The last indicator, Education Index (*Education*), measures the education level of each county through the evaluation of adult education and the progress of young cohorts through the school system. In addition, we examined other indicators that may be affected by hydropower development: the percentage of public access to electricity and piped water, population density, HIV cases, and teenage pregnancy rates.

We applied a differences-in-differences (DD) estimation strategy to estimate the effects of hydropower projects on human development indicators. We used the DD approach because data for the socio-economic indicators is only available every decade (1991, 2000, and 2010). The DD estimation strategy consists of identifying a specific intervention, then comparing the difference in the indices of interest before and after the intervention for the group affected by the treatment with the corresponding difference for the comparison group. In our case, the intervention is the beginning of the operation of hydropower plants. Again, the treatment group consists of counties that got hydropower and the control group consists of counties with plans to build hydropower that didn't materialize. The DD approach has been widely used for policy evaluation[34,35].

We cross-referenced the human development indices with the information organized by ANEEL about the Brazilian hydropower plants, creating a dummy variable (HP) that identifies which and when hydropower plants started operating in each county. We classified the counties with hydropower reservoirs in two groups. The first group (Group A) contains 46 counties where hydropower operations began in the first period of analysis (1991-2000). The second group (Group B) contains 101 counties that started operations during the second period (2000-2010). As multiple plants affect some counties, we restricted the analysis for groups A and B for the counties that were not receiving WRFC funds from plants built before 1991. The treatment parameter is the year that the power plant starts generating electricity, so we are not including a specific assessment of the construction stage.

Equation (7) defines the basic DD specification:

$$Model\ 2 - HumanDevelopmentIndex_{it} = \psi_1(HP_{it} * T_t) + T_t + HP_{it} + \alpha_i + \beta_k Z_{k,it} + \epsilon_{it} \qquad (7)$$

The dependent variable listed in equation (7) (Human Development Index) represents the indices selected for analysis, which include income, longevity, education, access to electricity and piped water, teenage pregnancy rates, and HIV cases. T is a dummy variable that identifies the post-construction period and controls for timing effects. We also separated the analysis in two periods: short term versus long term. The short term is the period between 1991 and 2000 for group A, and 2000 to 2010 for Group B (T=1 if year equals 2000 for group A, and 2010 for group B, respectively). The long term period is 1991 to 2010 (T=1 if year equals 2010, with 2000 values excluded), and is observed only for group A. HP is a dummy variable for each treated group (Group A and Group B) and controls for the time-invariant differences between control and treated counties. The interaction between HP and T defines the variable of interest, which evaluates the effect of the hydropower plant on socio-economic indicators. The Z_k matrix contains a list of control variables that include annual temperature and precipitation, and β_k is the vector of regression coefficients from those control variables. We applied the same model to estimate the impact on the log of population density as well.

County Creation Issue

Between 1991 and 2010, more than a thousand new counties were created in Brazil. This generates a problem for our analysis as the observation unit (county) changed over time. To overcome this issue, we mapped the changes between 1991 and 2010 and created an identifier to match new counties to their original territory. Then, we merged the new territories to their original one and applied the 1991 baseline county as our observation unit. We aggregated the variables of interest accordingly. This procedure leads to an additional problem because now we can have treated and not treated counties in the same territory. To deal with this additional problem, we weight the event-study and DD treatment dummy variables using the 2010 counties' territory as the weight. For example, if 60% of the territory of a county in 1991 becomes a separate 2010 county (where hydropower development took place), while the remaining 40% of the 1991 area became a non-treated county in 2010, the dummy variable value for the new treated county will be assumed to be 0.6.

Control Group

Despite the financial incentives available to support hydropower development in Brazil, many areas with hydropower potential do not succeed in developing their hydropower resources.

We employed those counties as our counterfactual control group. The reasons why some hydropower projects are still undeveloped include: lack of financial viability, environmental and social restrictions, and legal or regulatory issues. We include this constraint to control for biases associated with natural advantages[30,42], and siting decisions[43]. To identify those counties, we cross-referenced the counties' map with a database [44] provided by ANEEL that contains the precise location of hydropower plant sites studied and approved by the agency. This database has information about the projects' characteristics and their development stages (master plan, viability, basic design, under construction, operation). We selected the counties at stages before construction as our control group. Additionally, we constrained the control group by using only counties within 200km from our treated counties, resulting in a total of 111 counties.

3.4 Results and Discussion

3.4.1 Hydropower development and local economic activity

Figure 3-2 presents the results of the event-study analysis for the total GDP and its subcategories (industry, services, and agriculture). In order to test the validity of the event-study approach, we look at the behavior of the outcome variable prior to hydropower development. The coefficients represent the time path[29] of the GDP relative to the date when construction of a hydropower plant started. Except for one coefficient in agricultural GDP, there were no observable differences between treated and control groups before construction began, supporting the critical assumption that control and treated counties were on similar economic paths before hydropower development.

Figure 3-2 also shows that, during the construction period, treated counties had a greater average increase in total GDP than control counties. This growth is insignificant during the first two years, but achieves a peak in the third year after construction begins, when the average annual GDP growth is 10% (95% CI: 1% to 20%) larger than control counties. After this peak, such GDP difference substantially decreases, although it does not fully return to pre-construction levels. During the construction and operational stages, the average effect of hydropower on the local GDP is 4% (95% CI: -2% to 10%) and 5% (95% CI: 0% to 10%), respectively.

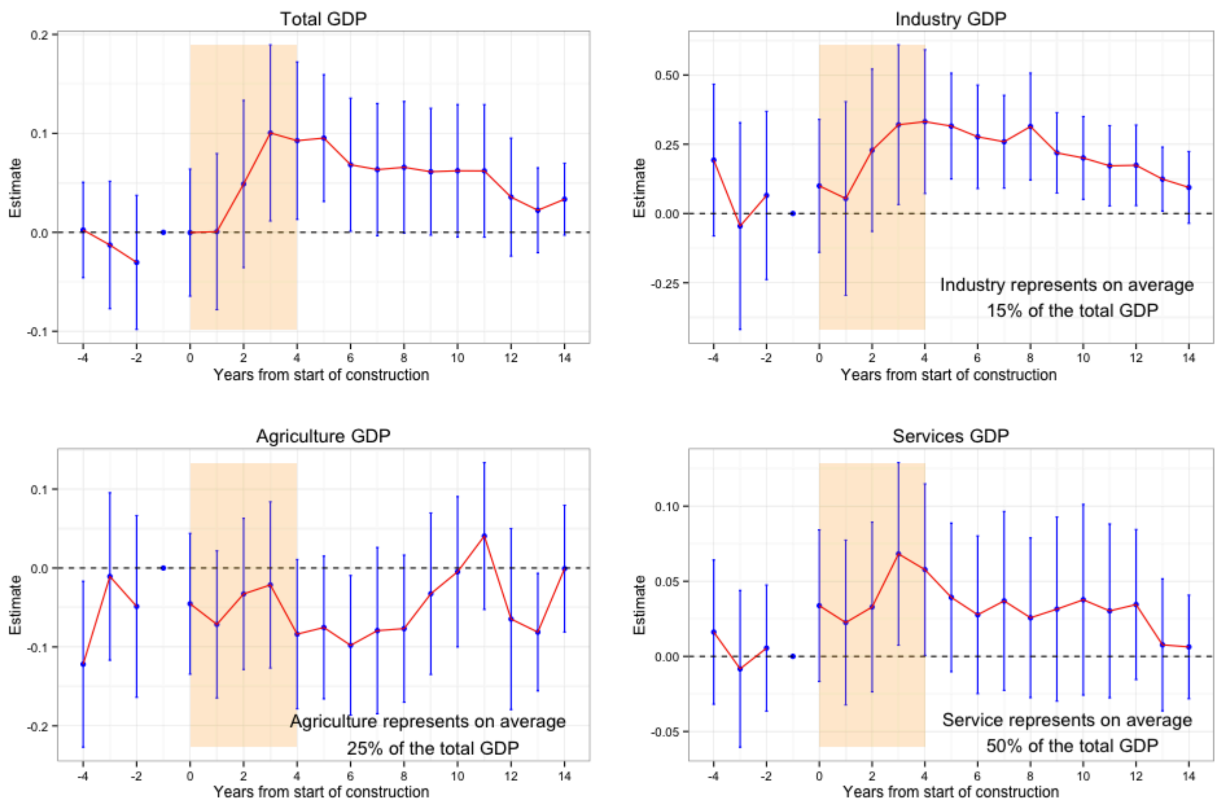

Figure 3-2: Gross domestic product (GDP) event-study regression results. Titles refer to dependent variables. The y-axis represents the coefficient estimates (b_y's from Model 1 defined in the Method section) for each gross domestic product indicator in log points. To obtain the results in percentage increase relative to the pre-construction period compute *exp(Estimate-1)*. The x-axis describes the coefficient outcome in each year relative to the first construction year (Year 0). The light orange boxes represent the average period of hydropower plant construction from our database (approximately 4 years). Points represent the average effect and bars represents the 95% confidence intervals defined as two times the standard errors (robust standard errors are clustered at the county level and hydropower plant).

Figure 3-2 shows that the increase in GDP is likely due to an increase in industrial GDP, which increases very fast a few years after the beginning of construction. At the peak (4^{th} year), hydropower development is associated with an industrial GDP increase of 39% (95% CI: 7% to 80%) per year compared to the pre-construction phase. However, 14 years after the start of construction this effect drops to an average of 9% (95% CI: -3% to 24%). A similar trend is observed in the services sector, where there is an increase of 7% (95% CI: 1% to 15%) in the third year with a gradual reduction thereafter.

In contrast, hydropower development is associated with a loss in agricultural GDP. In the sixth year after construction begins, there is a 10% reduction (95% CI: -3% to -18%) in agricultural GDP. This outcome is likely the result of two main factors. First, the flooding that occurs to create the reservoirs reduces the available land for agricultural production, and possibly affects fishing resources[13]. Second, new opportunities in the services and industrial sectors likely deprive the agricultural sector from workers.

Using the same event-study approach, we assess the relationship between hydropower development and public revenues. Figure 3-3 shows that public revenues increase an average of 6% (95% CI: 0% to 10%) after the beginning of construction. Public revenues continue to rise when operations start, achieving a peak (15%; 95% CI: 9% to 21%) eight years after construction begins. The first increase in public revenue is associated with the growth in the ISS (local tax). ISS revenues more than double during the construction period but their positive effects are limited to 11 years after construction begins.

ICMS revenues (state transfers) lead the second increase in the public revenue. This result is unsurprising given that the proportion of the ICMS received by each county varies by state, but is a function of the value each county adds to the overall state economy. As the treated counties' GDP increase due to the construction and operation of the power plants, the ICMS transfers to those counties also grow. The increasing part of the curve for ICMS is associated with additional electricity generation (and consumption) in the first years of operation. However, the ICMS return to pre-construction levels after the eighth year may be the result of continued growth in the rest of the state once construction is completed. This is the case if electricity generated in the hydropower plants is consumed in other parts of the state, and GDP in those places grows faster. Therefore, the relative contribution of the hydropower plant (and the county where it is located) to the overall state economy decreases with time, leading to a decrease in the ICMS transfers to the affected county.

Finally, our analysis indicates a long-run negative trend on FPM (federal transfers) to the county's budgets. The FPM distribution relies on complex criteria that include the size of the population and the state where the county is located. FPM transfers can decrease for a given county if the share of federal resources to other counties in the state increases in relation to total amount of resources available[31].

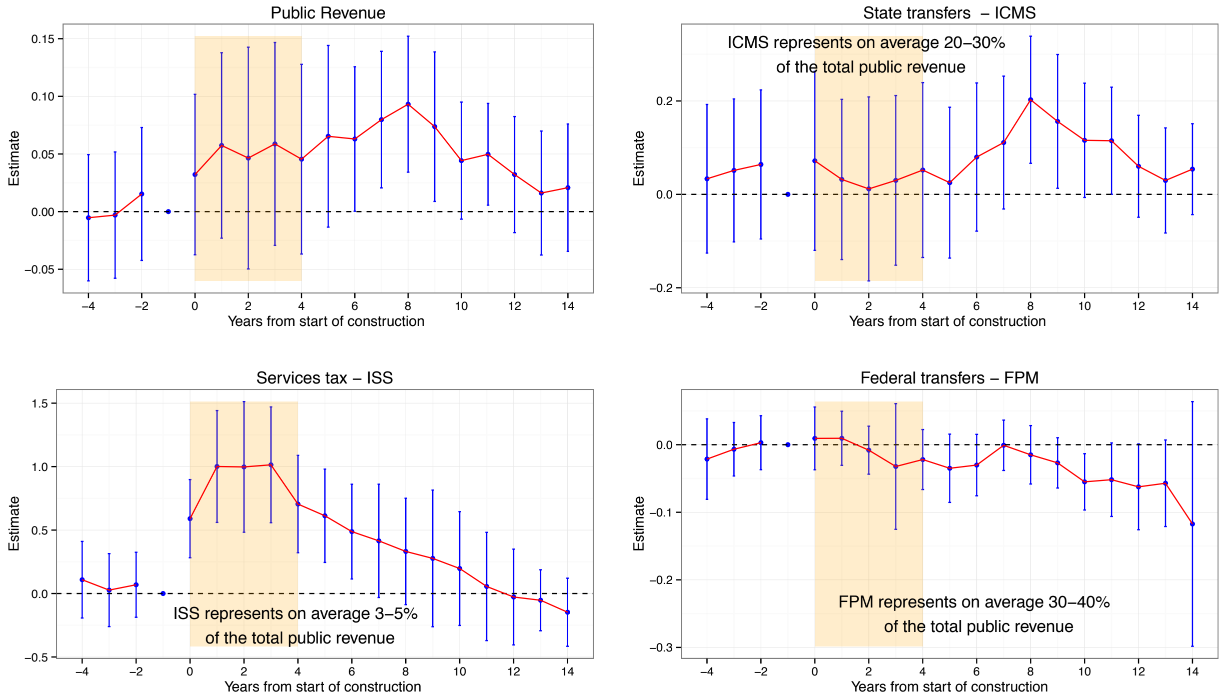

Figure 3-3: Public revenue event-study regression results. Titles refer to dependent variables. The y-axis represents the coefficient estimates (b_y's from Model 1 defined in the Method section) for each revenue indicator in log points. The x-axis describes the coefficient outcome as function of the years from beginning of the construction (Year 0). The light orange boxes represent the average period of construction the hydropower plants from our database (approximately 4 years). Points represent the average effect and error bars represent the 95% confidence intervals defined as two times the standard errors (robust standard errors are clustered at the county level and hydropower plant level).

Sensitivity and Heterogeneity

We assessed the sensitivity of our models to alternative specifications, including regressions without control variables, and using alternative control groups (see Appendix B). The removal of covariates did not affect the coefficients but increased the standard errors, suggesting that the control covariates help to explain part of the noise from our data. Furthermore, if we used all Brazilian counties that did not build hydropower plants as controls in our analysis, the effects of hydropower development are greater for GDP but lower for taxes, indicating that failing to control for natural advantages and siting decisions slightly biases the results. Appendix B (section 7.5) also includes assumption checks (e.g. the strict exogeneity assumption[32]) and a residual analysis. These additional model tests and sensitivity analysis qualitatively support our main findings.

We also evaluated the heterogeneity of hydropower development impacts by dividing the data in four criteria: 1) larger (greater than 500 MW) versus smaller plants (between 30 and 500 MW); 2) utility versus industrial ownership; 3) small (less than 30,000 people) versus large (greater than 30,000 people) counties, and 4) more developed (those with human development index greater than 0.4 in 1991) versus less developed counties (human development index less than 0.4). Most strikingly, we find that smaller hydropower plants perform better in terms of GDP and tax revenues than larger plants. Figure 3-4 describes the first potential reason: smaller plants did not negatively affect the agricultural sector (as they often required less flooded area) while larger plants were associated with substantial reductions in agricultural production. Second, ICMS revenues are greater for smaller power plants because they generate electricity that may be used locally, leading to increased ICMS revenues (See Figure S3, Appendix B, section 7.6.1.). Larger plants, in contrast, are often connected through interstate high voltage transmission lines to the load areas, increasing tax revenues in the state where the electricity is consumed. Therefore, the tax structure is a relevant driver to define the economic benefits allocation between hydropower producing regions and places with high electricity demand.

Our analysis suggests that counties where industry facilities and hydropower were simultaneously constructed have greater tax and GDP revenues than those without such involvement from the industry (See Figures S4 and S5, Appendix B, section 7.6.1). Industry-owned projects are likely developed to supply electricity to industries like mining and aluminum manufacturing, which contribute to industrial GDP. Those electro-intensive industries build power plants close to their facilities to ensure a steady supply of electricity. Finally, our results suggest that small counties were significantly affected by hydropower development while larger counties are barely affected (See Figures S6 and S7, Appendix B). We don't find a clear distinction between hydropower effects on more or less developed counties (See Figures S8 and S9, Appendix B). Appendix B (section 7.6.1) contains the detailed results and discussion about heterogeneity.

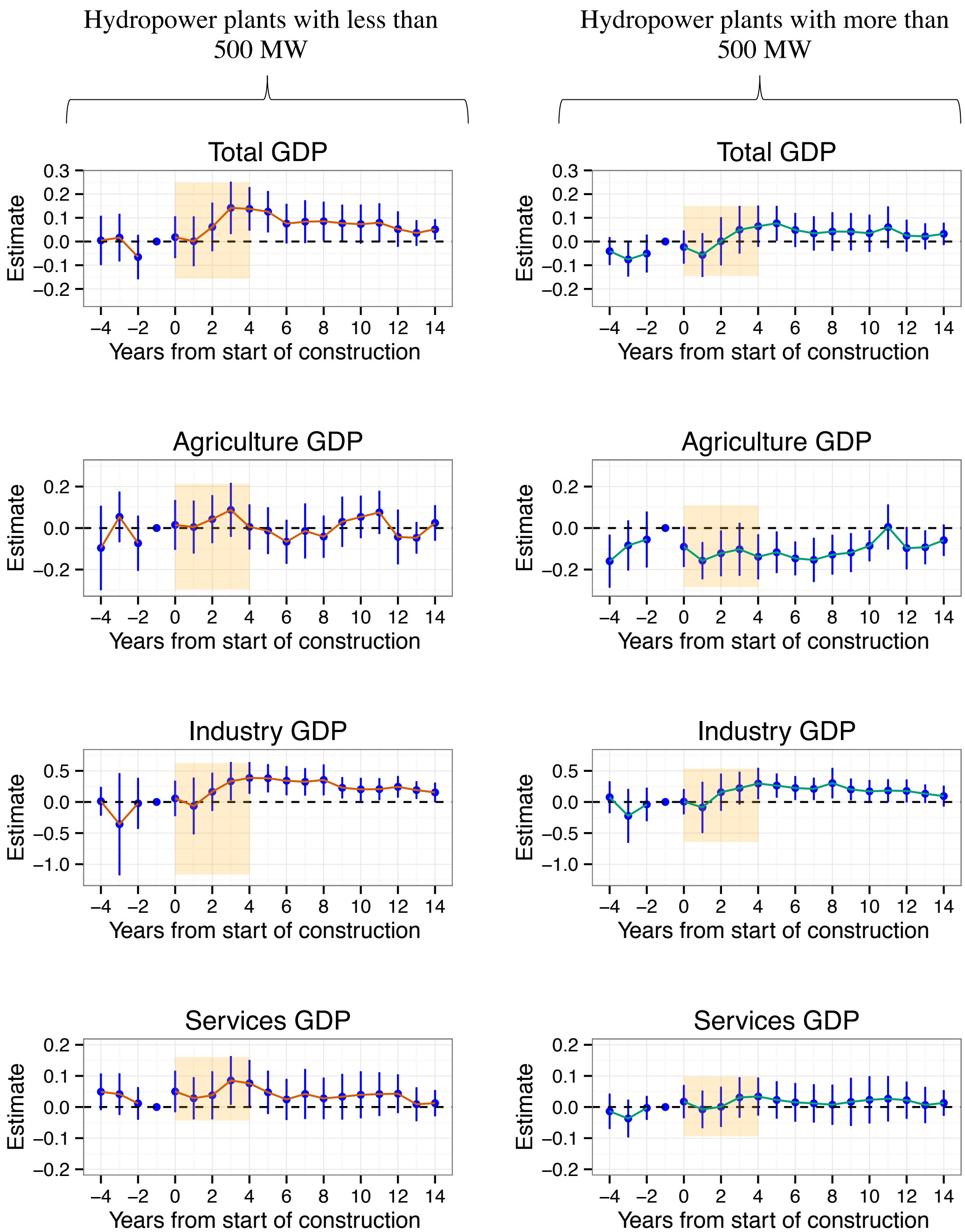

Figure 3-4: Smaller (< 500 MW of installed capacity) versus Larger hydropower plants (> 500 MW of installed capacity): gross domestic product event-study regression results. Titles refer to dependent variables. The y-axis represents the coefficient estimates (b_y's from Model 1 defined in the Method section) for each gross domestic product indicator in log points. To obtain the results in percentage increase relative to the pre-construction period compute *exp(Estimate-1)*.The x-axis describes the coefficient outcome in each year relative to the first construction year (Year 0). The light orange boxes represent the average period of hydropower plant construction from our database (approximately 4 years). Points represent the average effect and bars represents the 95% confidence intervals defined as two times the standard errors (robust standard errors are clustered at the county level and hydropower plant).

3.4.2 Hydropower development and socio-economic indicators

Figure 3-5 depicts the estimated coefficients for our three human development indicators as well as the other variables of interest. The regression results indicate that the socioeconomic indicators for counties that built hydropower plants were not significantly different (either in the short or long run) from counties in the control group. As in previous studies, we do not observe population agglomeration[30]. For education, access to piped water and electricity, and teenager pregnancy we cannot determine whether the relationship was negative or positive. The absence of long-term effects over the local economy likely explains the lack of positive social impacts.

Our results also suggest that the WRFC policy has been not effective in improving conditions relative to the control group that did not receive such payments. Appendix B (section 7.6.2) includes an additional analysis where we assess the socio-economic impacts of the WRFC policy alone. Specifically, we evaluate 379 counties affected by hydropower plants in operation before 1991 that started receiving WRFC funds only in 1991, when the compensation policy was put into effect. The WRFC implementation represents a discontinuity for the treatment group and allows us to investigate the effect of the WRFC alone, excluding the construction effect. We find that WRFC policy is associated with relative deterioration of socio-economic indicators (e.g., income and life expectancy) in the long run (See Figure S10, Appendix B).

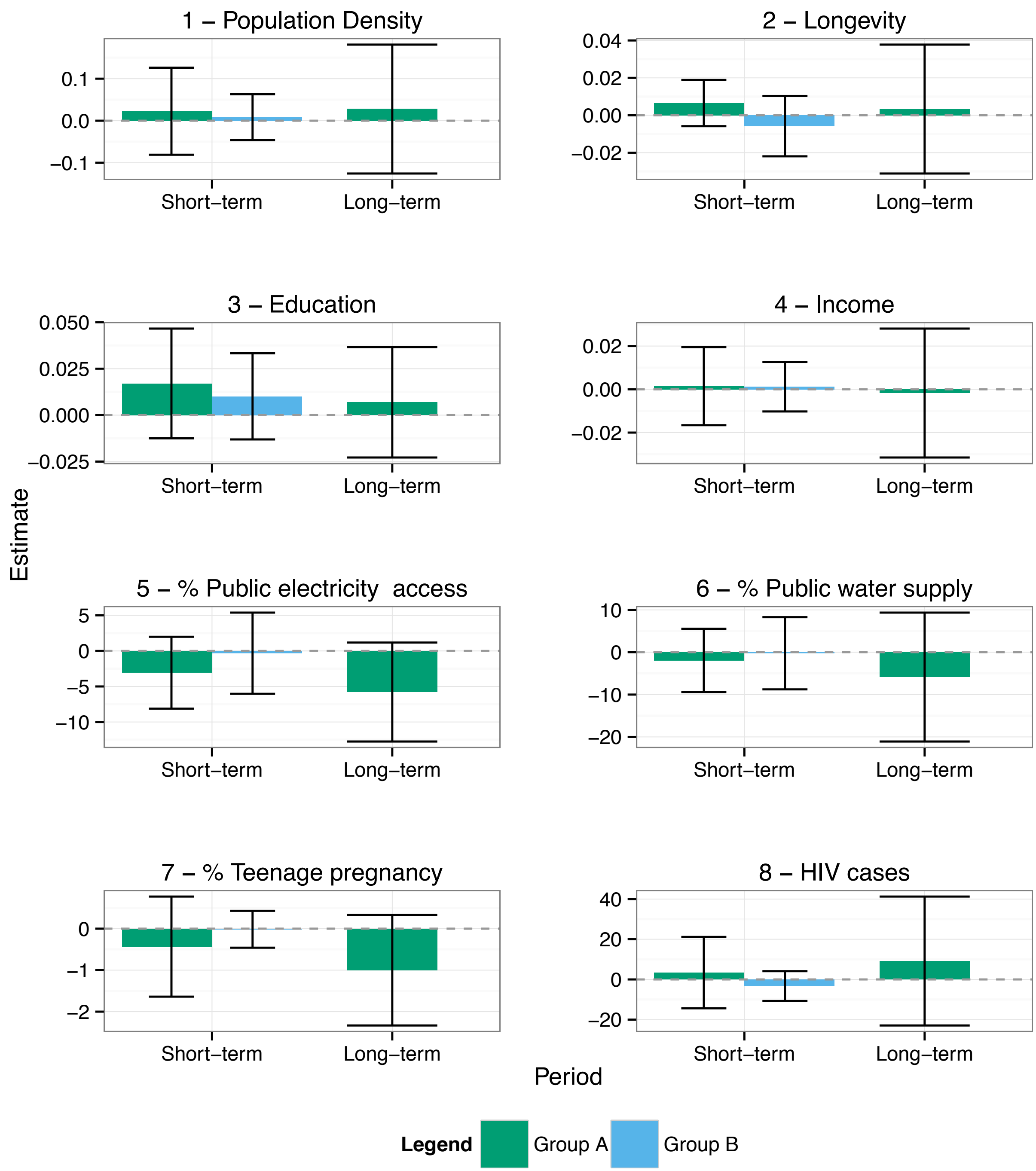

Figure 3-5: Difference-in-differences regression results for the human development indicators and other outcomes of interest for A and B treatment groups (described in the Methods section). Bars represent the average y_1 coefficient estimates from equation (7) described in the Methods section. Error bars represent the 95% confidence intervals defined as two times the standard errors (robust standard errors are clustered at the county level and hydropower plant level). Short term represents the first decade after hydropower development (A: 1991-2000 and B: 2000-2010). Long term represents two decades after hydropower development (Only A: 1991-2010).

3.5 Policy implications

In this chapter we have provided evidence that the positive effects of hydropower projects on local economies in Brazil are the result of two cycles: construction and operation. We found, however, that most of those effects are short-lived, and disappear in less than 15 years. This is particularly important because large hydropower dams (and their environmental consequences) last many decades or even centuries. Additionally, we did not find evidence that hydropower development contributes to long-term improvements for local social indicators. Hence, the empirical evidence does not support long-term positive economic and social impacts described in the environmental impact assessments for Brazilian projects. Our results highlight the need for empirically driven methods to assess the socio-economic viability of hydropower development in Brazil. We acknowledge, however, that this study focuses only on the local effects and does not evaluate the overall effects of the electricity transmitted to other parts of the Brazilian economy, which may in fact be more positive that our local results suggest.

This work also brings new empirical evidence to the debate about financial incentives for infrastructure and energy projects. Often, state and local governments use tax exemptions, subsidies, and changes in tax structure to try to attract industry and thus promote regional growth[36]. The quick reversion of local economic activity to pre-construction levels in Brazilian counties affected by hydropower plants relative to control counties reveals the lack of local agglomeration spillovers, and suggests that policies aimed at spurring hydropower development to support local well-being may not be effective.

References

1. Ansar, A., Flyvbjerg, B., Budzier, A. & Lunn, D. Should we build more large dams? The actual costs of hydropower megaproject development. Energy Policy 69, 43–56 (2014).

2. Jackson, S. & Sleigh, A. Resettlement for China's Three Gorges Dam: socio-economic impact and institutional tensions. Communist and Post-Communist Studies 33, 223–241 (2000).

3. Tilt, B., Braun, Y. & He, D. Social impacts of large dam projects: A comparison of international case studies and implications for best practice. Journal of Environmental Management 90, S249–S257 (2009).

4. Fearnside, P. M. Dams in the Amazon: Belo Monte and Brazil's Hydroelectric Development of the Xingu River Basin. Environmental Management 38, 16–27 (2006).

5. Fearnside, P. M. Tropical hydropower in the clean development mechanism: Brazil's Santo Antônio dam as an example of the need for change. Climatic Change 131, 575–589 (2015).

6. Egré, D. & Milewski, J. C. The diversity of hydropower projects. Energy Policy 30, 1225–1230 (2002).

7. IPCC, IPCC Special Report on Renewable Energy Sources and Climate Change Mitigation. (IPCC: 2011).

8. Hug-Glanzmann, G. A Hybrid Approach to Balance the Variability and Intermittency of Renewable Generation. 2011 IEEE PES PowerTech - Trondheim 1–8 (2011).doi:10.1109/PTC.2011.6019448

9. Sperling, von, E. Hydropower in Brazil: overview of positive and negative environmental aspects. Energy Procedia 18, 110–118 (2012).

10. James Feyrer, E. T. M. B. S. Geographic Dispersion of Economic Shocks: Evidence from the Fracking Revolution. 1–48 (2015).

11. Newell, R. G. & Raimi, D. Shale Public Finance: Local government revenues and costs associated with oil and gas development. National Bureau of Economic Research 1–87 (2015).

12. Kline, P. & Moretti, E. Local Economic Development, Agglomeration Economies, and the Big Push: 100 Years of Evidence from the Tennessee Valley Authority. The Quarterly Journal of Economics 129, 275–331 (2014).

13. da Silva Soito, J. O. L. & Freitas, M. A. V. Amazon and the expansion of hydropower in Brazil: Vulnerability, impacts and possibilities for adaptation to global climate change. Renewable and Sustainable Energy Reviews 15, 3165–3177 (2011).

14. Lerer, L. B. & Scudder, T. Health impacts of large dams. Environmental Impact Assessment Review (1999).

15. Rosenberg, D. M., Bodaly, R. A. & Usher, P. J. Environmental and social impacts of large scale hydroelectric development: who is listening? Global Environmental Change 5, 127–148 (1995).

16. Rosenberg, D. M. et al. Large-Scale Impacts of Hydroelectric Development. Environmental Rev. 5, 27–54 (1997).

17. Brown, P. H., Tullos, D., Tilt, B., Magee, D. & Wolf, A. T. Modeling the costs and benefits of dam construction from a multidisciplinary perspective. Journal of Environmental Management 90, S303–S311 (2009).

18. Friedl, G. & Wuest, A. A. Disrupting biogeochemical cycles – Consequences of damming. Aquatic Sciences 64, 55–65 (2002).

19. Manyari, W. V. & de Carvalho, O. A., Jr. Environmental considerations in energy planning for the Amazon region: Downstream effects of dams. Energy Policy 35, 6526–6534 (2007).

20. Fearnside, P. M. Environmental Impacts of Brazil's Tucurui Dam: Unlearned Lessons for Hydroelectric Development in Amazonia. Environmental Management 27, 377–396 (2001).

21. Sovacool, B. K. & Bulan, L. C. Behind an ambitious megaproject in Asia The history and implications of the Bakun hydroelectric dam in Borneo. Energy Policy 39, 4842–4859 (2011).

22. de Energia Eletrica Brazilian Electricity Agency, A. N. Brazilian Electricity Generation Information Databank (BIG - Banco De Informações De Geração - Aneel. at <http://www.aneel.gov.br/aplicacoes/capacidadebrasil/capacidadebrasil.cfm>

23. Eletrobras Relatório de Impacto Ambiental UHE Belo Monte. 1–100 (Eletrobrás: 2009).

24. EPE Relatorio de Impacto Ambiental UHE Teles Pires. 1–68 (Empresa de Pesquisa Energetica (EPE): 2010).

25. EPE Relatório de mpacto ambiental UHE Sinop. 1–88 (Empresa de Pesquisa Energetica (EPE): 2010).

26. EPE Relatório de Impacto Ambiental UHE São Manoel. 1–110 (Empresa de Pesquisa Energetica (EPE): 2011).

27. Jacobson, L. S., LaLonde, R. J. & Sullivan, D. G. Earnings Losses of Displaced Workers. The American Economic Review 83, 685–709 (1993).

28. McCrary, J. The Effect of Court-Ordered Hiring Quotas on the Composition and Quality of Police. The American Economic Review 97, 318–353 (2007).

29. Kline, P. The Impact of Juvenile Curfew Laws on Arrests of Youth and Adults. American Law and Economics Review 14, 44–67 (2012).

30. Severnini, E. R. The Power of Hydroelectric Dams: Agglomeration Spillovers. Institute for the Stufy of Labor (IZA) 1–70 (2014).

31. da Fazenda, M. & do Tesouro Nacional, S. Fundo de Participação dos Municípios – FPM. 1–15 (Brazilian government: 2013).

32. Wooldridge, J. M. Econometric Analysis of Cross Section and Panel Data. 1–753 (2004).

33. UNEP, U. N. D. P., de Pesquisa Economica Aplicada IPEA, I. & Pinheiro, F. J. Brazil's human development atlas (Atlas do desenvolvimento humano no Brasil). (2015).at <http://www.atlasbrasil.org.br/2013/pt/home/>

34. Meyer, B. D. Natural and Quasi-Experiments in Economics. Journal of Business & Economic Statistics 13, 151–161 (1995).

35. Bertrand, M., Duflo, E. & Mullainathan, S. How Much Should We Trust Differences-in-Differences Estimates? The Quarterly Journal of Economics 119, 249–275 (2004).

36. Morgan, W. E. & Hackbart, M. M. An analysis of state and local industrial tax exemption programs. Southern Economic Journal 41, 200 (1974).

37. de Energia Eletrica Brazilian Electricity Agency, A. N. Water resources use financial compensation data. (2015).at <http://www.aneel.gov.br/aplicacoes/cmpf/gerencial/>

38. de Geografia e Estatística IBGE, I. B. Instituto Brasileiro de Geografia e Estatística (IBGE).

39. do Tesouro Nacional, S. County public budget datafrom the Brazilian counties. (2010).at <http://www.ipeadata.gov.br/>

40. de Pesquisa Economica Aplicada IPEA, I. IPEADATA. (2015).

41. da Saúde, M. DATASUS. at <http://www2.datasus.gov.br/DATASUS/index.php?area=01>

42. Rosenthal, S. S. & Strange, W. C. Evidence on the nature and sources of agglomeration economies. Handbook of regional and urban economics (2004).doi:10.1016/S0169-7218(04)07049-2

43. Greenstone, M., Hornbeck, R. & Moretti, E. identifying agglomeration spillovers: evidence from million dollar plants. National Bureau of Economic Research (2008).

44. de Energia Eletrica Brazilian Electricity Agency, A. N. Sistema de informações georreferenciadas do setor elétrico - SIGEL. (2015).at <http://sigel.aneel.gov.br/sigel.html>

4. COMPARING ALTERNATIVES TO HYDROPOWER DEVELOPMENT IN THE AMAZON

This chapter is based on research by *Felipe A. M. de Faria*[+] and *Paulina Jaramillo*[+] *currently in preparation for submission to Nature Energy*

[+]Department of Engineering & Public Policy, Carnegie Mellon University.

4.1 Introduction

Since the middle of the 20th century, Brazil has been supplying most of its growing electricity demand by building large hydropower plants. Currently, hydropower plants larger than 30 MW comprise 61% of the total installed capacity (144 GW)[1]. Recently, the construction of new hydropower plants has been concentrated in the Amazon basin, where large plants like Jirau (3,750 MW), Santo Antônio (3,150 MW), and Belo Monte (11,200 MW) were recently built. The Amazon region is the focus of the recent hydropower development given that most of the hydropower capacity in other regions has already been constructed. In addition to the previously listed projects, there are several projects currently under construction, such as Teles Pires (1,820 MW), São Manoel (746 MW) and Sinop (461 MW). Moreover, the latest government energy plan indicates that most of the new power plants will continue to be built over the Amazonian forest with São Luis do Tapajos (6,133 MW) and São Simão Alto (3,509 MW)) as notable examples[2].

Although hydropower has been seen as the main supply source to meet the growing demand for electricity, projects located in the Amazon could have significant environmental and social impacts[3-5]. The reservoirs in these power plants replace river and land, flooding agricultural land, flora, and fauna. The dams also block the natural river flow affecting the migration of aquatic species and resulting in changes in the oxygen, thermal, and sediment conditions in the reservoir area and downstream[6-8]. In some cases, the flooding and decay of large stocks of biomass in the reservoir area lead to greenhouse gas emissions with magnitude comparable to fossil fuel power plants[9-12]. Furthermore, large hydropower projects also affect the local population through the resettlement of people living in the reservoir areas and the deterioration of social cohesion because of the high influx of workers[3,13-15], and loss of Agricultural GDP.

In order to better understand the potential tradeoffs associated with hydropower development in the Amazon, it is essential to develop methods and indicators to compare the costs and benefits of these power plants against other alternatives for power generation. In this study, we develop different capacity expansion scenarios for the Brazilian power system. We simulate the electric system operations in order to estimate performance indicators such as land use, electricity production and operational costs, quantity of stored energy in the reservoirs, level of wind curtailment, and greenhouse gas (GHG) emissions across the different scenarios. The alternative scenarios include replacing the Amazonian hydropower capacity with wind power in the northeast and south regions, or natural gas plants in the southeast.

The results of this modeling effort suggest that higher wind penetration will reduce land use requirements for electricity generation and increase the average capacity of the system to store water in hydropower reservoirs because of the negative correlation between the peaks and valleys of hydro and wind power generation through the year. However, when wind penetration reaches 24% to 28% of total system capacity, generation from thermal power plants increase, leading to higher operational costs and GHG emissions than the baseline, hydro-based scenario.

Moreover, we also assessed the impact on costs and GHG emissions of replacing the more polluting coal, diesel, and oil power plants by less polluting natural gas power plants. Finally, we assess the impact of replacing Amazon hydropower with natural gas power plants, which increases the costs and GHG emissions of energy development compared to the baseline. Our results indicate that a combination of an expansion of renewable resources and natural gas power plants is likely a more effective strategy to replace Amazonia hydropower while reducing emissions from the Brazilian electric system.

4.2 Data

4.2.1 Brazil's integrated electric system

As of May 2016, Brazil has 143 GW of installed power generation capacity comprising 204 large hydropower plants (87 GW), 2,888 thermal power plants (40 GW), 2 nuclear power plants (2 GW), 356 wind parks (9 GW), and 456 small hydropower plants with less than 30 MW (5 GW)[1]. A national system operator (*Operador Nacional do Sistema - ONS*) is responsible for the operations of the integrated power system and controls the dispatch of power plants to instantaneously match supply and demand for electricity, while minimizing operation costs.

Modelling the optimal operation of a complex and integrated hydrothermal power network like the Brazilian electric system requires extensive and detailed data about each power plant, transmission lines, and loads. The *Empresa de Pesquisa Energetica* (EPE) is the Brazilian state company responsible for creating the long-term energy plans for the country. Every year, EPE issues an expansion plan (*Plano Decenal de Energia*) that includes a set of files containing the detailed characteristics of each power plant used to model the hydrothermal operation of the future system[16]. Table 4-1 includes the major characteristics that are available about each power plant from the EPE report released in January 2015 (hereafter the 2015 EPE report files), which focused on modelling the system from 2013 to 2023 but provided data up to 2028. We used 2015 EPE report files as the reference scenario (baseline) to represent the electricity generation capacity expansion from 2013 to 2028.

Table 4-1: Major information about the Brazilian electric system available in the EPE database

Major variables	Characteristics
Hydropower plants	
Operating Data	
Minimum flow (m^3/s)	Represents the minimum outflow of the plant, which may be required because of technical constraints.
Maximum flow (m^3/s)	Represents the maximum outflow through the turbines.
Minimum total outflow (m^3/s)	Represents a lower bound on the sum of turbined and spilled outflows, required for example to assure navigation along the river.
Production coefficient ($MW/m^3/s$)	Represents the average production coefficient in the plant
Installed capacity (MW)	Maximum limit of the plant power production.
Number of generators	Number of generating units in the power plant
Forced outage rate	Represents the effect of random equipment outages on the hydro plant production capacity.
Composite outage rate	Represents the joint effect of equipment maintenance and equipment outage on the hydro plant production capacity.
Characteristics of the downstream reservoirs	Indicate the characteristics of the cascade structure
Plant parameters	
Minimum/maximum reservoir storage (hm^3)	Minimum and maximum reservoir storage capacities
Spillway type	Indicate if the plant can spill at any reservoir storage level.
Storage (hm^3)	Constant water volume of the run-of-the-river plant
Area (km^2)	Reservoir area
Production coefficient × storage	Represents the effect of head variation with storage.
Thermal plants	
Operating Data	
Fuel characteristics	Information about source, unit (ton, m^3, gallon, etc.) and price ($/unit)
Minimum generation (MW)	Minimum limit of the plant power output.
Maximum generation (MW)	Maximum limit of the plant power output.
Forced outage rate – FOR (%)	Represents the effect of random equipment outages on the thermal plant production capacity.
Composite outage rate – COR (%)	Represents the joint effect of equipment maintenance and equipment outage on the thermal plant production capacity.
Plant type	Standard or "must-run"
Loads by subsystem	The monthly load variability is represented by three load blocks (see method)
Subsystem interconnection	Information about the interconnection between subsystems

EPE models the Brazilian system by dividing it in 10 subsystems: 1) North, 2) Northeast, 3) Southeast, 4) South, 5) Paraná, 6) Itaipu, 7) Teles Pires and Tapajós, 8) Belo Monte, 9) Acre and Roraima, and 10) Manaus, Amapá and Boa Vista. Some of these subsystems contain power plants and loads (e.g. Southeast), but others contain just generation (e.g. Belo Monte). Figure 4-1 describes a scheme of the subsystems and their interconnection.

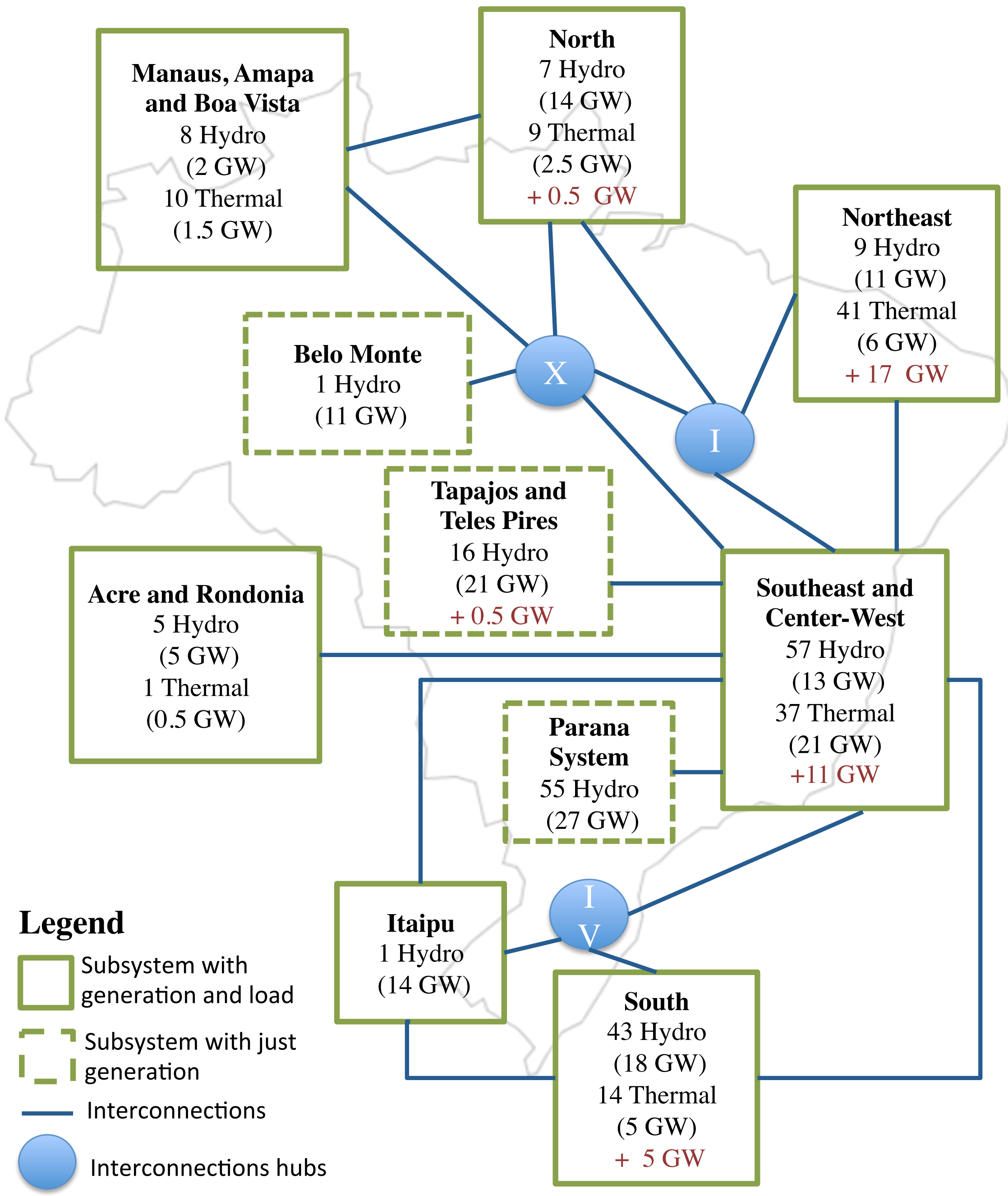

Figure 4-1:Brazilian integrated system scheme (forecasted capacity by 2028). Red figures inside the boxes represent the "other renewables" average power (wind, solar, biomass). Source: adapted from EPE, 2014.

4.2.2 Representation of the current system

The EPE's 2015 energy report database contains data for the Brazilian interconnected electric system as of May 2013 and contains 133 hydroelectric power plants (86 GW) and 99 thermal power plants (20 GW). Table S1 and S2 in the Appendix C (section 8.2) contain the main characteristics of the hydroelectric and thermal power plants represented in the current system, respectively. Other renewables like wind, biomass, solar, and small hydro account for less than 10 GW and their energy output are modelled as a group that includes all power plants by subsystem. Appendix C provides more details about the EPE's modelling assumptions about the wind, biomass, solar and small hydropower plants.

4.2.3 Baseline scenario

To supply growing demand for electricity, EPE defines a set of hydroelectric and thermal projects that should start operations by 2028 (database horizon). Each project listed has a unique operating start date such that the power plants in the database are under different development stages throughout the period of analysis (see the complete schedule in Appendix C). As a result, some power plants in the database are already in operation, under construction or in an advanced licensing stage, while others are just in the proposal stage and may ultimately remain undeveloped. For purposes of this analysis, we assume all these plants will be operational in our baseline scenario.

According to the EPE expansion plan, Brazil will need to build approximately 55 GW of new hydropower plants, 20 GW of thermal plants, and 26 GW of wind plants to meet electricity demand by 2028. Therefore, most of the new capacity will continue to come from hydropower plants. Hydropower plants located in the Amazon are expected to account for 46 out of 55 GW of the new hydropower capacity described in the EPE's plan (Table 4-2).

Table 4-2: Recent or planned large hydropower plants in the Amazon (2013 - 2028)

Name	Installed Capacity (MW)	Lat.	Long.	Reservoir Area (km^2)
Belo Monte	11,233	-3.1	-51.8	440
Bem Querer	708	1.9	-61.0	559
Cachoeira do Caldeirão	219	0.9	-51.3	51
Cachoeira do Caí	802	-5.1	-56.5	420
Cachoeira dos Patos	528	-5.9	-55.8	117
Carecuru	240	-0.1	-53.0	184
Colíder	300	-11.0	-55.8	123
Ferreira Gomes	252	0.9	-51.2	12
Jamanxim	881	-5.6	-55.9	74
Jardim de Ouro	227	-6.3	-55.8	426
Jatobá	2,338	-5.2	-56.9	646
Jirau	3,750	-9.3	-64.7	303
Marabá	1,708	-5.3	-49.1	1,115
Paradão A	199	2.9	-61.6	17
São Luís do Tapajós	8,040	-4.6	-56.8	722
Serra Quebrada	1,328	-5.7	-47.5	386
São Simão Alto	3,509	-8.2	-58.3	284
Santa Isabel	1,087	-6.1	-48.3	1,850
São Manoel	700	-9.2	-57.1	53
Sinop	400	-11.3	-55.5	330
Salto Augusto de Baixo	1,461	-8.9	-58.6	125
Santo Antônio do Jari	370	-0.7	-52.5	32
Santo Antônio	3,151	-8.8	-63.9	271
Tabajara	350	-8.9	-62.2	129
Teles Pires	1,820	-9.3	-56.8	123
Tucumã	453	-10.5	-58.4	219
Total	**46,055**			**9,012**

4.2.4 Introducing wind generation in the model

The baseline scenario forecasts the need for additional 26 GW of wind capacity by 2028. Brazilian wind resources are concentrated in the Northeast and South subsystems. Wind energy production variability introduces complexity to the system operation; however, this complexity is not represented by the current information provided by EPE. The EPE's database treats the renewable sources (excluding large hydropower plants) like groups of projects in each subsystem. The renewable sources are also assumed to be must-run plants with a constant monthly electricity output (Figure S2 in the Appendix C). Thus, the EPE's modelling approach accounts only for an average seasonal variability, but does not account for the stochastic nature of the wind speeds and the daily variability of wind output.

To overcome this issue, we created wind generation series using wind speed data from the National Centers for Environmental Prediction (NCEP) Climate Forecast System Reanalysis (CFSR)[17] for the current and future wind parks. NCEP-CFSR is an atmospheric reanalysis product available at an hourly time resolution from 1979 to the present and a horizontal resolution of 0.5° latitude × 0.5° longitude. Reanalysis data are attractive for wind-power studies because they can offer wind speed data for large areas and long time periods and in locations where historical data are not available[18]. To define the position of the current and future wind parks we used data from the Brazilian electricity agency ANEEL that provides the geographical position of each wind park in operation and under earlier development stages[19] (See Table S3 and Figure S3 in the Appendix C). We evaluated the validity of using CSFR wind speeds to generate wind power output series using real data from 32 wind parks in Brazil. The appendix for this chapter details this validation analysis (Appendix C, section 8.4).

4.2.5 Power plant investment costs

The Chamber of Electric Energy Trading (*Câmara de Comercialização de Energia Elétrica - CCEE*, in Portuguese), which is the Brazilian electricity market operator, provides a dataset of all new power plants that sold energy in public auction since 2005[20]. This database contains the installed capacity and the forecasted capital costs for 826 power plants built from 2005 to 2015. We applied the CCEE cost information to estimate the total construction costs of the future power plants. Appendix C (section 8.5) contains a detailed description about the CCEE data.

4.3 Method

4.3.1. Power systems model

We imported 2015 EPE report files to model current and future power plants using SDDP (stochastic dual dynamic programming), which is a hydrothermal dispatch model with the representation of the transmission network. The model calculates the least-cost stochastic operating policy of the electric system, taking into account operational details of the plants, such as water inflows and operational limits, and the stochastic behaviour of the system caused by renewable variability[21-23].

In purely thermal systems, the operation cost of each plant depends essentially on its fuel cost - the plants with the lower fuel costs are dispatched first. However, the operation of hydrothermal systems is more complex because the system operator needs to decide every time whether to save or use water from the reservoirs. If the operator decides to use hydro energy today, and future inflows are high, allowing for reservoir storage recovery, the system operation will be efficient[23]. In contrast, if a drought occurs, it may be necessary to use more expensive thermal generation in the future, or even interrupt the supply. Similarly, if storage levels are kept high through more use of thermal today, and high inflows occur in the future, reservoirs may spill, which results in a waste of energy and higher operational costs. If a drought occurs instead, storage displaces thermal generation and the operation is efficient[23]. The problem is stochastic because water inflow to the reservoirs is a result of a random process and it is impossible to have a perfect forecast of future inflows[22]. Additionally, most inflow sequences are serially correlated affecting the operation decisions[23]. In other words, if the inflow of the past month was wetter than the average, there is a tendency that the inflows in the next few months will be wetter too.

The SDDP application in this study allows the comparison of different expansion plans taking into account the hydrothermal scheduling issue. SDDP determines the sequence of hydro releases, which minimizes the expected thermal operation costs (given by fuel costs and penalties for rationing) during the planning horizon[21,23]. Renewable sources, like wind, are treated as a negative load with zero cost. The SDDP algorithm decomposes the multi-stage stochastic problem into several one-stage sub-problems. Each sub-problem corresponds to a linearized optimal power flow with additional constraints representing the hydro reservoir equations and a piecewise linear approximation of the expected future cost function[21,22]. For a given stage of the problem, the future cost is a function of the reservoir storage levels and inflows. SDDP incorporates inflow stochastic characteristic by solving the optimization problem several times (Monte Carlo simulation). We solve the optimization for each scenario using 400 simulations. The algorithm also incorporates serial autocorrelation of inflows by modeling the water inflows to the reservoirs using an autoregressive linear regression model based on the historical monthly inflows for each hydropower reservoir. Appendix C (section 8.3) contains more details about hydrothermal scheduling issue and the SDDP algorithm.

Moreover, a fair comparison between different expansion plans should take into account that each scenario should provide similar levels of system reliability. We built our alternative scenarios to provide system reliability levels comparable to the baseline. We measured the system reliability using the lost load probability over the planning horizon. Finally, we compared the baseline against the alternative expansion plans using environmental (e.g. land use and greenhouse gas emissions), system operation (e.g. level of stored energy in the hydroelectric reservoirs and wind curtailment) and cost (e.g. investment and operational costs) indicators.

4.3.2. Demand and interconnection representation

The EPE database represents electricity demand in a typical day in the Brazilian system using three load blocks within each month (stage): high, medium and low. EPE projects future electricity demand based on demographic, economic, and sectorial studies about residential and industrial electricity consumption[24]. The loads are grouped by subsystem[16] and in a typical day, the high load happens between 6 pm and 9 pm; the low load occurs from 0 am to 7 am; and the rest of hours of the day are considered medium load[25]. Therefore, three pairs of duration (hours) and demand (GWh) by month represent each load block. Given this information, we optimize system operations to meet the demand in monthly time steps where three different load levels (blocks) represent the daily load variability within each month. All scenarios have the same demand profile. Figure 4-2 shows the annual load duration curves for 2014 and 2028. Finally, we represent the interconnection between subsystems as described in Figure 4-1, but we relax the transmission capacity constraints assuming no restriction between the sub-systems.

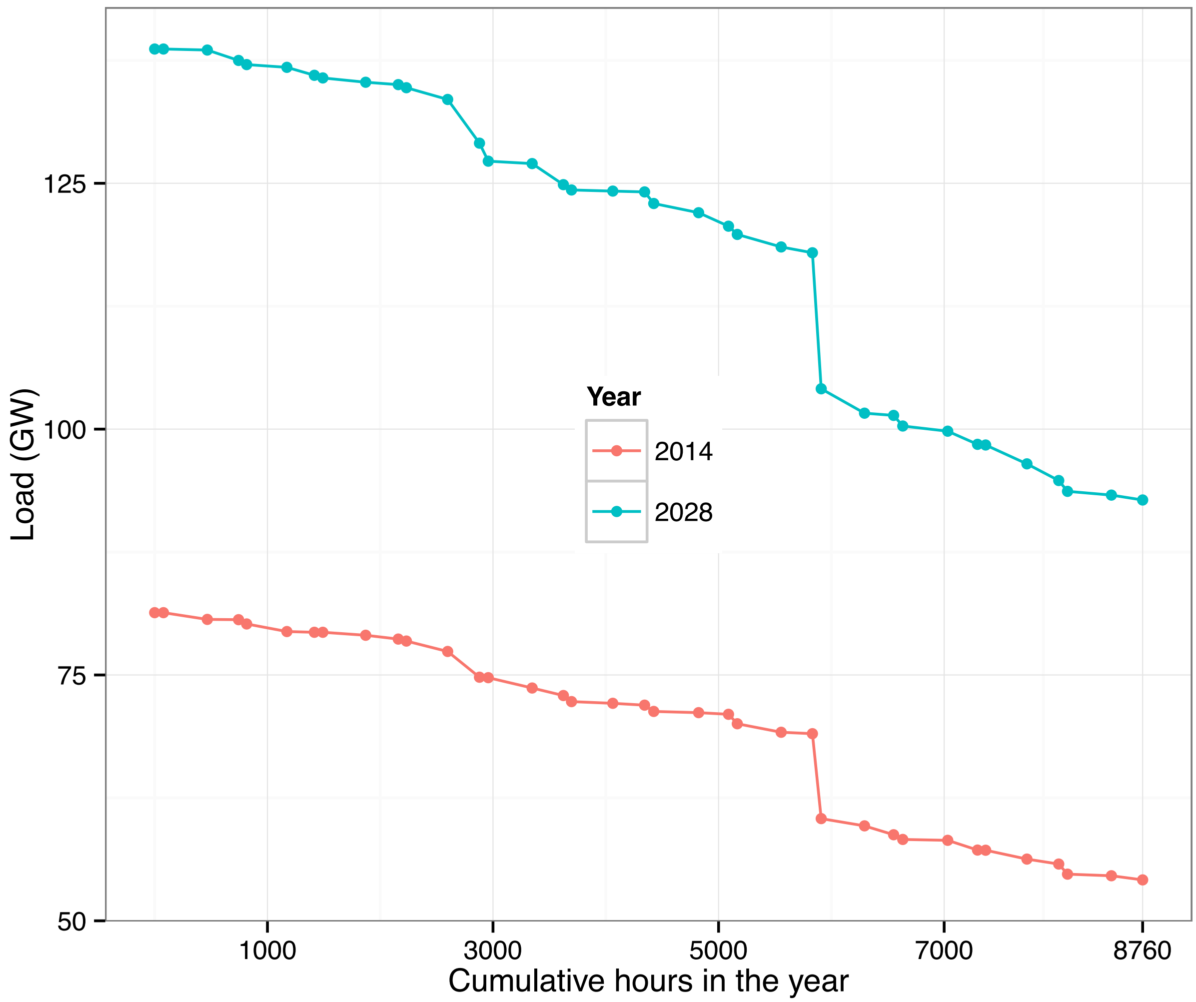

Figure 4-2: Load duration curves for 2014 and 2028. Load duration curve is a graphical representation of the association between generating capacity requirements and capacity utilization.

4.3.3. Alternative scenarios

The objective of this chapter is to compare different electricity generation expansion scenarios for the Brazilian integrated electric system using performance indicators that characterize the technical, economic, and environmental features of each scenario. The baseline scenario was created using government plans and relies heavily on large hydropower plants in the Amazon. According to the EPE plan, in 2028, wind power corresponds to only 15% of the total installed capacity. In addition, we developed four alternatives scenarios:

1. Scenario "Wind27": Replaces hydroelectric power plants scheduled for operation in the Amazon after 2020 with wind parks so that by 2028 wind power accounts for 27% of total installed capacity.
2. Scenario "Wind39": Replaces hydroelectric power plants scheduled for operation in the Amazon after 2013 with wind parks so that by 2028 wind power accounts for 39% of the total installed capacity.
3. Scenario "Natural Gas": Replaces hydroelectric power plants scheduled for operation in the Amazon after 2020 with natural gas power plants
4. Scenario "Coal/Oil/Diesel Retirement": Assumes the same conditions detailed in the "Wind39" scenario, but, additionally, all current and future coal, oil and diesel power plants are retired and replaced by natural gas power plants with the same capacity.

To estimate the installed capacity of wind parks needed in the "Wind 27" and "Wind39" scenarios that replace the hydropower in the baseline scenario, we did a first order approximation by multiplying the installed capacity of the new hydropower plants by 0.55 (average hydro capacity factor) and then dividing the result by 0.4 (average capacity factor for wind in Brazil). This approximation overestimated the installed capacity creating excessive wind curtailment in the SDDP simulations. Thus, we adjusted the wind expansion scenarios by reducing wind power capacity parametrically while maintaining similar levels of lost load across the alternative scenarios and the baseline. We followed an equivalent procedure to estimate natural gas capacity in the last scenario, but we multiplied the hydropower capacity in the schedule by 0.6.

We represented the new wind installed capacity in the model by creating groups of 25 fictitious wind parks of 30 MW of installed capacity each. Thus, each group has 750 MW of installed capacity. In order to define the location of each wind park in the group, we applied a lottery with replacement. This lottery is based on a sample of 1,065 wind parks that are under early licensing stage and located in the Northeast and South states (see Figure S3 in the Appendix C). We then created wind energy generation series for each group of wind parks (750 MW) by simulating the energy output from each fictitious power plant individually using the NCEP-CSFR hourly wind speeds during 32 years (1979 -2010). Next, we aggregated the results for the 25 wind parks within each group by month and load block. As a result, each group of 750 MW wind parks contains 96 monthly series of plant capacity factors (32 for each load block), which are inputs to SDDP. The introduction of the NCEP-CSFR capacity factor series to describe the wind variability by load block is the only difference between the government plans and our baseline scenario. SDDP draws a lottery from those monthly series and optimizes the hydrothermal schedule according the wind energy output from the selected series. Because of the system constraints, wind curtailment might occur but should be avoided as it represents a waste of energy. Wind curtailment is one of performance indicators we compared across scenarios.

Table 4-3 describes the evolution of installed capacity by source in the baseline scenario from 2013 to 2028, as well as the modifications implemented in the alternative expansion scenarios. Most of the new thermal power plants are powered by natural gas (92% of the total new capacity in the baseline scenario). Additionally, two new nuclear power plants (Angra 3, which is under construction, and another planned plant) correspond to 6% of the new thermal generation capacity in the baseline. Therefore, coal, diesel, and oil represent a just minor (~2%) share of the new capacity. In addition to the new capacity described in Table 4-3, the "Coal/Oil/Diesel Retirement" scenario includes the replacement of approximately 8 GW of coal, oil, and diesel power plants under operation by cleaner natural gas power plants. We assumed the Coal/Oil/Diesel power plants are replaced by natural gas power plants in the beginning of the simulation (May 2013).

Table 4-3:Additional capacity by year:baseline and alternative scenarios

Year	Baseline				Wind27		Wind39 and Coal/Oil/Diesel Retirement		Natural Gas	
	Non-Amazon Hydro	Amazon Hydro	Thermal	Wind	Amazon Hydro	Additional Wind in relation to the baseline	Amazon Hydro	Additional Wind in relation to the baseline	Amazon Hydro	Additional Natural Gas in relation to the baseline
2013	422	1,203	2925	0	1,203	0	0	1,500	1,203	0
2014	111	2,605	1343	0	2,605	0	0	3,000	2,605	0
2015	0	4,554	1102	3,750	4,554	0	0	6,000	4,554	0
2016	674	4,570	0	3,000	4,570	0	0	6,000	4,570	0
2017	45	3,886	316	1,500	3,886	0	0	4,500	3,886	0
2018	45	4,767	1705	1,500	4,767	0	0	6,000	4,767	0
2019	328	611	0	1,500	611	0	0	750	611	0
2020	1018	945	0	750	0	750	0	750	0	567
2021	290	2,533	0	750	0	3,000	0	3,000	0	1,520
2022	619	2,155	0	750	0	2,250	0	2,250	0	1,293
2023	819	2,419	0	1,500	0	2,250	0	2,250	0	1,451
2024	1292	4,235	0	1,500	0	4,500	0	4,500	0	2,541
2025	347	4,818	1000	2,250	0	5,250	0	5,250	0	2,891
2026	567	2,801	0	2,250	0	3,000	0	3,000	0	1,680
2027	1135	2,326	1300	3,000	0	2,250	0	2,250	0	1,396
2028	948	1,821	10300	2,250	0	2,250	0	2,250	0	1,093
Total	**8,658**	**46,247**	**19,990**	**26,250**	**22,195**	**25,500**	**-**	**53,250**	**22,195**	**14,431**

4.3.4. Performance indicators

We compared the baseline and the alternative scenarios using technical, economic, and environmental performance indicators. Land use and greenhouse gas emissions are the environmental impact metrics of interest for this chapter. Direct land use requirements (excludes transmission lines) for new projects were calculated using the following assumptions:

- Large hydro power reservoirs: sum of the reservoir areas
- Wind: 0.003 MW/km^2 [26].
- Thermal electricity from coal and natural gas: 0.035 MW/km^2 [27]

GHG emissions from hydropower are usually low; however, reservoirs located in tropical forested areas have the potential to emit large quantities of methane, a more powerful GHG gas compared to carbon dioxide[28]. Carbon dioxide (CO_2) and methane (CH_4) emissions from hydropower result from the oxic/anoxic decomposition of the flooded organic matter from different sources within the reservoir (e.g. vegetation and soils) and from outside the reservoir (e.g. sedimentary OM input from the upstream river basin)[10,29,30]. Estimates for eighteen new hydropower plants planned in the Amazon indicate total emissions that vary from 9-21 Tg of CH_4 and 81-310 Tg of CO_2 over a hundred years[12]. Based on the average lower and upper bounds values defined by Faria et al. 2015, we estimated the emissions from eighteen major Amazon reservoirs (Belo Monte, Bem Querer, Cachoeira do Caí, Cachoeira do Caldeirao, Cachoeira dos Patos, Colider, Ferreira Gomes, Jamanxim, Jatobá, Jirau, Marabá, Salto Augusto de Baixo, Santo Antônio, São Luís do Tapajos, São Manoel, Sao Simao Alto, Sinop, and Teles Pires) over the first 15 years of operation that are within the scope of this study.

GHG emissions from thermal plants were calculated using the following emission factors[31]:

- Nuclear: 16 t CO_2e/MWh
- Oil/Diesel: 840 t CO_2e /MWh
- Natural Gas: 470 t CO_2e /MWh
- Biomass: 40 t CO_2e /MWh
- Coal: 1,000 t CO_2e /MWh

Moreover, we compared the alternative scenarios in terms of investment costs for the new power plants and operating costs of the thermal system. Appendix C contains more details about this calculation. The EPE database provides the operation costs for each thermal power plant, which vary from 20 to 1,000 reais per MWh (6 to 285 US dollars per MWh)[16]. We assumed the same operational costs defined by EPE (250 reais/MWh, 70 US$/MWh) for the new natural gas power plants[16].

To evaluate the hydro performance of each alternative, we also compared the energy storage levels in the hydroelectric reservoirs, which is a measure of the system resilience against droughts. This value is calculated using the volume of water stored in each reservoir with storage capacity multiplied by its average production coefficient (MWh/m^3). Further, we used the wind curtailment levels in megawatts as an indicator of the system performance.

4.4 Results and Discussion

4.4.1 Generation output projections

Figure 4-3 describes the optimal generation output for each scenario from May 2013 to December 2028 by load block and fuel type. The coloured areas in Figure 4-3 define the average power output considering 400 simulations of the optimal system operation. In December 2013, wind power represents just 3% of the total generation (5% of the total capacity), while the total renewable generation (including large hydro) accounts for 80% of the total generation.

In the baseline scenario, 46 GW of hydropower plants in the Amazon fulfil most part of the future electricity demand. Wind generation plays a minor role in this scenario and, in 2028 wind power corresponds to only 15% of the total installed capacity (on average, 12% of the total generation in December 2028). Average hydropower output varies by load block indicating that these plants are dispatched to balance the load variability. In contrast, average thermal generation does not vary significantly by load block, and the power plants are dispatched with the same power output within the day ("base load"). The wet-dry season variability explains the peaks and valleys in the hydro and thermal generation. The limitation of water resources during the dry season (April-September) reduces the hydropower generation capacity and more thermal generation is necessary to meet demand. In December 2028, renewables sources (including large hydropower) represent 80% of the total generation. Thus, the baseline results indicate the same level of renewable generation throughout the study horizon.

The major difference between scenario "Wind27" and the baseline is the higher penetration of wind in the system after 2020. In December 2028, wind accounts for 20% of total generation, while the total renewable generation represents 84% of total. Most of the new wind plants are located in the Northeast subsystem where higher wind speeds occur from July to November. These higher wind speeds occur in July/August as the dry season peaks (when hydropower output decreases), thus maintaining thermal generation as base load. However, as the penetration of wind increases to 24% of installed capacity (2025), thermal generation starts to vary significantly by demand block to balance the daily wind variability.

Scenario “Wind39” presents a more aggressive policy towards wind generation. It characterizes an expansion scenario where wind replaces all 46 GW of recently built, under construction, and future hydropower plants in the Amazon. The major difference between the operating profiles in scenario “Wind39” and the baseline is the change in the thermal generation profile. From 2013 to 2018, wind power replaces large power plants in the Amazon like Jirau, Santo Antonio, and Belo Monte and average thermal generation decreases and continues to be dispatched as base load. By 2020, wind account for 28% of total installed capacity, and thermal power plants start being dispatched to meet high and medium demand periods during the low wind speed season (February-June). Between 2020 and 2028, average thermal generation also increases faster compared to the baseline and the “Wind27” scenarios. In December 2028, wind and total renewable generation account, on average, for 29% and 84% of the total electricity generated in the system, respectively. The “Coal/Oil/Diesel Retirement” average dispatch profile is similar to the “Wind39”.

In the last scenario, natural gas power plants (rather than wind) replace the same hydropower plants as in the “Wind27” scenario. Wind capacity in this scenario increases as in the baseline scenario. The lack of significant additional capacity from hydro or wind power plants in this scenario increases the average demand for thermal generation. After 2024, the thermal generation seasonal variability also increases because there is no wind to compensate for the seasonal changes in hydropower output. Furthermore, after 2024, when wind power accounts for 13% of the total installed capacity, the quantity of thermal generation necessary to supply the demand peak (high demand block) increases. In December 2028, total renewables generation corresponds to 75% of the total generation, representing the lowest share across the scenarios.

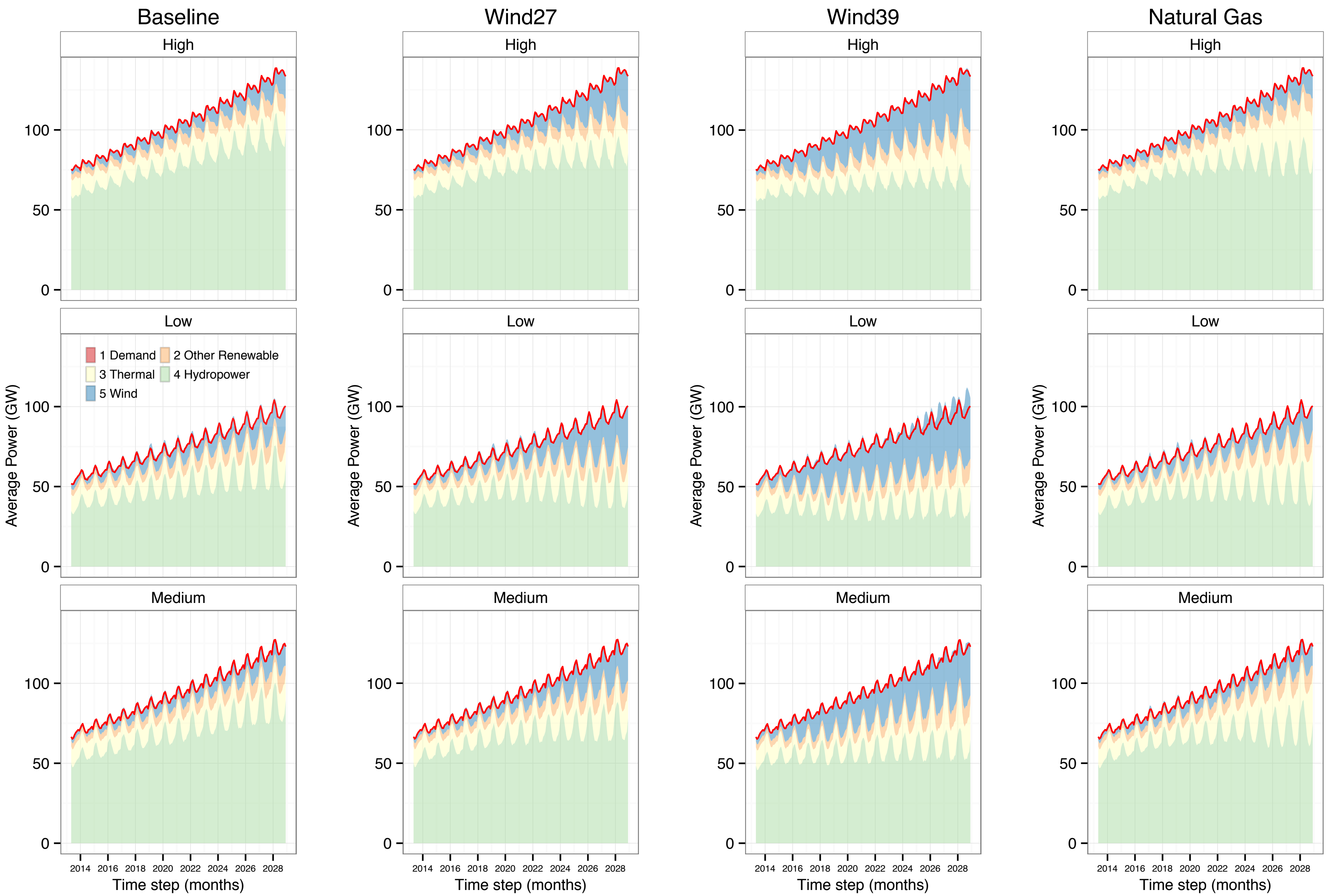

Figure 4-3: Average optimal dispatch for each scenario by source (wind, hydro and thermal power plants) and by load block (high, medium, load).

4.4.2 Energy storage

The quantity of water stored in the reservoirs is a pertinent performance indicator because storage adds resilience against droughts (seasonal variability) and flexibility to meet daily load variability. Figure 4-4 summarizes the energy storage in hydropower reservoirs during the study horizon for each scenario, measured as a percentage of total system storage capacity. For a given month, the energy storage is defined by the multiplication of the volume in each reservoir by its production coefficient taking into account the cascade of hydropower plants.

There are two sorts of variability represented in Figure 4-4. The first source of variability is the seasonal variability, which is illustrated by the average lines. The dry-wet seasons explain the peaks and valleys in the average energy storage profile in Figure 4-4. During the wet season, inflows tend to be above the annual average and the system operator manages the power plants dispatch to fill the storage reservoirs. On the other hand, inflows are below the annual average in the dry season, but the operator can use stored water from the reservoir to increase hydropower production to displace thermal generation.

The second variability is associated to the random inflows process over time. The stochastic process variability is captured in the model by simulating each expansion plan over the study horizon 400 times using different inflows series. As a result, SDDP output contains a distribution of the optimal dispatch under those 400 hundred simulated conditions. The shading defines the 95% confidence interval of the energy storage from the 400 simulated operations and characterizes the storage variance. Note that the wind seasonal and stochastic variability are also incorporated into the model affecting the optimal dispatch and, as a consequence, the storage levels.

By 2028, the seasonal variability of the hydro storage operations increase in the baseline scenario because of the greater seasonal variability integrated into the system by the large planned run-of-river hydropower plants in the Amazon without a proportional increase in storage capacity. These run-of-river designs aim to reduce the reservoir area (and volume) mitigating environmental and social impacts from the reservoir creation, at the cost of no storage capacity. Replacing Amazonian hydro with natural gas plants (Natural Gas scenario) reduces the system's capacity to store water but also reduces the storage variation between peaks and valleys compared to the baseline scenario.

The replacement of Amazonian hydropower by wind power plants has two major consequences to energy storage: 1) a reduction in the average storage variability between low and dry seasons because of the negative correlation between wind and inflows, and 2) an increase in the energy storage variance because of the wind/inflows stochastic features. Both characteristics are clear in the "Wind39" scenario, where the distance between average storage peaks and valleys is lower than the baseline, and the red shade is "thicker" indicating a higher variance compared to the baseline. The higher variance implies that storage capacity variability is higher under a high wind penetration. It happens because now the system operator needs to deal with two sources of electricity that present a random process: hydropower and wind. A system with high hydro and wind penetration is subject to more electricity output variability than a system with high hydro and low wind penetration. A similar but less evident effect occurs in the "Wind27" scenario after 2025 when the wind generation becomes more prominent.

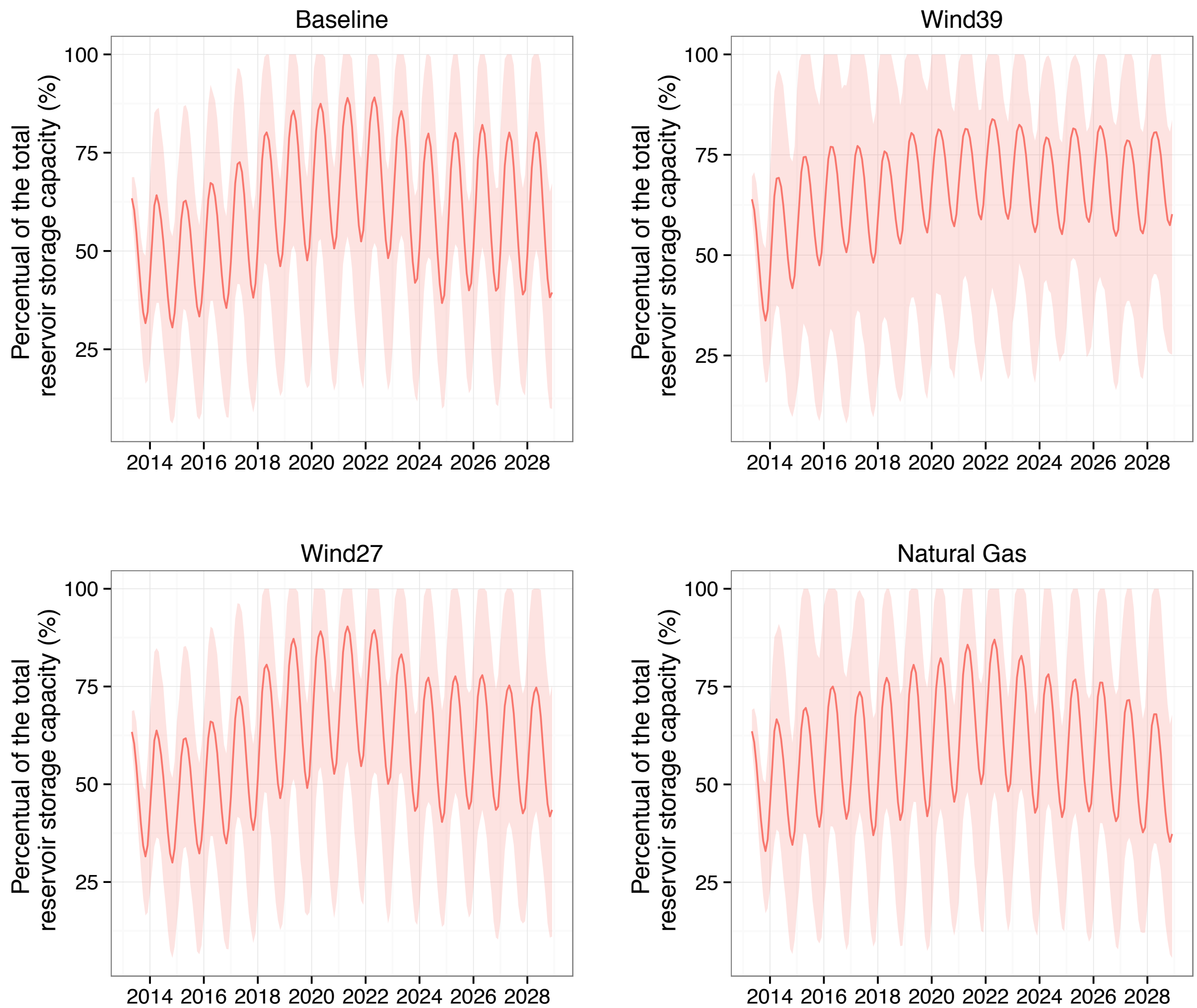

Figure 4-4: Average (lines) storage capacity in hydropower reservoir for each scenario presented in terms of the percentage of the total storage capacity. The shades represent the 95% confidence interval from 400 hundred simulation for each scenario. "Coil/Oil/Diesel Retirement" scenario has the same storage profile as the "wind39" scenario.

4.4.3 Wind curtailment and lost load

The probability of wind curtailment and the probability of lost load are also relevant technical performance indicators of an electric system. To calculate wind curtailment in the optimization, we created an elastic demand variable with a zero cost to "absorb" wind overproduction. In contrast, the lost load is defined by the ratio (in percentages) between the energy (in GWh) that the system was not able to supply and the total demand (in GWh). Figure 4-5 describes the cumulative distribution results for lost load and wind curtailment.

The central characteristic of the lost load distributions is the low probability of significant lack of energy during the study horizon. We developed the alternative scenarios to provide approximately the same reliability levels as those in the baseline scenario, measured by lost load. Figure 4-5 shows that 99% of the time there is no lost load. The highest lost load levels occur only when the system faces a sequence of seasons with low wind speeds and little precipitation in the "Wind39" scenario.

The probability of wasting energy through wind curtailments is higher in the "Wind39" and "Coal/Oil/Diesel Retirement" scenarios because of the higher wind penetration. The simulation results indicate zero wind curtailment for just 60% of the time for those scenarios (Figure 4-5). Wind curtailment typically happens during the period of low loads, high wind speed seasons, and when the reservoirs are already filled and there is no more capacity to store water. The baseline and "Wind27" scenarios have similar empirical distributions for wind curtailment. For those scenarios, the energy curtailed is close to zero during 87% of the time. The lower wind and hydropower penetration in the "Natural Gas" scenario leads to the lower probability of wind curtailment across the expansion scenarios.

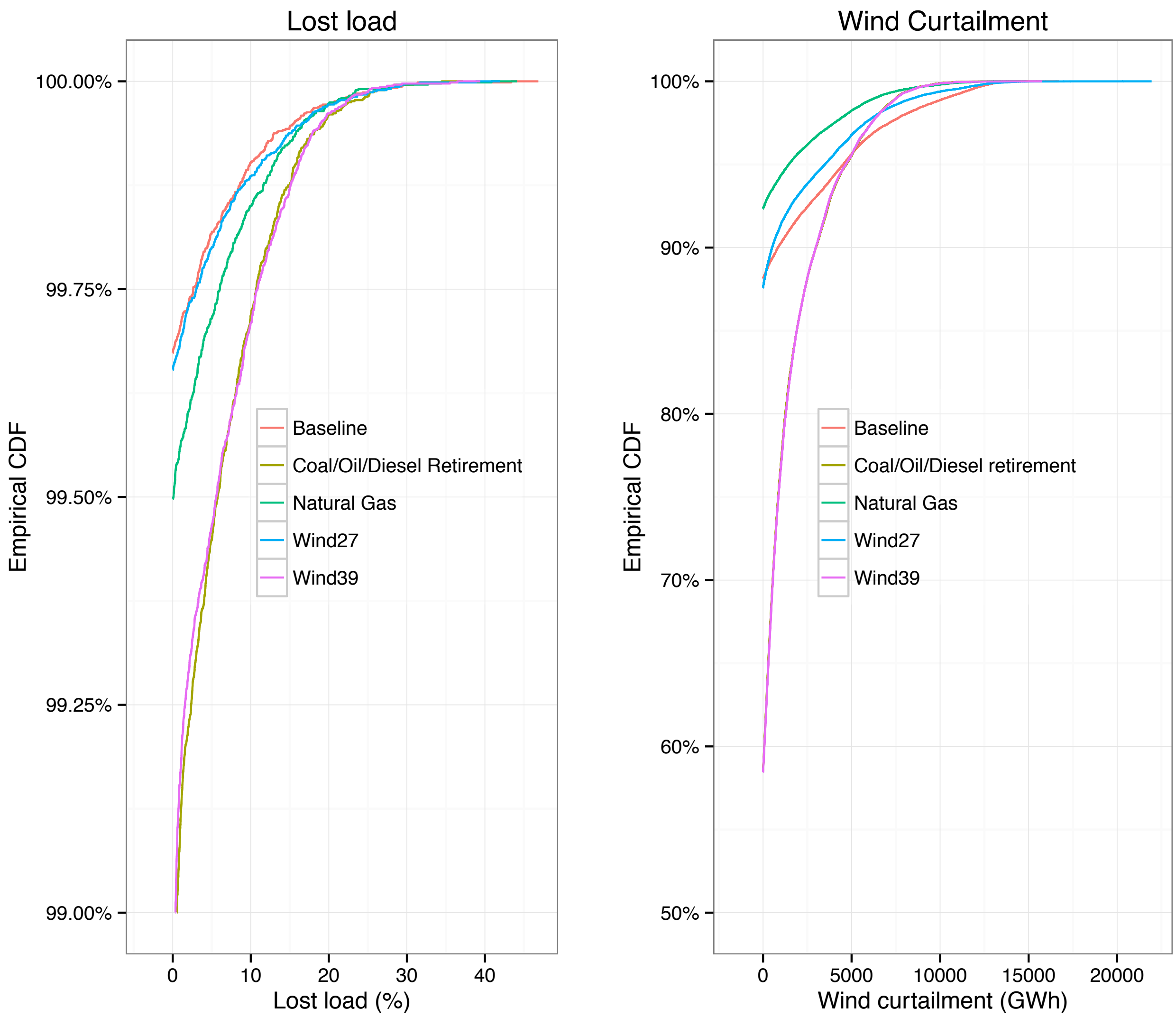

Figure 4-5: Cumulative distribution functions (CDF) of lost load (as a percentage of the total demand) and wind curtailment (in GWh) by scenario and load block.

4.4.4 Costs

We estimated the investment and operational costs of building the new power plants for each scenario. Table 4-4 summarizes the results and describes the capital costs, annual operational and maintenance (O&M) costs, and the annualized costs (Appendix C contains the calculation details for each source). The results indicate that the baseline and "Wind27" scenario have similar construction costs of around 300 billions reais (approximately 86 billion dollars). We estimated the cost of the hydropower plants using the project costs at the capacity auctions held by the Chamber of Electric Energy Trading (CCEE) and, thus, represent pre-construction estimates. However, large hydropower projects have historically suffered cost overruns, estimated at 96% globally[32]. In Brazil, for example, the Belo Monte hydropower plants was expected to cost 18 billions reais (approximately US$ 5 billion), but the actual cost was over 30 billion reais (approximately 9 billion US dollars). Considering a 50% and 96% cost overrun across the Amazonian hydropower projects, the capital costs in the baseline scenario would increase to an actual cost of 360 to 405 billion reais (100 to 115 billion US dollars), respectively. Total construction costs from the "Wind27", "Wind39", and "Coil/Oil/Diesel retirement" scenarios are 13%, 35% and 50% higher, respectively, than the baseline scenario. "Natural Gas" scenario construction costs are 20% cheaper than the baseline. Appendix C (section 8.5) provides details about the construction cost estimates.

Table 4-4: Construction, operation & maintenance (O&M), and annualized costs for each scenario

Source	Installed Capacity (MW)	**Total Construction Costs (million reais)*	*# Annual O&M (million reais)*	*^Annualized costs(million reais)*
Baseline				
Amazon hydro	46,247	108,658	2,173	15,258
Non-Amazon hydropower	8,657	29,995	600	4,212
Thermal	19,991	58,025	14,500	21,487
Wind	26,250	105,000	2,100	14,744
Total	**101,144**	**301,678**	**19,373**	**55,701**
Wind27				
Amazon hydro	22,195	47,132	943	6,618
Non-Amazon hydropower	8,657	29,995	600	4,212
Thermal	19,991	58,025	17,500	24,487
Wind	51,750	207,000	4,140	29,067
Total	**102,592**	**342,152**	**23,183**	**64,384**
Wind39				
Amazon hydro	-	-	-	-
Non-Amazon hydropower	8,657	29,995	600	4,212
Thermal	19,991	58,025	30,000	36,987
Wind	79,500	318,000	6,360	44,654
Total	**108,148**	**406,020**	**36,960**	**85,853**
Natural Gas				
Amazon hydro	22,195	47,132	943	6,618
Non-Amazon hydropower	8,657	29,995	600	4,212
Thermal	34,422	88,334	36,500	47,137
Wind	26,250	105,000	2,100	14,744
Total	**91,523**	**270,461**	**40,143**	**72,711**
Coal/Oil/Diesel retirement				
Amazon hydro	-	-	-	-
Non-Amazon hydropower	8,657	29,995	600	4,212
Thermal	27,707	104,537	30,300	42,888
Wind	79,500	318,000	6,360	44,654
Total	**115,863**	**452,532**	**37,260**	**91,754**

* Total construction costs are calculating considering the currency in reais on May, 2015
# Wind and hydropower power plants annual O&M costs are estimated in 2% of the total construction costs/ Thermal power plants O&M cost are calculated using the average annual O&M costs for the entire system according to the optimal dispatch in 2028. O&M costs for each thermal power plant are defined in the Appendix C and includes fuels costs.
^ We annualized the capital and O&M costs by assuming that the power plants have a lifetime of 50 years, and internal rate of return of 12%, which is equal to calculate: construction costs* 0.12042 + Annual O&M

To compare both construction and O&M costs in the same metric, we annualize the construction cost and sum this result with the annual O&M costs (including fuel costs) resulting in total annualized cost of building and operating the system. The annualized costs (last column in Table 4-4) show that the baseline has the lowest annualized cost (56 billion reais, 15 billion dollars) when hydropower cost overrun is not incorporated in the calculation. Considering a cost overrun from 50% to 96% over the Amazon hydropower plants, the annualized cost would increase from 63 to 70 billion reais (18 to 20 billion dollars). Annualized costs from the "Wind27", "Wind39", "Natural Gas", and "Coil/Oil/Diesel Retirement" scenarios are 15%, 54%, 40%, and 64% more expensive, respectively, than the baseline scenario.

Another indicator that is often applied to define the electric system costs is the operational marginal cost. The marginal cost is a SDDP output defined by the change in the operating cost with respect to an infinitesimal change in the load (reais/MWh). Figure 4-6 presents the simulated marginal cost results for each scenario. The historically low levels of the hydroelectric reservoirs in the beginning of the simulation (initial conditions in 2013) explain the high values of the upper confidence bounds in the first four years of analysis (2013-2016). Marginal costs are higher when more thermal generation is used to replace hydropower.

The marginal cost projections show that the baseline, "Wind27", and "Natural Gas" scenarios have similar marginal costs distributions with a median bellow or equal 250 reais/MWh (70 dollars/MWh) by 2028. The "Natural Gas" marginal costs variance, represented by the quartiles in the box plot, is lower than the baseline by the end of the analysis because of the new natural gas power plants operating costs. We assumed that the marginal cost of operating those new plants is 250 reais/MWh (70 dollars/MWh), which is the value projected by the government in the EPE report files. The new natural gas power plants operating cost is lower than the majority of the older thermal power plants, displacing more expensive thermal and reducing the marginal costs variance in the "Natural Gas" scenario.

In contrast, scenarios "Wind39" and "Coal/Oil/Diesel retirement" present a distinct average marginal cost profile because of the higher wind penetration, especially in the second half of the period of analysis. After 2020, the dispatch of thermal power plants increases during the low wind season, increasing the system marginal costs, especially during high load. By 2028, median marginal cost for both "Wind39" and ""Coal/Oil/Diesel Retirement" are above the 250 reais/MWh (70 dollars/MWh).

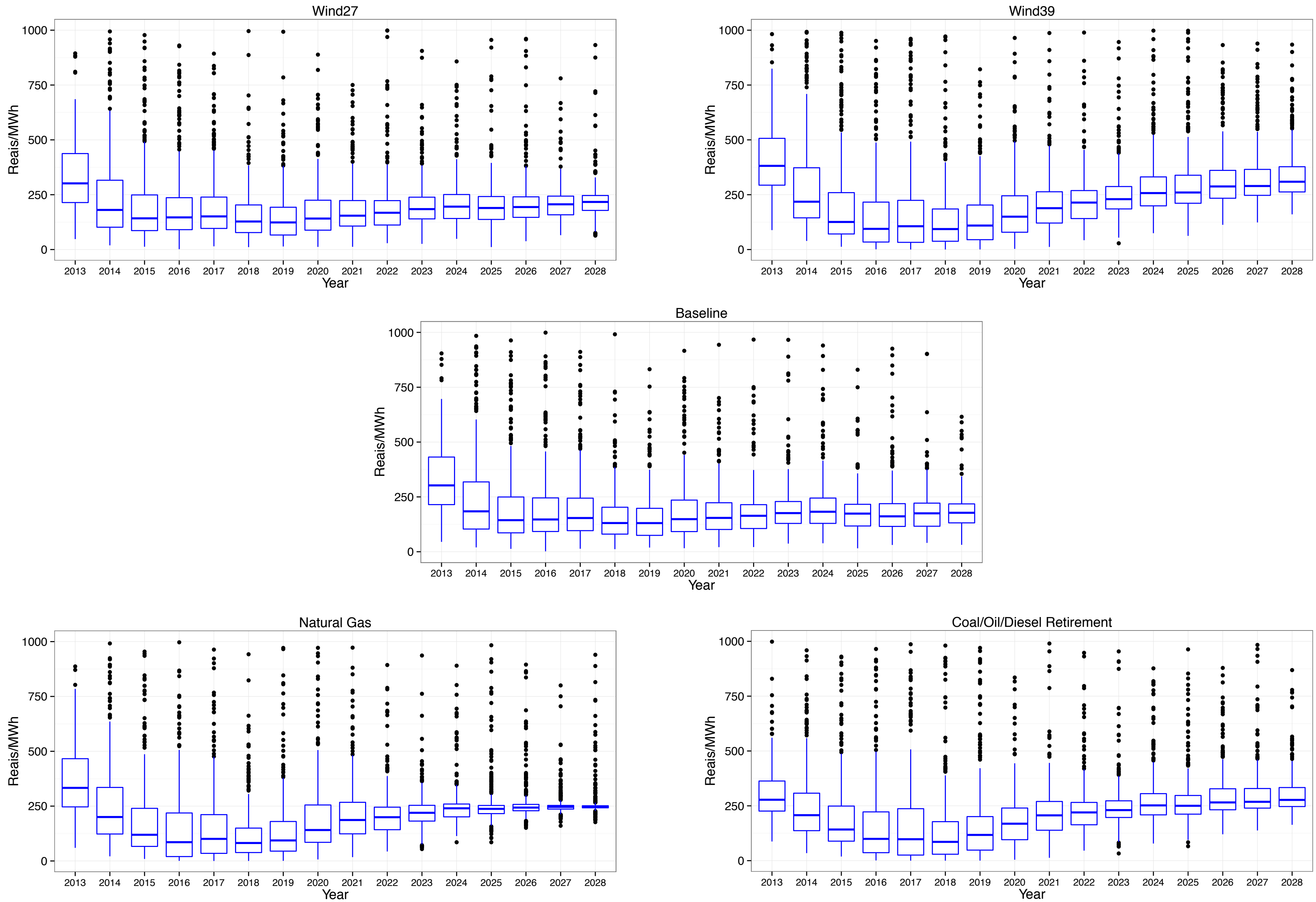

Figure 4-6: Marginal costs (reais/MWh) by year: box-plots from the 400 simulations

4.4.5 Greenhouse gas emissions

In 2012, GHG emissions from thermal electricity generation were estimated in 48.5 Tg of CO_2eq[33]. According to the Intended Nationally Determined Contributions (INDCs) presented to the United Nations Framework Convention on Climate Change (UNFCCC) Conference of the Parties (COP21) in Paris in December 2015[34], Brazil intends to reduce GHG emissions by 43% below 2005 levels by 2030. Brazilian GHG emissions in 2005 are estimated in 210 Tg CO_2eq. Among others, one of the measures to achieve the emissions reduction target is to expand the share of wind, biomass, and solar in the power system to at least 23% by 2030.

Figure 4-7 describes the total direct annual emissions from thermal power plants projected for each scenario (Box-plots). In the first complete year of analysis (2014), average annual direct emissions total 47 Tg of CO_2eq (95% CI: 21-99). In the baseline scenario direct emissions increase to 56 Tg of CO_2eq (95% CI: 26-103) in 2028, when the share of wind, biomass, and solar in the total power capacity is 18% (below the INDC value).

The "Wind27", "Wind39", and "Natural Gas" scenarios also result in increased direct GHG emissions from power generation between 2014 and 2028, and by 2028 such emissions would be higher than in the baseline scenario. In 2028, direct emissions from the "Wind27" scenario total 63 Tg of CO_2eq (95% CI: 30-107) when the share of non-hydro renewables is 30% of the total capacity. In the "Wind39" scenario, the higher renewables share (40% excluding hydro) leads to even higher GHG emissions that are estimated in 83 Tg of CO_2eq (95% CI: 47-118) in 2028. These results indicate that direct GHG emissions from the Brazilian power system will likely increase by 2028 under government plans, even as Amazonia hydro capacity grows. Furthermore, replacing the Amazonian hydropower plants with wind could even increase direct emissions from the power sector. These increases in direct GHG emissions occur because more thermal power generation is necessary to meet demand during dry and low wind speed seasons.

Not surprisingly, the “Natural Gas” scenario results in the highest direct annual GHG emissions (102 Tg of CO_2eq in 2028; 95% CI: 60-159) due to the increase in the thermal capacity. The “Coal/Oil/Diesel retirement” scenario evaluates the impact of replacing dirtier fossil fuel power plants by natural gas assuming the same level of wind penetration of the “Wind39” scenario. The exclusion of the dirtier fossil fuel power plants would reduce emissions in 2028 from 83 Tg of CO_2eq (95% CI: 47-118) in the “Wind39” to 73 Tg of CO_2eq (95% CI: 38-105) in the “Coal/Oil/Diesel Retirement” scenario. Those values do not include methane emissions from natural gas production, processing, and distribution, which have been shown to be significant[35,36].

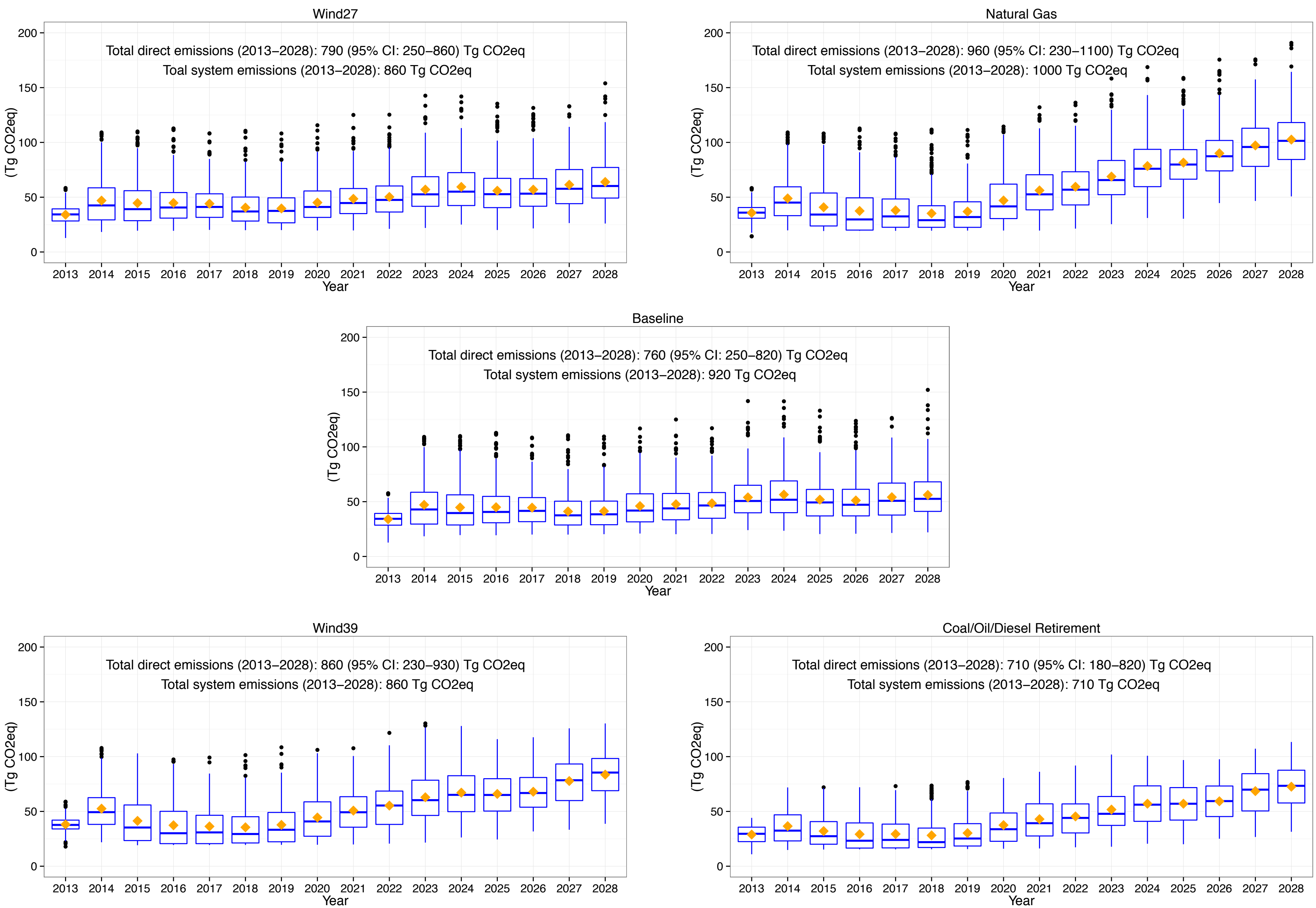

Figure 4-7: Box-plots: annual direct greenhouse gas (GHG) emissions from power generation by scenario (only thermal power plants). Total system emissions include GHG emissions from new Amazon reservoirs plus total direct emissions in the study horizon. The baseline Amazon GHG emissions include the results from the eighteen hydropower plants defined by Faria et al. 2015. "Wind27" and "Natural Gas" scenarios include only the emission from those eighteen hydropower plants build before 2020. Orange diamonds represent the mean

The box-plot results described in Figure 4-7 are limited to direct emissions from the power system that result from combustion of fossil fuels and do not include emissions associated with the degradation of the biomass in new Amazon hydropower reservoirs. Although there is significant uncertainty in estimates of GHG emissions from Amazon reservoir, using the values reported in Faria et al 2015, we estimate that the new major hydropower plants in the Amazon would emit an additional 25 to 300 Tg of CO_2eq into the atmosphere over the first 15 years of operation. While these emissions are still lower than the total direct emissions, they are not insignificant and further demonstrate that emissions associate with power generation could continue to increase by 2028 even if new renewable capacity is added to the system.

In Figure 4-7, we also estimate the expected total system emissions of each scenario across the study horizon considering hydropower emissions from new Amazonian reservoirs. The total system emissions consists in the sum of the annual direct emissions plus an average emissions from new Amazon hydropower plants (top-down and bottom-up models from Faria et al 2015). The results indicate that the "Coal/Oil/Diesel Retirement" scenario (which includes 40% wind) has the lowest GHG emissions (710 Tg of CO_2eq), followed by "Wind27" and "Wind39" (both with 860 Tg of CO_2eq). The baseline scenario results in a total GHG emission of 920 Tg of CO_2eq between 2013 and 2028. As expected, the "Natural Gas" scenario has the highest total system emissions (1000 Tg of CO_2eq).

4.4.6 Land use

Land use requirement for new power plants can serve as a proxy of non-climate related environmental and social impacts of generating capacity expansion. Table 4-5 describes the land use requirements for each scenario. Because of the reservoirs, hydropower plants require the most land. The construction of all hydropower plants in the Amazon would require 9,000 km^2 (to give a special perspective, this is 840 thousand soccer fields), resulting in a total land use requirement of approximately 9,800 km^2 in the baseline when accounting for all sources. The replacement of Amazon hydropower plants planned to be built after 2020 by wind parks and thermal power plants would reduce the total land use requirements by approximately 7,200 and 6,800 km^2, respectively.

Table 4-5: Land use requirements for each scenario by source (km^2)

	Amazon hydropower	Wind	Thermal	**Total**
Baseline	9,000	80	700	**9,780**
Wind27	1,700	160	700	**2,560**
Wind39 and Coal/Oil/Diesel retirement	0	240	700	**940**
Natural Gas	1,700	80	1,200	**2,980**

4.5 Summary, policy implications and limitations

To condense our findings and present an overall comparison between scenarios, we summarize each performance indicator across the scenarios (Table 4-6). The system represented in the starting date (May 2013) has 83% of renewable capacity, but only 12% when excluding large hydropower plants. Except for the “Natural Gas” scenario, Table 4-6 shows that the proportion of renewable capacity in 2028 corresponds to 83% of the total capacity, a similar value compared to the renewables fraction in 2013. However, the share of renewables excluding large hydropower plants varies significantly across the expansion plans scenarios affecting the performance indicators.

Table 4-6: Performance indicators summary

Performance indicators	Baseline	Wind27	Wind39	Natural Gas	Coal/Oil/Diesel Retirement
Share of renewable power in the system in 2028 (%)	82%	82%	82%	74%	82%
Share of renewable power in the system excluding hydropower in 2028 (%)	18%	30%	40%	19%	40%
Annualized costs (billion reais)	56	60	82	68	88
Annualized costs considering 50% hydropower cost overrun (billion reais)	65	63	82	72	88
Highest wind curtailment (ranking)	2	3	1	4	1
Average energy storage (n Dec. 2028, percentage of the total storage capacity)	39%	43%	58%	37%	58%
Total system GHG emissions 2013-2028 (Tg CO2eq)	920	860	860	1,000	710
Land use (km^2)	9,910	2,593	939	3,022	939

This chapter compares key performance indicators for an expanded power system in Brazil relying on different sources, including hydropower plants in the Amazon, wind, or natural gas power plants. Although our scenarios are extreme as we assume complete replacement of one source by another, they have the advantage of underscoring the consequences of choosing one "winner" and its main effect on system operation and costs. The outcomes comparison in Table 4-6 suggests that the optimal energy mix is likely a hybrid of lower impact hydropower plants, wind and natural gas - more similar to scenario "Wind27" than the baseline.

Our results indicate that when the wind share grows from 24% to 28% of total installed capacity, the fossil fuel thermal power plants start cycling more often, thus increasing marginal costs and GHG emissions. In order to achieve significant emissions reduction in the electric sector, Brazil would have to include other alternatives. One option would be replace part of the dirtier fossil fuel power plants by new natural gas or nuclear power plants. The comparison between the "Wind39" and "Coal/Oil/Diesel Retirement" scenarios shows that the replacement of the old coal, oil, and diesel power plants by new natural gas power plants would reduce total system emissions by 28% between 2013 and 2028. Another options would be increasing storage capacity by building low-impact storage reservoirs or rely on batteries and demand response mechanisms to reduce the thermal generation requirements in the peak loads.

Higher wind penetration also increases the supply variability at daily and seasonal scales such that the system operation complexity is greater. The wind variability issue should be more evident when modeling the system using a higher time resolution. We represented the daily variability using three demand blocks, which is a low resolution to represent the fast variations in wind or solar power output. Therefore, future research should increase the resolution and simulate the system using hourly or minute time steps. An important pre-condition for modeling improvements is the access to better wind and solar data. We thus suggest future efforts should focus on creating national database with high-resolution historical and simulated series of the wind speeds and energy output at higher temporal resolution than currently available.

Energy plans should not only focus on selecting one “winner” and only one pathway to follow. Capacity expansion studies should investigate the social, environmental, economic costs and benefits of building and operating new power plants by simulating and assessing several pathways to the future. This chapter underlines that hydroelectric development policy in the Amazon region deserves such a treatment.

References

1. Agencia Nacional de Energia Eletrica - ANNEL (Brazilian Electricity Agency). Electricity Generation Database (Banco De Informacoes De Geração - BIG). (2015).at <http://www.aneel.gov.br/aplicacoes/capacidadebrasil/capacidadebrasil.cfm>
2. MMEEPE Plano Decenal de Expansão de Energia. 1–434 (2014).
3. Fearnside, P. M. Brazil's Samuel Dam: Lessons for Hydroelectric Development Policy and the Environment in Amazonia. Environmental Management 35, 1–19 (2005).
4. Fearnside, P. M. Environmental Impacts of Brazil's Tucurui Dam: Unlearned Lessons for Hydroelectric Development in Amazonia. Environmental Management 27, 377–396 (2001).
5. da Silva Soito, J. O. L. & Freitas, M. A. V. Amazon and the expansion of hydropower in Brazil: Vulnerability, impacts and possibilities for adaptation to global climate change. Renewable and Sustainable Energy Reviews 15, 3165–3177 (2011).
6. Tundisi, J. G., Matsumura-Tundisi, T. & Calijuri, M. C. Limnology and Management of Reservoirs in Brazil. Comparative Reservoir Limnology and Water Quality Management 77, 22–55 (1993).
7. Tundisi, J. G. & Rocha, O. Reservoir management in South America. International Journal of Water Resources Development (1998).
8. Friedl, G. & Wuest, A. A. Disrupting biogeochemical cycles – Consequences of damming. Aquatic Sciences 64, 55–65 (2002).
9. Fearnside, P. M. Greenhouse gas emissions from a hydroelectric reservoir (Brazil Tucurui Dam) and the energy policy implications. Water, Air, & Soil Pollution 133, 69–96 (2002).
10. Rosa, L. P., Santos, dos, M. A., Matvienko, B., Santos, dos, E. O. & Sikar, E. Greenhouse Gas Emissions From Hydroelectric Reservoirs in Tropical Regions. Climatic Change 66, 9–21 (2004).
11. Demarty, M. & Bastien, J. GHG emissions from hydroelectric reservoirs in tropical and equatorial regions: Review of 20 years of CH4 emission measurements. Energy Policy 39, 4197–4206 (2011).
12. de Faria, F. A. M., Jaramillo, P., Sawakuchi, H. O., Richey, J. E. & Barros, N. Estimating greenhouse gas emissions from future Amazonian hydroelectric reservoirs. Environ. Res. Lett. 10, 1–13 (2015).
13. Jackson, S. & Sleigh, A. Resettlement for China's Three Gorges Dam: socio-economic impact and institutional tensions. Communist and Post-Communist Studies 33, 223–241 (2000).
14. Tilt, B., Braun, Y. & He, D. Social impacts of large dam projects: A comparison of international case studies and implications for best practice. Journal of Environmental Management 90, S249–S257 (2009).
15. Tundisi, J. G. Exploração Do Potencial Hidrelétrico Da Amazônia. Estudos Avancados 21, 1–9 (2007).
16. EPE's Newave input files. (2015).at <http://www.epe.gov.br/Estudos/Paginas/Plano%20Decenal%20de%20Energia%20%E2%80%93%20PDE/EPEpublicaarquivosdoprogramaNewavedoPDE2023.aspx?CategoriaID=345>
17. Saha, S. et al. NCEP Climate Forecast System Reanalysis (CFSR) Selected Hourly Time-Series Products, January 1979 to December 2010. (2016).

18. Rose, S. & Apt, J. What can reanalysis data tell us about wind power? Renewable Energy 83, 963–969 (2015).

19. de Energia Eletrica Brazilian Electricity Agency, A. N. Sistema de informações georreferenciadas do setor elétrico - SIGEL. (2015).at <http://sigel.aneel.gov.br/sigel.html>

20. CCEE Resultado consolidado dos leilões de energia. (2015).

21. Pereira, M. & Pinto, L. Multi-stage stochastic optimization applied to energy planning. Mathematical Programming (1991).

22. Gorenstin, B. G., M, C. N., da Costa, J. P. & Pereira, M. Sthocastic optimization of a hydro-thermal system including network constraints. IEEE Transactions Power Systems 1–7 (2004).

23. PSR SDDP Methodology Manual. 1–88 (Power Systems Research (PSR): 2014).

24. EPE Projeção da demanda de energia elétrica. 1–92 (Empresa de Pesquisa Energetica (EPE): 2014).

25. ONS Consolidação da previsão de carga para a elaboração do programa mensal da operação energética . 1–13 (Operador Nacional do Sistema - ONS: 2010).

26. P Denholm, M. H. M. J. A. S. O. N. Land-Use Requirements of Modern Wind Power Plants in the United States. 1–46 (2009).

27. Pasqualetti, M. J. & Miller, B. A. Land requirements for the solar and coal options. Geographical Journal (1984).

28. Barros, N. et al. Carbon emission from hydroelectric reservoirs linked to reservoir age and latitude. Nature Geoscience 4, 593–596 (2011).

29. Abril, G. et al. Carbon dioxide and methane emissions and the carbon budget of a 10-year old tropical reservoir (Petit Saut, French Guiana). Global Biogeochem. Cycles 19, 1–16 (2005).

30. Guérin, F., Abril, G., de Junet, A. & Bonnet, M.-P. Anaerobic decomposition of tropical soils and plant material: Implication for the CO2 and CH4 budget of the Petit Saut Reservoir. Applied Geochemistry 23, 2272–2283 (2008).

31. Moomaw, W. et al. IPCC special report on renewable energy sources and climate change mitigation. (2011).

32. Ansar, A., Flyvbjerg, B., Budzier, A. & Lunn, D. Should we build more large dams? The actual costs of hydropower megaproject development. Energy Policy 69, 43–56 (2014).

33. Ferreira, A. L., Tsai, D. S. & da Cunha, K. B. Análise da evolução das emissões de gee no brasil (1990-2012): setor de energia. 51 (Observatório do Clima: 2014).

34. Brazil, F. R. O. Federative Republic of Brazil Intended Nationally Determined Contribution . 1–10 (Fefderative Republic of Brazil: 2015).

35. Pétron, G. et al. Hydrocarbon emissions characterization in the Colorado Front Range: A pilot study. J. Geophys. Res. 117, n/a–n/a (2012).

36. Brandt, A. R., Heath, G. A., Kort, E. A., O'sullivan, F. & Pétron, G. Methane leaks from North American natural gas systems. Science (2014).

5. CONCLUSIONS AND POLICY RECCOMENDATIONS

The Brazilian government has proposed a significant expansion of hydropower plants in the Amazon in order to fulfill future electricity demand. The size of the investments (30 to 60 billion dollars by 2028) and the necessary area to build the reservoirs (9,000 km^2) illustrate the magnitude of the Amazon hydropower development policy. However, it is not clear that building hydropower plants in the middle of the biggest tropical forest in the Earth is the most cost-effective alternative to meet the majority of future electricity requirements in Brazil. Although the construction of large hydropower plants has significant benefits, including the generation of relatively cheap electricity and job creation, there are also several social (e.g. people resettlement), economic (e.g., loss of Agricultural GDP) and environmental costs (e.g. loss of fauna and flora, GHG emissions).

Despite the extensive scientific literature about hydropower impacts, most of the studies are qualitative and there is a lack of quantitative assessment of the social, economic and environmental hydropower impacts, especially in developing countries. In this dissertation, I identified three major issues relative to hydropower development in the Brazilian Amazon and employed quantitative methods for policy analysis to advance the knowledge about those issues and support informed decision.

In Chapter 2, I examined the GHG emissions from recently build and planned hydropower reservoirs in the Amazon. I helped to expand the literature by proposing the first predictive model for estimating GHG emissions from hydropower reservoirs based on a Monte Carlo simulation structure. Although the uncertainty on GHG emissions from hydropower reservoirs is still high, through this work, I showed that it is possible to identify hydropower plants with a high probability to emit significant levels of GHG emissions supporting future project selection.

In Chapter 3, I investigated the relationship between hydropower development and local socio-economic indicators using 56 Brazilian hydropower plants built over 1991-2010 applying econometric methods. I found that counties that built hydropower plants had greater GDP and tax revenues during the first years, but those positive economic effects lasts less than 15 years. I also found that that social indicators in counties that built hydropower did not statistically differ from those in the control counties. I showed, in particular, that the agricultural sector is negatively affected by hydropower development, especially by large dams. This is a critical contribution of the chapter given that most of the regions affected by dams are rural areas, and the negative impact on the agricultural sector significantly attenuates the positive economic impacts observed on the local industry and services sectors.

In Chapter 4, I simulated the operations of the Brazilian electric system operation under five capacity expansion scenarios. I found that wind energy has the potential to replace at least part of future hydropower plants in the Amazon at the same cost levels, bringing additional advantages to the electric system (e.g. increase average energy storage) and reducing land use requirements. However, I show that there is a limit for the wind expansion that varies from 24% to 28%. After this range, fossil fuel thermal power plants start cycling more often, increasing marginal costs and GHG emissions. My findings emphasize the need of including alternative scenarios in future capacity expansion plans.

Finally, this Dissertation underscores that there is a lack of understanding about the full costs and benefits of developing large hydropower plants in the Amazon. Analyzes of the costs and benefits of hydropower projects in Brazil has been restricted to the direct costs (e.g., construction costs) and direct benefits (e.g. electricity produced). This Dissertation stresses the need for accounting for indirect costs, such as the negative effect on the Agricultural GDP caused by large dams (Chapter 3). There is a lack of methods to assess and quantify the loss of ecosystem products and ecosystem services caused by hydropower plants. Scientist and engineers should fulfill this knowledge gap. My dissertation presents three examples on how quantitative methods for policy analysis (Monte Carlo simulation, econometrics, and optimization) can help to fulfill this gap. While the work in this thesis resulted in new quantitative information about the trade-offs associated with the expansion of the Brazilian hydropower system, there are still several unanswered questions about the impacts of new hydropower development. For instance, does the migration of people looking for new opportunities increase deforestation levels around hydropower projects? What are the impacts of climate change on precipitation patterns and their consequences on inflows and energy production? These unanswered questions should serve as motivation for future research that supports the design and operation of robust electricity systems under climate constraints.

6. APPENDIX A: CHAPTER 2

6.1 Model Details

This document includes details about the data and methods described in Chapter 2, as well as complementary results and discussion.

Figure S1 presents a representation of the main processes that lead to greenhouse gases (GHG) emissions. The figure describes the major sources of organic matter (OM) in the reservoir, as well as the production, consumption, and emissions of carbon dioxide (CO_2) and (CH_4) to the atmosphere.

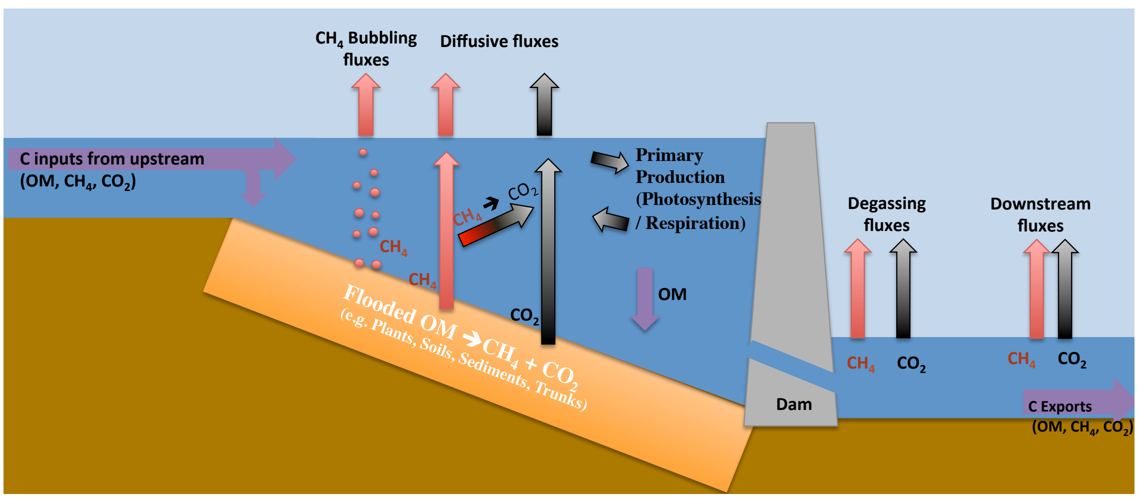

Figure S1: Scheme of GHG production (including OM sources), consumption and emissions to the atmosphere.

CO_2 and CH_4 production in tropical reservoirs results from the oxic/anoxic decomposition of OM from many sources, such as the flooded vegetation and soil, OM allochthonous (sedimentary) input from upstream, and macrophytes and algae produced in the reservoirs (Abril et al. 2005; Demarty & Bastien 2011; Guérin et al. 2008). The main pathways of GHG emissions to the atmosphere include ebbulitive fluxes, diffusive fluxes from the water surface of the reservoir, degassing right after the dam outlets structures (e.g. turbines, spillways), and fluxes through the downstream river.

Two temporal stages characterize the carbon (C) emissions from reservoirs. During the first stage, decomposition of easily decomposable biomass (like soil micro fauna and green parts of the vegetation) in the flooded area drives a sharp increase of emissions during the first few years. During the second phase, emissions tend to be reduced as the system reaches a steady state (St. Louis et al. 2000; Galy-Lacaux et al. 1999; Rosa et al. 2004; Demarty & Bastien 2011). The steady state results from shifts in the balance between the decomposition of flooded biomass at the reservoir bottom and CO_2 uptake by the phytoplankton in the epilimnion (the uppermost layer in a stratified reservoir)(Abril et al. 2005). Data from tropical reservoirs suggest that steady state conditions occur a few years (3 to 10 years) after reservoir creation (flooding), and that most of the emissions in this second stage continue to be derived from the flooded C pool in the reservoir area (Abril et al. 2005; Demarty & Bastien 2011; Guérin et al. 2008; Delmas, Galy-Lacaux & Richard 2001). For example, flooded biomass was still available in Petit Saut and Balbina 10 and 23 years after flooding, respectively (Abril et al. 2012).

We developed two independent approaches based on a Monte Carlo simulation structure to estimate CO_2 and CH_4 emissions in Amazonian reservoirs. The top-down (TD) approach relies on flux data measured in tropical reservoirs and rivers in South American equatorial forests. In the TD approach we modeled reservoir emissions, degassing emissions, downstream emissions, and natural river emissions (before flooding). The bottom-up (BU) approach is based on the potential emissions derived from the degradation of the removed and flooded OM in the reservoir areas, considering GHG production rates and CH_4 oxidation in the water column.

6.1.1 Top-down approach

We divided the GHG emissions from reservoir in two systems: the river system (before flooding) and the reservoir system (after flooding). The river system represents the environment before the reservoir construction, which is related to the natural conditions within the model boundaries. Rivers and wetlands in the Amazon are natural C sources as they transport, respire, and outgas C originating from OM from upland and flooded forests (Richey et al. 2002). The reservoir system characterizes the environment after the dam construction. The beginning of the reservoir in the upstream side defines the upper boundary of each system, which extends a 40km river distance downstream the dam. The differences in the fluxes to the atmosphere between the reservoir system and the river system define the reservoir net GHG emissions (NRE) (Equation S1).

$$NRE = Reservoir + Degassing + Downstream - Natural \qquad (S1)$$

Where**, Reservoir** represents the total annual surface emissions from the reservoir, defined by the annual CO_2 (Res_{CO2}) and CH_4 (Res_{CH4}) reservoir emissions. **Degassing** represents the total annual outlet degassing emissions and includes emissions of CO_2 (Deg_{CO2}) and CH_4 (Deg_{CH4}). **Downstream** represents the total annual emissions downstream the reservoir and includes emissions of CO_2 ($Down_{CO2}$) and CH_4 ($Down_{CH4}$). **Natural** represents the total annual emissions from the river in its natural state and also includes CO_2 (Nat_{CO2}) and CH_4 (Nat_{CH4}).

The GHG flux (daily flux mass per unit of area) multiplied by the surface area and number of days in the year defines the total annual emissions for each pathway (Res, Deg, Down and Nat) according to the equations S2 to S5.

$Reservoir = Res_{CO2} + Res_{CH4} = [(A_{RES} \times res_{CO2}) + (A_{RES} \times res_{CH4})] \times 365$ (S2)

$Degassing = Deg_{CO2} + Deg_{CH4} = [(A_{RES} \times deg_{CO2}) + (A_{RES} \times deg_{CH4})] \times 365$ (S3)

$Downstream = Down_{CO2} + Down_{CH4} = [A_{RIVERDOWN} \times down_{CO2}) + (A_{RIVERDOWN} \times down_{CH4})] \times 365$ (S4)

$Natural = Nat_{CO2} + Nat_{CH4} = [(A_{RIVER} \times nat_{CO2}) + (A_{RIVER} \times nat_{CH4})] \times 365$ (S5)

Where, $\mathbf{res_{CO2}}$ and $\mathbf{res_{CH4}}$ are the CO_2 and CH_4 reservoir emission fluxes, respectively. $\mathbf{deg_{CO2}}$ and $\mathbf{deg_{CH4}}$ are the CO_2 and CH_4 outlet degassing emission fluxes, respectively. $\mathbf{down_{CO2}}$ and $\mathbf{down_{CH4}}$ are the CO_2 and CH_4 downstream emission fluxes, respectively. $\mathbf{nat_{CO2}}$ and $\mathbf{nat_{CH4}}$ are the CO_2 and CH_4 natural river emission fluxes, respectively. All these fluxes are derived from empirical data, as discussed later in this document. $\mathbf{A_{RES}}$ is the reservoir area. $\mathbf{A_{RIVERDOWN}}$ is the river surface area downstream the dam, where the dam defines the upper limit, while a 40km distance downstream the dam defines the lower limit. $\mathbf{A_{RIVER}}$ is the river surface area within the model boundaries. We presented the fluxes in milligrams of the GHG gas per square meter per day (, e.g. mg CH_4 m^{-2} day^{-2}) and the surface areas in square kilometers. Thus, we multiplied the surface areas by 10^6 to obtain the annual emissions in grams. To convert the values from grams of the GHG to grams of C, we multiplied the results by the ratio of the atomic mass: 12/44 and 12/16 for CO_2 and CH_4, respectively.

Instead of applying conventional averages or ranges, we calculated the net reservoir emissions (*NRE*) using a Monte Carlo Simulation structure. Under this structure, the fluxes (res_{CO2}, res_{CH4}, deg_{CO2}, deg_{CH4}, $dowm_{CO2}$, $down_{CH4}$, nat_{CO2} and nat_{CH4}) are sampled from specific probability distributions; each sample set corresponds to one input scenario. Then, this input scenario is the basis to calculate the *NRE* and obtain one output scenario.

Each simulation corresponds to an annual steady state scenario *NRE*. Based on the emissions profile during the first ten years after flooding in Petit Saut (Abril et al. 2005), we modeled the first pulse of emissions by applying a multiplier factor to the annual steady state scenario. The multiplier factors for the reservoir system in the first five years are: three times the steady state emissions for the first three years, and two times the steady state emissions for the fourth and fifth years. After the fifth year, the annual emissions are assumed to be constant. Thus, the total net reservoir emissions in a hundred years are defined by the sum of the emissions in the first pulse (first five years) plus the steady state emissions during the next 95 years.

We repeat the whole process 10,000 times, producing 10,000 independent scenarios with corresponding output values. Therefore, the model results directly relate to the field data measurements compiled in this chapter and the adjusted probability distributions (See Section Data Analysis). One advantage of this method is the possibility to treat the uncertain derived from the flux data variability in an explicit and transparent form, through the application of standard statistical techniques (Morgan 1990).

We developed the simulation code using the open source language and environment for statistical computing and graphics "R" and its packages *ggplot2* (Wickham 2009). The R code is available upon request.

To convert all fluxes into CO_2 equivalents (CO_2eq), we used the 100-year and 20-year global CH_4 warming potential (GWP), which the IPCC reported as 34 and 86, respectively, in the 5th Climate Assessment Report (IPCC 2013).

We did not include pre-flooding terrestrial and post-flooding C burial fluxes in our estimates. Previous research suggests that mature forests are C neutral, as the gross production and community respiration ratio approaches 1 in old forests. In other words, emissions from respiration balance the uptake from photosynthesis (Odum 1969). Recent studies based on long-term monitoring have re-opened the discussion by demonstrating that old forests are not in balance. In the case of the Amazon forest, the average change in the above-the-ground stock from 0.36 to 0.62 metric tons of C per hectare per year (36 to 62 g **C** $m^{-2}yr^{-1}$) (Malhi 2010). However, changes in the soil C stocks are not included in these budgets (Sayer et al. 2011), because the knowledge about Amazon soils C dynamics is limited. Based on this uncertainty and low order of magnitude of potential sinks and emissions in mature forests in comparison to water related emissions, we did not model the behavior of the forests contained within the reservoir area before the impoundment.

Similarly, we did not include C burial in our estimates. Part of the organic C contained in the reservoir sediments can escape mineralization and accumulate in the reservoirs, resulting in a C sequestration within the reservoirs (Mendonça et al. 2012). It is very difficult to estimate the burial rates because of unknown and unconstrained factors that drive this process and the only theoretical model suggests that burial rates could vary from 1,000 to 4,000 g CO_2eq m^{-2} yr^{-1} in Amazon reservoirs (Mendonça et al. 2012). However, this estimate is based on long residence time lakes, which do not resemble the reservoir conditions of the new reservoirs in our database. Thus, we did not include the C burial in the balance because of lack of empirical data, and the high uncertainty about this process.

The TD approach has two sub models that account for limnological differences based on the stratification level of the reservoirs.

6.1.1.1 Reservoirs with high residence time and periods of stratification (TD - High RT)

The first model relies on fluxes from the classical "old" reservoirs of Tucuruí, Petit Saut, Samuel, and Balbina, which have average residence times (RT) of 50, 150, 115 and 350 days, respectively, and present long periods of stratification throughout the year (Abril et al. 2005;

Kemenes, Forsberg & Melack 2007; Guérin et al. 2006; Fearnside 2002). The section "Data Analysis" in this document includes a complete literature review of available flux data for the main GHG pathways in existing Amazonian hydropower reservoirs, which are the basis of the probability distributions that represent each flux component in the C balance of reservoirs in this model.

While the literature includes 141 estimates of CO_2 emissions and 89 estimates of CH_4 emissions in reservoirs across the world, these data showed that reservoirs located in the Amazon have significantly higher GHG emissions when compared to other non-Amazonian tropical and temperate reservoirs (Barros et al. 2011). For this reason, our statistical model (reservoir system) for reservoirs with high residence times only relies on data from four reservoirs built on tropical forest ecosystems in South America: Balbina, Petit Saut, Samuel, and Tucuruí.

6.1.1.2 Low residence time reservoirs (TD - Low RT)

The GHG flux literature about low RT reservoirs is scarce when compared to high RT reservoirs. The only available long-term measurements in low RT reservoirs were made in Lake Wohlen, a 2-day RT reservoir in Switzerland, where total CH_4 emission was on average greater than 150 mg CH_4 m^{-2} d^{-1} (DelSontro et al. 2010). In the case of Amazonian reservoirs, there is a first order estimate for the Santo Antônio dam, located at Madeira River. The estimate is based on data from just one campaign that took place five months after the reservoir started to be filled (Fearnside 2015b). The existing literature, however, provides important information that can be used to model the uncertainty in low RT reservoirs in the Amazon.

Low RT reservoirs have different fluxes to the atmosphere compared to high RT reservoirs, because the main reservoir channel has well-mixed water columns (oxic conditions) and limnological characteristics similar to river zones (StrašKraba 1973; Straškraba, Tundisi & Duncan 1993). In contrast to those of the high RT reservoirs, the main channels of low RT reservoirs do not stratify (see Section "Density Froude Number and Residence Time"). However, the bays and tributary zones of the low RT reservoirs are expected to stratify due to their lower flows in these areas. As a consequence, bays and tributary zones have higher CH_4 emissions than the main channel. The measurements in the Santo Antônio reservoir confirm this spatial variability (Fearnside 2015b). Thus, we divided the emissions estimates for low RT reservoirs in two different zones: main channel ($A_{CHANNEL}$)[1] and bays/tributaries (A_{BAYS}).

Because there is limited empirical data for low RT reservoirs, our model uses natural flux data as a proxy for low RT reservoirs (main channel fluxes). This substitution is valid because, first, prior research reports that GHG emissions are more strongly correlated to water column characteristics than flooded substrates (Duchemin et al. 2000; Pacheco et al. 2015). Second, we calculated the Densimetric Froude Number and RT for each reservoir under different flow scenarios. The high F-number and the low RT confirm that the main channel of these reservoirs resemble river conditions (StrašKraba 1973; Straškraba, Tundisi & Duncan 1993). Finally, data from the Santo Antônio reservoir also supports the assumption that natural river fluxes are good proxies for main channel emissions from low RT reservoir. Fearnside's (2015) data on fluxes from the Santo Antônio main channel (3 mg CH_4 $m^{-2}d^{-1}$) have the same order of magnitude as emissions average (10 mg CH_4 $m^{-2}d^{-1}$) from white water Amazonian rivers (See Table 2 in the main manuscript). Therefore, the probability distributions adopted for the main channel emissions fluxes in this model rely on data from large natural rivers in the Amazon, which are

[1] $A_{CHANNEL} = A_{RES} - A_{BAYS}$

classified according to water type. These probability distributions are the same ones that we used to estimate the emissions from the natural river in our TD-high RT model (nat_{CO2} and nat_{CH4}).

Note, however, that the adoption of natural river flux data to represent the emissions from the reservoir main channel is not the same of assuming low range of fluxes. Natural flux data from Amazonian river shows that CH_4 emissions rates can reach more than 600 mg CH_4 $m^{-2}d^{-1}$ (Sawakuchi et al. 2014). Natural river emissions have average, maximum, and minimum values with the same order of magnitude compared to surface reservoir emissions in the “old” Amazon reservoirs (See Table 3 in the main document). The main difference between river and reservoir fluxes in the Amazon is shape of the distributions. The natural river flux distributions are more skewed to the right (longer right tail). See section Data Analysis for details.

With respect to stratified bays and tributaries zones, we assumed that fluxes in these areas resemble the fluxes from stratified reservoirs (res_{CO2} and res_{CH4}). Data from the Santo Antônio reservoir also support this assumption (Fearnside 2015b). The reported flux for the tributary zones (340 mg CH_4 $m^{-2}d^{-1}$) is within the range adopted for res_{CH4} in the first year of operation (0 – 630 mg CH_4 $m^{-2}d^{-1}$).

Compared to those of high RT reservoirs, degassing and downstream emissions in low RT reservoirs are expected to be lower as the short RT and well-mixed conditions considerably reduce CH_4 concentrations in the water (DelSontro et al. 2010). Based on a single measurement of the CH_4 concentration in the air, a first order estimate from degassing and downstream emissions from the Santo Antônio dam shows that these pathways correspond to 35% of the total emissions in the first year of operation. Even though the measure was made at the peak of the emission (first two years), this value is lower when compared to the degassing estimates in the high RT reservoirs of Balbina (53% at age 18 (Kemenes, Forsberg & Melack 2007)), Petit Saut

(77% and 60% at age 9 and 10, respectively) and Tucuruí (88% at age 18) (Fearnside 2002). This result is expected because degasing/downstream emissions are positively correlated with CH_4 concentration in the reservoir (Abril et al. 2005; Guérin et al. 2006), which is then positively correlated with the RT (Galy-Lacaux et al. 1999; Delmas, Galy-Lacaux & Richard 2001).

Because only one degassing/downstream estimate is available for low RT reservoirs, we treated this variable parametrically in the TD-Low RT model. In other words, we did not fit a probability distribution for the degassing and downstream pathways. Instead, we treated the degassing/downstream fluxes as a single value based on the CH_4 value reported for the Santo Antônio reservoir ($deg/down_{CH4}$). Because of the high uncertainty (Fearnside 2015b), we present the results with and without the degassing/downstream estimates.

Based on the previously described assumptions, Equations S6 to S11 defines the mathematical formulation of the NRE for low RT reservoirs.

$$NRE_{lowRT} = \mathit{Reservoir} + \mathit{Degassing/Downstream} - \mathit{Natural} \quad (S6)$$

$$\mathit{Reservoir} = \mathit{Emissions\ from\ the\ main\ channel} + \mathit{Emissions\ from\ bays/tributaries} \quad (S7)$$

$$\mathit{Emissions\ from\ main\ channel} = [(A_{channel} \times nat_{CO2}) + (A_{channel} \times nat_{CH4})] \times 365 \quad (S8)$$

$$\mathit{Emissions\ from\ bays/tributaries} = [(A_{channel} \times res_{CO2}) + (A_{channel} \times res_{CH4})] \times 365 \quad (S9)$$

$$\mathit{Degassing/Downstream} = (A_{RES} \times deg/down_{CH4}) \times 365 \quad (S10)$$

$$\mathit{Natural} = [(A_{RIVERUP} \times res_{CO2}) + (A_{RIVERUP} \times res_{CH4})] \times 365 \quad (S11)$$

Where $A_{RIVERUP}$ is the natural surface of the river, delimited by the beginning of the reservoir and the dam, and A_{RES} is the reservoir area. $Deg/down_{CH4}$ corresponds to the degassing/downstream flux based on Santo Antônio reservoir. We presented the fluxes in milligrams of the GHG gas per square meter per day (, e.g. mg CH_4 m^{-2} day^{-2}) and the surface areas in square kilometers.

We applied the same Monte Carlo simulation structure described to the high RT model to estimate the total emissions in a 100-years.

6.1.1.3 Densimetric Froude number and residence time

As previously described, we applied the TD models for new reservoirs located in the Brazilian Amazon. We selected 18 projects for model application from the Brazilian Energy Plans (MME EPE 2013; MME EPE 2014). To select the TD model that better represents each reservoir (high or low RT), we performed an analysis of the Densimetric Froude number and the RT. The Densimetric Froude, F, provides a measure of the success with which the horizontal flow can shift the thermal structure of the reservoir from that of its gravitational static-equilibrium state (EPA 1969; Straškraba, Tundisi & Duncan 1993; StrašKraba 1973). The F-number is representative of the main channel of the reservoirs. F-numbers greater than $1/\pi$ indicate that the main channel will not stratify and will behave like river zones. F-numbers around $1/\pi$ are representative of weakly stratified conditions. Reservoirs stratify when the F-number is lower than $1/\pi$ (EPA 1969). The F-number is defined by equation S12.

$$F = 0.32\ (L/D)*(Q/V) \qquad \text{(S12)}$$

Where, L is the reservoir length (km), D is the average depth (m), Q is the volumetric discharge calculated using the mean flow (m^3/s), and V is the reservoir volume (hm^3).

The RT is also considered a reference value for reservoir stratification. Typical lake stratification occurs in reservoirs with high RT (>100 days) (StrašKraba 1973; Straškraba, Tundisi & Duncan 1993). Reservoirs with low RT (<10 days), on the other hand, have a completely mixed water column, with a homogenous flow rate and temperature distribution (StrašKraba 1973; Straškraba, Tundisi & Duncan 1993). Equation S13 defines RT.

$$RT = V/ Q \quad (S13)$$

Where, RT is the residence time (seconds), V is the reservoir volume (m^3) and Q is the volumetric discharge calculated using the flow (m^3/s) in the period of analysis. To obtain the values in days, we divided equation S13 by the number of seconds in a day (60 x 60 x 24).

We calculated the RT and F-number for two monthly flow conditions using the historical monthly natural flows time series of each reservoir in our database: average flow scenario and an drought scenario defined as the flow equivalent to the 95% exceedance percentile in a flow duration curve ($Q_{95\%}$). Tables S1 and S2 describe the flow conditions for each reservoir in this study, while Tables S3-S6 described the densimetric Froude number and RT computations.

For the average flow scenario, Cachoeira do Caí and Jamanxim resulted in F-numbers lower than $1/\pi$ during the driest months (August to October) indicating that these reservoirs will stratify during this period. The RT is also high in the dry season and reaches average of 230 days in Cachoeira do Caí and 100 days in Jamanxim in the driest months (August to October). The Sinop reservoir also presents weak stratification conditions and high RT (~60 days) during the dry season (July to October). In the case of the $Q_{95\%}$, the reservoirs of Cachoeira dos Patos and Ferreira Gomes also resulted in Froude numbers lower than $1/\pi$. The RT in this dry scenario is low in Ferreira Gomes (~15 days), but high in Cachoeira dos Patos (~200 days). The other reservoirs have high F-numbers and low RT throughout the year. Based on the characteristics of the reservoir operation, the RT and propensity to stratify, we suggest that the high RT model is representative of Cachoeira dos Patos, Cachoeira do Caí, Sinop, and Jamanxim reservoirs and the low RT model better represents the others reservoirs.

Table S1 – Average Reservoir Flows (m^3/s)

Project	Jan	Feb	Mar	Apr	May	Jun	Jul	Aug	Sep	Oct	Nov	Dec
Belo Monte	7797	12753	17954	19816	15698	7117	2883	1562	1065	1116	1880	3748
Bem Querer	1064	973	880	1409	3474	6216	7689	5984	3461	2024	1575	1207
Cachoeira do Caí	2328	3646	4878	4789	3202	1319	456	173	128	262	614	1486
Cachoeira do Caldeirão	570	921	1288	1635	1718	1528	1119	826	532	400	295	332
Cachoeira dos Patos	1593	2494	3337	3276	2190	902	312	118	88	180	420	1016
Colíder	1382	1676	1827	1345	856	642	550	471	444	516	654	960
Ferreira Gomes	513	977	1500	1854	1993	1591	1177	782	456	277	202	234
Jamanxim	1639	2567	3434	3371	2254	929	321	122	90	185	432	1046
Jatobá	13260	17437	20984	20869	14456	8430	5153	3782	3410	3646	5278	8375
Jirau	24337	29302	33562	29977	22943	16297	10987	7218	5902	7070	10641	16874
Marabá	14521	19340	22331	21946	13954	6647	3906	2768	2192	2556	4299	8483
Salto Augusto de Baixo	4774	6244	8109	7252	4839	3405	2456	2200	2180	2204	2876	3877
Santo Antônio	24742	29789	34119	30475	23324	16568	11170	7338	6000	7187	10818	17154
São Luís do Tapajos	15186	20885	25860	25647	17405	9200	4904	3191	2759	3147	5192	9299
São Manoel	3791	4164	4286	3065	2084	1425	1045	797	723	1047	1606	2708
São Simão Alto	4864	6378	8295	7510	5001	3479	2488	2215	2191	2217	2894	3914
Sinop	1529	1566	1565	1105	814	639	522	440	415	531	776	1218
Teles Pires	3441	4560	5281	3667	2066	1302	1010	790	732	904	1237	2111

Table S2 – Flow equivalent to the 95% exceedance percentile in a flow duration curve (m^3/s)

Project	Jan	Feb	Mar	Apr	May	Jun	Jul	Aug	Sep	Oct	Nov	Dec
Belo Monte	3880	6839	11067	12736	8372	3831	2017	1128	743	695	1179	1966
Bem Querer	408	313	317	308	762	2216	3308	2989	1215	841	589	540
Cachoeira do Caí	975	1799	2607	2638	1519	597	191	69	38	60	157	503
Cachoeira do Caldeirão	211	514	682	939	1034	891	745	538	295	149	95	98
Cachoeira dos Patos	668	1230	1783	1805	1039	409	131	47	26	41	108	344
Colíder	777	905	1076	834	551	480	428	381	340	357	383	459
Ferreira Gomes	149	346	831	1048	1173	822	582	429	217	118	64	81
Jamanxim	687	1266	1835	1857	1069	421	134	49	27	42	111	354
Jatobá	8533	10586	15140	14456	9843	6256	4095	3257	2960	2995	3624	5493
Jirau	14593	21264	23513	21112	15138	10241	7062	4657	3723	4205	5843	9501
Salto Augusto de Baixo	3503	4700	5927	5271	3441	2667	2100	1959	1943	1907	2371	3137
Santo Antônio	14835	21617	23904	21463	15389	10412	7180	4734	3785	4274	5940	9659
São Luís do Tapajos	9502	12182	18315	17809	12222	6331	3579	2607	2279	2288	3031	5485
São Manoel	1976	2250	2158	1744	1424	998	774	571	486	579	965	1312
São Simão Alto	3545	4727	6051	5407	3522	2701	2121	1965	1951	1915	2387	3152
Sinop	853	920	891	751	614	491	427	353	325	360	492	626
Teles Pires	1657	2452	2495	1763	1000	837	706	568	522	550	610	781

Data not available to Marabá

Table S3– Densimetric Froude (F)- Average flow scenario (m^3/s)

	Jan	Feb	Mar	Apr	May	Jun	Jul	Aug	Sep	Oct	Nov	Dec
Belo Monte	5.4	8.8	12.4	13.7	10.9	4.9	2.0	1.1	0.7	0.8	1.3	2.6
Bem Querer	3.9	3.6	3.2	5.2	12.8	23.0	28.4	22.1	12.8	7.5	5.8	4.5
Cachoeira do Caí	3.5	5.5	7.3	7.2	4.8	2.0	0.7	0.3	0.2	0.4	0.9	2.2
Cachoeira do Caldeirão	8.2	13.3	18.6	23.6	24.8	22.0	16.1	11.9	7.7	5.8	4.3	4.8
Cachoeira dos Patos	8.3	13.0	17.4	17.1	11.4	4.7	1.6	0.6	0.5	0.9	2.2	5.3
Colíder	3.2	3.8	4.2	3.1	2.0	1.5	1.3	1.1	1.0	1.2	1.5	2.2
Ferreira Gomes	1.5	2.9	4.4	5.4	5.8	4.6	3.4	2.3	1.3	0.8	0.6	0.7
Jamanxim	1.8	2.8	3.7	3.6	2.4	1.0	0.3	0.1	0.1	0.2	0.5	1.1
Jatobá	23.3	30.6	36.8	36.6	25.4	14.8	9.0	6.6	6.0	6.4	9.3	14.7
Jirau	44.1	53.1	60.8	54.3	41.6	29.5	19.9	13.1	10.7	12.8	19.3	30.6
Marabá	35.1	46.8	54.0	53.1	33.7	16.1	9.4	6.7	5.3	6.2	10.4	20.5
Salto Augusto de Baixo	12.0	15.7	20.4	18.3	12.2	8.6	6.2	5.5	5.5	5.6	7.2	9.8
Santo Antônio	63.9	76.9	88.1	78.7	60.2	42.8	28.9	19.0	15.5	18.6	27.9	44.3
São Luís do Tapajos	7.9	10.9	13.5	13.4	9.1	4.8	2.6	1.7	1.4	1.6	2.7	4.8
São Manoel	10.5	11.5	11.9	8.5	5.8	4.0	2.9	2.2	2.0	2.9	4.5	7.5
São Simão Alto	3.8	4.9	6.4	5.8	3.9	2.7	1.9	1.7	1.7	1.7	2.2	3.0
Sinop	3.0	3.1	3.1	2.2	1.6	1.2	1.0	0.9	0.8	1.0	1.5	2.4
Teles Pires	13.2	17.5	20.2	14.0	7.9	5.0	3.9	3.0	2.8	3.5	4.7	8.1

Red: F <0.3; Yellow: 0.3<F<1; Green: F>1

Table S4– Densimetric Froude (F)- Q95% scenario (m^3/s)

	Jan	Feb	Mar	Apr	May	Jun	Jul	Aug	Sep	Oct	Nov	Dec
Belo Monte	2.7	4.7	7.7	8.8	5.8	2.7	1.4	0.8	0.5	0.5	0.8	1.4
Bem Querer	1.5	1.2	1.2	1.1	2.8	8.2	12.2	11.0	4.5	3.1	2.2	2.0
Cachoeira do Caí	1.5	2.7	3.9	4.0	2.3	0.9	0.3	0.1	0.1	0.1	0.2	0.8
Cachoeira do Caldeirão	3.0	7.4	9.8	13.5	14.9	12.8	10.7	7.8	4.3	2.1	1.4	1.4
Cachoeira dos Patos	3.5	6.4	9.3	9.4	5.4	2.1	0.7	0.2	0.1	0.2	0.6	1.8
Colíder	1.8	2.1	2.5	1.9	1.3	1.1	1.0	0.9	0.8	0.8	0.9	1.0
Ferreira Gomes	0.4	1.0	2.4	3.1	3.4	2.4	1.7	1.3	0.6	0.3	0.2	0.2
Jamanxim	0.7	1.4	2.0	2.0	1.2	0.5	0.1	0.1	0.0	0.0	0.1	0.4
Jatobá	15.0	18.6	26.6	25.4	17.3	11.0	7.2	5.7	5.2	5.3	6.4	9.6
Jirau	26.4	38.5	42.6	38.3	27.4	18.6	12.8	8.4	6.7	7.6	10.6	17.2
Marabá	-	-	-	-	-	-	-	-	-	-	-	-
Salto Augusto de Baixo	8.8	11.8	14.9	13.3	8.7	6.7	5.3	4.9	4.9	4.8	6.0	7.9
Santo Antônio	38.3	55.8	61.7	55.4	39.8	26.9	18.5	12.2	9.8	11.0	15.3	25.0
São Luís do Tapajos	5.0	6.3	9.5	9.3	6.4	3.3	1.9	1.4	1.2	1.2	1.6	2.9
São Manoel	5.5	6.2	6.0	4.8	3.9	2.8	2.1	1.6	1.3	1.6	2.7	3.6
São Simão Alto	2.7	3.7	4.7	4.2	2.7	2.1	1.6	1.5	1.5	1.5	1.8	2.4
Sinop	1.7	1.8	1.7	1.5	1.2	1.0	0.8	0.7	0.6	0.7	1.0	1.2
Teles Pires	6.3	9.4	9.6	6.8	3.8	3.2	2.7	2.2	2.0	2.1	2.3	3.0

Red: F <0.3; Yellow: 0.3<F<1; Green: F>1

Table S5– Residence time, RT (days) - Average flow scenario (m^3/s)

	Jan	Feb	Mar	Apr	May	Jun	Jul	Aug	Sep	Oct	Nov	Dec
Belo Monte	6.8	4.1	2.9	2.7	3.4	7.4	18.4	33.9	49.7	47.4	28.1	14.1
Bem Querer	27.5	30.1	33.3	20.8	8.4	4.7	3.8	4.9	8.5	14.5	18.6	24.3
Cachoeira do Caí	17.0	10.9	8.1	8.3	12.4	30.0	86.8	228.7	309.1	151.0	64.4	26.6
Cachoeira do Caldeirão	4.7	2.9	2.1	1.6	1.6	1.7	2.4	3.2	5.0	6.7	9.1	8.1
Cachoeira dos Patos	5.1	3.2	2.4	2.5	3.7	8.9	25.8	68.3	91.5	44.8	19.2	7.9
Colíder	12.8	10.5	9.7	13.1	20.6	27.5	32.1	37.5	39.8	34.2	27.0	18.4
Ferreira Gomes	3.1	1.6	1.1	0.9	0.8	1.0	1.3	2.0	3.5	5.7	7.8	6.8
Jamanxim	7.1	4.5	3.4	3.5	5.2	12.5	36.2	95.3	129.2	62.9	26.9	11.1
Jatobá	3.5	2.7	2.2	2.2	3.2	5.5	9.0	12.3	13.6	12.7	8.8	5.5
Jirau	1.3	1.1	0.9	1.1	1.4	2.0	2.9	4.4	5.4	4.5	3.0	1.9
Marabá	4.3	3.2	2.8	2.8	4.4	9.3	15.8	22.4	28.2	24.2	14.4	7.3
Salto Augusto de Baixo	5.0	3.8	3.0	3.3	5.0	7.1	9.8	10.9	11.0	10.9	8.4	6.2
Santo Antônio	1.0	0.8	0.7	0.8	1.0	1.4	2.2	3.3	4.0	3.3	2.2	1.4
São Luís do Tapajos	5.8	4.2	3.4	3.4	5.0	9.5	17.8	27.4	31.7	27.8	16.8	9.4
São Manoel	1.8	1.6	1.6	2.2	3.2	4.7	6.4	8.4	9.2	6.4	4.2	2.5
São Simão Alto	9.1	6.9	5.3	5.9	8.8	12.7	17.8	19.9	20.2	19.9	15.3	11.3
Sinop	18.9	18.5	18.5	26.2	35.5	45.2	55.4	65.7	69.6	54.5	37.3	23.8
Teles Pires	3.0	2.3	2.0	2.9	5.1	8.0	10.4	13.3	14.3	11.6	8.5	5.0

Green: RT <30; Yellow: 30<RT<100; Red: RT>100

Table S6– Residence Time, RT (days) - Q95% scenario (m^3/s)

	Jan	Feb	Mar	Apr	May	Jun	Jul	Aug	Sep	Oct	Nov	Dec
Belo Monte	13.6	7.7	4.8	4.2	6.3	13.8	26.2	46.9	71.2	76.1	44.9	26.9
Bem Querer	71.8	93.5	92.4	95.2	38.4	13.2	8.9	9.8	24.1	34.8	49.7	54.2
Cachoeira do Caí	40.6	22.0	15.2	15.0	26.0	66.3	207.0	575.8	1041.1	661.5	251.5	78.6
Cachoeira do Caldeirão	12.7	5.2	3.9	2.8	2.6	3.0	3.6	5.0	9.1	17.9	28.1	27.3
Cachoeira dos Patos	12.1	6.5	4.5	4.5	7.8	19.7	61.4	172.5	309.8	196.0	74.7	23.4
Colíder	22.7	19.5	16.4	21.2	32.0	36.8	41.2	46.3	51.9	49.5	46.0	38.4
Ferreira Gomes	10.7	4.6	1.9	1.5	1.4	1.9	2.7	3.7	7.3	13.4	24.9	19.5
Jamanxim	16.9	9.2	6.3	6.3	10.9	27.7	86.5	238.8	435.7	276.3	105.0	32.8
Jatobá	5.4	4.4	3.1	3.2	4.7	7.4	11.3	14.3	15.7	15.5	12.8	8.5
Jirau	2.2	1.5	1.4	1.5	2.1	3.1	4.5	6.8	8.5	7.6	5.4	3.3
Marabá	-	-	-	-	-	-	-	-	-	-	-	-
Salto Augusto de Baixo	6.9	5.1	4.1	4.6	7.0	9.0	11.4	12.3	12.4	12.6	10.1	7.7
Santo Antônio	1.6	1.1	1.0	1.1	1.6	2.3	3.3	5.1	6.3	5.6	4.0	2.5
São Luís do Tapajos	9.2	7.2	4.8	4.9	7.2	13.8	24.4	33.5	38.4	38.2	28.8	15.9
São Manoel	3.4	3.0	3.1	3.8	4.7	6.7	8.6	11.7	13.8	11.5	6.9	5.1
São Simão Alto	12.5	9.3	7.3	8.2	12.5	16.4	20.8	22.5	22.6	23.1	18.5	14.0
Sinop	33.9	31.4	32.5	38.5	47.1	58.9	67.8	81.8	89.0	80.3	58.7	46.2
Teles Pires	6.3	4.3	4.2	5.9	10.5	12.5	14.8	18.5	20.1	19.1	17.2	13.4

Green: RT <30; Yellow: 30<RT<100; Red: RT>100

6.1.2 Bottom-up approach

The BU approach consists of a mass balance to estimate net reservoir emission using GHG production rates derived from incubation of soils and foliage from Petit Saut reservoir (Guérin et al. 2008). The model has three modules:

1. The first module computes the emissions related to the below the ground C stock (flooded soils).
2. The second module accounts for the emissions related to the biomass in the vegetation that was not properly cleared and stays in the reservoir after flooding (flooded foliage).
3. The third module accounts for the emissions related to the vegetation that is cleared in the reservoir area.

The sum of the emissions computed in each module defines the net reservoir emissions in the bottom-up model. The model represents a lower bound estimate of emissions, as it does not account for OM imported or produced within the reservoir through primary production. We also applied a Monte Carlo simulation structure to estimate the net reservoir emissions. We repeated the simulation 10,000 times for each reservoir.

6.1.2.1 Module 1 – Emissions from flooded soils

The net reservoir emissions in this module are defined by the difference between production and consumption of GHG in the sediment surface/water column, taking into account CH_4 oxidation fraction (MOX) and bacteria growth efficiency (BGE).

The initial soil C stock is defined by the multiplication of the flooded area (discounted the natural river area) and the soil OM C density. We modeled the uncertainty of the below-the-ground C stock density by assuming a uniform distribution that varies from 8 to 16 Gg C km^{-2} considering the 0-20cm layer (Cerri et al. 2007).

Equations S14 to S21 describe the mathematical formulation of the bottom-up model, which relies on monthly time steps to estimate emissions over 100 years:

$$CH_4\ Production_{soils}(t) = (CH_4\ production\ Rate_{soils}) * C\ Stock_{soils}(t) \quad (S14)$$

CO_2 Production $_{soils}$ (t) = (CO_2 production Rate $_{soils}$)* C Stock $_{soils}$ (t) (S15)

CH_4 Consumption from CH_4 oxidation (t) = CH_4 Production (t) * (1 - MOX) (S16)

CO_2 Production from CH_4 oxidation (t) = CH_4 Production (t) * (MOX)* BGE (S17)

CH_4 Emission $_{soils}$ (t) = CH_4 Production $_{soils}$ (t) - CH_4 Consumption from CH_4 oxidation (t) (S18)

CO_2 Emission $_{soils}$ (t) = CO_2 Production $_{soils}$ (t) + CO_2 Production from CH_4 oxidation (t) (S19)

NRE_{soils} (t) = CH_4 $Emission_{soils}$ (t) + CO_2 $Emission_{soils}$ (t) (S20)

C $Stock_{soils}$ (t+1) = C $Stock_{soils}$ (t) – CH_4/CO_2 $Production_{soils}$ (t) (S21)

A normal distribution defines the C production rates in this model. This probability distribution relies on the average and standard deviation of GHG potential production rates obtained from incubation of soils from Petit Saut reservoir (260 ± 56 nmol (CH_4) $g^{-1}h^{-1}$ and 350 ± 69 nmol (CO_2) $g^{-1}h^{-1}$). We assumed that production rates are the same for stratified and well mixed water column reservoirs, because soil saturation leads to anaerobic decomposition at this layer in both conditions (Davidson & Janssens 2006).

Methane Oxidation Fraction (MOX)

The aerobic methane-oxidizing bacteria consume part of the CH_4produced by methanogenesis. The literature shows that CH_4oxidation is a very efficient process in reducing CH_4 outgas to the atmosphere in freshwater environments (Bastviken 2009; Angelis & Scranton 1993; Guérin & Abril 2007; Kemenes, Forsberg & Melack 2007). CH_4 oxidation may occur in the sediment surface, as well as the water column, and it is positively correlated with CH_4 concentration, temperature, and availability of O_2 (Bastviken 2009). Our BU model requires an estimate of the fraction of the CH_4 produced that is oxidized before reaching the atmosphere (variable MOX).

CH_4 oxidation in stratified tropical reservoirs happens in both the reservoir and in the river below the dam (Guérin & Abril 2007; Kemenes, Forsberg & Melack 2007). In stratified water bodies, CH_4 oxidation occurs within the thermocline between the aerobic epilimnion and the anoxic and methane-saturated hypolimnion (Guérin & Abril 2007; Hanson & Hanson 1996). Below the dam, the reduction of CH_4 concentration with distance in the rivers is attributed to gas evasion and CH_4 oxidation (Guérin et al. 2006). In Petit Saut, about 90% of the CH_4 reaching the hypolimnion was oxidized in the reservoir or downstream (Guérin et al. 2006). In Balbina, 85% of the CH_4 loss downstream the dam was attributed to CH_4 oxidation (Kemenes, Forsberg & Melack 2007).

MOX data in reservoirs with well-mixed water column (low RT) are not available for Amazon reservoirs. The only measure for a low RT reservoir was made in Lake Wohlen, Switzerland, where the oxidation in water column was found to be negligible (DelSontro et al. 2010). However, the measurements made in Switzerland do not assess the oxidation in the sediment surface. In the case of methanogenic sediments overlain with oxic water in river and lakes, methanotrophic bacteria occur at the top of sediments, as well as in the water column (Hanson & Hanson 1996; Bastviken 2009; Angelis & Scranton 1993). A meta-analysis of CH_4 oxidation fractions in oxic lakes shows that 50% to 95% of the produced CH_4 is oxidized above the sediment (Bastviken 2009). In the case CH_4 oxidation in the water column, the data from lakes show that CH_4 oxidation fraction varies from 45% to 100% and that it is highly dependent on the mixing regime and depth (Bastviken 2009). With respect to rivers, a C balance for the Hudson River, United States, indicates that CH_4 oxidation in the water column removes from 13% to 70% of the produced CH_4 (Angelis & Scranton 1993).

The literature shows that MOX in different water column conditions vary significantly but overlap. As a result, we did not distinguish between high and low RT reservoirs in this approach. Instead, we assumed the same MOX for both water column conditions, which is defined by uniform distribution between 45% and 95%.

CH_4 oxidation results in CO_2 production, and we assume that the BGE (required in Equation S17) has a triangular distribution that ranges from 10% to 80% (Bastviken et al. 2003) and has the most probable value at 50% (Guérin et al. 2008).

6.1.2.2 Module 2 – Emissions from flooded foliage

Currently, the Brazilian environmental rules for reservoir construction specify the need to implement vegetation-clearing programs in the reservoir areas to reduce the hazardous effect of biomass decomposition in the water quality (Tundisi & Rocha 1998). However, the enforcement of this rule has been neglected in the past, such as the Teles Pires reservoir (CHTP 2015).

To address the issue of incomplete vegetation clearing in some reservoirs, we included a second degradation module. This module follows the same structure adopted to estimate emissions from soils (Guérin et al. 2008). The multiplication of the flooded area (discounting the natural river area) and C density of foliage (leaves and branches) defines the C stock. C densities of leaves and branches are assumed to be 0.6 Gg C km^{-2} and 5.8 Gg C km^{-2}, respectively (Malhi, Baldocchi & G 1999). Based on these values, we adopted a uniform distribution between 0.6 (only leaves) and 6.4 (sum of leaves and branches) Gg C/km^2 to represent the uncertainty in the C density of foliage that may remain in the reservoir. The net reservoir emissions from flooded foliage are defined as the difference between GHG production and consumption in the water column, taking into account MOX and BGE.

$$CH_4 \text{ Production}_{foliage}(t) = (CH_4 \text{ production Rate}_{foliage}) * \text{C Stock}_{foliage}(t) \qquad (S22)$$

CO_2 Production $_{foliage}$ (t) = (CO_2 production Rate)* C Stock $_{foliage}$ (t) (S23)

CH_4 Consumption from CH_4 oxidation (t) = CH_4 Production $_{foliage}$ (t) * (1 - MOX) (S24)

CO_2 Production from CH_4 oxidation (t) = CH_4 Production $_{foliage}$ (t) * (MOX)* BGE (S25)

CH_4 Emissions $_{foliage}$ (t) = CH_4 Production $_{foliage}$ (t) - CH_4 Consumption from CH_4 oxidation (t) (S26)

CO_2 Emissions $_{foliage}$ (t) = CO_2 Production $_{foliage}$ (t) + CO_2 Production from CH_4 oxidation (t) (S27)

NRE $_{foliage}$ (t) = CH_4 Emissions (t) + CO_2 Emissions (t) (S28)

C Stock $_{foliage}$ (t+1) = C Stock $_{foliage}$ (t) – CH_4/CO_2 Production $_{foliage}$ (t) (S29)

A lognormal distribution defines the C production rates in this module. This probability distribution relies on the average and standard deviation of GHG potential production rates obtained from incubation of foliage from Petit Saut reservoir (2400 ± 1000 mmol (CH_4) $g^{-1}h^{-1}$ and 3900 ± 5000 nmol (CO_2) $g^{-1}h^{-1}$) (Guérin et al. 2008).

MOX and BGE follow the same assumptions described for the Module 1– Emissions from flooded soils.

6.1.2.3 Module 3 – Emissions from the cleared vegetation

This module computes the GHG emissions related to C stock contained in the removed biomass from the reservoir area. As previously mentioned, Brazilian environmental rules require vegetation clearing of the flooded area before filling the reservoir (Kubistcheck 1960). Based on spatial information of the biomass density within each reservoir, we estimated the emissions related to the vegetation clearing for each reservoir according to the equation S30.

NRE $_{biomass}$ = Biomass density x (A_{RES}– $A_{RIVERUP}$) x C content (S30)

Where, Biomass density is defined by uniform distribution with maximum and minimum values described in Table S7. C content is the proportion of C in the biomass, which is assumed to be 50% (Martin & Thomas 2011; Feldpausch & Rondon 2004).

Table S7 – Biomass density range from the studied reservoirs (Gg km^{-2}). See section for the method to define the minimum and maximum values.

Project	Min (Gg km^{-2}).	Max (Gg km^{-2}).
Belo Monte	16	20
Bem Querer	12	17
Cachoeira do Caí	27	32
Cachoeira do Caldeirão	20	25
Cachoeira dos Patos	18	23
Colíder	9	13
Ferreira Gomes	9	12
Jamanxim	23	28
Jatobá	15	19
Jirau	20	24
Marabá	11	15
Salto Augusto de Baixo	19	24
Santo Antônio	16	21
São Luis do Tapajos	20	25
São Manoel	21	26
São Simão Alto	23	28
Sinop	9	13
Teles Pires	13	17

The biomass map (Saatchi et al. 2007), which is the base for the biomass density calculation, is calibrated using forest monitoring plots. Forest monitoring plots range from 0.5–50 ha in area, and within them, every individual tree over a certain threshold size (usually ≥100 mm diameter-at-breast-height) is identified, measured, and monitored over time (Lewis et al. 2009). Given the uncertainty related to the quality of the plots (Saatchi et al. 2007) and the limitation of these studies to account for the C below a certain threshold, we assumed that this C pool is independent of our estimates for foliage described in Module 2.

The fate of the C from vegetation clearing is variable and uncertain. According to Teles Pires reservoir vegetation clearing report (CHTP 2015), large trunks were used in the construction industry. Regarding smaller trunks and branches, the material was used to make charcoal and firewood. The small residues and vegetation were buried in the shallow excavations in the ground; a similar procedure was also applied in the Santo Antônio (Fearnside 2015b). We assumed that the C from the cleared biomass is released into the atmosphere, as CO_2, within a period of 30 years.

6.2 Data from new hydroelectric power plants in the Amazon

Data about the hydroelectric plants in this study came from the Brazilian Electric Agency (*Agencia Nacional de Energia Elétrica – ANEEL)*. These data came from river basin hydroelectric Master plans, known as "*estudos de inventario hidrelétrico",* and viability studies approved by ANEEL. The studies are public and provided by ANEEL. We selected 18 projects for model application from the Brazilian Energy Plans (MMEEPE 2010; EPEMME 2012). Figure S2 shows the spatial location of the studied reservoirs. Table 2-1 (Chapter 2) describes the characteristics of the studied reservoirs. Table S8 shows the ANEEL process number. The process number is the study reference identification in the agency and can be used to request the data.

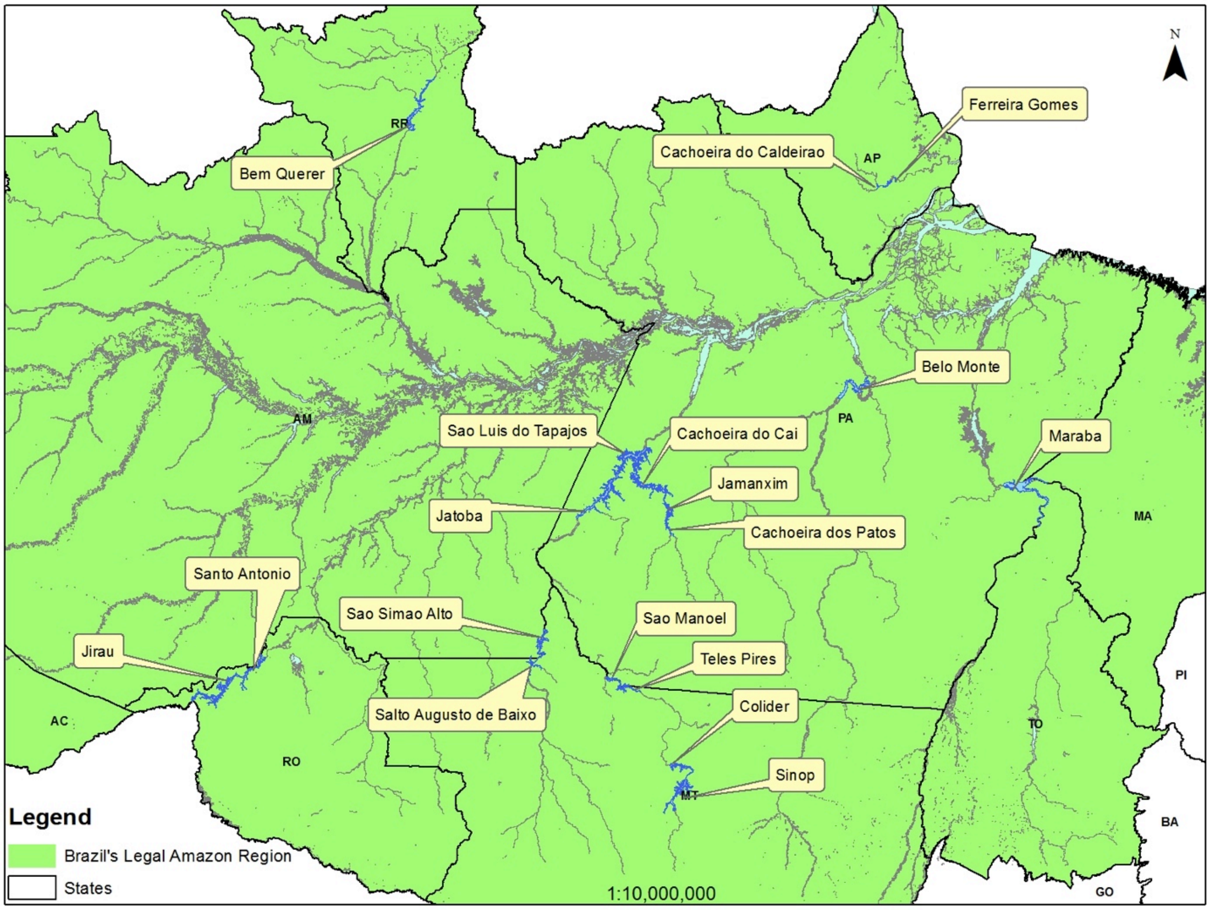

Figure S2 - Spatial distribution of the studied reservoirs

Table S8 - Information about the hydroelectric studies approved by ANEEL and used in this study.

Hydroelectric Power Plant Name	ANEEL Process Number	Stage
Belo Monte	48500.004313/2005-47	Master plan
Bem Querer	48500.002003/2006-60	Master plan
Cachoeira do Caí	48500.000623/2005-92	Master plan
Cachoeira do Caldeirão	48500.006127/2008-93	Viability
Cachoeira dos Patos	48500.000623/2005-92	Master plan
Colíder	48500.003933/2006-77	Viability
Ferreira Gomes	48100.003451/95-31	Master plan
Jamanxim	48500.000623/2005-92	Master plan
Jatobá	48500.000623/2005-92	Master plan
Jirau	48500.000291/2001-31	Master plan
Marabá	48500.000177/2001-65	Viability
Salto Augusto de Baixo	48500.001701/2006-11	Master plan
Santo Antônio	48500.000291/01-31	Master plan
São Luís do Tapajos	48500.000623/2005-92	Master plan
São Manoel	48500.004789/2006-78	Viability
São Simão Alto	48500.001701/2006-11	Master plan
Sinop	48500.004784/2006-54	Viability
Teles Pires	48500.004785/2006-17	Viability

The model inputs include two sets of variables, one related to landscape characteristics of the river/reservoir and another related to the flux rates per area per time. The variables related to the river/reservoirs, which we consider to be defined constants, include reservoir area (A_{RES}), the area of bays and tributary (A_{BAYS}), and natural river surface areas within the model boundaries ($A_{RIVERDOWN}$ and $A_{RIVERUP}$). Table S9 summarizes these data, which came from design documents cross-referenced to remote sense data using GIS techniques (See section 2.1 for details about the method to obtain the surface areas).

Table S9 – Surface area of rivers and reservoirs defined by the model boundaries and used as inputs for the models.

Hydroelectric Power Plant Name	River	Reservoir Area: A_{res} (km^2)	River Downstream Area: $A_{rRIVERDOWN}$ (km^2)	River Area: A_{RIVER} (km^2)	River Area upstream: $A_{RIVERUP}$ (km^2)	Bays/ Tributary Area (A_{BAYS})	Reservoir length (km)
Belo Monte	Xingu	516	245	484	239	28	89
Bem Querer	Branco	559	39	155	116	104	146
Cachoeira do Caí	Jamanxim	420	18	57	39	n/a	144
Cachoeira do Caldeirão	Araguari	48	32	48	16	11	52
Cachoeira dos Patos	Jamanxim	117	11	26	15	n/a	68
Colíder	Teles Pires	172	11	37	26	54	98
Ferreira Gomes	Araguari	18	20	26	6	3	10
Jamanxim	Jamanxim	74	13	19	6	n/a	44
Jatobá	Tapajós	646	106	474	368	173	132
Jirau	Madeira	303	53	124	71	97	140
Marabá	Tocantins	1,024	70	403	333	122	202
Salto Augusto de Baixo	Juruena	125	52	96	44	38	49
Santo Antônio	Madeira	271	44	140	96	66	134
São Luís do Tapajos	Tapajós	722	74	399	325	212	123
São Manoel	Teles Pires	64	34	44	10	17	45
São Simão Alto	Juruena	284	35	83	48	114	120
Sinop	Teles Pires	330	13	33	20	n/a	122
Teles Pires	Teles Pires	152	19	47	28	51	65

- n/a: not applied because high residence time reservoir are not divided in zones (main channel and tributary/bays).

We also compute the emission factor of each hydropower plant, based on the capacity factor and installed capacity described in Table 2-1 (Chapter 2) and according to the equation below:

$$\text{Emission factor} = (\text{NRE}) / (\text{number of years} * \text{Power} * \text{Capacity Factor} * 365 \text{ days} * 24 \text{ hours}) \quad \text{(S31)}$$

Where NRE is the net GHG reservoir emissions, in CO_2eq, estimated through the statistical models. Power is the installed capacity in MW. The emission factor (g CO_2eq MWh^{-1})

is an important parameter in evaluating the service provided by hydroelectric reservoir in comparison to other sources of electricity (Ometto et al. 2013). The scope and boundary of this study excludes emissions from construction of the physical infrastructure. Furthermore, the emissions factors reported for the different generating assets rely on net output at the power plant gate and do not include power losses associated with the long-distance transmission system.

6.2.1 Surface areas analysis

This section provides detailed information about the method employed to estimate the surface areas, which are inputs for our models. These surface areas include the reservoir area (A_{RES}), the natural river areas (A_{RIVER}, $A_{RIVERUP}$ and $A_{RIVERDOWN}$) and bays/tributary areas (A_{BAYS}).

First, we imported computer-aided design (CAD) files (*.dwf* file extension) containing the shape of the reservoirs to a shapefile (*.shp* file extension) using the software ArcGis. The CAD files are part of the design documents obtained from ANEEL. Figure S3 shows an example of this importing procedure for the Colíder reservoir. The reservoir area (A_{RES}) corresponds to the total reservoir area estimated using the imported polygon for each reservoir.

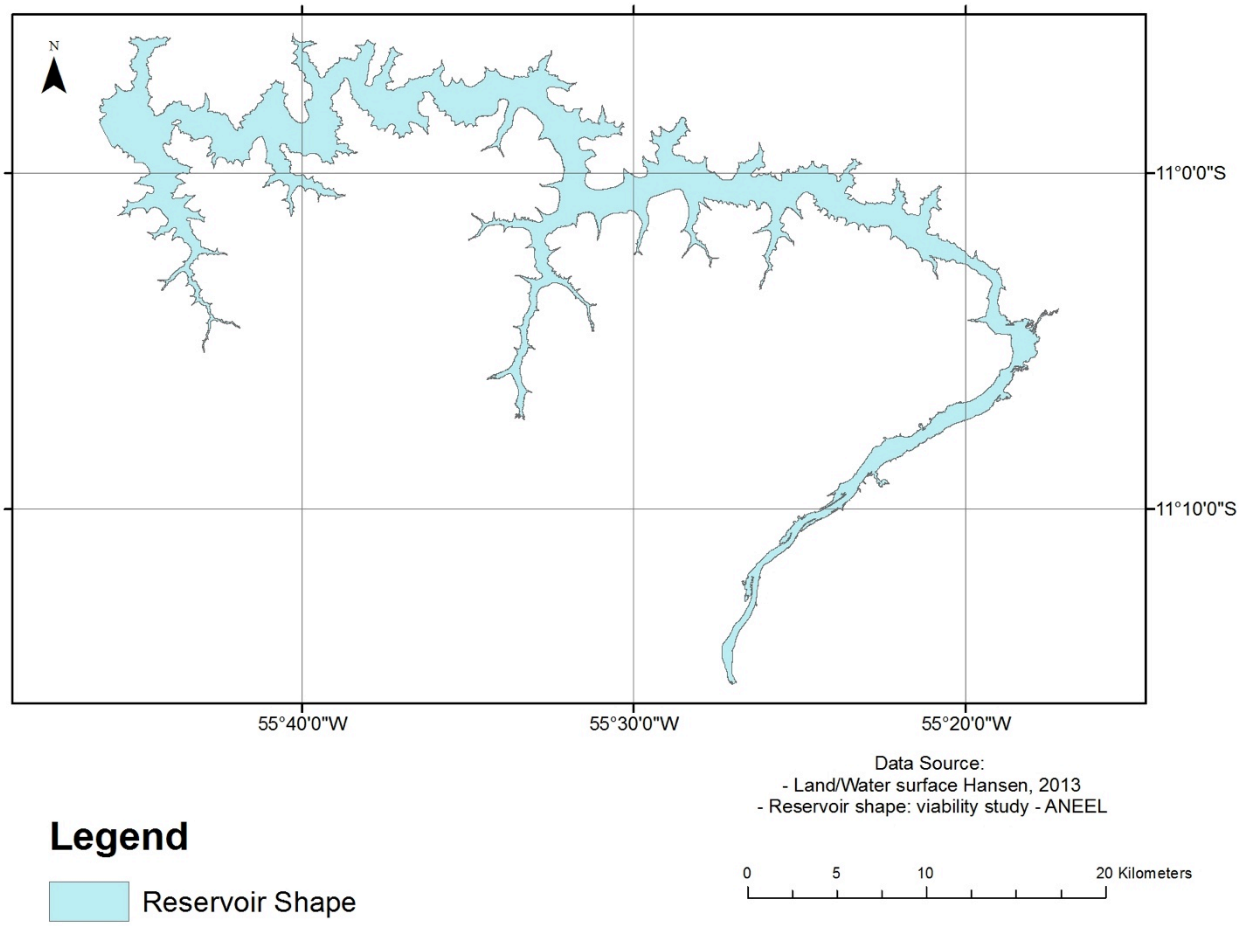

Figure S3 – Reservoir shape (A_{res}): example from Colíder reservoir.

In the case of run-of-river reservoirs, the reservoir water level does not suffer significant water level variation throughout the year. Therefore, the reservoir shape corresponds to the normal level of operation.

In the case of storage reservoirs, however, the definition of the reservoir area is a source of uncertainty because the variation of the water level can be significant. Table S10 presents the characteristics of the storage reservoirs. The data in Table S10 shows that the reservoirs of Cachoeira do Caí, Cachoeira dos Patos, and Sinop have an significant variation of the reservoir area.

Our baseline calculations assume A_{RES} at the maximum normal level for storage reservoir. To address effect of the variation of the area for storage reservoirs in our estimates, we performed a sensitivity analysis for these three reservoirs using the area (A_{RES}) at the normal level as new values in the simulations.

Table S10 – Storage reservoirs characteristics: operational water levels, volume and areas.

	Water Levels				Volume (hm^3)		Reservoir Area (km^2)	
Project	Normal Maximum	Normal Minimum	Normal (average)	Water level variation	Total	Storage	Area at Normal Maximum water level	Area at Normal (average) water level
São Luiz do Tapajós	50.0	49.6	49.8	0.4	7,553	277	722	716
Cachoeira do Caí	85.0	82.9	83.8	2.1	3,418	762	420	377
Jamanxim	143.0	142.2	142.5	0.8	1,004	61	74	73
Cachoeira dos Patos	176.0	173.1	174.3	2.9	696	265	117	93
Sinop	302.0	292.0	297.0	10	3,071	2,059	330	200

Second, we used the *shapefile* of the reservoir surface to clip a raster image containing the information about surface lands and water. This raster image defines global land surface and permanent water bodies based on Landsat 8 satellite data from 2000 to 2013 (Hansen et al. 2013). The image spatial resolution is 30 meters. Figure S4 shows an example of the result of this procedure. Based on these data and method, we defined the natural river surface within the reservoir area ($A_{RIVERUP}$), which corresponds to the blue area (permanent water bodies). We applied the same data and procedure to calculate the natural river area downstream the dam ($A_{RIVERDOWN}$). The only difference is that we clip the raster image containing the permanent water body using the dam as an upper bound, and 40-km distance downstream the dam as the lower bound.

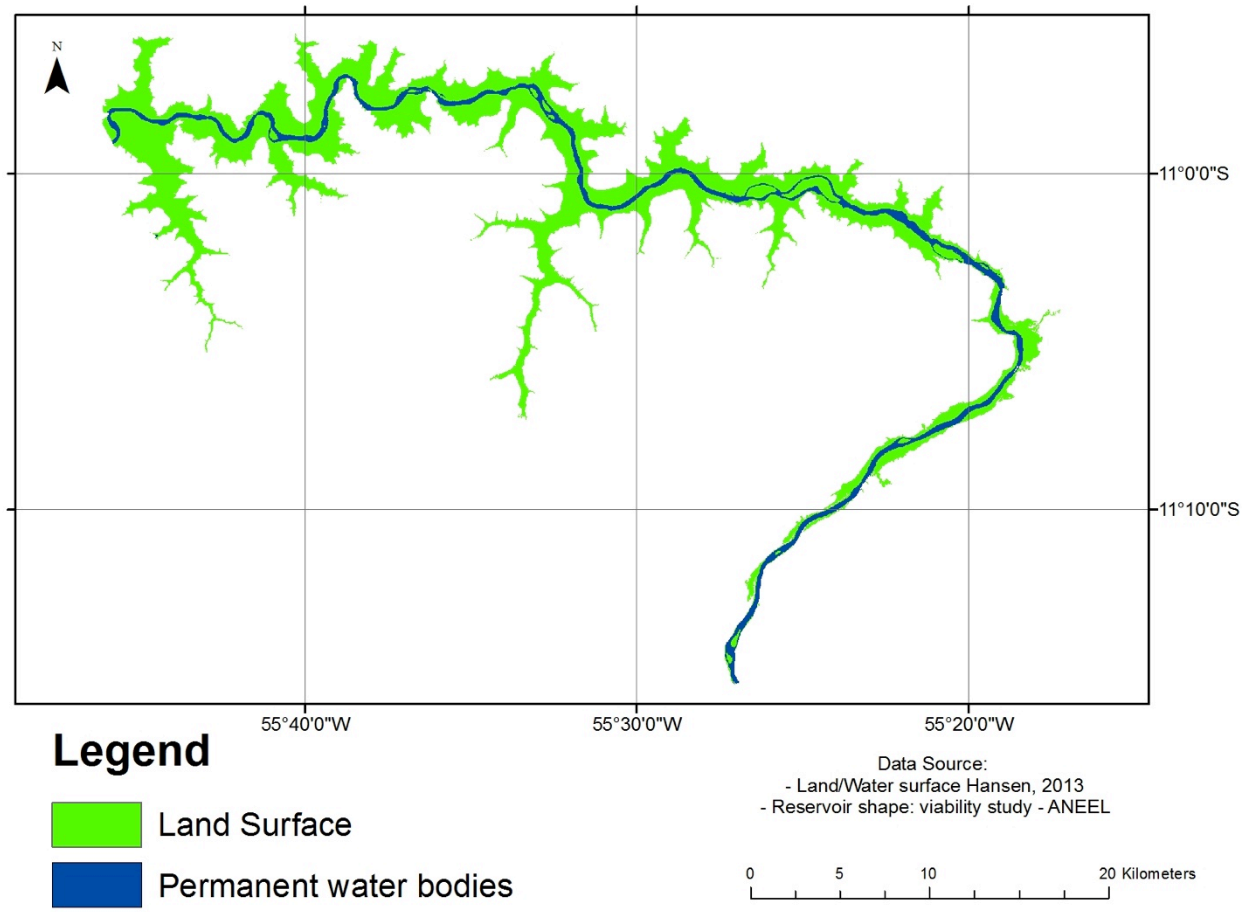

Figure S4 – $A_{RIVERUP}$ determination example for Colíder reservoir.

Third, we divided the total reservoir area in two groups: bays and tributaries, and main water body (main channel). This information is used to calculate the low RT reservoir emission in the TD approach. Low RT reservoirs have a well-mixed water column in the main reservoir water body, but stratified conditions in the bays and tributaries zones. Figure S5 shows an example of this division for Colíder reservoir.

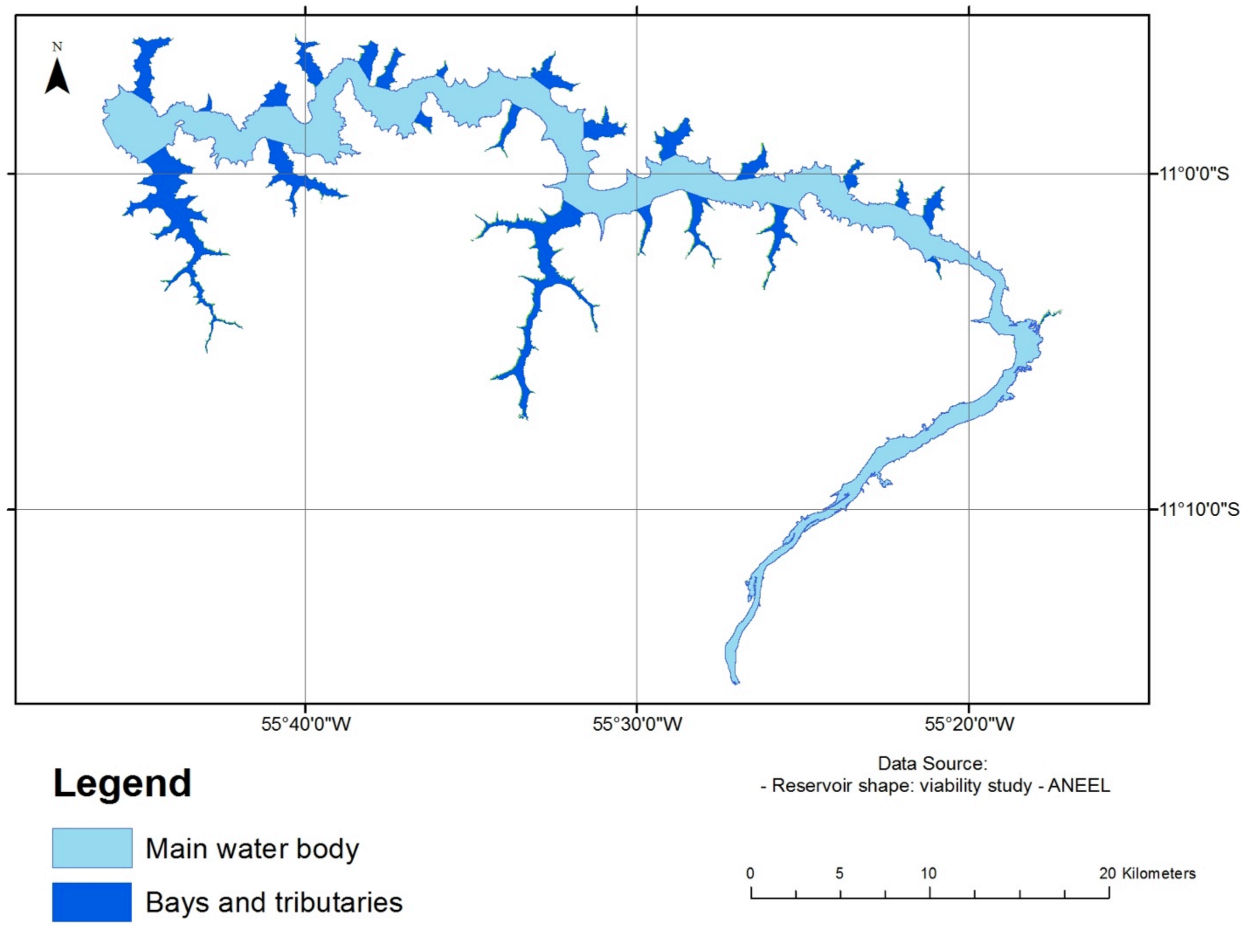

Figure S5– A_{BAYS} determination example for Colíder reservoir.

6.2.2 Above the ground biomass density in the reservoir area

The above the ground biomass density in the reservoir area is an input to calculate the above the ground C stock in the BU model (module 3). We calculated the amount of biomass in the reservoir using a similar procedure described to obtain the natural river areas. The data source is a raster file containing the Amazon basin aboveground live biomass spatial distribution (Saatchi et al. 2008). This raster image contains forest biomass density (in Mg ha^{-1}) divided among 11 classes at 1 km spatial resolution. Remote sensing and ground data used to produce these data were collected from 1990 to 2000. To estimate the total biomass in the reservoir area, we cut the raster image using the reservoir shape as illustrated in Figure S6.

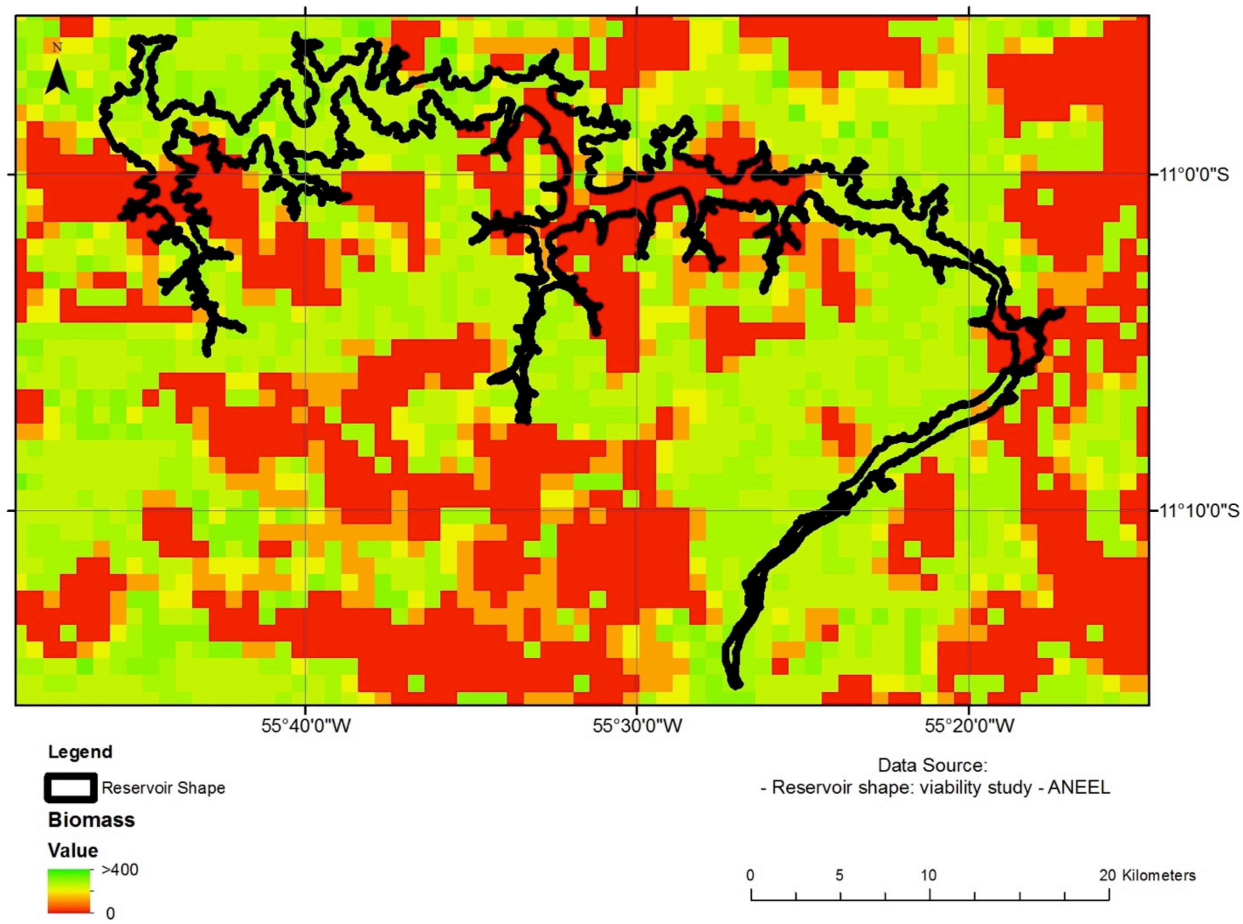

Figure S6 – Above the ground biomass determination example for Colíder reservoir. Legend values are in Mg ha^{-1}.

The result of the procedure is a table containing the number of pixels for each C density class within the reservoir area. Table S11 presents an example of this table to Colíder reservoir.

Table S11 – Biomass density estimation intermediary results: Colíder reservoir example.

Class	Biomass Density Range ($Mg\ km^{-2}$)	Number of pixels per class
1	0-0.25	29
2	0.25-0.50	45
3	0.50-0.75	12
4	0.75-1.00	18
5	1.00-1.50	85
6	1.50-2.00	70
7	2.00-2.50	22
8	2.50-3.00	0
9	3.00-3.50	0
10	3.50-4.00	0
11	>4.00	0
Total number of pixels (1 pixel = 1 km^2) =		281

Note that spatial resolution of the data generates an uncertainty when a pixel is not completely inside the reservoir shape. The GIS software algorithms integrate this pixel as part of the calculation resulting in a greater area compared to the area of the reservoir shape. For the Colíder example in Table S11, the total area is 281 km^2, while the correct reservoir area is 172 km^2. Thus, the estimation of the above the ground biomass using the total number of pixels would lead to an overestimation of the available biomass. To overcome this issue, we used the following procedure to define the minimum and maximum C density values for each reservoir:

1. We estimated a maximum value for the total above the ground biomass in the reservoir area by multiplying the maximum range from each class (e.g., Class 1 equals 0.25 Mg km^{-2} in Table S11) by the number of pixels (e.g., Class 1 equals 20 in Table S11), and summing these values across all classes.
2. We estimate a minimum value for the total above the ground biomass in the reservoir area by multiplying the minimum range from each class (e.g., Class 1 equals 0 Mg km^{-2} in Table S11) by the number of pixels, and summing these values across all classes.

3. We divided the maximum and minimum total mass values (results from step 1 and 2) by the total number of pixels obtaining a range for the above the ground biomass density in the reservoir area.
4. The maximum and minimum biomass density values are used as inputs to define the uncertainty of Equation S30.

The biomass density range results for each reservoir are presented in Table S7.

6.3 Data Analysis - Top-down approach

The TD model defines the flux rates (res_{CO2}, res_{CH4}, deg_{CO2}, deg_{CH4}, $down_{CO2}$, $doown_{CH4}$, nat_{CO2} and nat_{CH4}) by probability distributions that were fitted using published data from Amazon water bodies. The following paragraphs describe the data used to build TD approach. We fit several continuous distributions (Beta, Exponential, Extreme value, Gamma, Generalized extreme value, Generalized Pareto, Inverse Gaussian, Logistic, Log-logistic, Lognormal, Normal, Rayleigh and Weibull) to the data using MATLAB and its function *allfitdist* (Sheppard 2012). The MATLAB function fits most distributions using maximum likelihood estimation. We chose the best distribution through the calculation of the Bayesian Information Criterion (BIC) and Akaike Information Criterion (AIC), which are penalized criteria statistics for model selection. The sum of two terms characterizes the BIC and AIC. The first term is the difference of the maximized log-likelihoods and reflects the fit of the model to the observational data. The second term measures the complexity of the model and thus serves as a penalty for more complex models (Kuha 2004).

6.3.1 Natural River Emissions (nat_{CO2} and nat_{CH4})

We collected published data of CO_2 (Rasera et al. 2008; 2013; Ellis, Richey, Aufdenkampe, et al. 2012; Alin et al. 2011; Salimon et al. 2012) and CH_4 (Sawakuchi et al. 2014) fluxes in Amazon rivers (>100m) classifying the measurements by water-chemistry type. We selected a total of 184 and 453 data points for CO_2 and CH_4 flux rates, respectively. Data from Alin et al. (2011) and Ellis et al. (2012) are available for download from Oak Ridge National Laboratory Distributed Active Archive Center (Alin & Richey 2012; Ellis, Richey, Krusche, et al. 2012). Our database only includes measurements made on large rivers, because all the new power plants evaluated in this study are located in large rivers. The database is available upon request.

In the case of CO_2, the data points can be divided in two groups. The first group consists of data points where the reported values in the papers are averages from multiple measurements. The second group contains not only the averages, but also the raw data (individual field measurements). In other words, the second group contains independent measurements before any statistical treatment. To standardize the database, we calculated the average fluxes for measurements sampled on the same day and site (raw data), resulting in 95 data points for CO_2 fluxes. We used the database to fit distributions for the natural river flux rates according to the water chemistry type. Optical characteristics are the basis of the water type classification: *black water* is associated with a high content of humic compounds; *white water* is associated with a high content of suspended sediment; and *clear wat*er is characterized by the lack of turbidity caused by sediments and a dark color caused by humic compounds (Furch 1984; Junk et al. 2011).

Alin et. al (2011) studied the physical controls on CO_2 flux in low-gradient systems in the Amazon and Mekong river systems. CO_2 fluxes varied from 0.04 (150 mg CO_2 $m^{-2}d^{-1}$) to 14.2 mmol m^{-2} s^{-1} (54,000 mg CO_2 $m^{-2}d^{-1}$) in large rivers and from 0.7 (2661 mg CO_2 $m^{-2}d^{-1}$) to 12.4 mmol m^{-2} s^{-1} (47,000 mg CO_2 $m^{-2}d^{-1}$) in small rivers. They concluded that wind speed is the main physical control on gas exchange in estuaries and large rivers, while water current velocity and water depth become the drivers of these fluxes as the river size decreases (Alin et al. 2011).

Rasera et. al (2008) evaluated the factors controlling water-column respiration in small rivers of the central and southwestern Amazon basin. They reported CO_2 outgassing rates varying from 1 mmol C m^{-2} s^{-1} (3,800 mg CO_2 $m^{-2}d^{-1}$) to 12.7 mmol C m^{-2} s^{-1} (48,000 mg CO_2 $m^{-2}d^{-1}$). According to the authors, most rivers showed similar seasonal patterns, with CO_2 outgassing increasing during a high water period when compared to those observed at low water. Because this work focused on small rivers (width <100m), the selected data points from this reference come only from Ji-Paraná River (Rasera et al. 2008).

Rasera et. al (2013) assessed the spatial and temporal variability of CO_2 efflux in seven Amazonian Rivers and found rates varying from -0.8 (-3,000 mg CO_2 $m^{-2}d^{-1}$) to 15.3 (58,000 mg CO_2 $m^{-2}d^{-1}$). Negative fluxes were reported in Araguaia, Javaes and Teles Pires during dry season, indicating that the role of photosynthesis in fluvial systems of the Amazon should be better understood in estimates of the basin's C balance. The authors concluded that CO_2 flux variability is modulated by the seasonal cycle of CO_2 partial pressure (pCO_3), which is highly correlated with the water flow variability (Rasera et al. 2013).

Natural CH_4 emissions from rivers in the Amazon also exhibit significant spatial and temporal variability related to the water type, river morphology, and season. Average fluxes across measured Amazonian rivers range from 0.04 to 6.0 mmol CH_4 $m^{-2}d^{-1}$ (6.4 to 96 mg CH4 $m^{-2}d^{-1}$) (Sawakuchi et al. 2014).

Table S12 presents the summary of the statistics for each dataset. Figures S7, S8 and S9 show the histograms and adjusted distribution for CO_2 and CH_4 by water type.

Table S12 – Summary of statistics of each dataset (mg m^{-2} day^{-1})

	CH_4			CO_2		
Water Type	White	Black	Clear	White	Black	Clear
Average	12	7	73	19,948	21,923	5,869
Stand. Dev.	24	8	124	11,884	12,788	5,722
Min.	0	1	2	684	5,702	-760
Max.	160	54	644	53,983	48,280	24,178
Skew	4.0	2.6	2.4	0.8	0.6	1.3
n	214	73	165	26	27	42

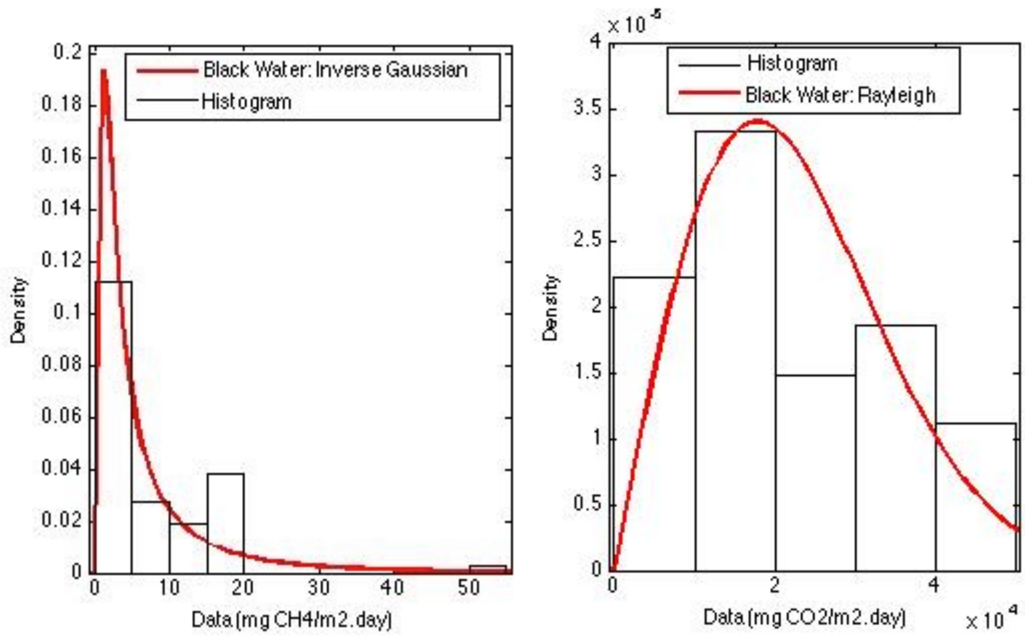

Figure S7 - Black water CH_4 and CO_2 flux data histograms and fitted distributions. CH_4 Black Water: Inverse Gaussian (mean (μ)= 7.18, shape (λ)=3.88); CO_2 Black Water: Rayleigh Distribution (scale (b)= 1.7862e+04).

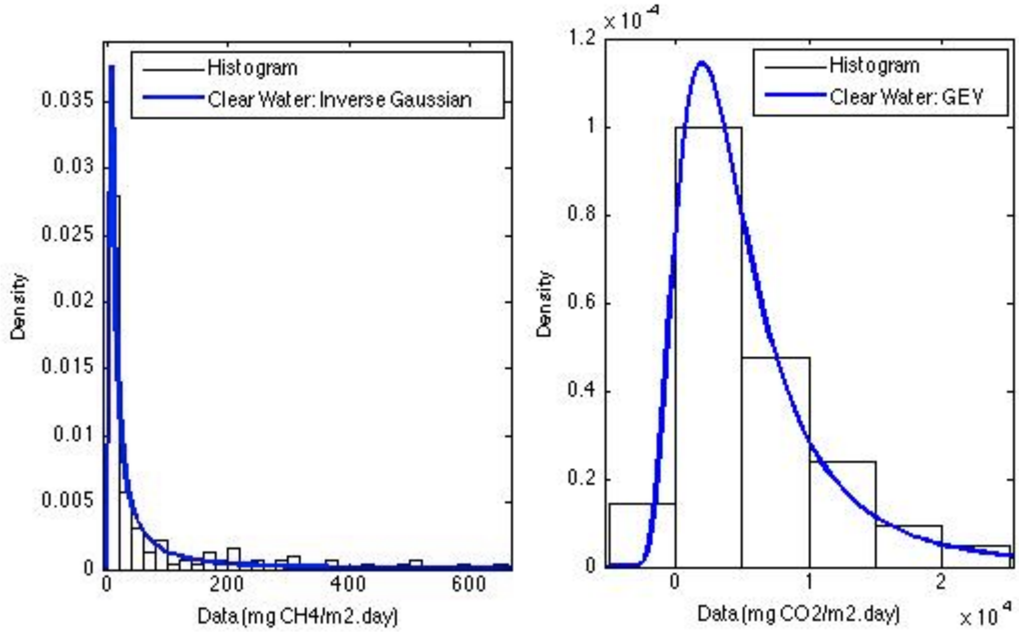

Figure S8 - Clear water CH_4 and CO_2 flux data histograms and fitted distributions. CH_4 Clear Water: Inverse Gaussian (mean (μ)= 72.95, shape (λ)=10.81). CO_2 Clear Water: Generalized Extreme Value distribution (shape (k) = 0.2964; Location (μ)=2.8263e+03; scale (σ) = 3.3465e+03).

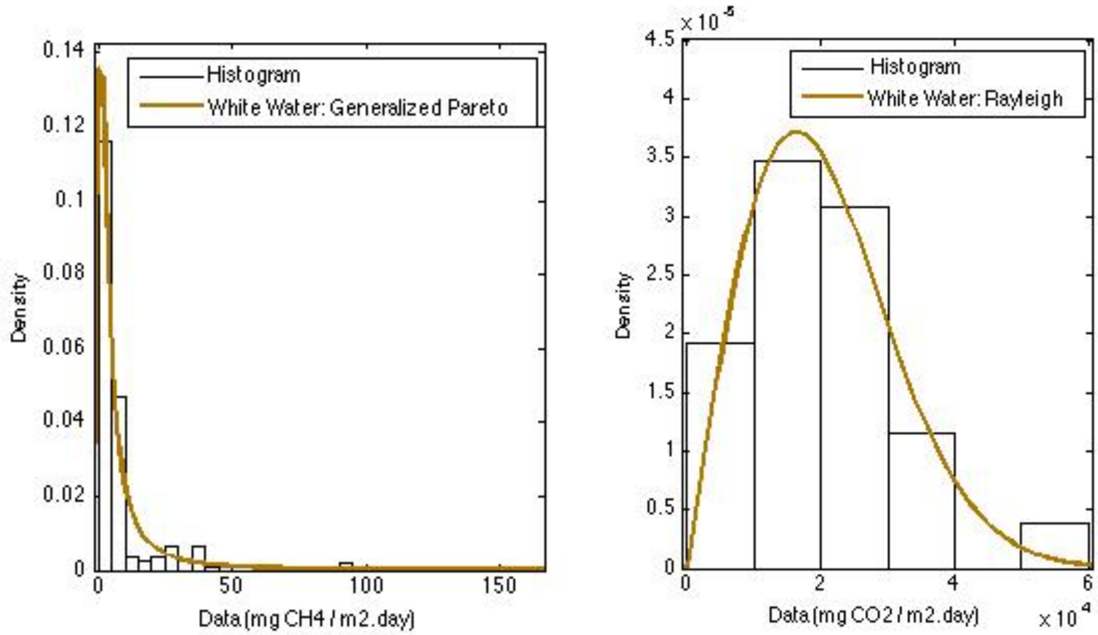

Figure S9 - White water CH_4 and CO_2 flux data histograms and fitted distributions. CH_4 white water: Generalized Pareto (shape (k) = 0.6947; scale (σ) = 4.4007; thresholds (θ)=0.0899). CO_2 white water: Rayleigh Distribution (scale (b)= 1.6336e+04).

6.3.2 Ebbulitive and diffusive emissions from the reservoir (res_{CO2} and res_{Ch4})

The reservoir surface emits CO_2 and CH_4 through ebullition and diffusion. The anaerobic decomposition of the OM present in the reservoir sediments produces CH_4, which is released from the sediments as bubbles because of its low solubility (Demarty & Bastien 2011). Diffusion is the flux that occurs in the air-water interface because of the difference in gas concentration at this layer (Demarty & Bastien 2011).

We selected data from four old forested tropical reservoirs (Balbina, Tucuruí, Samuel and Petit Saut) to fit the probability distributions that describe the reservoir surface fluxes in the TD approach (Abril et al. 2005; Guérin et al. 2006; Kemenes, Forsberg & Melack 2007; 2011; Santos et al. 2006; Lima 2005; Fearnside 2002). Table S13 details the characteristics of these reservoirs. We collected 15 data points for CO_2 diffusion and 20 data points for CH_4 fluxes (diffusion plus ebullition), which are described in Table S14.

Table S13 - Reservoirs Characteristics (Old Reservoirs).

Hydroelectric Power Plant Name	Latitude	Longitude	Power (MW)	Reservoir Area: A_{res} (km^2)	Reservoir Volume ($x10^6\ m^3$)	Mean Flow (m^3/s)	Residence Time (days)	Energy Density (MW/km^2)
Tucuruí	-3.834	-49.648	8370	2875	45500	11000	48	2.91
Samuel	-8.751	-63.457	216	560	3490	350	115	0.39
Balbina	-1.917	-59.481	250	2360	17500	577	351	0.11
Petit Saut	5.063	-53.048	116	310	3500	267	152	0.37

NOTE: We recalculated the annual residence time for the Tucuruí reservoir with the objective to standardize the calculation method with the other reservoirs. We estimated the annual average residence time by dividing volume and average annual flow. The average annual residence time provided in (Fearnside 2002) is 96, which is a result of the average of monthly residence time values (calculated with monthly flows)

Data from Petit Saut, where emissions have been measured since the impoundment in 1993 (Galy-Lacaux et al. 1999; Delmas et al. 2005; Abril et al. 2005), suggest that CO_2 diffusive and CH_4 diffusive and bubbling emissions stabilized 7 years and 4 years after the impoundment, respectively (Abril et al. 2005). For Petit Saut, we only included measurements after stabilization. The data points from the Balbina, Tucuruí, and Samuel reservoirs were sampled at least 9 years after the impoundment. We assumed that all these fluxes represent steady state conditions. (Kemenes, Forsberg & Melack 2007; 2011; Guérin et al. 2006; Lima 2005; Santos et al. 2006).

Average CO_2 emissions variability is high and range from 1,500 to 43,000 mg CO_2 $m^{-2}d^{-1}$. One data point for Samuel is responsible for the large upper bound. Without this extreme point, CO_2 emissions range from 1,500 to 14,000 mg CO_2 $m^{-2}d^{-1}$. The average value of the CO_2 flux reported in Samuel reservoir after 16 years of the impoundment (Guérin et al. 2006) is around three times higher than the second highest CO_2 emissions (found in Balbina). Exceptional weather conditions during the flux measurement campaign explain this high value (Guérin et al. 2006), which cannot be used to represent long-term average conditions. Additionally, a box plot analysis of the data indicates that this point is a statistical outlier. The physical conditions of the measurement and the statistical analysis indicate that this point is a potential outlier. As a consequence, our baseline calculations do not take this point into account. However, we present a sensitivity analysis of the simulation results considering this point latter in this Appendix.

With respect to CH_4, the reported fluxes variability is also high. Average CH_4 fluxes vary from 1 to 205 mg CH_4 $m^{-2}d^{-1}$. CH_4 fluxes include both diffusion and ebullition. Table S14 describes selected CO_2 diffusion (res_{CO2}) and CH_4 ebullition plus diffusion (res_{CH4}) fluxes, and Figure S10 shows the adjusted probability distributions.

Table S14 - Diffusion and ebullition emission fluxes measured in tropical forested reservoirs. Values in the brackets represent the reported standard deviation or range.

Reservoir	Reservoir Area (km^2)	Age when Sampled	**Diffusion CO_2 (mg CO_2 $m^{-2}.day^{-1}$)	Diffusion CH_4 (mg CH_4 $m^{-2}.day^{-1}$)	Ebullition CH_4 (mg CH_4 $m^{-2}.day^{-1}$)	Diffusion + ebullition CH_4 (mg CH_4 $m^{-2}.day^{-1}$)	Reference
Petit Saut [a]	7	4		12	6	19	Abril, et al 2005
Petit Saut [a]	300	5		28	5	34	Abril, et al 2005
Petit Saut [a]	300	6		11	4	15	Abril et al 2005
Petit Saut [a]	300	7	1808	26	4	30	Abril et al, 2005
Petit Saut [a]	300	8	1473	20	2	23	Abril et al, 2005
Petit Saut [a]	300	9	2009	18	1	19	Abril et al 2005
Petit Saut [a]	300	10	2511	17	1	18	Abril et al, 2005
Petit Saut [b]	270-365	10 (wet)	5852 (5104)	-	-	123.2 (140.8)	Guerin et al, 2006
Petit Saut [b]	270-365	10 (dry)	5764 (4840)	-	-	43.2 (25.6)	Guerin et al, 2006
Petit Saut [b]	270-365	12 (dry)	4532 (2992)	-	-	1.6 (1.6)	Guerin et al 2006
Petit Saut [b]	270-365	12 (wet)	4488 (6292)	-	-	11.2 (8)	Guerin et al, 2006
Balbina	1770	17-19	13845 (1260 -31270)	63* (7-460)	-	63	Kemenes et al, 2007, 2011
Balbina	1560 -2360	17	3344 (2024)	-	-	33.6* (48)	Guerin et al, 2006
Tucuruí	2430	14	10433 (1314-142723)	192.2 (0.03-2889)	13.2 (0.01-106)	205.4	Santos et al, 2006
Tucuruí	2430	15	6516 (457 - 32291)	10.9 (4.44 - 28.53)	2.5 (0.92-21.2)	13.4	Santos et al, 2006
Tucuruí	2800	16-17	-	13.82* (22.94)	-	13.82* (22.94)	Lima et al, 2005
Samuel	559	9	8087 (2313 - 16345)	164.3 (4.9 - 2375)	19.3 (0.0001 - 67)	183.6	Santos et al, 2006
Samuel	559	10	6808 (2200 - 24283)	10.8 (6.13 - 17.6)	13.6 (0.07 -37.6)	24.4	Santos et al, 2006
Samuel	559	11-12		71.19* (107.4)	-	71.19* (107.4)	Lima et al, 2005
Samuel	180-559	16	42944 (53372)	-	-	80 (94.4)	Guerin et al, 2006
Statistics		**Min**	1473			2	
		Max	42944			205	
		Average	8028			50	
		Standard Deviation	9891			55	
		n	15			20	

* Diffusion and ebullition

** The model does not account for CO_2 ebbulitive fluxes from the reservoir as these fluxes are negligible for the overall balance (Abril et al. 2005; Santos et al. 2006).

a - Flux rates calculated from the total annual emissions from Table 4 from Abril et al (2005), using average reservoir surface area of 300 km^2

b - Flux rates reported in Table 3 from Guerrin et al (2006)

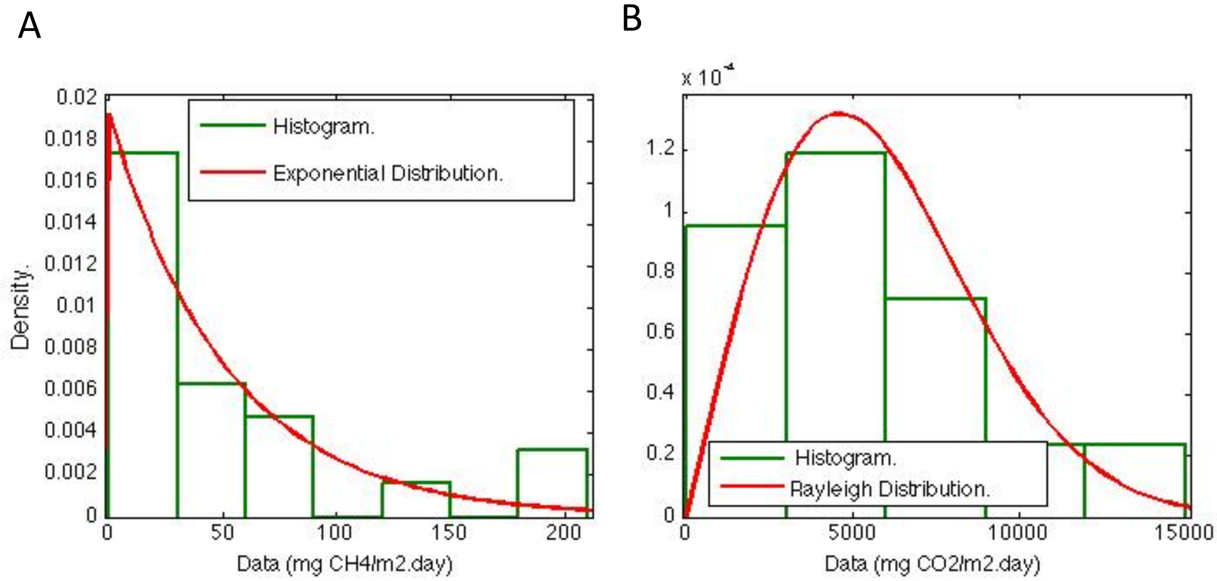

Figure S10 - A: Histogram and fitted distribution for res_{CH4}. Exponential distribution (scale parameter (μ)= 51.6) for the CH_4 diffusion plus ebullition dataset. B: Histogram and fitted distribution for res_{CO2}. Rayleigh fitted distribution (scale parameter (b) = 4589.8) for the CO_2 diffusion rates dataset excluding Samuel (16 years).

6.3.2 Outlet degassing (deg_{CO2} and deg_{Ch4})

Outlet degassing results from pressure and temperature changes that occur on discharge flows from low-level outlets, such as turbines and spillways. Outlet degassing emissions are estimated by the multiplication of the difference in gas concentration between upstream (reservoir) and downstream the dam (just after outlet structures), and the water volume that passes through the hydraulic structures (Kemenes, Forsberg & Melack 2007; 2011; Abril et al. 2005).

Degassing emissions were reported for the Petit Saut (Abril et al. 2005), Balbina (Kemenes, Forsberg & Melack 2007; 2011), and Tucuruí (Fearnside 2002) reservoirs (See Table S15). Most of the available data come from the Petit Saut reservoir, where degassing emission stabilization occurred after three years of the impoundment for CH_4 and 5 years for CO_2 (Abril et al. 2005). Unfortunately, there are not sufficient data (6 and 9 data points, for CO_2 and CH_4, respectively) to develop robust probability functions for these degassing rates. Thus, we assumed uniform distributions defined by the maximum and minimum values from our degassing data points to describe the uncertain of $\mathbf{deg_{CO2}}$ and $\mathbf{deg_{CH4}}$. $\mathbf{deg_{CO2}}$ varied from 50 to 90 mg of CO_2 m^{-2} day^{-1} and $\mathbf{deg_{CH4}}$ range from 50 to 900 mg of CH_4 m^{-2} day^{-1} .

Table S15 - Outlet Degassing Emissions in tropical reservoirs

Reservoir	Age when sampled	Mean Flow (m^3/s)	Reservoir Area (km^2)	CO_2 Degassing (t C $year^{-1}$)	CO_2 Degassing per reservoir area (mg CO_2 $m^{-2}.day^{-1}$)	CH_4 Degassing (t C $year^{-1}$)	CH_4 Degassing per reservoir area (mg CH_4 $m^{-2}.day^{-1}$)	Reference
Balbina	18	577***	2360	41000	48	34000	53	Kemenes et al, 2007, 2011
Petit Saut*	3			-	-	15280	186	Abril et al, 2005
	4			-	-	15230	185	Abril et al, 2005
	5			10100	92	11320	138	Abril et al, 2005
	6	267***	300	7700	70	18460	225	Abril et al, 2005
	7			5300	48	9380	114	Abril et al, 2005
	8			7300	67	12570	153	Abril et al, 2005
	9			9300	85	5189	63	Abril et al, 2005
Tucuruí**	5	3558	2875	-		702000	892	Fearnside, 2002
Statistics			**Min.**		48		53	
			Max.		92		892	
			Average		68		223	
			Standard Deviation		17		242	
			n		6		9	

*Include emission from the turbines and weir

** Indirectly estimated based on CH_4 concentration profile made by Tundisi in 1989 (unpublished) profile and degassing proportions at Petit Saut (Fearnside, 2002)

*** Mean flows values from Guerin et al, 2006

In the case of low RT reservoirs in the Amazon, the only available data for degassing fluxes comes from the Santo Antônio reservoir. Degassing/downstream CH_4 emissions from the

Santo Antônio dam in the first year were estimated to be 5.6 Gg (Fearnside 2015b). Thus, we applied the Santo Antônio flux (75 mg of $CH_4.m^{-2}.day^{-1}$) to define **deg/down$_{CH4}$** in TD-low RT model. As previously mentioned, due to the high uncertainty of this value (Fearnside 2015b), we present the results with and without this flux.

Note that degassing emissions are reported in total annual mass of CO_2 and CH_4. To standardize the degassing emissions, we divided the total annual emissions by the reservoir area (Table S15). In Table S16, we standardized the degassing emission from Amazonian reservoirs using two different criteria: degassing per water volume and degassing per reservoir area.

Table S16 – Standardization methods for degassing

Reservoir	Reservoir Age	Area (km^2)	Degassing (Mg C yr^{-1})	Mean Flow (m^3/s)	CH_4 Degassing (mg CH_4 per m^{-3} of water)	CH_4 Degassing (mg CH_4 $m^{-2}day^{-1}$)	References
Balbina	18	2360	34000	577	2.49	53	Kemenes et al, 2007, 2011
Petit Saut	3		15280	267	2.42	186	Abril et al, 2005
	4		15230	267	2.41	185	Abril et al, 2005
	5		11320	267	1.79	138	Abril et al, 2005
	6	300	18460	267	2.92	225	Abril et al, 2005
	7		9380	267	1.49	114	Abril et al, 2005
	8		12570	267	1.99	153	Abril et al, 2005
	9		5189	267	0.82	63	Abril et al, 2005
Tucuruí	5	2875	702000	3558	8.34	892	Fearnside, 2002
Santo Antônio*	1	273	5569	18806	0.01	75	Fearnside, 2015

**CH_4 degassing/downstream emission corresponds to 35% of total emissions (15,911 Mg C/year)*

We applied the area instead of the flow as the standardization for the degassing fluxes because this method is more physically appropriate. Degassing emissions are linearly correlated to CO_2 and CH_4 concentration in the reservoir water (Abril et al. 2005). Moreover, the gas concentrations in the reservoir are highly correlated to the RT, which is a function of reservoir flow and volume. However, the most important issue here is not the volume of water, but the quantity of the CH_4 produced. CH_4 production is correlated with the C stock, which is a function of the reservoir area. Finally, the standardization by area was also applied in previous literature (Goldenfum 2010).

In terms of degassing per water volume, the results for the Santo Antônio reservoir are two orders of magnitude lower compared to the other high-RT reservoirs. This result is predictable given that degassing/downstream emissions are positively correlated to CH_4 concentration in the reservoir (Abril et al. 2005), and CH_4 concentration is expected to be lower in low RT reservoirs when compared to those concentrations in high RT reservoirs (DelSontro et al. 2010).

With respect to the standardization by area, the Santo Antônio reservoir flux has one of the lowest values, but in the same order of magnitude compared to the other dams. Given that the estimate is based on data collect in the first operational year and reservoir emissions decrease after the first few years (Abril et al. 2005; Demarty & Bastien 2011), the standardization by area also suggests that the degassing emissions in low-RT reservoirs are lower compared to high RT reservoirs.

6.3.3 Downstream Emissions ($down_{CO2}$ and $down_{Ch4}$)

The water that passes through the dam structures and runs through the rivers still contains dissolved and particulate organic C, as well as dissolved CO_2 and CH_4 that were not released by degassing immediately after the dam and are thus transferred downstream (Guérin et al. 2006; Kemenes, Forsberg & Melack 2007; 2011).

Table S17 presents downstream emission fluxes ($down_{CO2}$ and $down_{CH4}$). Direct measurements of downstream fluxes from dams in tropical forests are available within a distance of around 30 to 40 km after the dam at Balbina (Guérin et al. 2006; Kemenes, Forsberg & Melack 2007; 2011), Samuel, and Petit Saut (Guérin et al. 2006). The authors found that rivers downstream of dams contained high concentrations of CH_4 and CO_2 originating from reservoir hypolimnions (the bottom layer of an stratified reservoir). Diffusive fluxes in the river gradually release this CH_4 and CO_2. Downstream CH_4 and CO_2 fluxes were on average 165 and 7 times higher than diffusive and ebbulitive fluxes measured in the reservoir, respectively (Guérin et al. 2006). Downstream concentrations presented a decreasing trend as a function of distance, but the slope of the relation varied across the dams. CH_4 concentrations decreased faster than CO_2 (Guérin et al. 2006). We defined the model downstream boundary as 40 km downstream the dam because the available data is constrained to this range.

Table S17 - Average downstream emissions in forested tropical reservoirs. Values in the brackets represent the reported standard deviation or range.

Reservoir	Reservoir Area (km^2)	Age when Sampled (season)	River Downstream Emissions (mg CO_2 /m^2.day)	River Downstream Emissions (mg CH_4/m^2.day)	Reference
Petit Saut	270-365	9 (wet)	41580 (14960)	720 (544)	Guerin, 2006
Petit Saut	270-365	9 (dry)	36476 (9152)	944 (944)	Guerin, 2006
Petit Saut	270-365	11 (dry)	35288 (16016)	1344 (608)	Guerin, 2006
Petit Saut	270-365	11 (wet)	29480 (4180)	752 (432)	Guerin, 2006
Balbina	1770	17-19	17563	1690 (8-4608)	Kemenes, 2007, 2011
Balbina	1560 - 2360	17	18128 (4180)	1824 (1056)	Guerin, 2006
Samuel	180-559	16	65736 (42372)	192 (208)	Guerin, 2006
Statistics		**Min**	17563	192	
		Max	65736	1824	
		Average	34893	1067	
		Standard Deviation	16378	583	
		n	7	7	

The limitation of data points for outlet degassing and downstream emissions led to the adoption of a uniform distribution to represent the uncertainty and variability in these flux rates. The uniform distributions were limited by the maximum and minimum data values for each emission rate distribution. We applied these fluxes only for the high RT reservoirs.

6.3.4 Fitted distributions summary

Table S18 summarizes the probability distributions assigned to each input of the Monte Carlo Simulation.

Table S18 - Fitted distributions summary

Flux	Distribution	Parameters
res $_{CO2}$	Rayleigh	scale parameter (b) = 4589.8
res $_{CH4}$	Exponential	(scale parameter (m)= 51.6)
deg $_{CO2}$	Uniform	(max=90, min=50)
deg $_{CH4}$	Uniform	(max=900, min=50)
down $_{CO2}$	Uniform	(max=65,700, min=17,600)
down $_{CH4}$	Uniform	(max=1,800, min= 190)
nat $_{CO2}$ - Black Water	Rayleigh	(scale (b)= 1.78e+04)
nat $_{CO2}$ - Clear Water	Generalized Extreme Value	(shape (k) = 0.296; Location (μ)=2.82e+03; scale (σ) = 3.34e+03)
nat $_{CO2}$ - White Water	Rayleigh	(scale (b)= 1.6336e+04)
nat $_{CH4}$ - Black Water	Inverse Gaussian	(mean (m)= 7.18, shape (l)=3.88);
nat $_{CH4}$ - Clear Water	Inverse Gaussian	(mean (m)= 72.95, shape (l)=10.81)
nat $_{CH4}$ - White Water	Generalized Pareto	(shape (k) = 0.6947; scale (s) = 4.4007; thresholds (q)=0.0899)

6.4 Complementary Results and Discussion

Table S19 reports the average and 95% confidence interval from the Monte Carlo simulation outcomes in a hundred years (NRE). These results correspond to the same values presented in Figure 2-1 in Chapter 2.

Table S19 -Simulation results: average and 95% Confidence Interval (2.5% - 97.5%). Net reservoir emissions in a hundred years.

	Bottom-up			Top-Down		
	CO_2	*CH_4*	*Total*	*CO_2*	*CH_4*	*Total*
	Tg C	Tg C	Tg C	Tg C	Tg C	Tg C
Belo Monte	5.5 (4-7)	0.6 (0-1)	6 (5-8)	18 (0-66)	1.9 (1-6)	20 (1-67)
Bem Querer	8.0 (6-10)	1 (0-2)	9 (7-11)	29 (2-99)	2.2 (1-7)	31 (4-101)
C. do Caí*	9.7 (8-12)	0.8 (0-2)	11 (9-13)	22 (-5-54)	6.9 (2-12)	29 (1-62)
C. do Caldeirão	0.7 (0.6-1)	0.1 (0-0.2)	0.8 (0.6-1)	2 (0-6)	0.1 (0-0.2)	2 (0-7)
C. dos Patos*	2.1 (2-3)	0.2 (0-0.5)	2 (1.9-3)	11 (2-20)	2.1 (1-4)	13 (4-22)
Colíder	2.4 (2-3)	0.3 (0-1)	3 (2-3)	9 (1-29)	0.7 (0-2)	10 (2-30)
F. Gomes	0.2 (0-0.24)	0.03 (0-0.06)	0.2 (0-0.3)	1 (0-2)	0.05 (0-0.1)	1 (0-3)
Jamanxim*	1.6 (1-2)	0.2 (0-0.3)	1.8 (1-2)	9 (3-16)	1.5 (0-3)	11 (4-18)
Jatobá	5.4 (4-7)	0.6 (0-1)	6 (5-7)	18 (4-42)	2.1 (2-4)	20 (6-44)
Jirau	5.0 (4-6)	0.5 (0-1)	6 (4-7)	36 (11-71)	0.9 (1-1)	37 (12-72)
Marabá	12 (9-15)	1.5 (0-3)	13 (10-17)	45 (2-160)	3.9 (3-12)	49 (5-164)
Salto A. de Baixo	1.7 (1-2)	0.2 (0-0.4)	2 (2-2)	5 (1-14)	0.5 (0-1)	6 (1-15)
Santo Antônio	3.5 (3-4)	0.4 (0-1)	4 (3-5)	28 (8-56)	0.8 (0.7-1)	29 (9-57)
São L. do Tapajos	8.7 (7-11)	0.9 (0-2)	10 (8-12)	25 (6-66)	2.5 (2-5)	28 (8-68)
São Manoel	1.2 (1-1)	0.1 (0-0.3)	1 (1-2)	3 (0-11)	0.3 (0-1)	4 (1-12)
São Simão Alto	5.5 (5-7)	0.5 (0-1)	6 (5-7)	15 (3-40)	1.1 (1-3)	16 (4-41)
Sinop*	5.0(4-7)	0.7 (0-2)	6 (4-7)	24 (6-48)	5.4 (1-10)	30 (11-54)
Teles Pires	2.3 (2-3)	0.3 (0-1)	3 (2-3)	8 (1-22)	0.6 (0-2)	8 (2-23)

** indicate storage dams*

Table S20 and S21 present the annual average and 95% confidence interval from the Monte Carlo simulation outcomes according to the reservoir age for both TD and BU approaches. The decreasing emissions through the time are explained by the modeling assumptions described in this document. In the case of the TD approaches, the steady state assumption (6° to 100° year) and the multiplier factors assumed model the first pulse of emissions (1° to 5°) explain the emissions temporal variability. On the other hand, the decreasing degradation function (module 1 and 2) justifies the reduction of emission over time in the BU model. These tables underline the higher impact from hydropower plants in the first years of operation.

Table S20 – Annual average CH_4 emissions according to the reservoir age (Gg C)

Project		Age				
	Approach	**1-3**	**4-5**	**5 -10**	**10 -20**	**20 -100**
Belo Monte	TD	52 (36-155)	34 (24-104)	17 (12-52)	17 (12-52)	17 (12-52)
	BU	5 (1 - 13)	3 (0 - 7)	2 (0 - 4)	1 (0 - 2)	0.2 (0 - 0.4)
Bem Querer	TD	62 (39-185)	42 (26-123)	21 (13-62)	21 (13-62)	21 (13-62)
	BU	8 (1 - 21)	5 (1 - 12)	3 (1 - 7)	2 (0 - 4)	0.3 (0 - 0.6)
Cachoeira do Caí	TD	191 (46-338)	128 (31-225)	64 (15-113)	64 (15-113)	64 (15-113)
	BU	7 (1 - 18)	4 (1 - 10)	3 (0 - 6)	1 (0 - 3)	0.2 (0 - 1)
Cachoeira do Caldeirão	TD	4 (3-5)	3 (2-3)	1 (1-2)	1 (1-2)	1 (1-2)
	BU	1 (0 - 1)	0 (0 - 1)	0 (0 - 0)	0 (0 - 0)	0 (0 - 0)
Cachoeira dos Patos	TD	58 (16-100)	38 (11-67)	19 (5-33)	19 (5-33)	19 (5-33)
	BU	2 (0 - 5)	1 (0 - 3)	1 (0 - 2)	0 (0 - 1)	0.1 (0 - 0)
Colíder	TD	19 (12-54)	13 (8-36)	6 (4-18)	6 (4-18)	6 (4-18)
	BU	3 (0 - 7)	2 (0 - 4)	1 (0 - 2)	1 (0 - 1)	0.1 (0 - 0.2)
Ferreira Gomes	TD	1.4 (1-2)	0.9 (1-1)	0.5 (0-1)	0.5 (0-1)	0.5 (0-1)
	BU	0.2 (0 - 0.5)	0.1 (0 - 0.3)	0.1 (0 - 0.2)	0 (0 - 0.1)	0 (0 - 0)
Jamanxim	TD	42 (13-71)	28 (9-47)	14 (4-24)	14 (4-24)	14 (4-24)
	BU	1 (0 - 3)	1 (0 - 2)	0 (0 - 1)	0 (0 - 1)	0 (0 - 0.1)
Jatobá	TD	57 (45-100)	38 (30-67)	19 (15-33)	19 (15-33)	19 (15-33)
	BU	5 (1 - 13)	3 (0 - 8)	2 (0 - 4)	1 (0 - 2)	0.2 (0 - 0.4)
Jirau	TD	25 (21-36)	16 (14-24)	8 (7-12)	8 (7-12)	8 (7-12)
	BU	4 (1 - 11)	3 (0 - 6)	2 (0 - 4)	1 (0 - 2)	0.1 (0 - 0.3)
Marabá	TD	108 (71-331)	72 (48-221)	36 (24-110)	36 (24-110)	36 (24-110)
	BU	13 (2 - 32)	7 (1 - 19)	5 (1 - 11)	2 (0 - 6)	0.4 (0 - 1)
Salto Augusto de Baixo	TD	13 (9-31)	8 (6-21)	4 (3-10)	4 (3-10)	4 (3-10)
	BU	1 (0 - 4)	1 (0 - 2)	0.5 (0 - 1.2)	0.3 (0- 0.6)	0 (0 - 0.1)
Santo Antônio	TD	22 (19-32)	15 (12-21)	7 (6-11)	7 (6-11)	7 (6-11)
	BU	3 (1 - 8)	2 (0 - 5)	1.2 (0.2 - 2.7)	0.6 (0.1 - 1.4)	0.1 (0 - 0.2)
São Luís do Tapajos	TD	69 (50-141)	46 (33-94)	23 (17-47)	23 (17-47)	23 (17-47)
	BU	7 (1 - 19)	4 (1 - 11)	2.6 (0.5 - 6.1)	1.4 (0.3 - 3.1)	0.2 (0 - 0.6)
São Manoel	TD	7 (5-22)	5 (3-15)	2 (2-7)	2 (2-7)	2 (2-7)
	BU	1 (0 - 3)	1 (0 - 2)	0.4 (0.1 - 0.8)	0.2 (0 - 0.4)	0 (0 - 0.1)
São Simão Alto	TD	31 (20-78)	21 (13-52)	10 (7-26)	10 (7-26)	10 (7-26)
	BU	4 (1 - 11)	3 (0.4- 6)	1.6 (0.3 - 3.6)	0.8 (0.2 - 1.9)	0.1 (0 - 0.3)
Sinop	TD	150 (37-265)	100 (25-176)	50 (12-88)	50 (12-88)	50 (12-88)
	BU	6 (1 - 14)	3 (1 - 8)	2.1 (0.4 - 4.8)	1.1 (0.2 - 2.5)	0.2 (0 - 0.4)
Teles Pires	TD	17 (11-45)	11 (7-30)	6 (4-15)	6 (4-15)	6 (4-15)
	BU	2 (0 - 6)	1 (0 - 3)	0.8 (0.1 - 1.9)	0.4 (0.1 - 1)	0.1 (0 - 0.2)

Table S21– Annual average CO_2 emissions according to the reservoir age (Gg C)

Project	Approach	Age 1-3	4-5	5 -10	10 -20	20 -100
Belo Monte	TD	497 (-9-1824)	331 (-6-1216)	166 (-3-608)	166 (-3-608)	166 (-3-608)
	BU	31 (18 - 54)	20 (14 - 28)	16 (12 - 20)	12 (10 - 14)	1.9 (1.6 - 2.4)
Bem Querer	TD	808 (60-2745)	539 (40-1830)	269 (20-915)	269 (20-915)	269 (20-915)
	BU	49 (27 - 85)	31 (21 - 43)	23 (17 - 30)	17 (13 - 21)	3 (2 - 4)
Cachoeira do Caí	TD	606 (-149-1497)	404 (-99-998)	202 (-50-499)	202 (-50-499)	202 (-50-499)
	BU	50 (31 - 81)	34 (26 - 45)	28 (22 - 34)	22 (19 - 26)	3.6 (3 - 4)
Cachoeira do Caldeirão	TD	57 (8-177)	38 (5-118)	19 (3-59)	19 (3-59)	19 (3-59)
	BU	4 (2 - 6)	3 (2 - 3)	2 (2 - 3)	2 (1 - 2)	0.3 (0 - 0)
Cachoeira dos Patos	TD	295 (58-558)	197 (38-372)	98 (19-186)	98 (19-186)	98 (19-186)
	BU	12 (7 - 20)	8 (6 - 11)	6 (5 - 8)	5 (4 - 6)	0.8 (1 - 1)
Colíder	TD	263 (38-812)	175 (26-541)	88 (13-271)	88 (13-271)	88 (13-271)
	BU	15 (8 - 27)	9 (6 - 13)	7 (5 - 9)	5 (4 - 6)	0.8 (1 - 1)
Ferreira Gomes	TD	21 (2-69)	14 (1-46)	7 (1-23)	7 (1-23)	7 (1-23)
	BU	1.2 (0.6 - 2.1)	0.7 (0.5 - 1.1)	0.5 (0.4 - 0.7)	0.4 (0.3 - 0.5)	0.1 (0 - 0.1)
Jamanxim	TD	262 (76-452)	175 (51-301)	87 (25-151)	87 (25-151)	87 (25-151)
	BU	9 (5 - 14)	6 (4 - 8)	5 (4 - 6)	4 (3 - 4)	0.6 (0 - 1)
Jatobá	TD	489 (111-1163)	326 (74-775)	163 (37-388)	163 (37-388)	163 (37-388)
	BU	31 (18 - 54)	20 (14 - 28)	15 (12 - 20)	12 (9 - 14)	1.9 (2 - 2)
Jirau	TD	993 (297-1971)	662 (198-1314)	331 (99-657)	331 (99-657)	331 (99-657)
	BU	28 (16 - 47)	18 (13 - 25)	14 (11 - 18)	11 (9 - 13)	1.8 (2 - 2)
Marabá	TD	1242 (54-4431)	828 (36-2954)	414 (18-1477)	414 (18-1477)	414 (18-1477)
	BU	74 (40 - 130)	46 (31 - 66)	34 (25 - 45)	25 (20 - 30)	4.1 (3 - 5)
Salto Augusto de Baixo	TD	142 (27-397)	95 (18-264)	47 (9-132)	47 (9-132)	47 (9-132)
	BU	10 (6 - 16)	6 (5 - 9)	5 (4 - 6)	4 (3 - 5)	0.6 (1 - 1)
Santo Antônio	TD	783 (220-1559)	522 (146-1039)	261 (73-520)	261 (73-520)	261 (73-520)
	BU	20 (11 - 34)	13 (9 - 18)	10 (8 - 13)	8 (6 - 9)	1.2 (1 - 2)
São Luís do Tapajos	TD	706 (155-1834)	471 (103-1223)	235 (52-611)	235 (52-611)	235 (52-611)
	BU	48 (28 - 79)	32 (23 - 43)	25 (19 - 31)	19 (16 - 23)	3.2 (3 - 4)
São Manoel	TD	96 (12-318)	64 (8-212)	32 (4-106)	32 (4-106)	32 (4-106)
	BU	7 (4 - 11)	4 (3 - 6)	3 (3 - 4)	3 (2 - 3)	0.4 (0 - 1)
São Simão Alto	TD	417 (83-1112)	278 (55-741)	139 (28-371)	139 (28-371)	139 (28-371)
	BU	29 (18 - 49)	20 (14 - 27)	16 (13 - 20)	13 (11 - 15)	2 (2 - 2)
Sinop	TD	674 (161-1346)	449 (107-897)	225 (54-449)	225 (54-449)	225 (54-449)
	BU	32 (17 - 57)	20 (13 - 29)	14 (10 - 19)	10 (8 - 13)	1.7 (1 - 2)
Teles Pires	TD	219 (37-620)	146 (25-413)	73 (12-207)	73 (12-207)	73 (12-207)
	BU	14 (8 - 24)	9 (6 - 12)	6 (5 - 8)	5 (4 - 6)	0.8 (1 - 1)

Figure S11 presents the total net reservoir emission over a period for a hundred years in CO_2eq. The results illustrate the higher contribution of CH_4 to the potential climate impacts from these reservoirs compared to the total emissions in terms of C mass (Figure 2-1 in Chapter 2).

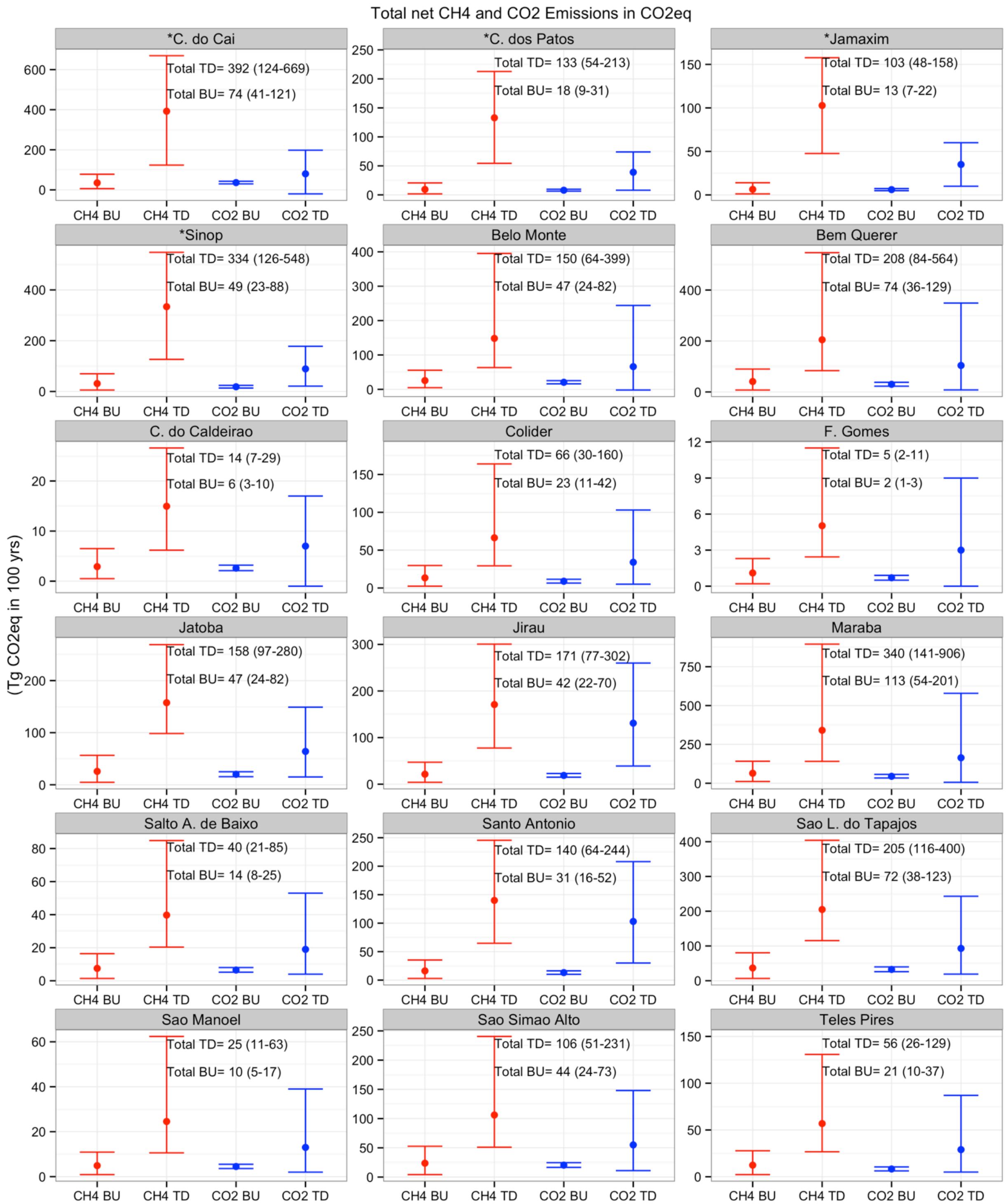

Figure S11 - Net reservoirs emissions in CO_2eq (methane GWP equals 34). Mean net GHG emission over 100 years (circle) and 95% confidence intervals (error bars). Black numbers represent the mean GHG net emissions and confidence intervals in parenthesis. (*) Indicates high RT reservoirs.

TD Approach Low RT Reservoirs

Figure S12 breaks down the contribution of each emission pathway to the net emissions (mean) for the top-down approach in low RT reservoirs and presents the results in total mass of C and in CO_2eq using methane GWP equal 86 (20-year) and 34 (100-year. It shows the gross fluxes from the reservoir system (Figures S12A, S12C and S12E) and the natural river system (Figures S12B, S12D and S12F).

In terms of C mass (Figures S12A and S12B), CO_2 emissions from the main channel and bays/tributaries are the largest contributors to C fluxes (reservoir system). On the other hand, when including the GWP as a metric for climate impacts, Figure S12C and S12F show that CH_4 fluxes account for the majority of the total emissions in CO_2 equivalents. In the average scenario, natural emissions before the impoundment account for 15% to 45% of the reservoir system emissions (comparing Figure S12A and S12B).

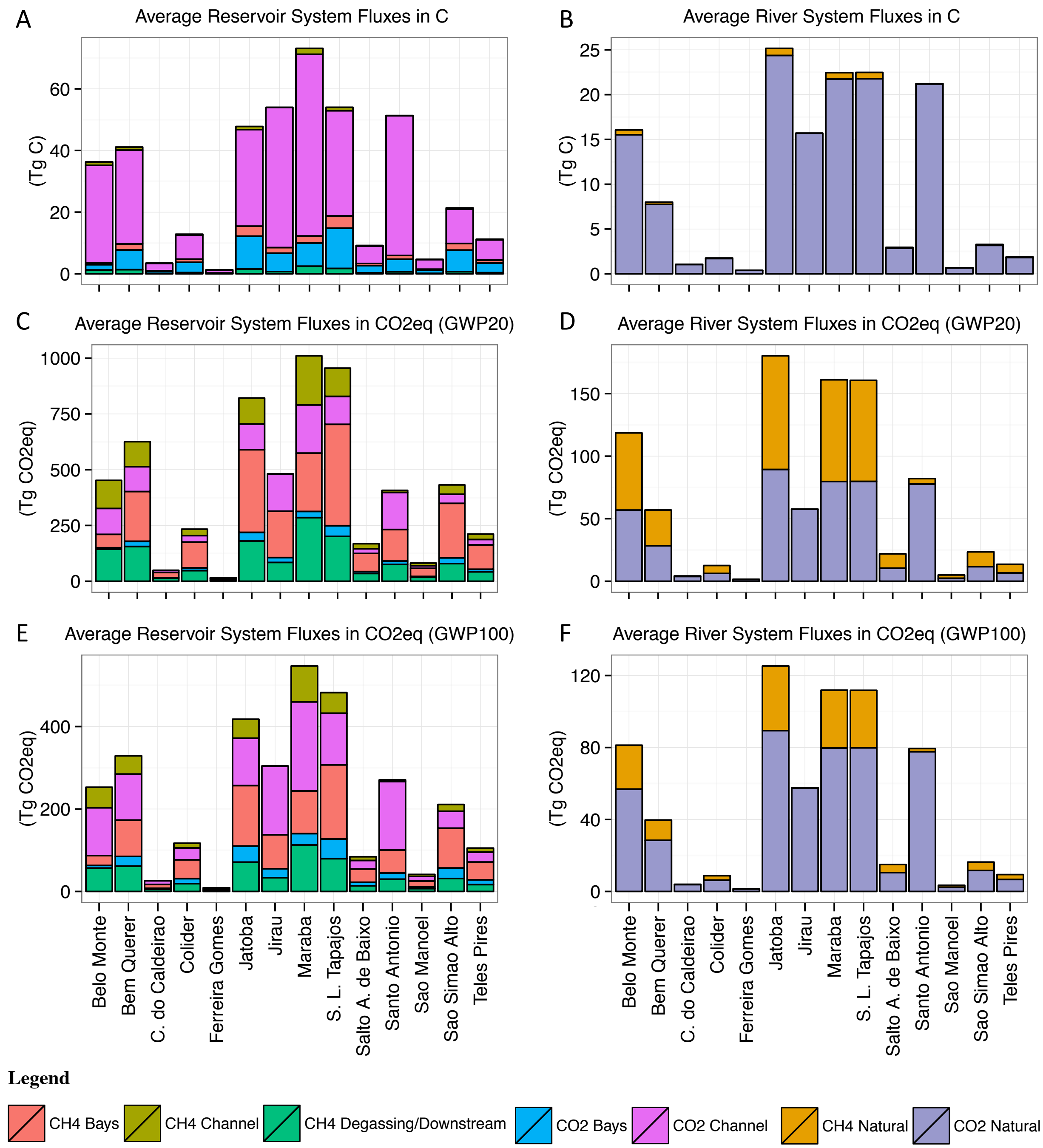

Figure S12: TD model mean results for the low residence time reservoirs in a hundred years by emission pathway. A- Reservoir system in C. B- River System (Natural Emissions) in C. C - Reservoir system in CO_2eq using the 20-year global warming potential (GWP) value for CH_4. D - River System in CO_2eq using the 20-year GWP value for CH_4. E - Reservoir system in CO_2eq using the 100-year GWP value for CH_4. F - River System in CO_2eq using the 100-year GWP value for CH_4.

6.4.1 Emission factors

Table S22 and S23 present the emission factor simulation results according to the reservoir age. Both approaches show the higher impact of hydropower in the first years of operation. Again, the model features and assumptions previously described in this document explain the decreasing emission factors according to the reservoir aging.

Table S22 – Annual emissions factors (kg CO_2eq MWh^{-1}) according to the reservoir age: average and 95% Confidence Interval (2.5% - 97.5%). Methane GPW equals 34.

		Age				
Project	Approach	**1-3**	**4-5**	**5 -10**	**10 -20**	**20 -100**
Belo Monte	TD	103 (44-274)	69 (29-183)	34 (15-91)	34 (15-91)	34 (15-91)
	BU	103 (39 - 217)	64 (27 - 127)	42 (20 - 77)	27 (15 - 44)	4 (2 - 8)
Bem Querer	TD	1668 (681-4450)	1112 (454-2966)	556 (227-1483)	556 (227-1483)	556 (227-1483)
	BU	1930 (697 - 4029)	1176 (476 - 2375)	770 (355 - 1408)	475 (253 - 796)	78 (40 - 139)
Cachoeira do Caí	TD	3031 (954-5171)	2021 (636-3448)	1010 (318-1724)	1010 (318-1724)	1010 (318-1724)
	BU	1672 (668 - 3385)	1056 (486 - 2021)	723 (388 - 1232)	484 (306 - 740)	79 (49 - 129)
Cachoeira do Caldeirão	TD	390 (161-693)	260 (107-462)	130 (54-231)	130 (54-231)	130 (54-231)
	BU	462 (177 - 958)	286 (125 - 569)	193 (97 - 345)	125 (74 - 198)	20 (12 - 35)
Cachoeira dos Patos	TD	2522 (1032-4037)	1681 (688-2691)	841 (344-1346)	841 (344-1346)	841 (344-1346)
	BU	1060 (401 - 2146)	654 (281 - 1302)	437 (217 - 776)	280 (162 - 453)	46 (26 - 79)
Colíder	TD	1249 (552-3087)	833 (368-2058)	416 (184-1029)	416 (184-1029)	416 (184-1029)
	BU	1453 (519 - 3020)	873 (343 - 1798)	563 (251 - 1057)	339 (172 - 588)	56 (27 - 104)
Ferreira Gomes	TD	106 (51-243)	71 (34-162)	35 (17-81)	35 (17-81)	35 (17-81)
	BU	129 (46 - 270)	78 (30 - 159)	50 (22 - 94)	30 (15 - 52)	5 (2 - 9)
Jamanxim	TD	695 (322-1066)	463 (215-711)	232 (107-355)	232 (107-355)	232 (107-355)
	BU	260 (103 - 526)	162 (73 - 319)	110 (57 - 194)	73 (44 - 114)	12 (7 - 20)
Jatobá	TD	390 (244-666)	260 (162-444)	130 (81-222)	130 (81-222)	130 (81-222)
	BU	370 (137 - 767)	226 (94 - 460)	150 (73 - 276)	94 (53 - 158)	16 (8 - 28)
Jirau	TD	248 (113-436)	165 (75-291)	83 (38-145)	83 (38-145)	83 (38-145)
	BU	187 (72 - 380)	116 (50 - 227)	78 (39 - 137)	50 (29 - 80)	8 (5 - 14)
Marabá	TD	921 (380-2420)	614 (254-1613)	307 (127-807)	307 (127-807)	307 (127-807)
	BU	995 (362 - 2108)	602 (243 - 1245)	392 (179 - 734)	240 (125 - 404)	40 (20 - 71)
Salto Augusto de Baixo	TD	159 (82-340)	106 (54-227)	53 (27-113)	53 (27-113)	53 (27-113)
	BU	180 (68 - 370)	111 (48 - 220)	74 (37 - 132)	48 (28 - 76)	8 (4 - 13)
Santo Antônio	TD	216 (100-379)	144 (67-252)	72 (33-126)	72 (33-126)	72 (33-126)
	BU	148 (55 - 304)	91 (38 - 183)	60 (29 - 108)	38 (22 - 62)	6 (3 - 11)
São Luís do Tapajos	TD	206 (116-406)	137 (77-270)	69 (39-135)	69 (39-135)	69 (39-135)
	BU	223 (85 - 452)	138 (59 - 275)	93 (46 - 166)	60 (35 - 96)	10 (6 - 17)
São Manoel	TD	215 (93-546)	143 (62-364)	72 (31-182)	72 (31-182)	72 (31-182)
	BU	265 (100 - 549)	164 (72 - 322)	110 (56 - 194)	72 (43 - 114)	12 (7 - 20)
São Simão Alto	TD	175 (84-398)	117 (56-265)	58 (28-133)	58 (28-133)	58 (28-133)
	BU	218 (86 - 437)	136 (61 - 263)	92 (48 - 161)	61 (37 - 96)	10 (6 - 16)
Sinop	TD	5283 (2001-8670)	3522 (1334-5780)	1761 (667-2890)	1761 (667-2890)	1761 (667-2890)
	BU	2579 (929 - 5337)	1550 (604 - 3192)	1003 (445 - 1874)	605 (307 - 1041)	100 (49 - 182)
Teles Pires	TD	184 (87-424)	123 (58-282)	61 (29-141)	61 (29-141)	61 (29-141)
	BU	215 (78 - 451)	131 (53 - 271)	86 (40 - 160)	53 (28 - 90)	9 (5 - 16)

For these calculations, we assumed that the emissions from the cleared vegetation (BU – Module 3) are uniformly released within a period of 30 years.

Table S23 – Annual emissions factor (kg CO_2eq MWh^{-1}) according to the reservoir age: average and 95% Confidence Interval (2.5% - 97.5%). Methane GPW equals 86.

		Age				
Project	Approach	**1-3**	**4-5**	**5 -10**	**10 -20**	**20 -100**
Belo Monte	TD	190 (110-490)	130 (73-320)	64 (36-160)	64 (36-160)	64 (36-160)
	BU	210 (58 - 489)	127 (38 - 286)	81 (28 - 165)	47 (19 - 90)	8 (3 - 16)
Bem Querer	TD	2900 (1600-7800)	2000 (1000-5200)	980 (521-2600)	980 (521-2600)	980 (521-2600)
	BU	3966 (1102 - 9166)	2385 (705 - 5387)	1502 (501 - 3106)	868 (334 - 1658)	143 (53 - 293)
Cachoeira do Caí	TD	6800 (2000-12000)	4500 (1300-7700)	2300 (670-3800)	2300 (670-3800)	2300 (670-3800)
	BU	3269 (943 - 7533)	2007 (649 - 4491)	1303 (495 - 2619)	798 (364 - 1451)	132 (58 - 256)
Cachoeira do Caldeirão	TD	700 (400-1200)	470 (270-800)	230 (134-400)	230 (134-400)	230 (134-400)
	BU	929 (256 - 2161)	561 (171 - 1268)	360 (129 - 742)	215 (91 - 399)	35 (14 - 70)
Cachoeira dos Patos	TD	5300 (1900-8600)	3500 (1300-5700)	1800 (640-2900)	1800 (640-2900)	1800 (640-2900)
	BU	2122 (595 - 4926)	1286 (396 - 2884)	821 (289 - 1672)	487 (201 - 925)	80 (32 - 164)
Colíder	TD	2100 (1200-5000)	1400 (790-3300)	710 (395-1700)	710 (395-1700)	710 (395-1700)
	BU	2963 (783 - 6901)	1774 (494 - 4001)	1111 (349 - 2314)	635 (229 - 1237)	105 (36 - 217)
Ferreira Gomes	TD	180 (120-320)	120 (79-210)	59 (40-110)	59 (40-110)	59 (40-110)
	BU	265 (69 - 619)	159 (44 - 366)	100 (31 - 209)	57 (20 - 110)	9 (3 - 19)
Jamanxim	TD	1400 (570-2200)	940 (380-1500)	470 (190-740)	470 (190-740)	470 (190-740)
	BU	523 (146 - 1190)	318 (98 - 708)	204 (74 - 414)	123 (53 - 227)	20 (9 - 40)
Jatobá	TD	740 (530-1200)	500 (360-810)	250 (178-410)	250 (178-410)	250 (178-410)
	BU	753 (205 - 1741)	455 (133 - 1031)	288 (98 - 593)	169 (67 - 323)	28 (11 - 56)
Jirau	TD	340 (190-530)	230 (130-350)	110 (64-180)	110 (64-180)	110 (64-180)
	BU	373 (106 - 857)	227 (70 - 503)	145 (52 - 294)	86 (37 - 161)	14 (6 - 28)
Marabá	TD	1600 (900-4300)	1100 (600-2900)	550 (300-1400)	550 (300-1400)	550 (300-1400)
	BU	2029 (536 - 4777)	1217 (345 - 2787)	765 (246 - 1593)	441 (164 - 863)	73 (26 - 150)
Salto Augusto de Baixo	TD	280 (180-610)	190 (120-410)	95 (59-200)	95 (59-200)	95 (59-200)
	BU	358 (100 - 838)	217 (66 - 485)	139 (49 - 282)	83 (35 - 154)	14 (6 - 27)
Santo Antônio	TD	300 (180-470)	200 (120-310)	100 (60-160)	100 (60-160)	100 (60-160)
	BU	298 (82 - 698)	181 (53 - 408)	115 (39 - 236)	67 (27 - 127)	11 (4 - 22)
São Luís do Tapajos	TD	380 (250-700)	250 (170-470)	130 (84-230)	130 (84-230)	130 (84-230)
	BU	441 (125 - 1031)	267 (84 - 588)	171 (62 - 344)	102 (43 - 189)	17 (7 - 34)
São Manoel	TD	380 (200-1000)	250 (130-660)	130 (67-330)	130 (67-330)	130 (67-330)
	BU	524 (149 - 1225)	318 (101 - 706)	204 (74 - 415)	122 (52 - 226)	20 (8 - 40)
São Simão Alto	TD	310 (180-690)	200 (120-460)	100 (59-230)	100 (59-230)	100 (59-230)
	BU	434 (127 - 1001)	265 (85 - 589)	171 (64 - 346)	103 (46 - 191)	17 (7 - 33)
Sinop	TD	11000 (3700-19000)	7500 (2500-13000)	3800 (1200-6300)	3800 (1200-6300)	3800 (1200-6300)
	BU	5296 (1401 - 12231)	3160 (895 - 7133)	1981 (624 - 4137)	1135 (408 - 2206)	188 (64 - 394)
Teles Pires	TD	320 (180-760)	210 (120-500)	110 (60-250)	110 (60-250)	110 (60-250)
	BU	436 (118 - 1033)	262 (76 - 602)	166 (55 - 345)	96 (37 - 185)	16 (6 - 33)

For these calculations, we assumed that the emissions from the cleared vegetation (BU – Module 3) are uniformly released within a period of 30 years.

6.4.2 The importance of vegetation clearing

To investigate the importance of vegetation clearing in the GHG emissions from Amazon reservoirs, we compared the emissions results from each BU approach module. Table S24 presents the simulation mean and 95% confidence interval in total mass of C for each module: only flooded soils, only flooded foliage, and cleared vegetation.

Table S24 – Total reservoir emissions over a 100-years in terms of carbon mass: average and 95% Confidence Interval (2.5% - 97.5%) according to the carbon stock.

	Only flooded soils (Module 1)		Only flooded foliage (Module 2)		Cleared Vegetation (Module 3)	Total
	CH_4	*CO_2*	*CH_4*	*CO_2*	*CO_2*	*Total*
Projects	Tg C	Tg C	Tg C	Tg C	Tg C	Tg C
Belo Monte	0.5 (0-1)	2.3 (1-3)	0.1 (0-0.3)	0.65 (0.6-0.7)	2 (2-3)	6 (5-8)
Bem Querer	0.7 (0-2)	3.8 (2-5)	0.2 (0-0.5)	1.03 (1-1.1)	3.2 (3-4)	9 (7-11)
Cachoeira do Caí	0.6 (0-1)	3.2 (2-5)	0.2 (0-0.5)	0.88 (0.8-0.9)	5.6 (5-6)	11 (9-13)
Cachoeira do Caldeirão	0.1 (0-0.1)	0.3 (0-0)	0.02 (0-0.04)	0.07 (0.1-0.1)	0.36 (0.3-0.4)	0.8 (0.6-1)
Cachoeira dos Patos	0.2 (0-0.4)	0.9 (1-1)	0.06 (0-0.1)	0.24 (0.2-0.2)	1 (0.9-1.2)	2 (1.9-3)
Colíder	0.2 (0-1)	1.2 (1-2)	0.1 (0-0.2)	0.35 (0.3-0.4)	0.8 (0.7-0.9)	3 (2-3)
Ferreira Gomes	0.02 (0-0.04)	0.1 (0.06-0.14)	0.01 (0-0.01)	0.03 (0-0)	0.06 (0.05-0.1)	0.2 (0-0.3)
Jamanxim	0.1 (0-0.3)	0.6 (0-1)	0.04 (0-0.1)	0.16 (0.2-0.2)	0.9 (0.8-0.96)	1.8 (1-2)
Jatobá	0.5 (0-1)	2.4 (1-3)	0.2 (0-0.3)	0.64 (0.6-0.8)	2.4 (2.1-2.6)	6 (5-7)
Jirau	0.4 (0-1)	2 (1-3)	0.1 (0-0.3)	0.54 (0.5-0.6)	2.5 (2.3-2.8)	6 (4-7)
Marabá	1.2 (0-3)	5.8 (4-8)	0.4 (0.1-0.9)	1.62 (1.4-1.8)	4.5 (4-5)	13 (10-17)
Salto Augusto de Baixo	0.1 (0-0.3)	0.7 (0-1)	0.04 (0-0.1)	0.19 (0.2-0.2)	0.9 (0.8-1)	2 (2-2)
Santo Antônio	0.3 (0-1)	1.5 (1-2)	0.1 (0-0.2)	0.41 (0.4-0.4)	1.6 (1-2)	4 (3-5)
São Luis do Tapajos	0.7 (0-1)	3.3 (2-5)	0.2 (0-0.5)	0.93 (0.9-1)	4.5 (4-5)	10 (8-12)
São Manoel	0.1 (0-0.2)	0.5 (0-1)	0.03 (0-0.1)	0.13 (0.1-0.1)	0.63 (0.6-0.7)	1 (1-2)
São Simão Alto	0.4 (0-1)	2 (1-3)	0.1 (0-0.3)	0.55 (0.5-0.6)	3 (2.7-3.3)	6 (5-7)
Sinop	0.5 (0-1)	2.6 (2-4)	0.2 (0-0.4)	0.73 (0.6-0.8)	1.7 (1-2)	6 (4-7)
Teles Pires	0.2 (0-0)	1 (1-1)	0.1 (0-0.2)	0.29 (0.3-0.3)	0.9 (0.8-1)	3 (2-3)

Compared to the emissions from soils only, Table S24 results show that the flooded foliage contributes to an average increase of 33% and 28% of the CH_4 and CO_2 emissions, respectively. These results underline the importance of the vegetation clearing requirement and the effect of an inefficient biomass removal. CO_2 emissions from the cleared vegetation are in the same order of magnitude compared to the CO_2 emissions from soils alone, representing a significant component of the budget.

Table S25 shows the effect of flooded foliage and vegetation clearing on the emissions factors of each reservoir. Compared to the C in the soils only, Table S25 results indicate the emission factors increase on average 64% when taking into account the emissions from flooded foliage and cleared biomass.

Table S25 – Total reservoir emissions over a 100-years in terms CO_2eq: average and 95% Confidence Interval (2.5% - 97.5%) according to the carbon stock. GWP equal 34 (100 years)

	Flooded soils only		Flooded soils and foliage, plus cleared biomass	
	Total	Average Emission Factor	*Total*	Average Emission Factor
Projects	Tg CO_2eq	kg CO_2eq MWh^{-1}	Tg CO_2eq	kg CO_2eq MWh^{-1}
Belo Monte	29 (11-55)	7 (3-14)	47 (24-82)	12 (6-21)
Bem Querer	47 (18-89)	138 (54-261)	74 (36-129)	216 (104-377)
Cachoeira do Caí	40 (16-76)	112 (44-211)	74 (41-121)	205 (115-336)
Cachoeira do Caldeirão	3 (1-6)	32 (12-60)	6 (3-10)	54 (29-93)
Cachoeira dos Patos	11 (4-21)	74 (29-140)	18 (9-31)	123 (64-209)
Colíder	15 (6-30)	105 (41-200)	23 (11-42)	158 (74-283)
Ferreira Gomes	1 (0-2)	9 (4-18)	2 (1-3)	14 (7-25)
Jamanxim	7 (3-14)	18 (7-34)	13 (7-22)	31 (17-52)
Jatobá	29 (12-57)	26 (10-50)	47 (24-82)	42 (21-73)
Jirau	25 (10-47)	13 (5-24)	42 (22-70)	22 (11-37)
Marabá	74 (28-139)	72 (27-135)	113 (54-201)	110 (53-196)
Salto Augusto de Baixo	9 (3-16)	12 (5-23)	14 (8-25)	21 (11-36)
Santo Antônio	19 (7-35)	10 (4-20)	31 (16-52)	17 (9-29)
São Luis do Tapajos	42 (16-81)	15 (6-29)	72 (38-123)	26 (14-45)
São Manoel	6 (2-11)	18 (7-34)	10 (5-17)	31 (16-53)
São Simão Alto	25 (10-47)	15 (6-28)	44 (24-73)	26 (14-44)
Sinop	33 (13-62)	187 (73-354)	49 (23-88)	281 (132-501)
Teles Pires	13 (5-25)	15 (6-29)	21 (10-37)	24 (12-43)

With respect to vegetation clearing, the following mitigation measures are recommended:

1. Instead of burning or burying the cleared vegetation, the wood resources should only be employed in low decay end uses such as construction material and furniture.
2. The reforestation of a previously deforested area with at least the same size of the reservoir area to replace the C stock lost by the vegetation clearing.
3. Improve the enforcement of the vegetation clearing and authorize the reservoir filling just after a complete biomass removal including leaves and small foliage.

4. Vegetation clearing should take place just before the reservoir filling starts in order to reduce the period for biomass regrowth in the reservoir area.

6.4.3 Sensitivity Analysis: reservoir area from projects with storage capacity

The reservoir surface area (A_{RES}) is a source of uncertainty for storage reservoirs because of the seasonal water level variation related to variability of river flows and reservoir operation. A_{RES} variations can affect our estimates, particularly the TD approach, where A_{RES} is an important input to scale the GHG fluxes.

In the case of the BU approach, the periodical variation of the reservoir level may affect the proliferation of biomass in the drawdown zone, annually increasing the flooded C stock available for CH_4 production. The variation of the reservoir area, however, does not affect the initial C stock assessed by the BU model as the C stock available continues to be defined by the maximum water level. At this point, we cannot estimate the seasonal increment of the biomass in the drawdown zones because of lack of studies regarding the specific contribution related to these areas. The TD model estimates, however, indirectly account for these inputs because the probability distributions for the TD model are based on measurements in the air/water interface, which captures emissions from all input sources, including the upstream and lateral inputs, such as the biomass from drawdown zones.

To evaluate the effect of the variation of the A_{RES} in the TD model, we performed a sensitivity analysis using an alternative reference value to define the A_{RES}. Table S26 present the sensitivity analysis results using two reservoir areas: at the normal maximum (baseline), and at normal average water level (see Table S10 for details). As expected, Table S26 shows that the use of a lower reservoir area leads to lower emissions. However, the variation of the surface area does not change the conclusion about the high level of emissions from these reservoirs, which are comparable to those of thermal power plants.

Table S26 - Sensitivity Analysis results for storage reservoirs. Simulation results over a period of 100 years: average and 95% Confidence Interval (2.5% - 97.5%). GWP equals 34.

	Normal Maximum Water Level					Normal Average Water Level				
	CO_2	*CH_4*	*Total*	*Total*	*Emission Factor*	*CO_2*	*CH_4*	*Total*	*Total*	*Emission Factor*
Projects	Tg C	Tg C	Tg C	Tg CO_2eq	kg CO_2eq MWh^{-1}	Tg C	Tg C	Tg C	Tg CO_2eq	kg CO_2eq MWh^{-1}
Cachoeira do Caí	22	7	29	392	1000 (320-1,700)	19	6	25	353	910 (280-1,500)
Cachoeira dos Patos	11	2	13	133	840 (340-1,300)	9	2	11	111	700 (290-1,100)
Sinop	24	5	30	334	1800 (670-2,900)	16	3	19	213	1100 (440-1,800)

6.4.4 Sensitivity Analysis: degassing/downstream fluxes in low RT reservoirs

Because only one estimate from Santo Antônio reservoirs (Fearnside 2015b) is available for modeling the degasing/downstream fluxes in low RT reservoirs (TD approach), we present the results for low RT reservoir with and without the degassing/downstream estimate. Table S27 presents the results in terms of mass of C and Table S28 presents the effect of degassing in CO_2eq. The results show that degassing/downstream emissions can be an important part of the budget for low RT reservoirs. Nevertheless, more data are necessary to confirm the contribution of these pathways in low RT reservoirs.

Table S27 - Degassing/downstream sensitivity analysis of total emission fluxes for low RT reservoirs. Simulation results over a period of 100 years: average and 95% Confidence Interval (2.5% - 97.5%).

Projects	**Reservoir Surface Emissions**		**Degassing/ downstream**	**Total with degassing/ downstream**	**Total without degassing/ downstream**
	CO_2 Tg C	*CH_4* Tg C	*CH_4* Tg C	*Total* Tg C	*Total* Tg C
Belo Monte	18 (0-66)	0.6 (0-4.3)	1.25	20 (1-67)	18 (0-66)
Bem Querer	29 (2-99)	0.9 (0.1-5.3)	1.36	31 (4-100)	30 (3-99)
Cachoeira do Caldeirão	2 (0-6.4)	0 (0-0.1)	0.12	2.2 (0-6.5)	2.1 (0-6.4)
Colíder	9.5 (1-29)	0.3 (0-1.5)	0.42	10 (2-30)	9.7 (2-30)
Ferreira Gomes	0.75 (0-2.5)	0.01 (0-0.02)	0.04	0.8 (0-2.5)	0.76 (0-2.5)
Jatobá	18 (4-42)	0.5 (0-2)	1.57	20 (6-44)	18 (4-42)
Jirau	36 (11-71)	0.1 (0-0.5)	0.74	37 (12-72)	36 (11-71)
Marabá	45 (2-160)	1.4 (0.1-9.4)	2.49	49 (5-160)	46 (3-160)
Salto Augusto de Baixo	5.1 (1-14)	0.2 (0-0.8)	0.30	5.6 (1-15)	5.3 (1-14)
Santo Antônio	28 (8-56)	0.1 (0-0.5)	0.66	29 (9-57)	28 (8-56)
São Luís do Tapajos	25 (6-66)	0.7 (0.1-3.3)	1.76	28 (8-68)	26 (6-66)
São Manoel	3.5 (0-11)	0.1 (0-0.6)	0.16	3.7 (1-12)	3.6 (1-12)
São Simão Alto	15 (3-40)	0.4 (0-2.1)	0.69	16 (4-41)	15 (3-41)
Teles Pires	7.9 (1-22)	0.2 (0-1.3)	0.37	8.5 (2-23)	8.1 (2-22)

Table S28 - Degassing/downstream sensitivity analysis of the emission factor for low RT reservoirs. Simulation results over a period of 100 years: average and 95% Confidence Interval (2.5% - 97.5%). Methane GWP equals 34.

	Emission Factor with degassing/downstream kg CO_2eq MWh^{-1}	**Emission factor without degassing/downstream** kg CO_2eq MWh^{-1}
Belo Monte	35 (15-92)	21 (2-79)
Bem Querer	570 (227-1500)	400 (60-1400)
Cachoeira do Caldeirão	120 (61-260)	73 (15-210)
Colíder	420 (186-1000)	300 (67-880)
Ferreira Gomes	35 (17-80)	21 (3-66)
Jatobá	130 (80-230)	71 (21-170)
Jirau	83 (37-150)	67 (21-130)
Marabá	310 (127-820)	200 (25-710)
Salto Augusto de Baixo	53 (28-110)	35 (9-95)
Santo Antônio	72 (33-130)	56 (17-110)
São Luís do Tapajos	69 (39-130)	42 (12-110)
São Manoel	72 (31-190)	52 (10-160)
São Simão Alto	58 (28-130)	41 (11-110)
Teles Pires	61 (29-140)	43 (10-120)

6.4.5 Sensitivity Analysis: effect of including data outlier from Samuel

Based on the statistical analysis of the data and the weather conditions reported during the sampling, we considered the diffusion point from Samuel reservoir at 16 years old an outlier. The goal of this section is to evaluate the influence of this outlier in our results and conclusions.

The inclusion of the outlier changes the best distribution for reservoir surface CO_2 emissions for both model selection criteria (Akaike information criterion and Bayesian information criterion). Instead of the Rayleigh distribution (scale parameter: 4589.8), the best distribution is a log-logistic distribution (parameters: location = 8.53, scale = 0.46). Table S29 shows the effect of the inclusion of this outlier in total CO_2 emissions. As expected, the inclusion of the outlier and the change in the probability distribution affects our estimates, because the log-logistic distribution is more skewed to the right than the Rayleigh distribution. As a result, the main effect of the shift happens to the upper bound confidence interval. The effect in the upper bound is only substantial for Cachoeira do Caí, Cachoeira do Caldeirão, Cachoeira dos Patos and Sinop.

Table S29 - Sensitivity analysis of the impact of Samuel outliers in total CO_2 emissions. Simulation results over a period of 100 years (in Tg of C): mean, median and 95% Confidence Interval (2.5% - 97.5%).

	Without Samuel at 16 years old				**With Samuel at 16 years old**			
	Mean	Median	2.5% CI	97.5% CI	Mean	Median	2.5% CI	97.5% CI
Belo Monte	18	13	0	66	18	13	0	68
Bem Querer	29	22	2	99	30	23	2	100
Cachoeira do Caí	22	21	0	54	29	20	0	120
Cachoeira do Caldeirão	2	2	0	6	3	2	0	11
Cachoeira dos Patos	11	10	2	20	13	10	2	38
Colíder	9	8	1	29	10	8	1	33
Ferreira Gomes	1	1	0	2	1	1	0	3
Jamanxim	9	9	3	16	11	9	3	27
Jatobá	18	16	4	42	21	16	4	64
Jirau	36	34	11	71	38	35	10	77
Marabá	45	33	2	160	47	35	1	163
Salto Augusto de Baixo	5	4	1	14	6	5	1	19
Santo Antônio	28	27	8	56	29	27	8	61
São Luís do Tapajos	25	22	6	66	29	23	5	92
São Manoel	3	3	0	11	4	3	0	12
São Simão Alto	15	13	3	40	17	13	3	55
Sinop	24	23	6	48	30	22	6	101
Teles Pires	8	7	1	22	9	7	1	29

Table S30 and Table S31 show the effect of the outlier inclusion in total net reservoir emissions and emission factors, respectively. The results confirm that the only significant effect in the emissions output happens only to the upper bound 95% confidence interval. The outlier inclusion does not change our conclusions about the level of emissions from each reservoir compared to thermal power plants.

Table S30 - Sensitivity analysis of the impact of Samuel outliers in total net reservoir GHG emissions. Simulation results over a period of 100 years (in Tg of CO_2eq): average, median and 95% Confidence Interval (2.5% - 97.5%).

	Without Samuel at 16 years old				**With Samuel at 16 years old**			
	Mean	Median	2.5% CI	97.5% CI	Mean	Median	2.5% CI	97.5% CI
Belo Monte	150	123	64	399	150	125	64	400
Bem Querer	208	171	84	564	212	176	85	565
Cachoeira do Caí	392	393	124	669	419	406	117	814
Cachoeira do Caldeirão	14	12	7	29	18	14	6	47
Cachoeira dos Patos	133	133	54	213	140	137	52	252
Colíder	66	57	30	160	70	59	29	179
Ferreira Gomes	5	4	2	11	5	4	2	12
Jamanxim	103	103	48	158	107	106	48	181
Jatobá	158	149	97	280	170	151	96	350
Jirau	171	165	77	302	178	169	76	323
Marabá	340	280	141	906	349	288	141	920
Salto Augusto de Baixo	40	35	21	85	42	37	20	97
Santo Antônio	140	135	64	244	145	137	63	263
São Luís do Tapajos	205	190	116	400	220	192	114	490
São Manoel	25	21	11	63	26	22	10	67
São Simão Alto	106	95	51	231	114	97	50	283
Sinop	334	333	126	548	354	345	120	668
Teles Pires	56	49	26	129	60	51	26	150

Table S31 - Sensitivity analysis of the impact of Samuel outliers in the emission factors. Simulation results over a period of 100 years (in Tg of CO_2eq): average, median and 95% Confidence Interval (2.5% - 97.5%).

	Without Samuel at 16 years old				**With Samuel at 16 years old**			
	Mean	Median	2.5% CI	97.5% CI	Mean	Median	2.5% CI	97.5% CI
Belo Monte	35	28	15	92	35	29	15	92
Bem Querer	565	465	227	1530	576	479	229	1533
Cachoeira do Caí	1010	1011	318	1724	1078	1045	301	2097
Cachoeira do Caldeirão	119	107	61	256	152	124	53	408
Cachoeira dos Patos	841	841	344	1346	886	865	330	1594
Colíder	416	357	186	1002	440	369	181	1125
Ferreira Gomes	35	31	17	80	37	32	17	87
Jamanxim	232	232	107	355	242	238	108	408
Jatobá	130	123	80	231	140	125	79	289
Jirau	83	80	37	146	86	82	37	156
Marabá	306	252	127	816	315	259	127	829
Salto Augusto de Baixo	53	47	28	113	57	49	27	130
Santo Antônio	72	70	33	126	74	70	33	135
São Luís do Tapajos	69	64	39	134	74	64	38	164
São Manoel	72	60	31	185	75	63	30	196
São Simão Alto	58	52	28	127	63	54	27	156
Sinop	1761	1758	667	2890	1868	1818	633	3523
Teles Pires	61	53	29	139	65	55	28	162

6.4.6 Energy density vs. emission factor

Figures S13 and S14 confirms that the relationship between energy density and emissions factors is strong and negatively correlated. The use of both approaches provides a reasonable range of values for comparing futures reservoir emissions in the Amazon with those from other sources of electricity generation.

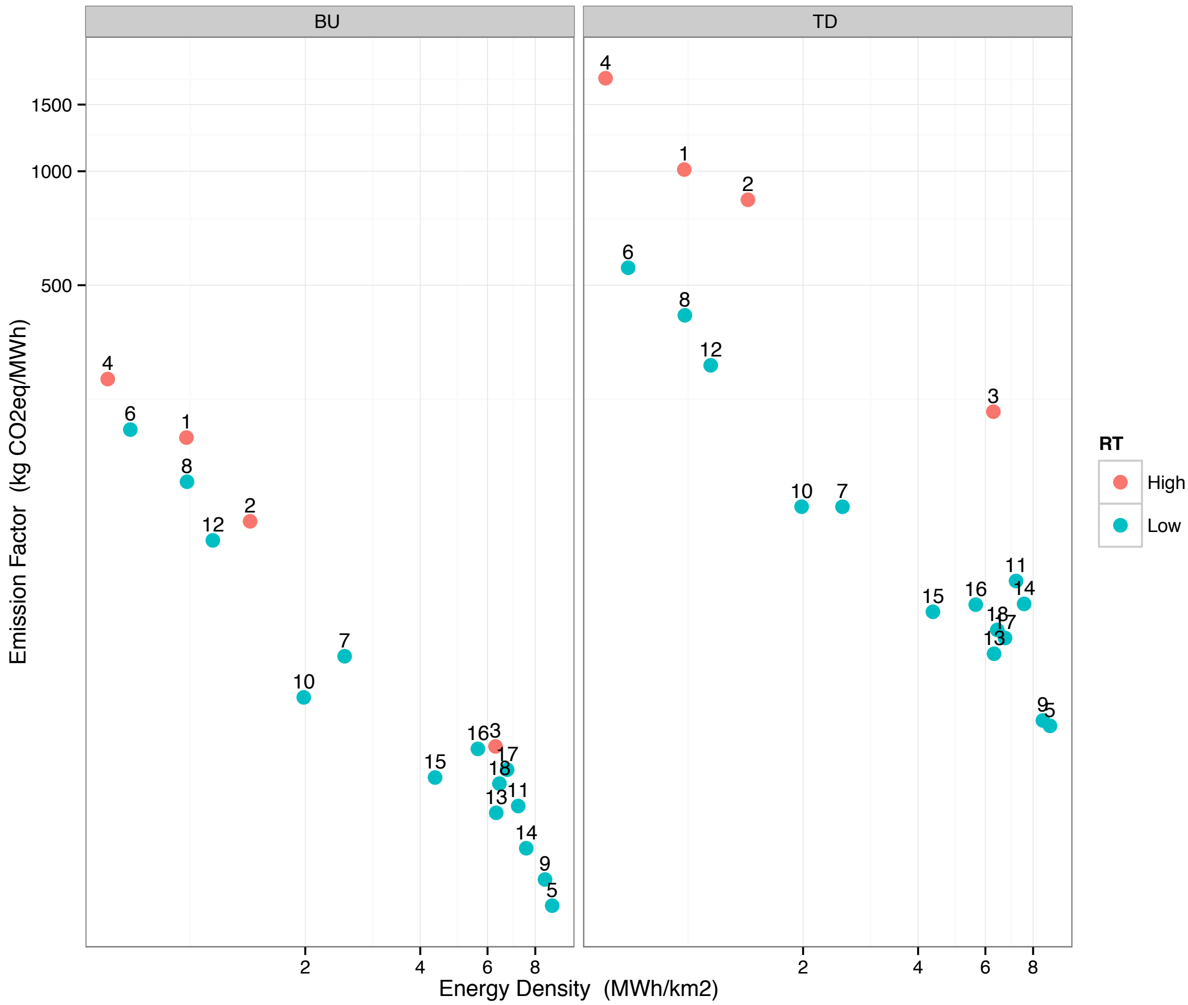

Figure S13 – Average emission factor (over 100 years period, GWP -34) plotted against energy density from each studied reservoirs. Number Identification: 1 - C. do Caí, 2 - C. dos Patos, 3 – Jamanxim, 4 – Sinop, 5 - Belo Monte, 6 - Bem Querer, 7 - C. do Caldeirão, 8 – Colíder, 9 - F. Gomes, 10 – Jatobá, 11 – Jirau , 12 – Marabá, 13 - Salto A. de Baixo, 14 - Santo Antônio, 15 - São L. do Tapajos, 16 - São Manoel, 17 - São Simão Alto, 18 - Teles Pires.

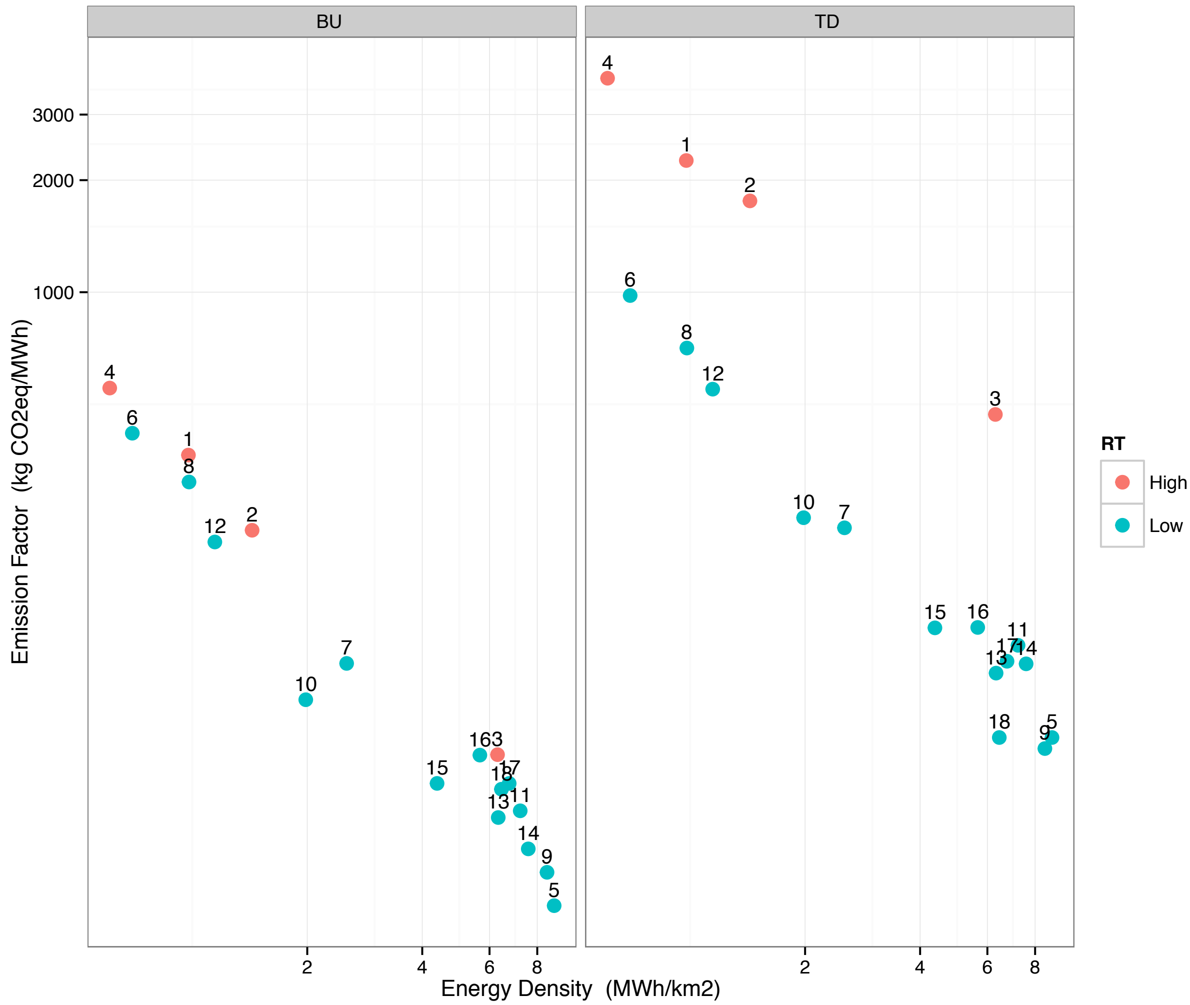

Figure S14 – Average emission factor (over 20 years period, GWP -86) plotted against energy density from each studied reservoirs. Number Identification: 1 - C. do Caí, 2 - C. dos Patos, 3 – Jamanxim, 4 – Sinop, 5 - Belo Monte, 6 - Bem Querer, 7 - C. do Caldeirão, 8 – Colíder, 9 - F. Gomes, 10 – Jatobá, 11 – Jirau , 12 – Marabá, 13 - Salto A. de Baixo, 14 - Santo Antônio, 15 - São L. do Tapajos, 16 - São Manoel, 17 - São Simão Alto, 18 - Teles Pires.

6.4.7 Climate change and land used change uncertainty

Climate change and deforestation in the Amazon are factors that may affect atmospheric and surface conditions in the future, which then would impact GHG emissions from reservoirs. Amazon precipitation pattern changes are considered one of the main impacts from land use change and global warming (Malhi et al. 2008). Precipitation controls discharge variability of the Amazon rivers (Villar et al. 2009), which affects limnological conditions of reservoirs. For instance, lower discharges increase reservoir RT, which is positively correlated to emissions (Pacheco et al. 2015; Abril et al. 2005). Changes in flow patterns also affect energy production, and consequently, the emission factor of the hydropower projects. For example, projections for Belo Monte reservoir shows that land use change in the Xingu Basin reduce flows patterns, and expected energy production decreases by 5% to 40% (Stickler, Coe & Costa 2013).

IPCC projections indicate temperature increase in South America are very likely to occur, with greatest warming projected in the southern Amazon region (IPCC 2013). Less rainfall is very likely to also occur in the eastern Amazon region during the dry season, but the effect in the rainy season is still very uncertain (IPCC 2013; Joetzjer et al. 2013). Regarding extremes precipitations, there is a high likelihood of the intensification of these events (IPCC 2013). The impacts of climate change on freshwater systems will likely 1) increase water temperatures and eutrophication, 2) decrease dissolved-oxygen levels, and 3) strengthen stratification (Roland, Huszar & Farjalla 2012).

Deforestation also affects Amazon hydrometeorology (Baidya Roy 2002; Costa & Pires 2009; Wang, Chagnon & Williams 2009), and can itself be a factor of climate change and a positive feedback on externally forced climate change (Malhi et al. 2008). Shifts in the regional climate patterns can influence reservoir emissions by changing the heat balance and surface mixed layer dynamics of hydroelectric reservoirs (Curtarelli et al. 2014). Any modification on precipitation and wind patterns can also affect emissions, as they are important factors to define gas exchange flux variability (Abril et al. 2005). Additionally, land use change from forest to agriculture or urban areas can increase eutrophication and cause a reversal in the role played by oligotrophic systems by increasing atmospheric C sequestration as sediment and dissolved organic C (Pacheco, Roland & Downing 2014). Finally, hydroelectric development can promote indirect deforestation, which increases emissions related to the projects (Fearnside 2015a).

At this point, we are unable to quantify the magnitude of future climate and land use change on our estimates. The direction of most of the effects, however, indicates that these factors will likely contribute to the increase in emission factors from hydropower plants in the Amazon.

References

Abril, G, Guérin, F, Richard, S, Delmas, R, Galy-Lacaux, C, Gosse, P, Tremblay, A, Varfalvy, L, Santos, dos, M A & Matvienko, B 2005, 'Carbon dioxide and methane emissions and the carbon budget of a 10-year old tropical reservoir (Petit Saut, French Guiana)', *Global Biogeochemical Cycles*, vol. 19, no. 4, p. 1–16.

Abril, G, Parize, M, Pérez, M A P & Filizola, N 2012, 'Wood decomposition in Amazonian hydropower reservoirs: an additional source of greenhouse gases', *Journal of South American Earth Sciences*.

Alin, S R, Rasera, M de F F L, Salimon, C I, Richey, J E, Holtgrieve, G W, krusche, A V & Snidvongs, A 2011, 'Physical controls on carbon dioxide transfer velocity and flux in low-gradient river systems and implications for regional carbon budgets', *Journal of Geophysical Research*, vol. 116, no. G1, p. G01009.

Alin, SR & Richey, JE 2012, 'LBA-ECO CD-06 CO_2 Exchange in River Systems Across the Amazon Basin: 2004-2007', Oak Ridge National Laboratory Distributed Active Archive Center (ed.), *daac.ornl.gov*, Oak Ridge National Laboratory Distributed Active Archive Center.

Angelis, M A & Scranton, M I 1993, 'Fate of methane in the Hudson River and estuary', *Global Biogeochemical Cycles*.

Baidya Roy, S 2002, 'Impact of land use/land cover change on regional hydrometeorology in Amazonia', *Journal of Geophysical Research*, vol. 107, no. D20, p. 8037.

Barros, N, Cole, J J, Tranvik, L J, Prairie, Y T, Bastviken, D, Huszar, V L M, del Giorgio, P & Roland, F 2011, 'Carbon emission from hydroelectric reservoirs linked to reservoir age and latitude', IPOC Change (ed.), *Nature Geoscience*, vol. 4, no. 9, Nature Publishing Group, pp. 593–596, viewed <http://www.nature.com/doifinder/10.1038/ngeo1211>.

Bastviken, D, Ejlertsson, J, Sundh, I & Tranvik, L 2003, 'Methane as a source of carbon and energy for lake pelagic food webs', *Ecology*.

Bastviken, D 2009, 'Methane', in GE Likens (ed.), *Encyclopedia of Inland Waters*, Academic Press, pp. 783–805.

Cerri, C E P, Easter, M, Paustian, K, Killian, K, Coleman, K, Bernoux, M, Falloon, P, Powlson, D S, Batjes, N H, Milne, E & Cerri, C C 2007, 'Predicted soil organic carbon stocks and changes in the Brazilian Amazon between 2000 and 2030', *Agriculture, Ecosystems & Environment*, vol. 122, no. 1, pp. 58–72.

CHTP (Companhia Hidrelétrica Teles Pires) 2015, 'Informativo de Supressão Vegetal - UHE Teles Pires', pp. 1–4, viewed <http://www.uhetelespires.com.br/site/2015/08/24/informativo-supressao-vegetal-uhe-teles-pires-2/#body>.

Costa, M H & Pires, G F 2009, 'Effects of Amazon and Central Brazil deforestation scenarios on the duration of the dry season in the arc of deforestation', P A Dirmeyer, D Niyogi, N de Noblet-Ducoudré, R E Dickinson & P K Snyder (eds), *International Journal of Climatology*, vol. 30, no. 13, pp. 1970–1979.

Curtarelli, M P, Ogashawara, I, Araújo, C A S, Alcântara, E H, Lorenzzetti, JA & Stech, J L 2014, 'Influence of summertime mesoscale convective systems on the heat balance and surface mixed layer dynamics of a large Amazonian hydroelectric reservoir', *Journal of Geophysical Research: Oceans*, vol. 119, no. 12, pp. 8472–8494.

Davidson, E A & Janssens, I A 2006, 'Temperature sensitivity of soil carbon decomposition and feedbacks to climate change', *Nature*, vol. 440, no. 7081, pp. 165–173.

Delmas, R, Galy-Lacaux, C & Richard, S 2001, 'Emissions of greenhouse gases from the Tropical hydroelectric reservoir of Petit Saut (French Guiana) compared with emissions from thermal alternatives', *Global Biogeochemical Cycles*, vol. 15, no. 4, pp. 993–1003.

Delmas, R, Richard, S, Guerin, F, Abril, G, Galy-Lacaux, CR, Delon, C & Gregoire, A 2005, 'Long Term Greenhouse Gas Emissions From the Hydroelectric Reservoir of Petit Saut (French Guiana) and Potential Impacts', Greenhouse Gas Emissions — Fluxes and Processes, pp. 293–312.

DelSontro, T, McGinnis, D F, Sobek, S, Ostrovsky, I & Wehrli, B 2010, 'Extreme Methane Emissions from a Swiss Hydropower Reservoir: Contribution from Bubbling Sediments', *Environmental Science & Technology*, vol. 44, no. 7, pp. 2419–2425.

Demarty, M & Bastien, J 2011, 'GHG emissions from hydroelectric reservoirs in tropical and equatorial regions: Review of 20 years of CH4 emission measurements', *Energy Policy*, vol. 39, no. 7, Elsevier, pp. 4197–4206, viewed <http://linkinghub.elsevier.com/retrieve/pii/S0301421511003168>.

Duchemin, É, Lucotte, M, Canuel, R, Queiroz, AG, Almeida, DC, Pereira, HC & Dezincourt, J 2000, 'Comparison of Greenhouse Gas Emissions From an Old Tropical Reservoir with Those From Other Reservoirs Worldwide', *Verh. Internat. Verein. Limnol.*, vol. 27, Sttugart, pp. 1391–1395.

Ellis, E E, Richey, J E, Aufdenkampe, A K, Krusche, A V, Quay, P D, Salimon, C & Brandão da Cunha, H 2012, 'Factors controlling water-column respiration in rivers of the central and southwestern Amazon Basin', *Limnology and Oceanography*, vol. 57, no. 2, pp. 527–540.

Ellis, E E, Richey, J E, Krusche, A V, Quay, P D, Salimon, C & Brandão da Cunha, H 2012, 'LBA-ECO CD06 Carbon Sources and Respiration Rates in Rivers in Amazonas and Acre: 2005-2006', Oak Ridge National Laboratory Distributed Active Archive Center (ed.), *daac.ornl.gov*, Oak Ridge National Laboratory Distributed Active Archive Center.

Environmental Protection Agency (EPA) 1969, *Mathematical Models for the Prediction of Thermal Energy Changes in Impoundments*, pp. 1–190.

Fearnside, PM 2002, 'Greenhouse gas emissions from a hydroelectric reservoir (Brazil Tucurui Dam) and the energy policy implications', *Water, Air, & Soil Pollution*, vol. 133, pp. 69–96.

Fearnside, PM 2015a, 'Emissions from tropical hydropower and the IPCC', *Environmental Science and Policy*, vol. 50, Elsevier Ltd, pp. 225–239.

Fearnside, PM 2015b, 'Tropical hydropower in the clean development mechanism: Brazil's Santo Antônio dam as an example of the need for change', *Climatic Change*, vol. 131, no. 4, pp. 575–589.

Feldpausch, T R & Rondon, M A 2004, 'Carbon and nutrient accumulation in secondary forests regenerating on pastures in central Amazonia', *Ecological Applications,* vol 14, no. 4, pp. 164-176.

Furch, K 1984, *Water chemistry of the Amazon basin: The distribution of chemical elements among freshwaters*, HJ Dumont & H Sioli (eds),, Monographiae Biologicae, Dordrecht, pp. 167–199.

Galy-Lacaux, C, Delmas, R, Kouadio, G, Richard, S & Gosse, P 1999, 'Long-term greenhouse gas emissions from hydroelectric reservoirsin tropical forest regions', *Global Biogeochemical Cycles*, vol. 13, no. 2, pp. 503–517.

Goldenfum, J 2010, *Guidelines on GHG Measurement Preliminary GHG Assessment Tool Proposal for CDM Methodology Revision*, J Goldenfum (ed.), The World Bank, pp. 1–166.

Guérin, F, Abril, G, Richard, S, Burban, B, Reynouard, C, Seyler, P & Delmas, R 2006, 'Methane and carbon dioxide emissions from tropical reservoirs: Significance of downstream rivers', *Geophysical Research Letters*, vol. 33, no. 21, p. L21407.

Guérin, F & Abril, G 2007, 'Significance of pelagic aerobic methane oxidation in the methane and carbon budget of a tropical reservoir', *Journal of Geophysical Research*, vol. 112, no. G3, p. G03006.

Guérin, F, Abril, G, de Junet, A & Bonnet, M-P 2008, 'Anaerobic decomposition of tropical soils and plant material: Implication for the CO_2 and CH_4 budget of the Petit Saut Reservoir', *Applied Geochemistry*, vol. 23, no. 8, pp. 2272–2283.

Hansen, M C, Potapov, P V, Moore, R, Hancher, M, Turubanova, S A, Tyukavina, A, Thau, D, Stehman, S V, Goetz, S J, Loveland, T R, Kommareddy, A, Egorov, A, Chini, L, Justice, C O & Townshend, J R G 2013, 'High-Resolution Global Maps of 21st-Century Forest Cover Change', *Science*, vol. 342, no. 6160, pp. 850–853.

Hanson, R S & Hanson, T E 1996, 'Methanotrophic bacteria.', *Microbiological reviews*.

IPCC 2013, *Climate Change 2013. The Physical Science Basis. Working Group I Contribution to the Fifth Assessment Report of the Intergovernmental Panel on Climate Change*, TF Stocker, D Qin, G-K Plattner, M Tignor, S K Allen, J Boschung, A Nauels, V Bex, Y Xia & P M Midgley (eds), Groupe d'experts intergouvernemental sur l'evolution du climat/Intergovernmental Panel on Climate Change-IPCC, C/O World Meteorological Organization, 7bis Avenue de la Paix, CP 2300 CH-1211 Geneva 2 (Switzerland).

Joetzjer, E, Douville, H, Delire, C & Ciais, P 2013, 'Present-day and future Amazonian precipitation in global climate models: CMIP5 versus CMIP3', *Climate Dynamics*, vol. 41, no. 11-12, pp. 2921–2936.

Junk, W J, Piedade, M T F, Schöngart, J, Cohn-Haft, M, Adeney, JM & Wittmann, F 2011, 'A Classification of Major Naturally-Occurring Amazonian Lowland Wetlands', *Wetlands*, vol. 31, no. 4, pp. 623–640.

Kemenes, A, Forsberg, B R & Melack, J M 2007, 'Methane release below a tropical hydroelectric dam', *Geophysical Research Letters*, vol. 34, no. 12, p. L12809.

Kemenes, A, Forsberg, B R & Melack, J M 2011, 'CO_2 emissions from a tropical hydroelectric reservoir (Balbina, Brazil)', *Journal of Geophysical Research*, vol. 116, no. G3, p. G03004.

Kubistcheck, J 1960, *Lei N^O 3.824, De 23 De Novembro De 1960.*, Brazil, pp. 1–1.

Kuha, J 2004, 'AIC and BIC: Comparisons of Assumptions and Performance', *Sociological Methods & Research*, vol. 33, no. 2, pp. 188–229.

Lewis, S L, Lloyd, J, Sitch, S, Mitchard, E T A & Laurance, W F 2009, 'Changing Ecology of Tropical Forests: Evidence and Drivers', *Annual Review of Ecology, Evolution, and Systematics*, vol. 40, no. 1, pp. 529–549.

Lima, I B T 2005, 'Biogeochemical distinction of methane releases from two Amazon hydro reservoirs', *Chemosphere*, vol. 59, no. 11, pp. 1697–1702.

Malhi, Y, Baldocchi, D D & Jarvis, P G 1999, 'The carbon balance of tropical, temperate and boreal forests', *Plant, Cell and Environment*, vol. 22,, pp. 715–740.

Malhi, Y, Roberts, J T, Betts, R A, Killeen, T J & Li, W 2008, 'Climate change, deforestation, and the fate of the Amazon', *Science*, pp. 1–5.

Malhi, Y 2010, 'The carbon balance of tropical forest regions, 1990 - 2005', *Current Opinion in Environmental Sustainability*, vol. 2, no. 4, Elsevier B.V., pp. 237–244.

Martin, A R & Thomas, S C 2011, 'A Reassessment of Carbon Content in Tropical Trees', J Chave (ed.), *PLoS ONE*, vol. 6, no. 8, p. e23533.

Mendonça, R, Kosten, S, Sobek, S, Barros, N, Cole, J J, Tranvik, L & Roland, F 2012, 'Hydroelectric carbon sequestration', *Nature Geoscience*, vol. 5, no. 12, pp. 838–840.

MME (Ministério de Minas e Energia) EPE (Empresa de Pesquisa Energética) 2013, 'Plano Decenal de Expansão Energia 2022', pp. 1–410.

MME (Ministério de Minas e Energia) EPE (Empresa de Pesquisa Energética) 2014, 'Plano Decenal de Expansão Energia 2023', pp. 1–434.

Morgan, G 1990, *Uncertainty*, Cambridge University Press (ed.).

Odum, E P 1969, 'The strategy of ecosystem development', *Science*, vol. 164, pp. 262–270.

Ometto, J P, Cimbleris, A X C P, Santos, dos, M A, Rosa, L P, Abe, D, Tundisi, J X G, Stech, JXL, Barros, N & Roland, FXB 2013, 'Carbon emission as a function of energy generation in hydroelectric reservoirs in Brazilian dry tropical biome', *Energy Policy*, Elsevier, pp. 1–8.

Pacheco, F, Roland, F & Downing, J 2014, 'Eutrophication reverses whole-lake carbon budgets', *Inland Waters*, vol. 4, no. 1, pp. 41–48.

Pacheco, F S, Soares, M C S, Assireu, A T, Curtarelli, M P, Abril, G, Stech, J L, Alvalá, P C & Ometto, J P 2015, 'The effects of river inflow and retention time on the spatial heterogeneity of chlorophyll and water–air CO_2 fluxes in a tropical hydropower reservoir', *Biogeosciences*, vol. 12, no. 1, pp. 147–162.

Rasera, M de F F L, Ballester, M V R, Krusche, A V, Salimon, C, Montebelo, L A, Alin, S R, Victoria, R L & Richey, J E 2008, 'Estimating the Surface Area of Small Rivers in the Southwestern Amazon and Their Role in CO_2 Outgassing', *Earth Interactions*, vol. 12, no. 6, pp. 1–16.

Rasera, M de F F L, Krusche, A V, Richey, J E, Ballester, M V R & Victoria, R L 2013, 'Spatial and temporal variability of pCO_2 and CO_2 efflux in seven Amazonian Rivers', *Biogeochemistry*, vol. 116, no. 1-3, pp. 241–259.

Richey, J E, Melack, J M, Aufdenkampe, A K & Hess, V M B L L 2002, 'Outgassing From Amazonian Rivers and Wetlands as a Large Tropical Source of Atmospheric CO_2', *Nature*, vol. 416, pp. 1–5.

Roland, F, Huszar, V & Farjalla, V F 2012, 'Climate change in Brazil: perspective on the biogeochemistry of inland waters', *Brazilian Journal of Biology*, vol. 72, no. 3, pp. 709–722.

Rosa, L P, Santos, dos, M A, Matvienko, B, Santos, dos, E O & Sikar, E 2004, 'Greenhouse Gas Emissions From Hydroelectric Reservoirs in Tropical Regions', *Climatic Change*, vol. 66, no. 1-2, pp. 9–21.

Saatchi, SS, Houghton, RA, Alvala, R C S, Soares J V & Yu, Y 2007, 'Distribution of aboveground live biomass in the Amazon basin', *Global Change Biology*, vol. 13, no. 4, pp. 816–837.

Saatchi, S S, Houghton, R A, Alves, D & Nelson, B 2008, 'LBA-ECO LC-15 Amazon Basin Aboveground Live Biomass Distribution Map: 1990-2000', Oak Ridge National Laboratory Distributed Active Archive Center, viewed <https://daac.ornl.gov/LBA/guides/LC15_AGLB.html>.

Salimon, C, Santos Sousa, E, Alin, S R, Krusche, A V & Ballester, M V 2012, 'Seasonal variation in dissolved carbon concentrations and fluxes in the upper Purus River, southwestern Amazon', *Biogeochemistry*, vol. 114, no. 1-3, pp. 245–254.

Santos, dos, M A, Rosa, L P, Sikar, B, Sikar, E & Santos, dos, EO 2006, 'Gross greenhouse gas fluxes from hydro-power reservoir compared to thermo-power plants', *Energy Policy*, vol. 34, no. 4, pp. 481–488.

Sawakuchi, H O, Bastviken, D, Sawakuchi, A O, krusche, A V, Ballester, M V R & Richey, J E 2014, ‘Methane emissions from Amazonian Rivers and their contribution to the global methane budget’, *Global Change Biology*, Wiley Online Library.

Sayer, E J, Heard, M S, Grant, H K, Marthews, T R & Tanner, E V J 2011, ‘Soil carbon release enhanced by increased tropical forest litterfall’, *Nature Climate Change*, vol. 1, no. 9, Nature Publishing Group, pp. 1–4.

Sheppard, M 2012, ‘ALLFITDIST’, *mathworks.com*, Matlab Central.

St. Louis, V L, Kelly, C A, Duchemin, É, Rudd, J W M & Rosenberg, D M 2000, ‘Reservoir Surfaces as Sources of Greenhouse Gases to the Atmosphere: A Global Estimate’, *BioScience*, vol. 50, no. 9, pp. 766–775.

Stickler, C M, Coe, M T & Costa, M H 2013, ‘Dependence of hydropower energy generation on forests in the Amazon Basin at local and regional scales’, *PNAS*, vol. 110, no. 23, pp. 9601–9606.

StrašKraba, M 1973, ‘Limnological basis for modeling reservoir ecosystems’, *Geophysical Monograph Series - Man-made Lakes: Their Problems and Environmental Effects*, vol. 17, Wiley Online Library, pp. 517–535.

Straškraba, M, Tundisi, J G & Duncan, A 1993, ‘State-of-the-Art of Reservoir Limnology and Water Quality Management’, *Comparative Reservoir Limnology and Water Quality Management*, vol. 77, pp. 213–288.

Tundisi, J G & Rocha, O 1998, ‘Reservoir management in South America’, *International Journal of Water Resources Development*.

Villar, J C E, Guyot, J L, Ronchail, J, Cochonneau, G, Filizola, N, Fraizy, P, Labat, D, de Oliveira, E, Ordoñez, JJ & Vauchel, P 2009, ‘Contrasting regional discharge evolutions in the Amazon basin (1974–2004)’, *Journal of Hydrology*, vol. 375, no. 3-4, Elsevier B.V., pp. 297–311.

Wang, J, Chagnon, F & Williams, E R 2009, ‘Impact of deforestation in the Amazon basin on cloud climatology’, *PNAS*.

Wickham, H 2009, ‘ggplot2: elegant graphics for data analysis’, Springer New York, viewed <http://had.co.nz/ggplot2/book>.

7. APPENDIX B: CHAPTER 3

7.1 Introduction

This chapter includes details about the data and outcomes described in Chapter 3, along with additional results and analyses. First, we provide a more detailed description of the data used in the study, such as the characteristics of the hydropower plants and additional statistics about the variables of interest. Second, we employ various methods to assess the robustness of the main findings of Chapter 3, such as alternative assumptions about clustering and model specification. Third, we present a complementary assessment of the heterogeneity of the economic impacts of hydropower development by some critical characteristics, such as project size (installed capacity) and plant ownership (utility or industry).

7.2 Data

7.2.1 Hydropower plants built between 1991 and 2010

Table S1 characterizes the main features of the 56 hydropower plants built in Brazil between 1991 and 2010 that were used in the study. The projects include a total of 23 gigawatts of installed capacity and 10,000 km2 of reservoir area. We identified the counties affected by power plants listed on Table 1 using the water resources compensation policy database organized by the Brazilian Electricity Regulatory Agency (ANEEL – Agencia Nacional de Energia Eletrica, 2015b). The reservoirs from these hydropower plants affected 242 counties based on the 2010 county territory map. Annex C1 contains the list of the control counties.

Table S1: Hydropower plants built in Brazil from 1991 to 2010

ANEEL Identification	Name	Installed Capacity (kW)	Reservoir Area (km^2)	Beginning of Construction	Beginning of Operation (First turbine)	Owner	Industry or Utility
12	14 de Julho	100,000	7	2004	2008	Companhia Energética Rio das Antas	Utility
42	Aimorés	330,000	37	2001	2005	Companhia Vale do Rio Doce	Industry
630	Cana Brava	450,000	140	1999	2002	Tractebel Energia S/A	Utility
641	Risoleta Neves (Antiga Candonga)	140,000	3	2001	2004	Companhia Vale do Rio Doce	Industry
647	Canoas I	82,500	35	1992	1999	Companhia Brasileira de Alumínio	Industry
718	Castro Alves	130,000	6	2004	2008	Companhia Energética Rio das Antas	Utility
866	Corumbá I	375,000	63	1991	1996	Furnas Centrais Elétricas S/A.	Utility
1006	Funil	180000	37	2000	2002	Companhia Vale do Rio Doce	Industry
1066	Guaporé	120,000	5	2001	2003	Tangara Energia S/A	Utility
1079	Guilman-Amorim	140,000	2	1995	1997	Arcelor Mittal Brasil S.A.	Industry
1098	Igarapava	210,000	51	1995	1998	Companhia Vale do Rio Doce	Industry
1146	Irapé	360,000	149	2002	2006	CEMIG Geração e Transmissão S/A	Utility
1152	Itá	1,450,000	126	1996	2000	Ita Energética S/A	Utility
1175	Itapebi	462,011	62	2001	2003	Itapebi Geração de Energia S/A	Utility
1245	Jauru	121,500	5	2000	2003	Queiroz Galvão Energética S/A.	Industry
1304	Luís Eduardo Magalhaes (Lajeado)	902,500	704	1998	2001	Rede Lajeado Energia S/A	Utility
1356	Machadinho	1,140,000	89	1998	2002	Companhia Brasileira de Alumínio	Industry
1401	Manso	210,000	402	1998	2000	Furnas Centrais Elétricas S/A.	Utility
1469	Miranda	408,000	53	1991	1998	CEMIG	Utility
1574	Nova Ponte	510,000	459	1991	1994	CEMIG	Utility
2077	Pirajá	70,000	17	1999	2002	Companhia Brasileira de Alumínio	Industry
2103	Ponte de Pedra	176,100	16	2002	2005	Ponte de Pedra Energética S/A	Utility
2127	Porto Primavera (Eng. Sergio Motta)	1,540,000	2,977	1991	1999	Companhia Energética de São Paulo	Utility

2167	Quebra Queixo	120,000	6	2000	2003	Companhia Energetica Chapeco	Utility
2176	Queimado	105,000	36	2000	2004	CEMIG	Utility
2591	Governador Jose Richa (Salto Caxias)	1,240,000	144	1995	1999	Copel Geração e Transmissão S.A.	Utility
2731	Serra da Mesa	1,275,000	1,254	1993	1998	Furnas Centrais Elétricas S/A.	Utility
2873	Três Irmãos	807,500	670	1991	1993	Companhia Energética de Sπo Paulo	Utility
27012	Dona Francisca	125,000	22	1998	2001	Dona Francisca Energética S/A	Utility
27053	Xingó	3,162,000	59	1991	1994	Companhia Hidro Elétrica do São Francisco	Utility
27196	Porto Estrela	112,000	4	1999	2001	CEMIG Geração e Transmissãoπo S/A	Utility
27244	Itiquira	156,000	4	1998	2002	Itiquira Energética S/A	Utility
27401	Campos Novos	880,000	41	2001	2007	Campos Novos Energia S/A.	Utility
27483	Amador Aguiar I	240,000	21	2003	2006	Companhia Vale do Rio Doce	Industry
27484	Amador Aguiar II	210,000	44	2004	2007	Companhia Vale do Rio Doce+AN16	Industry
27556	Barra Grande	690,000	100	2001	2005	Energética Barra Grande S/A	Utility
27795	Corumbá IV	127,000	187	2001	2006	Corumbá Concessões S/A	Utility
27968	Monte Claro	130,000	2	2001	2004	Companhia Energética Rio das Antas	Utility
28352	Corumbá III	96,447	70	2006	2009	Geração CIII S.A.	Utility
28353	Peixe Angical	498,750	318	2002	2006	Enerpeixe S/A	Utility
28354	Foz do Chapeco	855,000	86	2004	2010	Foz do Chapecó≤ Energia S/A	Utility
28355	Serra do Facão	212,580	226	2004	2010	Serra do Facão Energia S.A.	Utility
28360	Fundão	120,168	3	2004	2006	Centrais Elétricas do Rio Jordao S/A	Utility
28361	Santa Clara	120,168	25	2002	2005	Centrais Elétricas do Rio Jordao S/A	Utility
28564	Salto Pilão	191,890	0	2006	2009	Companhia Brasileira de Alumínio	Industry
28565	Pedra do Cavalo	160,000	199	2003	2004	Votorantim Cimentos N/NE S/A	Industry
28567	Sπo Salvador	243,200	100	2006	2009	Companhia Energética Sπo Salvador	Utility

28757	Barra dos Coqueiros	90,000	25	2007	2010	Gerdau S/A	Industry
28758	Salto	116,000	60	2007	2010	Rio Verde Energia S.A.	Utility
28760	Salto do Rio Verdinho	93,000	44	2007	2010	Rio Verdinho Energia S/A	Utility
28863	Estreito	1,087,000	1,271	2006	2011	Renova Energia Renovável S.A.	Utility
29453	Baguari	140,000	17	2006	2009	Baguari I Geração de Energia Elétrica S/A	Utility
29457	Retiro Baixo	83,657	28	2007	2010	Retiro Baixo Energética S.A	Utility
908	Espora	32,000	28	2001	2006	Espora Energética S/A	Utility
2696	Santa Branca	56,050	28	1996	1999	Light Energia S/A	Utility
27092	Canoas II	72,000	26	1992	1999	Companhia Brasileira de Alumínio	Industry

7.2.2 Undeveloped hydropower plants: control group

The regulatory process to develop power plants in Brazil can be summarized by three major stages: 1) watershed master plan, 2) viability study, and 3) basic design. Each stage adds complexity to the level of details in the engineering and environmental studies. ANEEL assesses, manage and approves those studies, and make part of this information publicly available (ANEEL, 2015a). We used hydropower plants that were not built yet to identify our group of control counties. Table S2 contains the list of undeveloped hydropower plants sites. The reasons why some hydropower projects are still undeveloped include: lack of financial viability, environmental and social restrictions, legal or regulatory issues, or project still completing different stages of the regulatory process. For example, in 2001, a private company obtained the legal rights to build the Murta project, a 120 MW power plant sited in the state of Minas Gerais. The project is still under discussion because many households would need to be relocated out of the area that would be flooded by the reservoir. Another example is the Garabi project that has been “under development” since 1970. This project is on the border of Brazil and Argentina, a condition that adds complexity to the regulatory process and project development because of the need of agreement between the two countries. In the main model, we include as counterfactuals only the counties within a distance of 200 kilometers from our treatment group.

Table S5: Undeveloped hydropower plants used to identify control counties

ID	Name	Installed Capacity (kW)	ID	Name	Installed Capacity (kW)	ID	Name	Installed Capacity (kW)
1	Água Branca	73,000	45	Encantado	36,200	90	Pedra Branca	320,000
2	Água Clara	32,450	46	Ercilândia	96,600	91	Perdida 2	48,000
3	Água Limpa	320,000	47	Escada Grande	41,000	92	Pompeu	209,100
4	Águas Lindas	40,000	48	Escaramuça	50,000	93	Ponte Indaiá	51,400
5	A38PA100	177,800	49	Escura	75,000	94	Porto Ferreira	49,300
6	Almenara	100,000	50	Espigão Preto	34,000	95	Porto Guarita	47,350
7	Alta Floresta	127,800	51	Estreito	56,000	96	Pouso Alto	76,000
8	Apertados	135,500	52	Formoso	342,000	97	Quebra Remo	267,800
9	Araguainha	48,000	53	Foz do Atalaia	72,000	98	Riacho Seco	276,000
10	Araguanã	960,000	54	Foz do Piquiri	101,200	99	Ribeiro Goncalves	113,000
11	Arroio do Meio 30.0	68,600	55	Foz do xaxim	63,200	100	Rio Sono Baixo	56,700
12	Bambu I	84,000	56	Galileia	238,000	101	Rochedo II	70,000
13	Bananeiras	200,000	57	Garabi	1,152,000	102	Roncador	134,000
14	Banharão	67,000	58	Guatambó	34,500	103	Sao Cristóvão	47,820
15	Barra do Claro	61,000	59	Ilha São Pedro	131,000	104	São Jeronimo	340,000
16	Barretos	46,500	60	Iraí	330,000	105	São Joao	60,000
17	Bem Querer J1A	708,400	61	Itaocara I	150,000	106	São Manuel	51,000
18	Berimbau	66,000	62	Itapiranga	724,600	107	São Marcos	57,000
19	Biboca	57,000	63	Jamanxim	881,000	108	São Roque	135,000
20	Boaventura	32,100	64	Januária	180,000	109	Sacos	114,000
21	Bois 12	74,900	65	Jenipapo	96,300	110	Salto Ariranha	36,670
22	Bois 13	64,500	66	Jequitinhonha	101,400	111	Salto Duran	36,100
23	Bom Retiro	45,000	67	JRN-277	1,248,000	112	Santa Isabel	108,700
24	Brejão	75,000	68	JRN-466	510,000	113	Santa Rita	61,000
25	BUR-039	37,500	69	JRN-530	415,000	114	Santo Antônio	84,300
26	Cachoeirão	64,000	70	JRN-577	225,000	115	Santo Hipólito	95,000
27	Cachoeira	63,000	71	JRN-720	150,000	116	Saudade	61,400
28	Cachoeira Caracol	32,600	72	JUI-048	53,000	117	Serra Quebrada	1,328,000
29	Cachoeira do Caí	802,000	73	Lagoinha	37,100	118	Sinop	775,000
30	Cachoeira Galinha	399,800	74	Lajeadao III	46,800	119	Sucuri	38,000
31	Cachoeira Velha	81,000	75	Limoeiro	142,000	120	Sumauma	458,200
32	Cachoeirinha	45,000	76	Lua Cheia	103,000	121	Tabajara	350,000
33	Cambuci	50,000	77	Magessi	53,000	122	Taboa	98,000
34	Canto do Rio	44,000	78	Marabi	2,160,000	123	Telemaco Borba	118,000
35	Cantu	36,700	79	Maranhão	125,000	124	Tibagi Montante	32,000

36	Castelhano	64,000	80	Mocoto	95,000	125	Tijuco Alto	144,000
37	Cebolão Médio	120,000	81	Mortes 2	310,400	126	Torixoreu	408,000
38	Chacorão	3,336,000	82	Mutum	79,500	127	Traíra	60,000
39	Comissário	105,300	83	Murta	120,000	128	Uniao II Montante	67,800
40	Couto Magalhães	150,000	84	Nova Roma	51,000	129	Uruçuí	134,000
41	Cruzeiro do Sul	43,000	85	Paicandu	103,290	130	Urucuia	42,000
42	Cubatão	45,000	86	Panorama	54,000	131	Urucupatá	291,500
43	Davinópolis	107,000	87	Paranhos	62,500	132	Verde 11 Alto	48,300
44	Diamantino	46,000	88	Paredão A	199,300	133	Vila Rica	39,100
45	Doresópolis	60,000	89	Pau D'Arco	64,000	134	Volta Grande Baixa	54,700

7.2.3 Precipitation and air temperature data

Annual precipitation and air temperature data for each county was estimated using the global precipitation and temperature series developed by Willmott & Matsuura from the University of Delaware (Willmott & Matsuura, 2015). The database contains time series (1900-2010) of global terrestrial air temperature and precipitation at a spatial grid resolution of 0.5x0.5 degree. We defined the county value based on the smallest Euclidian distance from the county to the precipitation and temperature grid.

7.2.4 Tax data characteristics

This section describes the characteristics of the variables used to describe county public revenues: total public revenue, services tax – ISS, state transfers – ICMS, and federal transfers FPM.

The first indicator is the total income of the county (Public revenue), which represents on average 95% of the total revenues for a county, excluding capital revenues (e.g. credit operations and disposal of assets). The second public budget indicator is the local service tax (*Imposto Sobre Serviços* – ISS, in Portuguese). Although the ISS corresponds to a small fraction of the budget for most counties (around 3% of the total public revenues), the tax is a very good proxy to evaluate the effect of the construction and operation of hydropower plants on the local economy, because it is a direct measure of the level of economic activity in the services sector. The third indicator is the Brazilian state excise tax (*Imposto sobre Circulaçaão de Mercadorias e Serviços – ICMS*, in Portuguese). The ICMS is paid over the purchase of goods and transportation and communication services, including electricity. On average, ICMS transfers accounted for 20% to 30% of a county's income between 1991 and 2010. The last indicator is a federal transfer to the counties called "counties' participation fund" (*Fundo de Participação dos Municípios* – FPM, in Portuguese). The share received by each county is a function of county population and the state where the county is located. The FPM is one of the most important sources of income for counties, and its proportion of the total revenues ranges from 30% to 40% (averages from 1991 to 2010). Most of the counties in Brazil depend heavily on state and federal transfers, representing on average 85% of their total public revenues.

7.3 Socioeconomic Indicators – Summary Statistics

Table S3 presents the statistical summary of the socioeconomic indicators according to treated groups (A and B) and control group in 1991. Treated group A represents counties with hydropower plants built between 1991 and 2000 and treated group B represents counties with hydropower plants built between 2000 and 2010. Table 2 shows that control and treated groups have similar statistics for some indicators (e.g. education and teenage pregnancy) but different statistics for others (e.g. longevity and percentage of households with access to piped water).

Because of this heterogeneity, we include covariates in the regression to be able to control for observables and time-invariant unobservables.

Table S3 - Socioeconomic indicator sample statistics

	Mean	Standard deviation	Mean	Standard deviation	Mean	Standard deviation
Socioeconomic indicators (1991)	Group A (n=46)		Group B (n=101)		Control Group (n=106)	
Education	0.21	0.07	0.18	0.07	0.20	0.07
Longevity	0.57	0.05	0.54	0.08	0.68	0.05
Income	0.69	0.06	0.67	0.06	0.55	0.07
% of households with access to electricity	83	15	70	21	76	21
% of households with access to piped water	73	19	58	25	66	22
% teenager pregnancy	3.1	2.1	2.3	1.5	2.5	1.7
Number of HIV cases	3.9	16.1	3.4	21.3	1.9	10.0

7.4 Sensitivity Analysis

To evaluate the robustness of our main findings, we implemented a sensitivity analysis consisting of two parts. First, we evaluated the effect of different clustering alternatives on the variance of estimated parameters. We assessed the results for three different clustering assumptions: no clustering, clustering by county, and clustering by county and hydropower plant (Model 1 from Chapter 3). Second, we assessed the effect on the regression estimates of (i) relaxing the restriction of using only counties with unexplored hydropower potential as controls, and (ii) excluding and including covariates from our main model specification. The sensitivity analysis confirms that the event-time dummy results from the main model (Model 1) are stable under alternative conditions.

7.4.1. Gross domestic product

Table S4 to Table S7 present the regression results for total GDP and its subaccounts (industry, agriculture and services). The column called “Main model” describes the results presented in the main document (Model 1). Columns A and B represent the results of distinct clustering assumptions and the last three columns present the coefficients assuming alternative conditions: 1) relaxing the restriction of using only counties with hydropower plants that didn’t materialize as controls, 2) without covariates (temperature, precipitation, royalties and state GDP, and 3) adding another covariate (population).

Overall, the estimates of the sensitivity analysis are qualitatively similar. Regarding the clustering alternatives, it is possible to see that, in general, the standard errors follow a pattern:

Clustered by county and hydropower plants > Clustered by county > No clustering

This result is expected given that failure to control for within-cluster error correlation can lead to misleadingly small standard errors, and consequent misleadingly narrow confidence intervals, large t-statistics, and low p-values (Cameron & Miller, 2015).

Regarding the alternative condition “1” (where we relax the restriction of using only counties with unexplored hydropower potential as controls), the outcomes indicate that the failure to control for natural advantages and siting decisions tends to result in a slight overestimation of the average coefficients, consistent with other findings in the literature (e.g. Severnini, 2014). Furthermore, the covariates exclusion (condition “2”) and inclusion (condition “3”) do not result in major effects for the event-time dummy coefficients (ED) and standard errors. We did not add population as a covariate in the main model because of the potential feedbacks between economic output and population that could bias the ED coefficients.

Table S5: Sensitivity Analysis – regression results (dependent variable Total GDP)

	Clustering Alternatives			Specification alternatives		
	Main Model	*A*	*B*	*1) Relaxing the restriction of using only counties with unexplored hydropower potential as controls*	*2) Without covariates (temperature, precipitation, royalties and state GDP)*	*3) Adding a covariate (population)*
Standard errors clustered by county:	*Yes*	*Yes*	*No*	*Yes*	*Yes*	*Yes*
Standard errors clustered by hydropower plant:	*Yes*	*No*	*No*	*No*	*Yes*	*Yes*
County and Year Fixed Effects	*Yes*	*Yes*	*Yes*	*Yes*	*Yes*	*Yes*
EDminus5	0.028 (0.045)	0.028 (0.035)	0.028 (0.035)	-0.017 (0.037)	0.028 (0.045)	0.028 (0.045)
EDminus4	0.004 (0.028)	0.004 (0.025)	0.004 (0.030)	-0.030 (0.026)	0.004 (0.032)	0.004 (0.028)
EDminus3	-0.021 (0.031)	-0.021 (0.026)	-0.021 (0.028)	-0.034 (0.028)	-0.021 (0.034)	-0.021 (0.031)
EDminus2	-0.037 (0.033)	-0.037 (0.025)	-0.037 (0.025)	-0.055** (0.025)	-0.037 (0.035)	-0.037 (0.033)
EDzero	-0.011 (0.031)	-0.011 (0.025)	-0.011 (0.022)	-0.015 (0.026)	-0.011 (0.034)	-0.011 (0.031)
EDplus1	-0.005 (0.038)	-0.005 (0.025)	-0.005 (0.021)	-0.004 (0.026)	-0.005 (0.042)	-0.005 (0.038)
EDplus2	0.040 (0.040)	0.040 (0.027)	0.040* (0.021)	0.048* (0.027)	0.040 (0.043)	0.040 (0.040)
EDplus3	0.099** (0.042)	0.099*** (0.029)	0.099*** (0.020)	0.107*** (0.028)	0.099** (0.045)	0.099** (0.042)
EDplus4	0.091** (0.037)	0.091*** (0.026)	0.091*** (0.019)	0.098*** (0.025)	0.091** (0.039)	0.090** (0.037)
EDplus5	0.092*** (0.032)	0.092*** (0.027)	0.092*** (0.020)	0.100*** (0.028)	0.092*** (0.034)	0.091*** (0.032)
EDplus6	0.065** (0.032)	0.065** (0.026)	0.065*** (0.020)	0.075*** (0.027)	0.065* (0.035)	0.064** (0.032)
EDplus7	0.060* (0.031)	0.060** (0.024)	0.060*** (0.020)	0.074*** (0.024)	0.060* (0.034)	0.059* (0.031)
EDplus8	0.050 (0.031)	0.050* (0.026)	0.050*** (0.018)	0.058** (0.028)	0.050 (0.035)	0.049 (0.031)
EDplus9	0.045 (0.029)	0.045* (0.026)	0.045** (0.018)	0.060** (0.027)	0.045 (0.032)	0.044 (0.029)
EDplus10	0.046 (0.031)	0.046* (0.025)	0.046** (0.019)	0.064*** (0.024)	0.046 (0.033)	0.045 (0.031)
EDplus11	0.041 (0.030)	0.041* (0.024)	0.041** (0.021)	0.068*** (0.023)	0.041 (0.034)	0.040 (0.030)
EDplus12	0.020 (0.026)	0.020 (0.022)	0.020 (0.021)	0.064*** (0.021)	0.020 (0.029)	0.019 (0.026)
EDplus13	0.009 (0.018)	0.009 (0.025)	0.009 (0.023)	0.051** (0.022)	0.009 (0.020)	0.008 (0.018)
EDplus14	0.023 (0.015)	0.023 (0.021)	0.023 (0.023)	0.041** (0.019)	0.023 (0.016)	0.023 (0.015)
EDplus15	0.045*** (0.016)	0.045** (0.019)	0.045* (0.024)	0.035** (0.018)	0.045** (0.017)	0.044*** (0.016)
log (state GDP)	0.177* (0.101)	0.177** (0.075)	0.177*** (0.037)	-0.072*** (0.017)		0.185* (0.106)
Itaipu royalties	-0.001 (0.002)	-0.001 (0.002)	-0.001 (0.003)	-0.001*** (0.000)		-0.001 (0.002)
Precipitation	-0.000** (0.000)	-0.000*** (0.000)	-0.000*** (0.000)	-0.000*** (0.000)		-0.000** (0.000)
Temperature	-0.014 (0.010)	-0.014 (0.010)	-0.014** (0.007)	-0.007*** (0.002)		-0.014 (0.010)
Population						0.000 (0.000)

Notes: ***Significant at the 1 percent level;**Significant at the 5 percent level;*Significant at the 10 percent level.

Table S5: Sensitivity Analysis – regression results (dependent variable Industry GDP)

	Clustering Alternatives			Specification alternatives		
	Main Model	*A*	*B*	*1) Relaxing the restriction of using only counties with unexplored hydropower potential as controls*	*2) Without covariates (temperature, precipitation, royalties and state GDP)*	*3) Adding a covariate (population)*
Standard errors clustered by county:	*Yes*	*Yes*	*No*	*Yes*	*Yes*	*Yes*
Standard errors clustered by hydropower plant:	*Yes*	*No*	*No*	*No*	*Yes*	*Yes*
County and Year Fixed Effects	*Yes*	*Yes*	*Yes*	*Yes*	*Yes*	*Yes*
EDminus5	0.249** (0.125)	0.249*** (0.082)	0.249*** (0.090)	-0.008 (0.073)	0.249* (0.147)	0.248** (0.125)
EDminus4	0.209* (0.121)	0.209** (0.085)	0.209*** (0.079)	0.000 (0.076)	0.209 (0.134)	0.208* (0.121)
EDminus3	-0.057 (0.177)	-0.057 (0.118)	-0.057 (0.073)	-0.215* (0.129)	-0.057 (0.197)	-0.058 (0.177)
EDminus2	0.059 (0.141)	0.059 (0.084)	0.059 (0.065)	-0.117 (0.077)	0.059 (0.150)	0.059 (0.141)
EDzero	0.075 (0.113)	0.075 (0.075)	0.075 (0.058)	-0.003 (0.071)	0.075 (0.127)	0.075 (0.113)
EDplus1	0.044 (0.166)	0.044 (0.092)	0.044 (0.054)	-0.027 (0.093)	0.044 (0.181)	0.044 (0.166)
EDplus2	0.202 (0.133)	0.202** (0.082)	0.202*** (0.054)	0.175** (0.079)	0.202 (0.146)	0.202 (0.133)
EDplus3	0.318** (0.128)	0.318*** (0.082)	0.318*** (0.052)	0.278*** (0.077)	0.318** (0.142)	0.317** (0.128)
EDplus4	0.326*** (0.118)	0.326*** (0.075)	0.326*** (0.050)	0.302*** (0.071)	0.326** (0.128)	0.325*** (0.117)
EDplus5	0.306*** (0.087)	0.306*** (0.071)	0.306*** (0.053)	0.311*** (0.070)	0.306*** (0.095)	0.305*** (0.087)
EDplus6	0.266*** (0.082)	0.266*** (0.067)	0.266*** (0.051)	0.271*** (0.069)	0.266*** (0.092)	0.264*** (0.082)
EDplus7	0.245*** (0.073)	0.245*** (0.062)	0.245*** (0.052)	0.270*** (0.064)	0.245*** (0.087)	0.244*** (0.073)
EDplus8	0.265*** (0.080)	0.265*** (0.067)	0.265*** (0.047)	0.241*** (0.068)	0.265*** (0.103)	0.263*** (0.080)
EDplus9	0.165*** (0.061)	0.165*** (0.059)	0.165*** (0.047)	0.205*** (0.061)	0.165** (0.072)	0.163*** (0.061)
EDplus10	0.141** (0.059)	0.141** (0.055)	0.141*** (0.051)	0.199*** (0.057)	0.141** (0.071)	0.140** (0.059)
EDplus11	0.102* (0.055)	0.102** (0.051)	0.102* (0.054)	0.181*** (0.053)	0.102 (0.072)	0.101* (0.054)
EDplus12	0.122** (0.059)	0.122** (0.051)	0.122** (0.055)	0.208*** (0.051)	0.122* (0.064)	0.122** (0.059)
EDplus13	0.090* (0.047)	0.090* (0.052)	0.090 (0.060)	0.171*** (0.048)	0.090* (0.049)	0.090* (0.047)
EDplus14	0.062 (0.045)	0.062 (0.047)	0.062 (0.059)	0.147*** (0.047)	0.062 (0.050)	0.061 (0.045)
EDplus15	0.106** (0.051)	0.106** (0.044)	0.106* (0.063)	0.154*** (0.044)	0.106*** (0.040)	0.105** (0.051)
log (state GDP)	0.740** (0.322)	0.740*** (0.247)	0.740*** (0.097)	0.097** (0.044)		0.751** (0.335)
Itaipu royalties	-0.018** (0.009)	-0.018** (0.008)	-0.018*** (0.007)	-0.003*** (0.001)		-0.018** (0.009)
Precipitation	-0.000*** (0.000)	-0.000*** (0.000)	-0.000*** (0.000)	-0.000*** (0.000)		0
Temperature	-0.080** (0.040)	-0.080*** (0.028)	-0.080*** (0.018)	-0.022*** (0.005)		-0.080** (0.040)
Population						0.000 (0.000)

Notes: ***Significant at the 1 percent level;**Significant at the 5 percent level;*Significant at the 10 percent level.

Table S7: Sensitivity Analysis – regression results (dependent variable Services GDP)

	Clustering Alternatives			Specification alternatives		
	Main Model	*A*	*B*	*1) Relaxing the restriction of using only counties with unexplored hydropower potential as controls*	*2) Without covariates (temperature, precipitation, royalties and state GDP)*	*3) Adding a covariate (population)*
Standard errors clustered by county:	*Yes*	*Yes*	*No*	*Yes*	*Yes*	*Yes*
Standard errors clustered by hydropower plant:	*Yes*	*No*	*No*	*No*	*Yes*	*Yes*
County and Year Fixed Effects	*Yes*	*Yes*	*Yes*	*Yes*	*Yes*	*Yes*
EDminus5	0.049 (0.035)	0.049* (0.029)	0.049** (0.023)	0.021 (0.029)	0.049 (0.037)	0.049 (0.035)
EDminus4	0.019 (0.025)	0.019 (0.020)	0.019 (0.020)	0.006 (0.021)	0.019 (0.029)	0.019 (0.025)
EDminus3	-0.010 (0.026)	-0.010 (0.019)	-0.010 (0.019)	-0.012 (0.019)	-0.010 (0.027)	-0.011 (0.026)
EDminus2	0.004 (0.020)	0.004 (0.015)	0.004 (0.016)	-0.002 (0.015)	0.004 (0.021)	0.004 (0.020)
EDzero	0.030 (0.025)	0.030* (0.016)	0.030** (0.015)	0.034** (0.016)	0.030 (0.026)	0.030 (0.025)
EDplus1	0.022 (0.027)	0.022 (0.017)	0.022 (0.014)	0.027 (0.017)	0.022 (0.028)	0.022 (0.027)
EDplus2	0.031 (0.027)	0.031* (0.018)	0.031** (0.014)	0.045*** (0.018)	0.031 (0.029)	0.031 (0.027)
EDplus3	0.070** (0.029)	0.070*** (0.018)	0.070*** (0.013)	0.080*** (0.017)	0.070** (0.031)	0.070** (0.029)
EDplus4	0.059** (0.028)	0.059*** (0.017)	0.059*** (0.013)	0.070*** (0.017)	0.059** (0.029)	0.059** (0.027)
EDplus5	0.040 (0.025)	0.040** (0.017)	0.040*** (0.013)	0.053*** (0.018)	0.040 (0.026)	0.039 (0.025)
EDplus6	0.028 (0.025)	0.028* (0.016)	0.028** (0.013)	0.039** (0.017)	0.028 (0.027)	0.027 (0.025)
EDplus7	0.037 (0.029)	0.037** (0.018)	0.037*** (0.013)	0.053*** (0.018)	0.037 (0.030)	0.037 (0.029)
EDplus8	0.020 (0.025)	0.020 (0.016)	0.020* (0.012)	0.034* (0.018)	0.020 (0.027)	0.020 (0.025)
EDplus9	0.026 (0.029)	0.026 (0.017)	0.026** (0.012)	0.042** (0.018)	0.026 (0.030)	0.025 (0.029)
EDplus10	0.032 (0.030)	0.032* (0.018)	0.032** (0.013)	0.048*** (0.018)	0.032 (0.031)	0.032 (0.030)
EDplus11	0.022 (0.028)	0.022 (0.017)	0.022 (0.014)	0.045*** (0.017)	0.022 (0.029)	0.022 (0.028)
EDplus12	0.028 (0.025)	0.028 (0.018)	0.028** (0.014)	0.060*** (0.016)	0.028 (0.026)	0.028 (0.025)
EDplus13	0.002 (0.022)	0.002 (0.018)	0.002 (0.015)	0.031** (0.016)	0.002 (0.023)	0.002 (0.022)
EDplus14	0.002 (0.018)	0.002 (0.015)	0.002 (0.015)	0.018 (0.014)	0.002 (0.018)	0.002 (0.018)
EDplus15	0.011 (0.014)	0.011 (0.012)	0.011 (0.016)	0.021* (0.011)	0.011 (0.014)	0.011 (0.014)
log (state GDP)	0.040 (0.078)	0.040 (0.055)	0.040 (0.025)	-0.178*** (0.014)		0.044 (0.081)
Itaipu royalties	0.002 (0.002)	0.002 (0.003)	0.002 (0.002)	-0.001*** (0.000)		0.002 (0.002)
Precipitation	-0.000*** (0.000)	-0.000*** (0.000)	-0.000*** (0.000)	-0.000*** (0.000)		-0.000*** (0.000)
Temperature	-0.002 (0.007)	-0.002 (0.006)	-0.002 (0.005)	-0.006*** (0.002)		-0.002 (0.007)
Population						0.000 (0.000)

Notes: ***Significant at the 1 percent level;**Significant at the 5 percent level;*Significant at the 10 percent level.

Table S8: Sensitivity Analysis – regression results (dependent variable Agriculture GDP)

	Clustering Alternatives			Specification alternatives		
	Main Model	*A*	*B*	*1) Relaxing the restriction of using only counties with unexplored hydropower potential as controls*	*2) Without covariates (temperature, precipitation, royalties and state GDP)*	*3) Adding a covariate (population)*
Standard errors clustered by county:	*Yes*	*Yes*	*No*	*Yes*	*Yes*	*Yes*
Standard errors clustered by hydropower plant:	*Yes*	*No*	*No*	*No*	*Yes*	*Yes*
County and Year Fixed Effects	*Yes*	*Yes*	*Yes*	*Yes*	*Yes*	*Yes*
EDminus5	-0.107 (0.069)	-0.107** (0.046)	-0.107** (0.049)	-0.132*** (0.044)	-0.107 (0.066)	-0.108 (0.069)
EDminus4	-0.127** (0.058)	-0.127*** (0.046)	-0.127*** (0.043)	-0.172*** (0.047)	-0.127** (0.058)	-0.127** (0.058)
EDminus3	-0.026 (0.054)	-0.026 (0.044)	-0.026 (0.040)	-0.043 (0.043)	-0.026 (0.053)	-0.027 (0.054)
EDminus2	-0.059 (0.058)	-0.059 (0.037)	-0.002065	-0.091** (0.036)	-0.059 (0.060)	-0.059 (0.058)
EDzero	-0.059 (0.045)	-0.059** (0.030)	-0.001888	-0.090*** (0.029)	-0.059 (0.046)	-0.059 (0.045)
EDplus1	-0.081* (0.047)	-0.081** (0.032)	-0.081*** (0.030)	-0.099*** (0.031)	-0.081* (0.048)	-0.081* (0.047)
EDplus2	-0.047 (0.047)	-0.047 (0.031)	-0.047 (0.029)	-0.076** (0.032)	-0.047 (0.050)	-0.047 (0.047)
EDplus3	-0.046 (0.055)	-0.046 (0.037)	-0.046 (0.028)	-0.07* (0.037)	-0.046 (0.055)	-0.047 (0.054)
EDplus4	-0.089* (0.047)	-0.089*** (0.034)	-0.089*** (0.027)	-0.107*** (0.034)	-0.089* (0.047)	-0.09* (0.046)
EDplus5	-0.083* (0.046)	-0.083** (0.033)	-0.083*** (0.029)	-0.109*** (0.033)	-0.083* (0.046)	-0.084* (0.046)
EDplus6	-0.105** (0.043)	-0.105*** (0.033)	-0.105*** (0.028)	-0.120*** (0.034)	-0.105** (0.045)	-0.106** (0.043)
EDplus7	-0.086* (0.052)	-0.086** (0.038)	-0.086*** (0.028)	-0.094** (0.039)	-0.086 (0.054)	-0.087* (0.052)
EDplus8	-0.09* (0.047)	-0.090*** (0.031)	-0.090*** (0.025)	-0.099*** (0.032)	-0.09* (0.047)	-0.092** (0.046)
EDplus9	-0.047 (0.051)	-0.047 (0.033)	-0.001222	-0.055 (0.034)	-0.047 (0.053)	-0.048 (0.050)
EDplus10	-0.019 (0.048)	-0.019 (0.033)	-0.019 (0.028)	-0.027 (0.033)	-0.019 (0.050)	-0.021 (0.048)
EDplus11	0.021 (0.044)	0.021 (0.032)	0.021 (0.029)	0.010 (0.033)	0.021 (0.047)	0.021 (0.044)
EDplus12	-0.077 (0.055)	-0.077** (0.035)	-0.077*** (0.030)	-0.001972	-0.077 (0.056)	-0.078 (0.055)
EDplus13	-0.091** (0.038)	-0.091** (0.036)	-0.091*** (0.033)	-0.082** (0.034)	-0.091** (0.037)	-0.091** (0.038)
EDplus14	-0.007 (0.042)	-0.007 (0.033)	-0.007 (0.032)	-0.019 (0.030)	-0.007 (0.043)	-0.008 (0.042)
EDplus15	0.044 (0.039)	0.044 (0.031)	0.044 (0.035)	-0.029 (0.032)	0.044 (0.044)	0.044 (0.039)
log (state GDP)	0.186 (0.167)	0.186** (0.091)	0.186*** (0.053)	0.162*** (0.025)		0.195 (0.173)
Itaipu royalties	-0.003 (0.004)	-0.003 (0.003)	-0.003 (0.004)	0.000 (0.001)		-0.003 (0.004)
Precipitation	-0.000** (0.000)	-0.000*** (0.000)	-0.000*** (0.000)	0.000 (0.000)		-0.000** (0.000)
Temperature	-0.000 (0.014)	-0.000 (0.011)	-0.000 (0.010)	0.000 (0.003)		-0.000 (0.014)
Population						0.000 (0.000)

Notes: ***Significant at the 1 percent level; **Significant at the 5 percent level;*Significant at the 10 percent level.

7.4.2. Tax revenues

Table S8 to S11 present the detailed regression results for the total public revenues and its subaccounts (Services tax - ISS, State transfers - ICMS, and Federal transfers - FPM). Overall, the conclusions reported for the GDP sensitivity hold for the tax revenues sensitivities. A minor difference occurs for condition “1” (where we relax the restriction of using only counties with hydropower potential that didn’t materialize as controls), where instead of an overestimation, the outcomes are sometimes underestimated in relation to the main model event-time dummy coefficients. However, the results are still qualitative similar.

Table S6: Sensitivity Analysis – regression results (dependent variable Public revenues)

	Clustering Alternatives			Specification alternatives		
	Main Model	*A*	*B*	*1) Relaxing the restriction of using only counties with unexplored hydropower potential as controls*	*2) Without covariates (temperature, precipitation, royalties and state GDP)*	*3) Adding a covariate (population)*
Standard errors clustered by county:	*Yes*	*Yes*	*No*	*No*	*Yes*	*Yes*
Standard errors clustered by hydropower plant:	*Yes*	*No*	*No*	*No*	*Yes*	*Yes*
County and Year Fixed Effects	*Yes*	*Yes*	*Yes*	*Yes*	*Yes*	*Yes*
EDminus5	0.008 (0.021)	0.008 (0.020)	0.008 (0.021)	0.011 (0.022)	0.008 (0.020)	0.010 (0.021)
EDminus4	-0.005 (0.020)	-0.005 (0.020)	-0.005 (0.020)	-0.003 (0.022)	-0.005 (0.021)	-0.005 (0.020)
EDminus3	-0.003 (0.021)	-0.003 (0.020)	-0.003 (0.021)	-0.009 (0.022)	-0.003 (0.021)	-0.003 (0.021)
EDminus2	0.015 (0.021)	0.015 (0.020)	0.015 (0.020)	0.000 (0.022)	0.015 (0.021)	0.014 (0.021)
EDzero	0.032 (0.023)	0.032 (0.023)	0.032* (0.018)	0.027 (0.018)	0.032 (0.024)	0.033 (0.023)
EDplus1	0.057** (0.026)	0.057** (0.026)	0.057*** (0.017)	0.034* (0.018)	0.057** (0.026)	0.058** (0.026)
EDplus2	0.046 (0.028)	0.046* (0.027)	0.046*** (0.018)	0.014 (0.018)	0.046* (0.028)	0.046* (0.028)
EDplus3	0.059** (0.028)	0.059** (0.027)	0.059*** (0.018)	0.028 (0.018)	0.059** (0.028)	0.058** (0.027)
EDplus4	0.045 (0.028)	0.045* (0.027)	0.045** (0.018)	0.005 (0.019)	0.045 (0.028)	0.045 (0.028)
EDplus5	0.065** (0.027)	0.065** (0.026)	0.065*** (0.019)	0.021 (0.019)	0.065** (0.027)	0.062** (0.027)
EDplus6	0.063** (0.027)	0.063** (0.026)	0.063*** (0.019)	0.024 (0.019)	0.063** (0.028)	0.061** (0.027)
EDplus7	0.080*** (0.024)	0.080*** (0.023)	0.080*** (0.020)	0.036* (0.020)	0.080*** (0.023)	0.078*** (0.024)
EDplus8	0.093*** (0.025)	0.093*** (0.024)	0.093*** (0.021)	0.045** (0.021)	0.093*** (0.024)	0.092*** (0.025)
EDplus9	0.074*** (0.026)	0.074*** (0.025)	0.074*** (0.021)	0.022 (0.021)	0.074** (0.029)	0.074*** (0.026)
EDplus10	0.044* (0.026)	0.044* (0.026)	0.044** (0.023)	-0.008 (0.023)	0.044* (0.026)	0.048* (0.026)
EDplus11	0.050** (0.024)	0.050** (0.023)	0.050** (0.024)	-0.007 (0.024)	0.050** (0.024)	0.053** (0.024)
EDplus12	0.032 (0.024)	0.032 (0.023)	0.032 (0.025)	-0.023 (0.025)	0.032 (0.022)	0.032 (0.024)
EDplus13	0.016 (0.023)	0.016 (0.022)	0.016 (0.027)	-0.045 (0.027)	0.016 (0.022)	0.016 (0.022)
EDplus14	0.021 (0.022)	0.021 (0.022)	0.021 (0.027)	-0.046* (0.027)	0.021 (0.021)	0.021 (0.022)
EDplus15	0.017 (0.021)	0.017 (0.020)	0.017 (0.029)	-0.05* (0.029)	0.017 (0.021)	0.015 (0.020)
log (state GDP)	0.451*** (0.068)	0.451*** (0.066)	0.451*** (0.026)	0.356*** (0.010)		0.432*** (0.067)
Itaipu royalties	0.000* (0.000)	0.000** (0.000)	0.000*** (0.000)	0.000 (0.000)		0.000* (0.000)
Precipitation	0.000* (0.000)	0.000* (0.000)	0.000* (0.000)	0.000*** (0.000)		0.000** (0.000)
Temperature	0.002 (0.008)	0.002 (0.008)	0.002 (0.007)	-0.024*** (0.002)		0.005 (0.008)
Population						0.000*** (0.000)

Notes: ***Significant at the 1 percent level;**Significant at the 5 percent level;*Significant at the 10 percent level.

Table S7: Sensitivity Analysis – regression results (dependent variable: Services Tax-ISS)

	Clustering Alternatives			Specification alternatives		
	Main Model	*A*	*B*	*1) Relaxing the restriction of using only counties with unexplored hydropower potential as controls*	*2) Without covariates (temperature, precipitation, royalties and state GDP)*	*3) Adding a covariate (population)*
Standard errors clustered by county:	*Yes*	*Yes*	*No*	*No*	*Yes*	*Yes*
Standard errors clustered by hydropower plant:	*Yes*	*No*	*No*	*No*	*Yes*	*Yes*
County and Year Fixed Effects	*Yes*	*Yes*	*Yes*	*Yes*	*Yes*	*Yes*
EDminus5	0.052 (0.108)	0.052 (0.105)	0.052 (0.114)	0.023 (0.098)	0.052 (0.107)	0.048 (0.108)
EDminus4	0.109 (0.130)	0.109 (0.126)	0.109 (0.110)	0.068 (0.120)	0.109 (0.132)	0.110 (0.129)
EDminus3	0.027 (0.132)	0.027 (0.128)	0.027 (0.112)	-0.044 (0.118)	0.027 (0.131)	0.029 (0.132)
EDminus2	0.069 (0.134)	0.069 (0.130)	0.069 (0.110)	-0.032 (0.120)	0.069 (0.137)	0.074 (0.133)
EDzero	0.590*** (0.144)	0.590*** (0.140)	0.590*** (0.096)	0.506*** (0.138)	0.590*** (0.146)	0.587*** (0.143)
EDplus1	1.001*** (0.161)	1.001*** (0.156)	1.001*** (0.095)	0.905*** (0.152)	1.001*** (0.163)	1.000*** (0.160)
EDplus2	0.997*** (0.168)	0.997*** (0.163)	0.997*** (0.096)	0.898*** (0.161)	0.997*** (0.170)	0.998*** (0.167)
EDplus3	1.014*** (0.158)	1.014*** (0.153)	1.014*** (0.097)	0.898*** (0.149)	1.014*** (0.160)	1.017*** (0.156)
EDplus4	0.705*** (0.145)	0.705*** (0.140)	0.705*** (0.098)	0.587*** (0.130)	0.705*** (0.144)	0.707*** (0.143)
EDplus5	0.613*** (0.145)	0.613*** (0.140)	0.613*** (0.102)	0.468*** (0.126)	0.613*** (0.141)	0.622*** (0.142)
EDplus6	0.488*** (0.144)	0.488*** (0.139)	0.488*** (0.102)	0.337*** (0.125)	0.488*** (0.139)	0.494*** (0.142)
EDplus7	0.415*** (0.148)	0.415*** (0.143)	0.415*** (0.107)	0.254* (0.130)	0.415*** (0.136)	0.421*** (0.146)
EDplus8	0.332** (0.151)	0.332** (0.146)	0.332*** (0.111)	0.169 (0.134)	0.332** (0.141)	0.335** (0.150)
EDplus9	0.277* (0.148)	0.277* (0.143)	0.277** (0.113)	0.091 (0.132)	0.277* (0.142)	0.275* (0.147)
EDplus10	0.197 (0.142)	0.197 (0.138)	0.197 (0.122)	-0.044 (0.129)	0.197 (0.131)	0.183 (0.142)
EDplus11	0.056 (0.141)	0.056 (0.137)	0.056 (0.128)	-0.0252	0.056 (0.134)	0.044 (0.140)
EDplus12	-0.027 (0.133)	-0.027 (0.129)	-0.027 (0.135)	-0.274** (0.117)	-0.027 (0.127)	-0.029 (0.132)
EDplus13	-0.053 (0.118)	-0.053 (0.114)	-0.053 (0.147)	-0.342*** (0.117)	-0.053 (0.113)	-0.052 (0.116)
EDplus14	-0.147 (0.130)	-0.147 (0.125)	-0.147 (0.145)	-0.404*** (0.123)	-0.147 (0.120)	-0.148 (0.128)
EDplus15	-0.142 (0.145)	-0.142 (0.141)	-0.142 (0.158)	-0.365** (0.145)	-0.142 (0.131)	-0.138 (0.144)
log (state GDP)	1.561*** (0.409)	1.561*** (0.395)	1.561*** (0.147)	0.895*** (0.069)		1.641*** (0.402)
Itaipu royalties	-0.000 (0.000)	-0.000 (0.000)	-0.000* (0.000)	-0.001 (0.001)		-0.000 (0.000)
Precipitation	0.000*** (0.000)	0.000*** (0.000)	0.000*** (0.000)	0.000*** (0.000)		0.000*** (0.000)
Temperature	0.013 (0.046)	0.013 (0.044)	0.013 (0.038)	-0.000 (0.012)		0.003 (0.045)
Population						-0.000*** (0.000)

Notes: ***Significant at the 1 percent level;**Significant at the 5 percent level;*Significant at the 10 percent level.

Table S8: Sensitivity Analysis – regression results (dependent variable: state transfers - ICMS)

	Clustering Alternatives			Specification alternatives		
	Main Model	*A*	*B*	*1) Relaxing the restriction of using only counties with unexplored hydropower potential as controls*	*2) Without control covariates (temperature, precipitation, royalties and state GDP)*	*3) Adding a control covariate (population)*
Standard errors clustered by county:	*Yes*	*Yes*	*No*	*No*	*Yes*	*Yes*
Standard errors clustered by hydropower plant:	*Yes*	*No*	*No*	*No*	*Yes*	*Yes*
County and Year Fixed Effects	*Yes*	*Yes*	*Yes*	*Yes*	*Yes*	*Yes*
EDminus5	0.061 (0.051)	0.061 (0.050)	0.061 (0.050)	0.052 (0.048)	0.061 (0.055)	0.062 (0.051)
EDminus4	0.033 (0.053)	0.033 (0.051)	0.033 (0.048)	0.014 (0.046)	0.033 (0.055)	0.033 (0.053)
EDminus3	0.051 (0.052)	0.051 (0.050)	0.051 (0.049)	0.031 (0.047)	0.051 (0.052)	0.051 (0.052)
EDminus2	0.064 (0.053)	0.064 (0.052)	0.064 (0.048)	0.027 (0.046)	0.064 (0.053)	0.063 (0.053)
EDzero	0.072 (0.062)	0.072 (0.060)	0.072* (0.042)	0.037 (0.040)	0.072 (0.063)	0.072 (0.062)
EDplus1	0.032 (0.054)	0.032 (0.052)	0.032 (0.042)	0.018 (0.039)	0.032 (0.054)	0.032 (0.054)
EDplus2	0.012 (0.060)	0.012 (0.058)	0.012 (0.042)	-0.024 (0.039)	0.012 (0.059)	0.012 (0.060)
EDplus3	0.030 (0.057)	0.030 (0.055)	0.030 (0.043)	-0.002 (0.040)	0.030 (0.057)	0.029 (0.057)
EDplus4	0.052 (0.059)	0.052 (0.058)	0.052 (0.043)	0.005 (0.040)	0.052 (0.059)	0.052 (0.060)
EDplus5	0.025 (0.057)	0.025 (0.055)	0.025 (0.045)	-0.002 (0.042)	0.025 (0.054)	0.023 (0.057)
EDplus6	0.080 (0.055)	0.080 (0.053)	0.080* (0.045)	0.051 (0.042)	0.080 (0.055)	0.079 (0.055)
EDplus7	0.111** (0.055)	0.111** (0.053)	0.111** (0.047)	0.070 (0.044)	0.111** (0.052)	0.110** (0.055)
EDplus8	0.203*** (0.061)	0.203*** (0.059)	0.203*** (0.049)	0.156*** (0.045)	0.203*** (0.059)	0.202*** (0.061)
EDplus9	0.156** (0.063)	0.156** (0.061)	0.156*** (0.050)	0.099** (0.046)	0.156** (0.064)	0.156** (0.063)
EDplus10	0.116** (0.057)	0.116** (0.056)	0.116** (0.054)	0.060 (0.049)	0.116** (0.058)	0.118** (0.058)
EDplus11	0.115** (0.054)	0.115** (0.053)	0.115** (0.057)	0.052 (0.052)	0.115** (0.052)	0.117** (0.054)
EDplus12	0.060 (0.052)	0.060 (0.050)	0.060 (0.059)	0.003 (0.054)	0.060 (0.052)	0.060 (0.051)
EDplus13	0.030 (0.050)	0.030 (0.049)	0.030 (0.065)	-0.015 (0.059)	0.030 (0.048)	0.030 (0.050)
EDplus14	0.054 (0.044)	0.054 (0.043)	0.054 (0.065)	0.017 (0.058)	0.054 (0.041)	0.054 (0.044)
EDplus15	0.044 (0.044)	0.044 (0.043)	0.044 (0.070)	0.003 (0.063)	0.044 (0.041)	0.043 (0.044)
log (state GDP)	0.874*** (0.158)	0.874*** (0.153)	0.874*** (0.063)	0.821*** (0.021)		0.860*** (0.154)
Itaipu royalties	0.000 (0.000)	0.000 (0.000)	0.000 (0.000)	-0.000*** (0.000)		0.000 (0.000)
Precipitation	0.000 (0.000)	0.000 (0.000)	0.000 (0.000)	0.000*** (0.000)		0.000 (0.000)
Temperature	0.040** (0.020)	0.040** (0.019)	0.040** (0.017)	0.008* (0.004)		0.042** (0.020)
Population						0.000 (0.000)

Notes: ***Significant at the 1 percent level;**Significant at the 5 percent level;*Significant at the 10 percent level.

Table S9: Sensitivity Analysis – regression results (dependent variable: federal transfers - FPM)

	Clustering Alternatives			Specification alternatives		
	Main Model	*A*	*B*	*1) Relaxing the restriction of using only counties with unexplored hydropower potential as controls*	*2) Without covariates (temperature, precipitation, royalties and state GDP)*	*3) Adding a covariate (population)*
Standard errors clustered by county:	*Yes*	*Yes*	*No*	*No*	*Yes*	*Yes*
Standard errors clustered by hydropower plant:	*Yes*	*No*	*No*	*No*	*Yes*	*Yes*
County and Year Fixed Effects	*Yes*	*Yes*	*Yes*	*Yes*	*Yes*	*Yes*
EDminus5	-0.005 (0.019)	-0.005 (0.019)	-0.005 (0.024)	0.008 (0.028)	-0.005 (0.019)	-0.004 (0.019)
EDminus4	-0.021 (0.029)	-0.021 (0.028)	-0.021 (0.023)	0.004 (0.028)	-0.021 (0.029)	-0.021 (0.028)
EDminus3	-0.007 (0.018)	-0.007 (0.018)	-0.007 (0.023)	0.010 (0.028)	-0.007 (0.019)	-0.007 (0.018)
EDminus2	0.003 (0.018)	0.003 (0.018)	0.003 (0.023)	0.028 (0.027)	0.003 (0.018)	0.002 (0.018)
EDzero	0.009 (0.019)	0.009 (0.019)	0.009 (0.020)	0.032 (0.024)	0.009 (0.019)	0.010 (0.019)
EDplus1	0.009 (0.018)	0.009 (0.017)	0.009 (0.020)	0.020 (0.023)	0.009 (0.017)	0.010 (0.018)
EDplus2	-0.008 (0.017)	-0.008 (0.017)	-0.008 (0.020)	-0.002 (0.023)	-0.008 (0.016)	-0.008 (0.017)
EDplus3	-0.032 (0.048)	-0.032 (0.047)	-0.032 (0.020)	-0.026 (0.024)	-0.032 (0.048)	-0.033 (0.048)
EDplus4	-0.022 (0.021)	-0.022 (0.020)	-0.022 (0.020)	-0.014 (0.024)	-0.022 (0.020)	-0.023 (0.021)
EDplus5	-0.035 (0.027)	-0.035 (0.026)	-0.000735	-0.034 (0.025)	-0.035 (0.025)	-0.037 (0.026)
EDplus6	-0.030 (0.024)	-0.030 (0.023)	-0.030 (0.021)	-0.014 (0.025)	-0.030 (0.023)	-0.032 (0.024)
EDplus7	-0.001 (0.018)	-0.001 (0.018)	-0.001 (0.022)	0.022 (0.026)	-0.001 (0.017)	-0.002 (0.019)
EDplus8	-0.015 (0.021)	-0.015 (0.020)	-0.015 (0.023)	-0.001 (0.027)	-0.015 (0.019)	-0.016 (0.020)
EDplus9	-0.027 (0.019)	-0.027 (0.018)	-0.027 (0.023)	-0.014 (0.027)	-0.027 (0.020)	-0.027 (0.018)
EDplus10	-0.055*** (0.021)	-0.055*** (0.020)	-0.055** (0.025)	-0.038 (0.029)	-0.055*** (0.020)	-0.052** (0.020)
EDplus11	-0.052** (0.022)	-0.052** (0.021)	-0.052* (0.027)	-0.000 (0.031)	-0.052*** (0.020)	-0.049** (0.022)
EDplus12	-0.062*** (0.023)	-0.062*** (0.022)	-0.062** (0.028)	-0.058* (0.032)	-0.062*** (0.019)	-0.062*** (0.023)
EDplus13	-0.057** (0.025)	-0.057** (0.025)	-0.057* (0.031)	-0.064* (0.035)	-0.057** (0.023)	-0.057** (0.025)
EDplus14	-0.117 (0.087)	-0.117 (0.085)	-0.117*** (0.030)	-0.141*** (0.035)	-0.117 (0.088)	-0.117 (0.088)
EDplus15	-0.040* (0.024)	-0.040* (0.024)	-0.040 (0.033)	-0.048 (0.038)	-0.040** (0.020)	-0.041* (0.024)
log (state GDP)	0.095 (0.078)	0.095 (0.075)	0.095*** (0.029)	0.004 (0.012)		0.079 (0.077)
Itaipu royalties	0.000 (0.000)	0.000 (0.000)	0.000 (0.000)	0.000 (0.000)		0.000 (0.000)
Precipitation	-0.000 (0.000)	-0.000 (0.000)	-0.000 (0.000)	0.000 (0.000)		-0.000 (0.000)
Temperature	0.002 (0.008)	0.002 (0.008)	0.002 (0.008)	-0.003 (0.003)		0.004 (0.008)
Population						0.000** (0.000)

Notes: ***Significant at the 1 percent level;**Significant at the 5 percent level;*Significant at the 10 percent level.

7.4.3 Socioeconomic indicators

We applied a similar sensitivity analysis for the eight socioeconomic indicators: average income, life expectancy, educational level, access to piped water, access to public electricity, teenage pregnancy levels, and HIV cases. Annex B3 contains the detailed regression tables. Those estimates also indicate that failure to control for within-cluster error correlation lead to misleadingly small standard errors. Overall, the use of alternative specifications also suggests that the selected socioeconomic indicators are not affected by hydropower development after construction at the 5% level, supporting the results presented in Chapter 3.

7.5 Regressions checks

To provide additional information about the validity of our model assumptions, we developed a series of regression checks. First, we examined the residuals from our main regression to confirm that the basic ordinary least squares assumptions are valid. Second, we tested the strict exogeneity assumption by running alternative specifications using lagged covariates, and provided a lower bound estimate for the main model using an autoregressive model.

7.5.1 Residual diagnostics and clustered bootstrapping

Annex B2 contains six plots with standard regression diagnostics (distribution of the studentized residual, residuals vs. fitted values, Q-Q plot, scale location, cook's distance, and a residuals vs. leverage) for each dependent economic variable evaluated in this study. The analysis of the results confirms that the residual distributions have constant variance. However, the residuals vs. fitted values plot review the existence of outliers, and the distribution of the studentized residuals and Q-Q plots indicate that error distributions have a longer tail compared to the normal distribution. Although the cook's distance and leverage vs. residuals plot indicate that those outliers are not influential, the normality assumption of the variance seems to be violated. This violation can affect the standard errors and, as a consequence, our inferences.

To investigate the effect of the lack of normal variance in regression standard errors, we performed a standard clustered bootstrapping procedure. Bootstrap methods generate a number of pseudo-samples from the original sample, for each pseudo-sample we calculate the statistic of interest, and use the distribution of this statistic across pseudo-samples to infer the distribution of the original sample statistic (Cameron, Gelbach & Miller 2008).

Table S12 and Table S13 compare the results from the clustered robust standard errors from the main model with clustered bootstrap standard errors for GDP and taxes, respectively. Table S12 shows that clustered bootstrap and the main model standard errors are qualitative similar. In contrast, Table S13 indicates that bootstrap standard errors are, in general, greater compared to the main model ones. This occurs because the deviation from the normal distribution is greater for taxes (Compare Q-Q plots in Annex B2). As a result, the substitution of the bootstrap standard errors for inference attenuates the statistical significance from our results. However, this analysis does not change our main conclusions, as most of the significant coefficients under the main model assumptions are still significant at 5% level using the average bootstrap standard errors.

Table S6: Comparison between the clustered robust standard errors from the main model and clustered bootstrap standard error statistics: Total GDP, Industry GDP, Services GDP and Agriculture GDP. Bootstrapping results: average and 95%confidence interval.

	Total GDP		Industry GDP		Services GDP		Agriculture GDP	
	Main Model	Bootstrapping	Main Model	Bootstrapping	Main Model	Bootstrapping	Main Model	Bootstrapping
EDminus5	0.045	0.043 (0.029-0.057)	0.125	0.109 (0.068-0.149)	0.035	0.033 (0.015-0.051)	0.069	0.072 (0.055-0.091)
EDminus4	0.028	0.034 (0.023-0.046)	0.121	0.103 (0.058-0.142)	0.025	0.028 (0.021-0.036)	0.058	0.066 (0.048-0.089)
EDminus3	0.031	0.031 (0.021-0.04)	0.177	0.154 (0.076-0.23)	0.026	0.023 (0.017-0.03)	0.054	0.06 (0.046-0.077)
EDminus2	0.033	0.03 (0.024-0.035)	0.141	0.105 (0.07-0.142)	0.020	0.016 (0.012-0.019)	0.058	0.06 (0.05-0.071)
EDzero	0.031	0.028 (0.022-0.036)	0.113	0.092 (0.068-0.123)	0.025	0.02 (0.016-0.026)	0.045	0.046 (0.037-0.055)
EDplus1	0.038	0.03 (0.024-0.037)	0.166	0.142 (0.103-0.179)	0.027	0.022 (0.018-0.028)	0.047	0.049 (0.039-0.059)
EDplus2	0.040	0.033 (0.027-0.041)	0.133	0.11 (0.081-0.14)	0.027	0.024 (0.019-0.03)	0.047	0.047 (0.039-0.056)
EDplus3	0.042	0.034 (0.028-0.042)	0.128	0.104 (0.078-0.13)	0.029	0.023 (0.019-0.028)	0.055	0.056 (0.045-0.068)
EDplus4	0.037	0.032 (0.026-0.037)	0.118	0.093 (0.075-0.116)	0.028	0.023 (0.019-0.027)	0.047	0.05 (0.042-0.056)
EDplus5	0.032	0.033 (0.026-0.039)	0.087	0.086 (0.071-0.099)	0.025	0.024 (0.02-0.028)	0.046	0.048 (0.041-0.056)
EDplus6	0.032	0.031 (0.026-0.037)	0.082	0.083 (0.069-0.098)	0.025	0.024 (0.019-0.028)	0.043	0.047 (0.038-0.055)
EDplus7	0.031	0.03 (0.024-0.036)	0.073	0.073 (0.061-0.085)	0.029	0.027 (0.022-0.032)	0.052	0.056 (0.043-0.068)
EDplus8	0.031	0.03 (0.022-0.038)	0.080	0.076 (0.06-0.094)	0.025	0.022 (0.018-0.026)	0.047	0.052 (0.044-0.062)
EDplus9	0.029	0.029 (0.021-0.036)	0.061	0.072 (0.059-0.089)	0.029	0.025 (0.02-0.03)	0.051	0.056 (0.045-0.07)
EDplus10	0.031	0.028 (0.023-0.035)	0.059	0.069 (0.054-0.09)	0.030	0.026 (0.02-0.031)	0.048	0.052 (0.039-0.063)
EDplus11	0.030	0.029 (0.022-0.036)	0.055	0.062 (0.049-0.078)	0.028	0.025 (0.019-0.031)	0.044	0.046 (0.037-0.055)
EDplus12	0.026	0.031 (0.023-0.039)	0.059	0.076 (0.059-0.096)	0.025	0.024 (0.019-0.031)	0.055	0.059 (0.048-0.071)
EDplus13	0.018	0.026 (0.019-0.035)	0.047	0.066 (0.053-0.08)	0.022	0.025 (0.019-0.031)	0.038	0.044 (0.031-0.057)
EDplus14	0.015	0.022 (0.016-0.03)	0.045	0.064 (0.045-0.085)	0.018	0.021 (0.016-0.026)	0.042	0.049 (0.037-0.061)
EDplus15	0.016	0.02 (0.013-0.028)	0.051	0.068 (0.041-0.097)	0.014	0.018 (0.014-0.022)	0.039	0.044 (0.033-0.056)

Table S7: Comparison between the clustered robust standard errors from the main model and clustered bootstrap standard error statistics: Public revenues, Services tax, State transfers and federal transfers. Bootstrapping results: average and 95%confidence interval.

	Public revenues		Services tax - ISS		State transfer - ICMS		Federal transfer - FPM	
	Main Model	Bootstrapping	Main Model	Bootstrapping	Main Model	Bootstrapping	Main Model	Bootstrapping
EDminus5	0.021	0.029 (0.023-0.035)	0.108	0.142 (0.114-0.172)	0.051	0.083 (0.064-0.101)	0.019	0.022 (0.017-0.027)
EDminus4	0.020	0.031 (0.026-0.037)	0.130	0.178 (0.144-0.21)	0.053	0.088 (0.068-0.11)	0.029	0.036 (0.021-0.047)
EDminus3	0.021	0.032 (0.026-0.037)	0.132	0.174 (0.134-0.215)	0.052	0.085 (0.065-0.105)	0.018	0.024 (0.02-0.03)
EDminus2	0.021	0.033 (0.027-0.039)	0.134	0.161 (0.131-0.194)	0.053	0.088 (0.067-0.109)	0.018	0.024 (0.019-0.03)
EDzero	0.023	0.039 (0.028-0.049)	0.144	0.188 (0.15-0.225)	0.062	0.106 (0.079-0.128)	0.019	0.027 (0.022-0.033)
EDplus1	0.026	0.044 (0.031-0.056)	0.161	0.248 (0.199-0.301)	0.054	0.094 (0.068-0.117)	0.018	0.024 (0.017-0.03)
EDplus2	0.028	0.052 (0.037-0.065)	0.168	0.282 (0.225-0.342)	0.060	0.108 (0.076-0.134)	0.017	0.022 (0.017-0.027)
EDplus3	0.028	0.048 (0.033-0.062)	0.158	0.252 (0.201-0.31)	0.057	0.1 (0.072-0.124)	0.048	0.051 (0.02-0.079)
EDplus4	0.028	0.046 (0.031-0.06)	0.145	0.218 (0.186-0.258)	0.059	0.104 (0.079-0.127)	0.021	0.027 (0.02-0.033)
EDplus5	0.027	0.044 (0.031-0.056)	0.145	0.21 (0.171-0.248)	0.057	0.091 (0.065-0.113)	0.027	0.032 (0.024-0.04)
EDplus6	0.027	0.037 (0.029-0.046)	0.144	0.21 (0.167-0.263)	0.055	0.088 (0.068-0.109)	0.024	0.028 (0.021-0.036)
EDplus7	0.024	0.034 (0.028-0.042)	0.148	0.241 (0.185-0.315)	0.055	0.082 (0.066-0.1)	0.018	0.023 (0.019-0.028)
EDplus8	0.025	0.035 (0.027-0.041)	0.151	0.231 (0.17-0.303)	0.061	0.081 (0.065-0.1)	0.021	0.026 (0.021-0.033)
EDplus9	0.026	0.038 (0.027-0.047)	0.148	0.283 (0.198-0.367)	0.063	0.085 (0.063-0.107)	0.019	0.023 (0.018-0.03)
EDplus10	0.026	0.032 (0.024-0.04)	0.142	0.242 (0.169-0.314)	0.057	0.074 (0.057-0.094)	0.021	0.026 (0.018-0.033)
EDplus11	0.024	0.028 (0.022-0.034)	0.141	0.23 (0.162-0.301)	0.054	0.069 (0.054-0.089)	0.022	0.031 (0.021-0.041)
EDplus12	0.024	0.03 (0.022-0.038)	0.133	0.206 (0.146-0.275)	0.052	0.066 (0.052-0.088)	0.023	0.035 (0.026-0.046)
EDplus13	0.023	0.031 (0.024-0.039)	0.118	0.146 (0.106-0.198)	0.050	0.066 (0.051-0.087)	0.025	0.037 (0.028-0.046)
EDplus14	0.022	0.031 (0.023-0.041)	0.130	0.162 (0.112-0.22)	0.044	0.057 (0.043-0.08)	0.087	0.104 (0.032-0.16)
EDplus15	0.021	0.03 (0.022-0.041)	0.145	0.188 (0.124-0.261)	0.044	0.062 (0.047-0.083)	0.024	0.039 (0.025-0.051)

7.5.2 Robustness checks

The basic unobserved effects model can be written, for a randomly drawn cross section observation i, as

$$y_{it} = x_{it}\beta + c_i + u_{it} \qquad (1)$$

where, x_{it} is a vector of observable variables that change across *t* but not *i*, variables that change across *i* but not *t*, and variables that change across *i* and *t*. c_i is the individual effect and u_{it} the idiosyncratic errors (Wooldridge 2004). For a linear panel data model, the strict exogeneity assumption can be formally stated by the following equation:

$$E(y_{it}|x_{i1}, x_{i2}, \dots x_{iT}, c_i) = E(y_{it}|x_{it}, c_i) = x_{it}\beta + c_i \quad (2)$$

For t=1,2,…,T.

It means that, once x_{it} and c_i are controlled for, x_{is} has no partial effect on y_{is} for s¹t (Wooldridge 2004). Given equation (1), the idiosyncratic errors can be stated as

$$E(u_{it}|x_{it}, c_i) = 0 \quad (3)$$

This assumption denotes that explanatory variables in each time period are uncorrelated with the idiosyncratic errors in each time period (Wooldridge 2004):

$$E(x'_{is}u_{it}) = 0 \quad (4)$$

To check the strict exogeneity assumption, we employed a test proposed by Wooldridge (2004) using the following specification:

$$y_{it} = x_{it}\beta + \delta w_{i,t+1} + c_i + u_{it} \quad (5)$$

where, $w_{i,t+1}$ is a subset of $x_{i,t+1}$ (that would exclude time dummies). Under the strict exogeneity, d should be equal to zero. The usual *F* statistic is valid here. Table S14 to Table S21 describes the results from this analysis in the last column (column 5). Further, we include a similar analysis but with lagged regressors (column 4) instead of the leads. The last row of the tables contains the F-statistics and the correspondent p-values.

Moreover, we apply an autoregressive (AR) model to investigate a lower bound estimate to be compared to our main model results. Angrist & Pischke (2008) shows that if the unobserved effects model is correct and we mistakenly estimate an equation using lagged outcomes like the equation 6 below, estimates of a positive treatment effect will tend to be too small (Angrist & Pischke 2008). Therefore, the autoregressive model can be used as a lower bound estimate and an additional check to our main model.

$$y_{it} = x_{it}\beta + \delta y_{i,t-h} + c_i + u_{it} \quad (6)$$

where $y_{i,t-h}$ is a vector including lagged dependent variables for multiple periods.

Table S14 to Table S21 contain the regression estimates from five different specifications. The first column reports the results from the main model. The second column is similar to the main model but instead of 20 event-time dummies, we simplified the specification by including only two event-time dummies that represent the averages in the construction (EDzero to EDplus4) and operation (EDplus5 to EDplus15) stages. Based on this simpler model, the third column presents the autoregressive (AR) specification (equation 6) with a lagged dependent variable (Ylag), and fourth and fifth column present the strict exogeneity tests using lags or leads of a subset of regressors (equation 5), respectively.

The lead regressors joint F-test (column 5) indicate that the strict exogeneity assumption is violated for most of the indicators. The inconsistency from using fixed effects when the strict exogeneity assumption fails is of order T^{-1}. Thus, with large T the bias may be minimal

(Wooldridge 2004). For our data, the estimated bias would be around 5% (T=20). Furthermore, our coefficients of interest (construction and operation) are not affected supporting the argument that our main results are robust.

As expected, the AR model construction and operation coefficients indicate a lower estimate in comparison to the main simpler event-time model. The AR values provide a lower bound for our main estimates and confirm the direction and order of magnitude of our main estimates.

Table S14: Comparison between the main model and other alternative specifications: a simpler event-time, an autoregressive, and lag/lead regressors model. Dependent variable: Total GDP

	Main Model (1)	Simple Model (2)	AR (3)	Lag Regressors (t-1) (4)	Lead Regressors (t+1) (5)
EDminus5	0.025 (0.042)				
EDminus4	0.005 (0.025)				
EDminus3	-0.012 (0.032)				
EDminus2	-0.030 (0.034)				
EDzero	-0.000 (0.033)				
EDplus1	0.001 (0.040)				
EDplus2	0.048 (0.043)				
EDplus3	0.099^{**} (0.045)				
EDplus4	0.092^{**} (0.040)				
EDplus5	0.094^{***} (0.032)				
EDplus6	0.066^{**} (0.034)				
EDplus7	0.062^{*} (0.034)				
EDplus8	0.066^{**} (0.033)				
EDplus9	0.061^{*} (0.032)				
EDplus10	0.061^{*} (0.033)				
EDplus11	0.059^{*} (0.033)				
EDplus12	0.033 (0.030)				
EDplus13	0.016 (0.022)				
EDplus14	0.030^{*} (0.018)				
EDplus15	0.047^{***} (0.018)				
Construction		0.047 (0.030)	0.017^{*} (0.009)	0.040^{***} (0.013)	0.044^{***} (0.013)
Operation		0.052^{**} (0.022)	-0.006 (0.006)	0.048^{***} (0.011)	0.047^{***} (0.012)
Ylag			0.987^{***} (0.002)		
log (state GDP)	-121.633^{***} (25.338)	-129.437^{***} (26.654)	-7.255^{***} (1.814)	-98.748^{***} (23.564)	-107.543^{***} (24.189)
Itaipu royalties	0.006^{**} (0.003)	0.007^{**} (0.003)	0.000^{***} (0.000)	0.008^{**} (0.004)	0.008^{*} (0.004)
Precipitation	-0.000^{**} (0.000)	-0.000^{**} (0.000)	0.000 (0.000)	-0.000 (0.000)	-0.000 (0.000)
Temperature	-0.011 (0.011)	-0.011 (0.012)	0.003^{***} (0.001)	0.020^{**} (0.008)	-0.001 (0.010)
log (state GDP): t-1				-38.538 (23.526)	
Precipitation: t-1				0.000 (0.000)	
Air Temperature: t-1				-0.034^{***} (0.009)	
log (state GDP): t+1					-25.555 (24.128)
Precipitation: t+1					-0.000 (0.000)
Air Temperature: t+1					0.022^{***} (0.008)
Wald test for the subset of lag/lead covariates (F-statistic/p-values)				F = 7.51 / p= 5.2e-05	F = 3.97 / p= 0.007

Note: ***Significant at the 1 percent level;**Significant at the 5 percent level;*Significant at the 10 percent level.

Table S15: Comparison between the main model and other alternative specifications: a simpler event-time, an autoregressive, and lag/lead regressors model. Dependent variable: Industry GDP

	Main Model (1)	Simple Model (2)	AR (3)	Lag Regressors (t-1) (4)	Lead Regressors (t+1) (5)
EDminus5	0.247* (0.136)				
EDminus4	0.221 (0.139)				
EDminus3	-0.023 (0.185)				
EDminus2	0.087 (0.154)				
EDzero	0.110 (0.122)				
EDplus1	0.064 (0.175)				
EDplus2	0.233 (0.148)				
EDplus3	0.325** (0.146)				
EDplus4	0.335** (0.132)				
EDplus5	0.315*** (0.096)				
EDplus6	0.275*** (0.093)				
EDplus7	0.256*** (0.084)				
EDplus8	0.320*** (0.098)				
EDplus9	0.219*** (0.073)				
EDplus10	0.195*** (0.074)				
EDplus11	0.164** (0.071)				
EDplus12	0.164** (0.071)				
EDplus13	0.111** (0.055)				
EDplus14	0.082 (0.062)				
EDplus15	0.115** (0.055)				
Construction		0.148* (0.086)	0.053 (0.034)	0.114*** (0.031)	0.126*** (0.032)
Operation		0.177*** (0.051)	-0.002 (0.017)	0.154*** (0.024)	0.156*** (0.026)
Ylag			0.944*** (0.015)		
log (state GDP)	-293.048*** (74.784)	-316.459*** (77.630)	-41.039*** (12.540)	-246.480*** (58.150)	-271.969*** (60.342)
Itaipu royalties	0.003 (0.006)	0.004 (0.006)	-0.000 (0.001)	0.011** (0.005)	0.013** (0.006)
Precipitation	0	0	0.000*** (0.000)	0.000 (0.000)	-0.000 (0.000)
Temperature	-0.003256	-0.076 (0.046)	0.016*** (0.005)	0.022 (0.018)	-0.022 (0.022)
log (state GDP): t-1				-97.63* (58.838)	
Precipitation: t-1				-0.000 (0.000)	
Air Temperature: t-1				-0.048** (0.021)	
log (state GDP): t+1					-53.539 (59.876)
Precipitation: t+1					0.000 (0.000)
Air Temperature: t+1					0.039** (0.018)
Wald test for the subset of lag/lead covariates (F-statistic/p-values)				F = 4.759/ p= 0.002	F = 2.407/ p= 0.065

Note: ***Significant at the 1 percent level;**Significant at the 5 percent level;*Significant at the 10 percent level.

Table S16: Comparison between the main model and other alternative specifications: a simpler event-time, an autoregressive, and lag/lead regressors model. Dependent variable: Services GDP

	Main Model (1)	Simple Model (2)	AR (3)	Lag Regressors (t-1) (4)	Lead Regressors (t+1) (5)
EDminus5	0.046 (0.033)				
EDminus4	0.018 (0.025)				
EDminus3	-0.007 (0.027)				
EDminus2	0.007 (0.021)				
EDzero	0.035 (0.026)				
EDplus1	0.023 (0.028)				
EDplus2	0.033 (0.029)				
EDplus3	0.069** (0.031)				
EDplus4	0.058** (0.029)				
EDplus5	0.039 (0.025)				
EDplus6	0.028 (0.026)				
EDplus7	0.037 (0.030)				
EDplus8	0.026 (0.027)				
EDplus9	0.031 (0.031)				
EDplus10	0.038 (0.032)				
EDplus11	0.029 (0.029)				
EDplus12	0.034 (0.025)				
EDplus13	0.006 (0.023)				
EDplus14	0.006 (0.018)				
EDplus15	0.012 (0.014)				
Construction		0.037* (0.022)	0.003 (0.004)	0.032*** (0.008)	0.032*** (0.008)
Operation		0.024 (0.022)	-0.002 (0.004)	0.024*** (0.007)	0.019** (0.008)
Ylag			0.995*** (0.001)		
log (state GDP)	-73.878*** (16.264)	-76.872*** (16.766)	-3.727*** (0.797)	-69.087*** (15.425)	-68.235*** (16.620)
Itaipu royalties	0.006* (0.003)	0.006** (0.003)	0.000*** (0.000)	0.006 (0.004)	0.006 (0.005)
Precipitation	-0.000*** (0.000)	-0.000** (0.000)	0.000* (0.000)	-0.000 (0.000)	-0.000 (0.000)
Temperature	-0.000 (0.007)	-0.001 (0.007)	0.003*** (0.001)	0.014*** (0.005)	0.000 (0.006)
log (state GDP): t-1				-4.716 (13.275)	
Precipitation: t-1				0.000 (0.000)	
Air Temperature: t-1				-0.008 (0.006)	
log (state GDP): t+1					-0.024 (13.999)
Precipitation: t+1					-0.000 (0.000)
Air Temperature: t+1					0.017*** (0.006)
Wald test for the subset of lag/lead covariates (F-statistic/p-values)				F = 2.100 / p= 0.097	F = 4.781/ p= 0.002

Note: ***Significant at the 1 percent level;**Significant at the 5 percent level;*Significant at the 10 percent level.

Table S17: Comparison between the main model and other alternative specifications: a simpler event-time, an autoregressive, and lag/lead regressors model. Dependent variable: Agriculture GDP

	Main Model (1)	Simple Model (2)	AR (3)	Lag Regressors (t-1) (4)	Lead Regressors (t+1) (5)
EDminus5	-0.108 (0.068)				
EDminus4	-0.123** (0.052)				
EDminus3	-0.018 (0.054)				
EDminus2	-0.052 (0.058)				
EDzero	-0.050 (0.045)				
EDplus1	-0.076 (0.048)				
EDplus2	-0.039 (0.048)				
EDplus3	-0.045 (0.054)				
EDplus4	-0.087* (0.047)				
EDplus5	-0.081* (0.046)				
EDplus6	-0.103** (0.044)				
EDplus7	-0.083 (0.053)				
EDplus8	-0.003496				
EDplus9	-0.033 (0.051)				
EDplus10	-0.006 (0.048)				
EDplus11	0.037 (0.045)				
EDplus12	-0.067 (0.056)				
EDplus13	-0.086** (0.038)				
EDplus14	-0.002 (0.043)				
EDplus15	0.047 (0.042)				
Construction		-0.029 (0.037)	-0.032 (0.020)	-0.021 (0.017)	-0.017 (0.018)
Operation		-0.043 (0.028)	-0.018 (0.012)	-0.037** (0.015)	-0.026 (0.016)
Ylag			0.957*** (0.006)		
log (state GDP)	-75.930*** (25.728)	-68.068*** (25.872)	-13.121*** (2.474)	-64.790** (32.286)	-66.343** (32.397)
Itaipu royalties	0.002 (0.002)	0.003 (0.002)	0.001*** (0.000)	0.003 (0.003)	0.004 (0.004)
Precipitation	-0.000** (0.000)	-0.000** (0.000)	0.000 (0.000)	-0.000*** (0.000)	-0.000** (0.000)
Temperature	0.001 (0.015)	0.002 (0.014)	0.001 (0.001)	0.026** (0.012)	0.033** (0.015)
log (state GDP): t-1				32.085 (30.829)	
Precipitation: t-1				0.000 (0.000)	
Air Temperature: t-1				-0.047*** (0.015)	
log (state GDP): t+1					37.424 (31.487)
Precipitation: t+1					-0.000*** (0.000)
Air Temperature: t+1					0.020* (0.012)
Wald test for the subset of lag/lead covariates (F-statistic/p-values)				F = 6.043 / p= 0.0004	F = 6.829 / p= 0.0001

Note: ***Significant at the 1 percent level;**Significant at the 5 percent level;*Significant at the 10 percent level.

Table S18: Comparison between the main model and other alternative specifications: a simpler event-time, an autoregressive, and lag/lead regressors model. Dependent variable: Public revenues

	Main Model (1)	Simple Model (2)	AR (3)	Lag Regressors (t-1) (4)	Lead Regressors (t+1) (5)
EDminus5	0.013 (0.023)				
EDminus4	0.007 (0.030)				
EDminus3	0.013 (0.027)				
EDminus2	0.030 (0.029)				
EDzero	0.052 (0.034)				
EDplus1	0.076* (0.039)				
EDplus2	0.068 (0.047)				
EDplus3	0.078* (0.044)				
EDplus4	0.070 (0.043)				
EDplus5	0.087** (0.041)				
EDplus6	0.083** (0.035)				
EDplus7	0.099*** (0.030)				
EDplus8	0.115*** (0.032)				
EDplus9	0.094*** (0.034)				
EDplus10	0.059** (0.025)				
EDplus11	0.058** (0.023)				
EDplus12	0.032 (0.024)				
EDplus13	0.001 (0.023)				
EDplus14	0.006 (0.026)				
EDplus15	0.005 (0.028)				
Construction		0.066* (0.036)	0.042 (0.045)	0.069*** (0.010)	0.067*** (0.010)
Operation		0.071*** (0.025)	0.029 (0.037)	0.079*** (0.010)	0.074*** (0.011)
Ylag			0.701*** (0.002)		
log (state GDP)	-95.564*** (17.461)	-94.871*** (17.850)	-126.098*** (8.405)	-40.820 (25.346)	-24.140 (26.771)
Itaipu royalties	0.005 (0.003)	0.005 (0.003)	-0.000 (0.001)	0.004*** (0.002)	0.004*** (0.001)
Precipitation	0.000* (0.000)	0.000* (0.000)	0.000 (0.000)	0.000 (0.000)	0.000** (0.000)
Temperature	0.005 (0.011)	0.004 (0.012)	-0.001 (0.004)	-0.012 (0.008)	-0.020** (0.009)
log (state GDP): t-1				-56.383** (22.693)	
Precipitation: t-1				0.000*** (0.000)	
Air Temperature: t-1				0.014 (0.011)	
log (state GDP): t+1					-66.354*** (23.834)
Precipitation: t+1					0.000*** (0.000)
Air Temperature: t+1					-0.007 (0.009)
Wald test for the subset of lag/lead covariates (F-statistic/p-values)				F = 9.703/ p= 2.2e-06	F = 11.281/ p= 2.2e-07

Note: ***Significant at the 1 percent level;**Significant at the 5 percent level;*Significant at the 10 percent level.

Table S19: Comparison between the main model and other alternative specifications: a simpler event-time, an autoregressive, and lag/lead regressors model. Dependent variable: Services tax - ISS

	Main Model (1)	Simple Model (2)	AR (3)	Lag Regressors (t-1) (4)	Lead Regressors (t+1) (5)
EDminus5	0.093 (0.119)				
EDminus4	0.148 (0.158)				
EDminus3	0.053 (0.141)				
EDminus2	0.065 (0.146)				
EDzero	0.606*** (0.165)				
EDplus1	1.015*** (0.228)				
EDplus2	1.021*** (0.258)				
EDplus3	1.047*** (0.228)				
EDplus4	0.749*** (0.192)				
EDplus5	0.634*** (0.182)				
EDplus6	0.495*** (0.182)				
EDplus7	0.432* (0.222)				
EDplus8	0.339 (0.207)				
EDplus9	0.252 (0.267)				
EDplus10	0.153 (0.234)				
EDplus11	-0.026 (0.226)				
EDplus12	-0.118 (0.206)				
EDplus13	-0.162 (0.143)				
EDplus14	-0.237 (0.162)				
EDplus15	-0.191 (0.175)				
Construction		0.896*** (0.177)	0.313*** (0.077)	0.913*** (0.060)	0.906*** (0.062)
Operation		0.294* (0.162)	0.059 (0.051)	0.327*** (0.055)	0.338*** (0.061)
Ylag			0.761*** (0.005)		
log (state GDP)	411.180*** (88.229)	411.537*** (90.221)	-165.455*** (13.522)	-280.317** (131.101)	-271.488** (135.569)
Itaipu royalties	0.010 (0.022)	0.006 (0.021)	-0.004*** (0.001)	0.006 (0.012)	0.005 (0.013)
Precipitation	0.000** (0.000)	0.000** (0.000)	0.000 (0.000)	0.000*** (0.000)	0.000*** (0.000)
Temperature	0.011 (0.072)	0.002 (0.072)	0.010 (0.007)	0.006 (0.041)	-0.067 (0.046)
log (state GDP): t-1				695.212*** (114.909)	
Precipitation: t-1				0.000*** (0.000)	
Air Temperature: t-1				-0.071 (0.044)	
log (state GDP): t+1					704.592*** (116.487)
Precipitation: t+1					0.000*** (0.000)
Air Temperature: t+1					0.000 (0.041)
Wald test for the subset of lag/lead covariates (F-statistic/p-values)				F = 24.663 / p= 7.74e-16	F = 22.998/ p= 8.9e-15

Note: ***Significant at the 1 percent level;**Significant at the 5 percent level;*Significant at the 10 percent level.

Table S20: Comparison between the main model and other alternative specifications: a simpler event-time, an autoregressive, and lag/lead regressors model. Dependent variable: State transfers - ICMS

	Main Model (1)	Simple Model (2)	AR (3)	Lag Regressors (t-1) (4)	Lead Regressors (t+1) (5)
EDminus5	0.071 (0.080)				
EDminus4	0.056 (0.085)				
EDminus3	0.074 (0.078)				
EDminus2	0.079 (0.082)				
EDzero	0.095 (0.100)				
EDplus1	0.055 (0.087)				
EDplus2	0.040 (0.099)				
EDplus3	0.059 (0.093)				
EDplus4	0.089 (0.099)				
EDplus5	0.054 (0.086)				
EDplus6	0.105 (0.086)				
EDplus7	0.137* (0.078)				
EDplus8	0.230*** (0.071)				
EDplus9	0.176** (0.073)				
EDplus10	0.125** (0.061)				
EDplus11	0.109* (0.061)				
EDplus12	0.041 (0.055)				
EDplus13	-0.012 (0.055)				
EDplus14	0.016 (0.047)				
EDplus15	0.019 (0.053)				
Construction		0.045 (0.076)	0.034 (0.062)	0.019 (0.019)	0.010 (0.019)
Operation		0.087* (0.050)	0.070* (0.037)	0.075*** (0.019)	0.068*** (0.021)
Ylag			0.705*** (0.010)		
log (state GDP)	-32.879 (59.995)	-31.217 (60.710)	-137.638*** (11.731)	-119.176** (50.885)	-101.486** (50.757)
Itaipu royalties	0.004 (0.004)	0.004 (0.003)	0.002 (0.001)	0.004** (0.002)	0.004** (0.002)
Precipitation	0.000 (0.000)	0.000 (0.000)	0.000 (0.000)	0.000 (0.000)	0.000** (0.000)
Temperature	0.043 (0.029)	0.042 (0.029)	-0.000144	-0.011 (0.017)	-0.010 (0.019)
log (state GDP): t-1				109.719** (45.483)	
Precipitation: t-1				0.000*** (0.000)	
Air Temperature: t-1				0.070*** (0.020)	
log (state GDP): t+1					99.999** (45.714)
Precipitation: t+1					0.000*** (0.000)
Air Temperature: t+1					-0.034** (0.017)
Wald test for the subset of lag/lead covariates (F-statistic/p-values)				F = 12.339/ p= 4.8e-08	F = 15.701/ p= 3.6e-10

Note: ***Significant at the 1 percent level;**Significant at the 5 percent level;*Significant at the 10 percent level.

Table S21: Comparison between the main model and other alternative specifications: a simpler event-time, an autoregressive, and lag/lead regressors model. Dependent variable: Federal transfers - FPM

	Main Model (1)	Simple Model (2)	AR (3)	Lag Regressors (t-1) (4)	Lead Regressors (t+1) (5)
EDminus5	-0.005 (0.016)				
EDminus4	-0.018 (0.029)				
EDminus3	-0.000 (0.020)				
EDminus2	0.011 (0.021)				
EDzero	0.020 (0.023)				
EDplus1	0.020 (0.020)				
EDplus2	0.003 (0.018)				
EDplus3	-0.023 (0.048)				
EDplus4	-0.012 (0.022)				
EDplus5	-0.024 (0.023)				
EDplus6	-0.020 (0.024)				
EDplus7	0.009 (0.018)				
EDplus8	-0.004 (0.022)				
EDplus9	-0.014 (0.019)				
EDplus10	-0.044** (0.021)				
EDplus11	-0.041 (0.027)				
EDplus12	-0.054* (0.031)				
EDplus13	-0.055* (0.031)				
EDplus14	-0.116 (0.090)				
EDplus15	-0.041 (0.033)				
Construction		0.008 (0.018)	-0.006 (0.036)	0.009 (0.011)	0.010 (0.011)
Operation		-0.019 (0.017)	-0.043 (0.042)	-0.011 (0.010)	-0.000198
Ylag			0.678*** (0.003)		
log (state GDP)	-77.510*** (16.144)	-76.961*** (16.170)	-89.898*** (6.905)	-51.604*** (18.624)	-52.374*** (19.299)
Itaipu royalties	0.002 (0.002)	0.002 (0.002)	-0.003** (0.001)	0.001 (0.001)	0.001 (0.001)
Precipitation	-0.000 (0.000)	-0.000 (0.000)	0.000 (0.000)	-0.000 (0.000)	-0.000 (0.000)
Temperature	0.004 (0.009)	0.003 (0.008)	0.004 (0.003)	-0.008 (0.008)	0.001 (0.008)
log (state GDP): t-1				-17.107 (14.752)	
Precipitation: t-1				0.000*** (0.000)	
Air Temperature: t-1				0.011 (0.010)	
log (state GDP): t+1					-15.393 (15.359)
Precipitation: t+1					-0.000 (0.000)
Air Temperature: t+1					-0.003 (0.009)
Wald test for the subset of lag/lead covariates (F-statistic/p-values)				F = 2.496 / p= 0.057	F = 1.265/ p= 0.284

Note: ***Significant at the 1 percent level;**Significant at the 5 percent level;*Significant at the 10 percent level.

7.6 Complementary results and discussion

The number of people employed by a hydropower project varies according to power plant size and project phase. When construction starts, there is an immediate growth in local population and investments related to the construction of the hydropower plant. Each project creates direct jobs that are associated with dam construction, and indirect jobs, which are related to the additional demand for goods and services. When construction ends, part of the migrant workers leave, looking for new opportunities elsewhere. Figure S1 is an example (Teles Pires hydropower plant) of the variation in the number of people employed for each construction stage. It is interesting to note how the shape of ISS curve (Figure 3-3 from the Chapter 3) follows a pattern that is similar to the intensity of labor in the construction of hydropower plants. The ISS curve is characterized by a steep increase in the first year, achieving a peak during the second to fourth year, then followed by a steady decrease in the intensity. The fact that hydropower projects start operation in stages and the construction does not end abruptly drives this slow decrease in the ISS intensity. In the operation phase, the number of direct jobs varies from dozens to thousands of people, depending on the size of the power plant. Hydropower companies become a new industry in the area, providing new tax revenue. Usually, after construction the majority of jobs related to the dam disappear from the region.

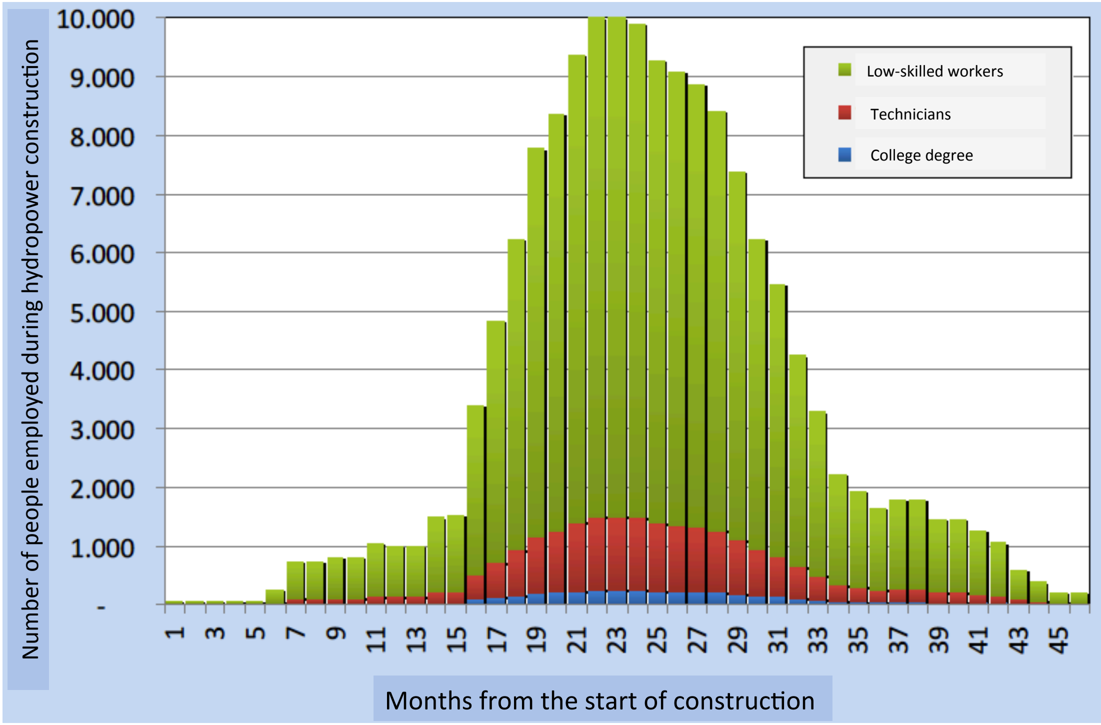

Figure S1: Number of people directly employed at the Teles Pires hydropower plant (1820 MW). Source: Adapted from the Teles Pires Environmental Impact Assessment Report (p.95, Volume I).

7.6.1 Heterogeneity

In the Chapter 3, we present the average impact of hydropower development for the counties in our sample. Here, we explore how the different characteristics of projects (size and ownership) and counties (population size and level of human development) influenced our average estimates.

7.6.1.1 Larger (>500 MW) versus Smaller Dams (>30MW and <500 MW)

First, we evaluated how project size (based on installed capacity) affects our average estimates. Using our main model, we divided our sample into two groups: counties affected by power plants with more than 500 MW (larger dams) and counties with hydropower plants between 30 and 500 MW of installed capacity (smaller dams). Figure S2 shows that the main difference between counties affected by larger and smaller dams is the negative Agriculture GDP associated with projects with more than 500 MW. As discussed in Chapter 3, this negative effect is probably associated with two main reasons: displacement of productive agricultural land by the reservoir flooding, and attraction of agricultural workers to new opportunities in the other economic sectors. Larger hydropower plants are often associated with larger reservoirs supporting the belief that flooding a large area significantly contribute to displace local agriculture output. As a result of this substantial negative effect on agricultural GDP, the overall performance of smaller hydropower plants is better when compared to the larger ones.

Hydropower plants with less than 500 MW also perform better in terms of tax revenues (Figure S3). Although the effect on the services tax is slightly superior for larger projects, smaller hydropower plants perform much better in terms of state transfers (ICMS). This result largely occurs because the ICMS is charged over the use of electricity in the point of consumption. Larger hydropower plants are usually connected to high voltage interstate transmission lines directly to the load centers and, therefore, the consumption of electricity does not happen in the region surrounding the dam. As a consequence, tax revenues increase on other regions. In contrast, smaller dams can be connected to regional grids, boosting local ICMS revenues.

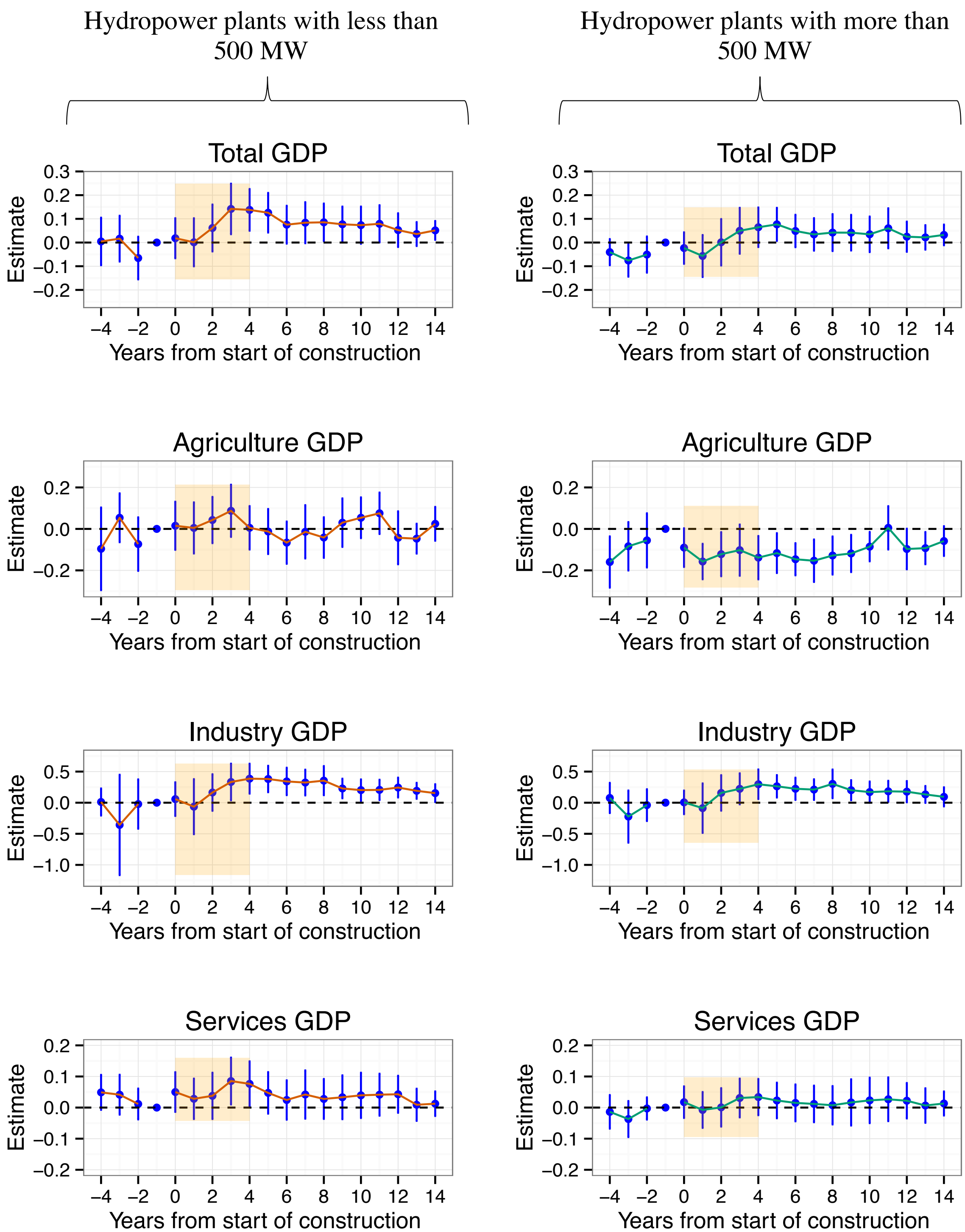

Figure S2: Regression results for counties affected by hydropower plants of different sizes based on installed capacity: GDP

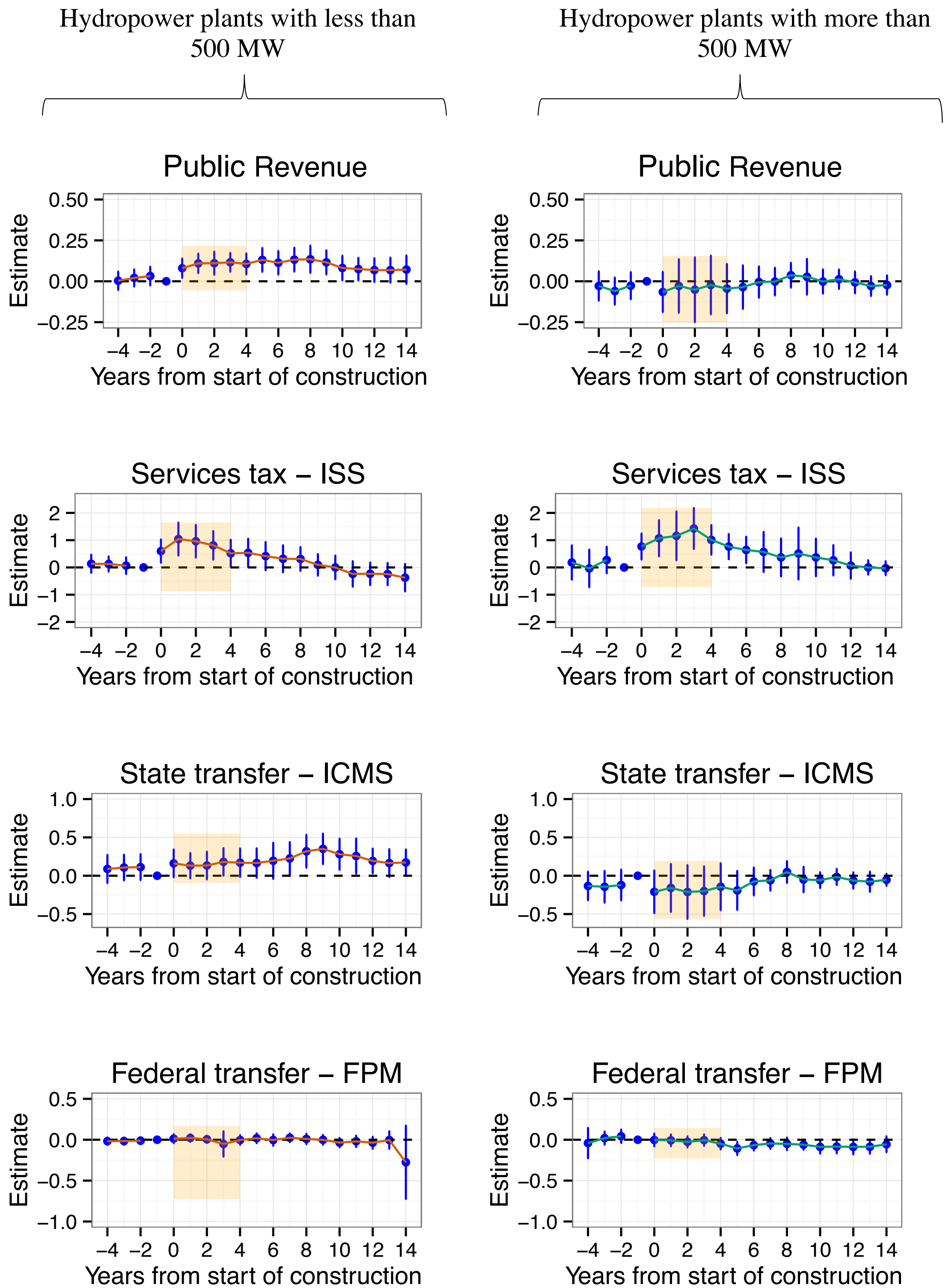

Figure S3: Regression results for counties affected by hydropower plants of different sizes based on installed capacity: tax revenues

7.6.1.2 Utility versus Industry ownership

We also assess the importance of the ownership of hydropower plants on the economic outcomes. Industrial companies such as mining and aluminum manufacturing own some of the hydropower plants in our sample. Those hydropower plants are often associated with electric-intensive industrial projects from the same company. Thus, the industrial facilities consume most of the electricity generated by the associated hydropower plant, which we presume are close to the hydropower plants. Utility companies dedicated to the electricity business own the rest of the projects in our database. To explore the heterogeneity between those types of project owners, we divided the dataset into two groups: counties affected by power plant owned by utility companies or by industrial companies.

Figure S4 and Figure S5 present the comparison between those groups and show that the association between a hydropower project and an industrial facility results in better and more persistent economic outcomes. In terms of GDP, industrial-owned projects have a greater effect on the services sector, such that the total GDP is expressively more affected than the utility-owned projects. Industrial-owned projects also perform better in term of tax revenues, because of the greater local services tax and state transfers. The synergy between the hydropower plant construction and the industrial activity likely amplifies and extends the economic shock explaining the empirical difference observed in Figure S4 and Figure S5. However, we acknowledge that our analysis does not take into account the negative environmental and social impacts from this association.

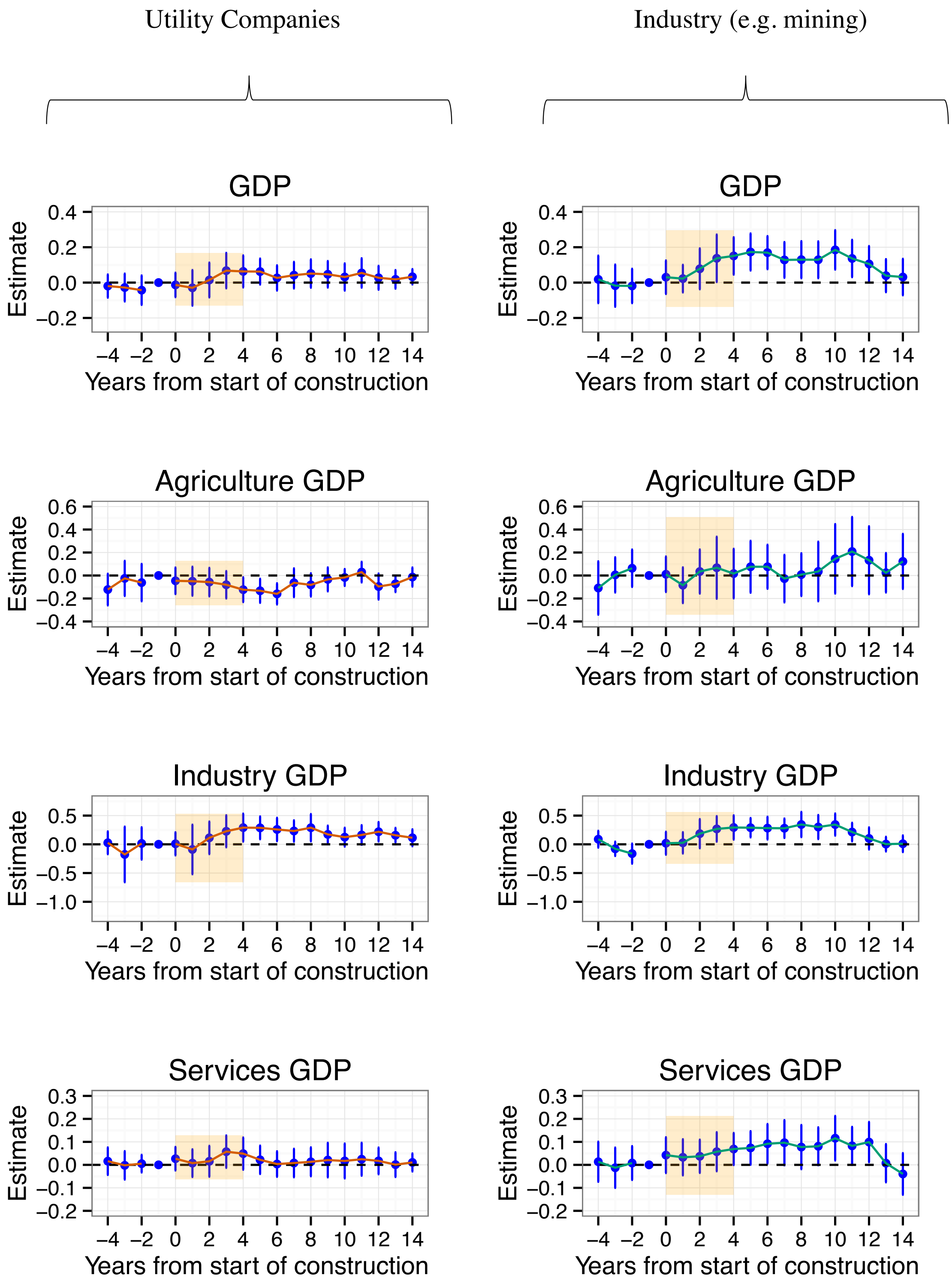

Figure S4: Regression results for counties affected by hydropower plants with different ownership: GDP

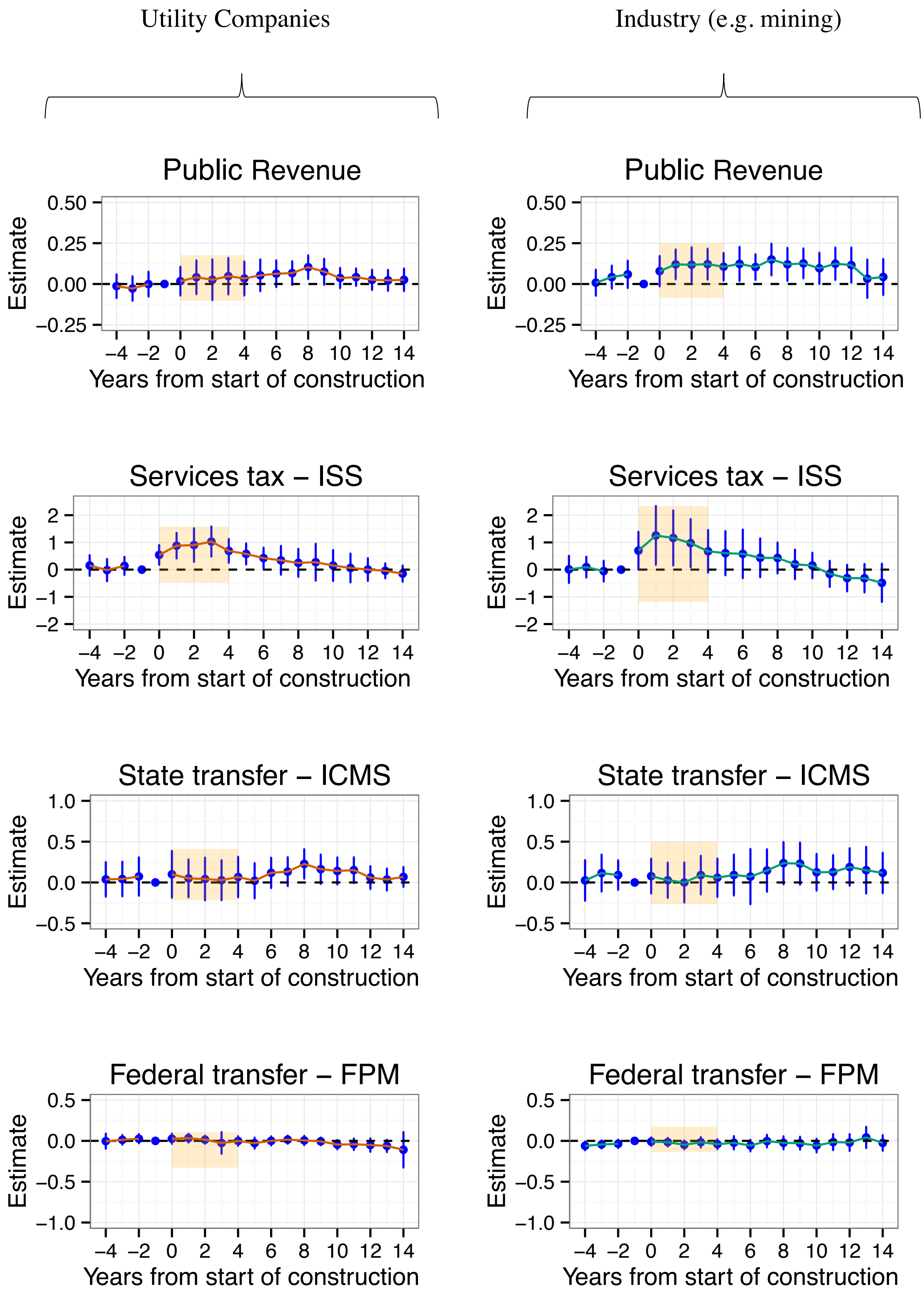

Figure S5: Regression results for counties affected by hydropower plants with different ownership: tax revenues

7.6.1.3 Population Size

The population size of a county affected by a hydropower project is also expected to be a key factor driving heterogeneity in the economic outcomes. To explore the strength of this hypothesis, we divided the dataset into two groups: counties with less than 30,000 people in 1991 ("Small counties") and counties with more than 30,000 people in 1991 ("Large counties"). We chose the value 30,000 because it is around the median population of the counties in our sample.

Figure S6 and S7 indicate that hydropower plants installed in large counties barely have an effect in either GDP or tax revenues indicators. On the other hand, the effect in the small counties is significant for all indicators demonstrating a clear distinction between small and large counties. This result is expected given that the shock produced by the hydropower plant should be greater in a small economy compared to the same shock in a lager economy.

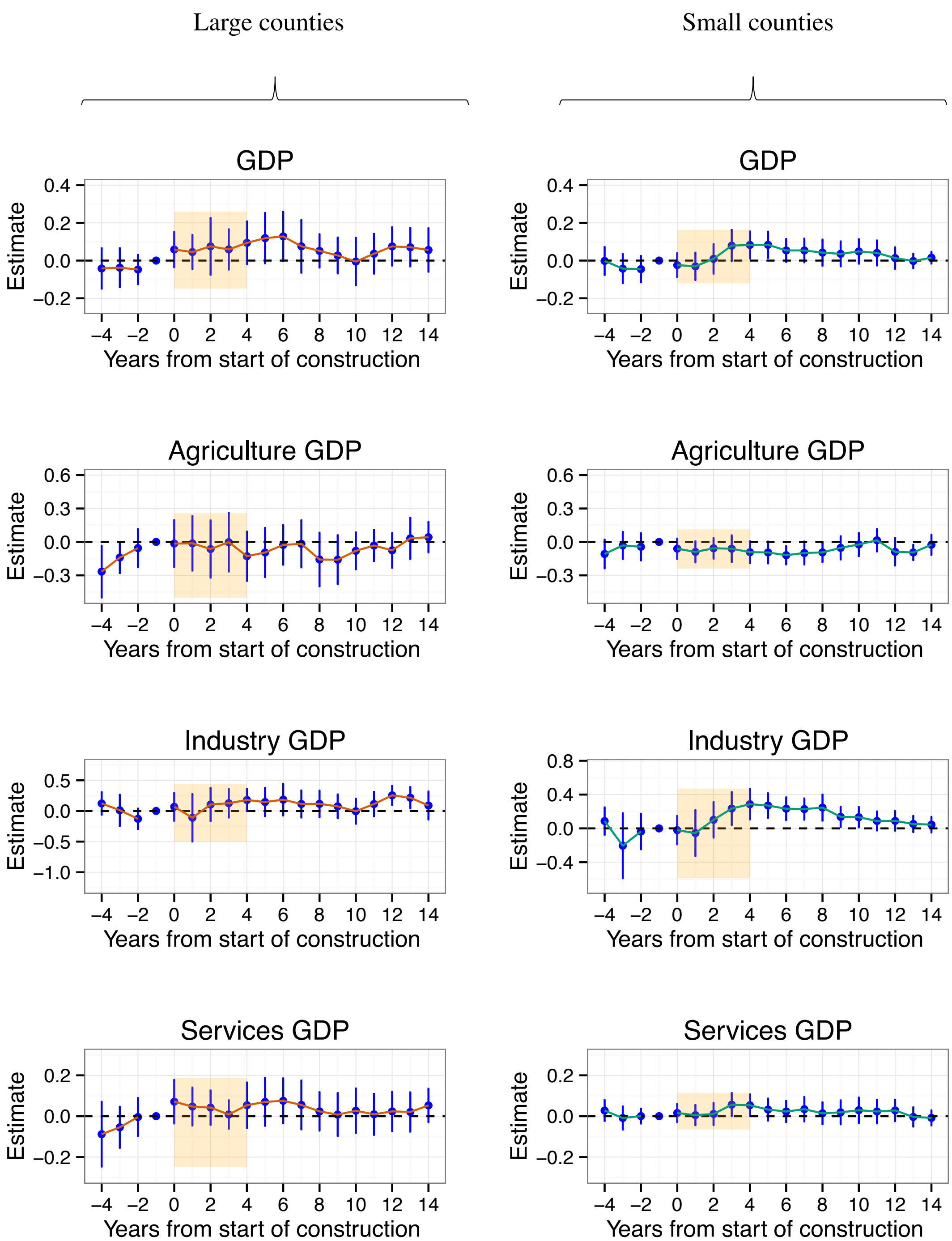

Figure S6: Regression results for large vs. small counties affected by hydropower plants: GDP

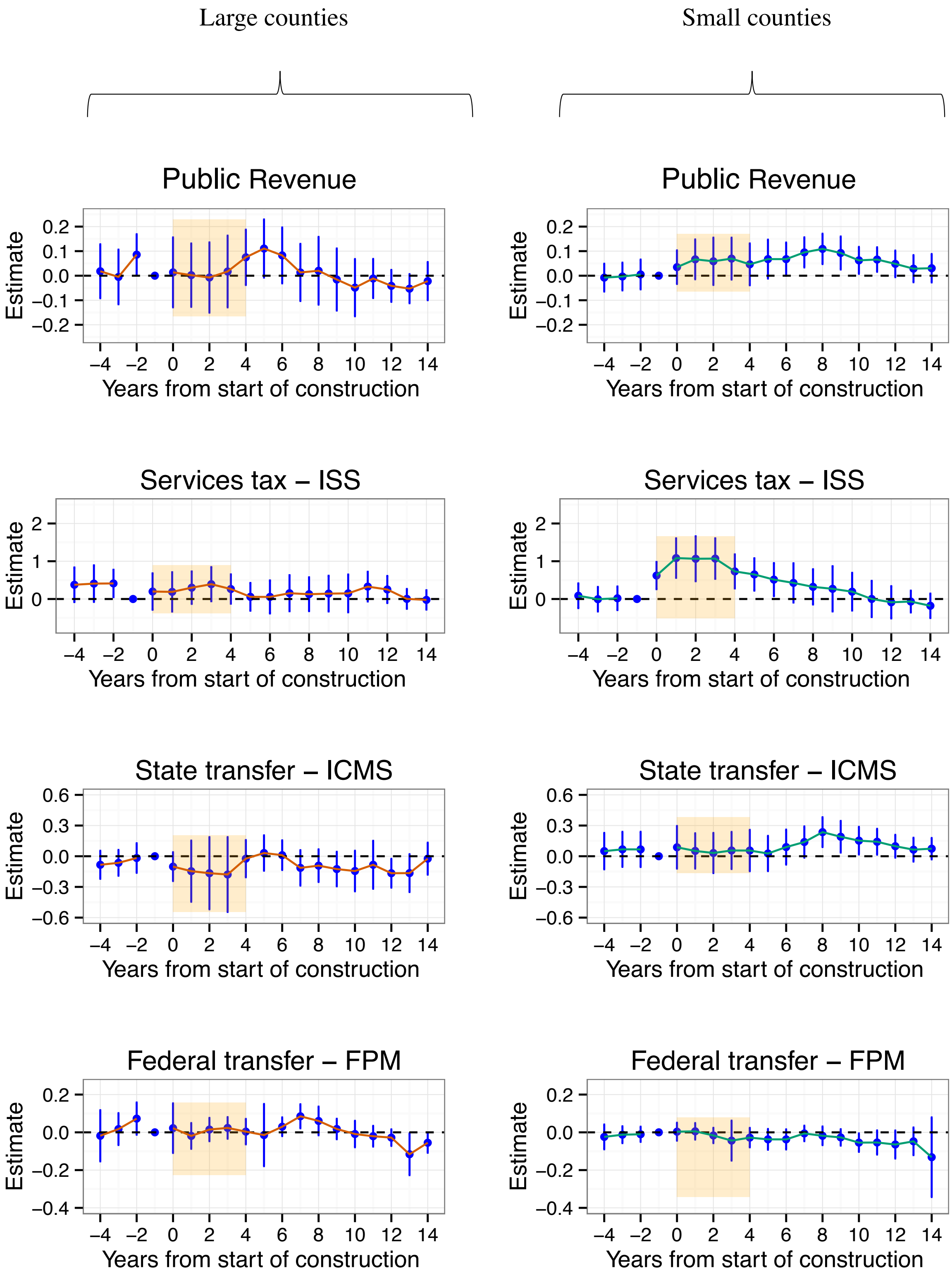

Figure S7: Regression results for large vs. small counties affected by hydropower plants: tax revenues

7.6.1.4 Human development

The county human development levels should also be a central factor driving heterogeneity in the economic indicators. For example, a better-educated population should be more likely to be employed in new activities associated to the hydropower plant development, as well as to create new businesses to supply the new demand for goods and services. This characteristic should reduce the need for bringing temporary professionals or services to fulfill the additional demands, such that the benefit to the local economy is anticipated to be greater and longer. Similarly, more developed counties are expected to have a better infrastructure to alleviate the negative impacts and improve the positive ones. To investigate the importance of the human development level on the impacts of hydropower development on the local economy, we divided the counties into two groups: more developed counties (those with human development indexes greater than 0.4 in 1991) and less developed counties (those with human development indexes lower than 0.4 in 1991)

Figure S8 and Figure S9 indicate that more and less developed counties have qualitative similar results in terms of GDP and taxes. For some indicators, such as industry GDP and ISS, the average effect seems to be greater on less developed counties. However, the variance for the less developed counties is larger, such that it is difficult to characterize a clear difference between more and less developed counties.

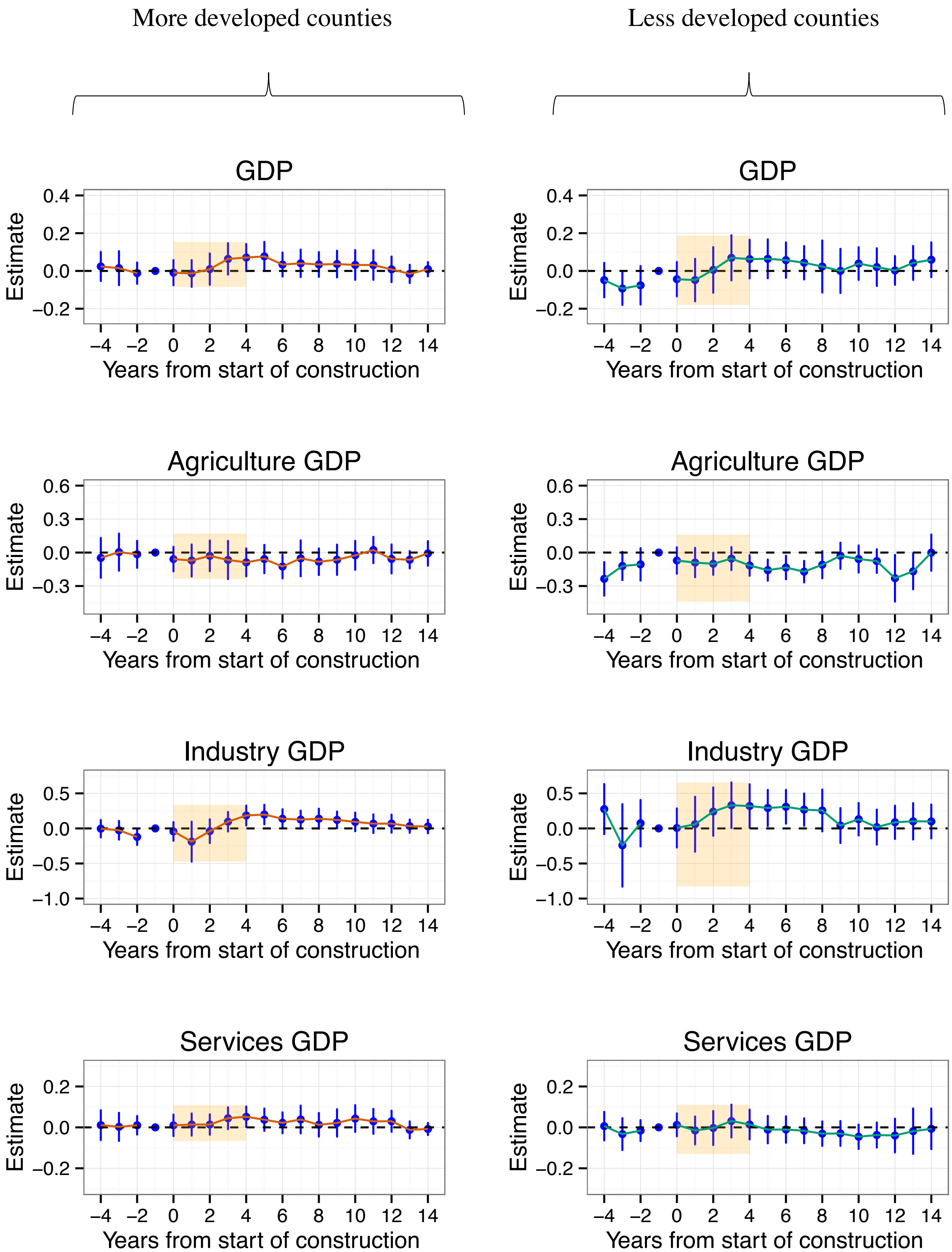

Figure S8: Regression results for more vs. less developed counties affected by hydropower plants: GDP

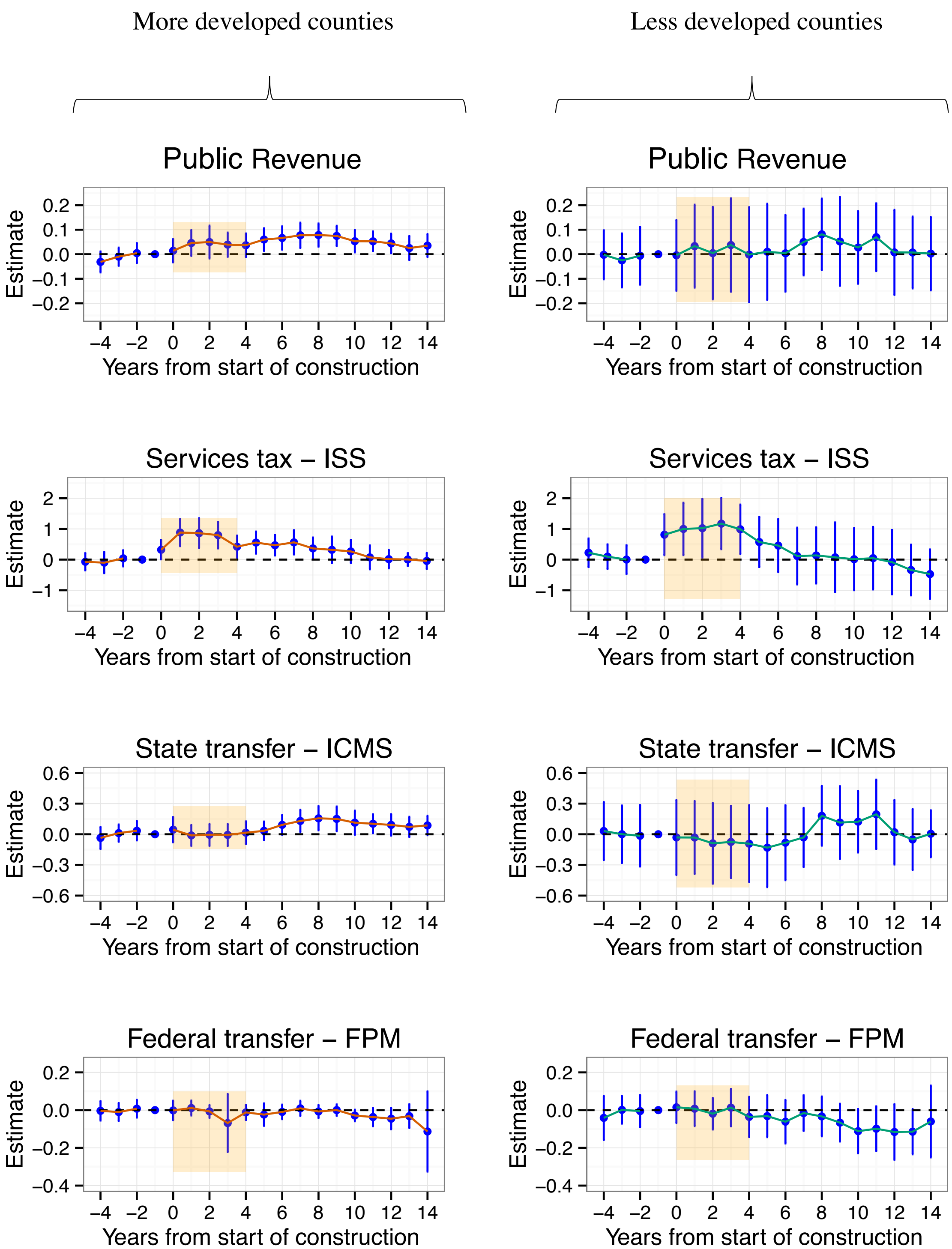

Figure S9: Regression results for more vs. less developed counties affected by hydropower plants: tax revenues

7.6.2 The effect of the water resources financial compensation (WRFC) on counties affected by hydropower plants built before 1991

The water resources financial compensation (in Portuguese, *compensação financeira pela utilização dos recursos hídricos)* is a legal mechanism that requires hydro dam owners to pay a fee for the water used to produce electricity. The fee is 6.75% of the monthly total energy produced by power plants multiplied by an energy tariff. The energy tariff is defined annually by the Brazilian electricity agency – ANEEL (Agencia Nacional de Energia Eletrica) – that is also responsible for collecting and distributing the WRFC fees. According to the law, 45% of the total WRFC resources are allocated to counties affected by the reservoirs, 45% to the states where the counties are located, and 10% to the federal government. In 2014, 183 hydropower reservoirs paid WRFC fees to ANEEL totaling 1.7 billion reais (~470 million USD given March 2016 foreign exchange rates). The idea behind the WRFC is to compensate places affected by hydropower reservoirs to mitigate social and environmental impacts, hoping to improve local welfare.

Here, we investigate the effects of the WRFC on the human development indicators alone by using a new group of counties as the treatment sample. This new group, called Group C, contains counties with a hydropower plant built before 1991 but that started receiving WRFC funds only in 1991, when the compensation policy was put into effect. The WRFC implementation represents a discontinuity for the treatment group and allows us to investigate the effect of the WRFC alone (excluding the construction effect). We applied the difference-in-difference specification (model 2 in Chapter 3) for the same socioeconomic indicators applied to groups A and B in Chapter 3.

Figure S10 reveals that the compensation policy positively affected the education indicator in the first decade of analysis and is significant at the 5% level. The average magnitude of the effect is approximately 1% greater (95% CI: 0% to 2%), but the coefficient is negative in the second period (-0.07%, 95% CI: 0% to -2%). Moreover, both the short- and long-run effects of the policy on income are negative and statistically significant, indicating a deleterious effect that increased over time. Additionally, the population density analysis suggests that the policy leads to an increase in population density by 8% (95% CI: 3% to 15%) in the long run.

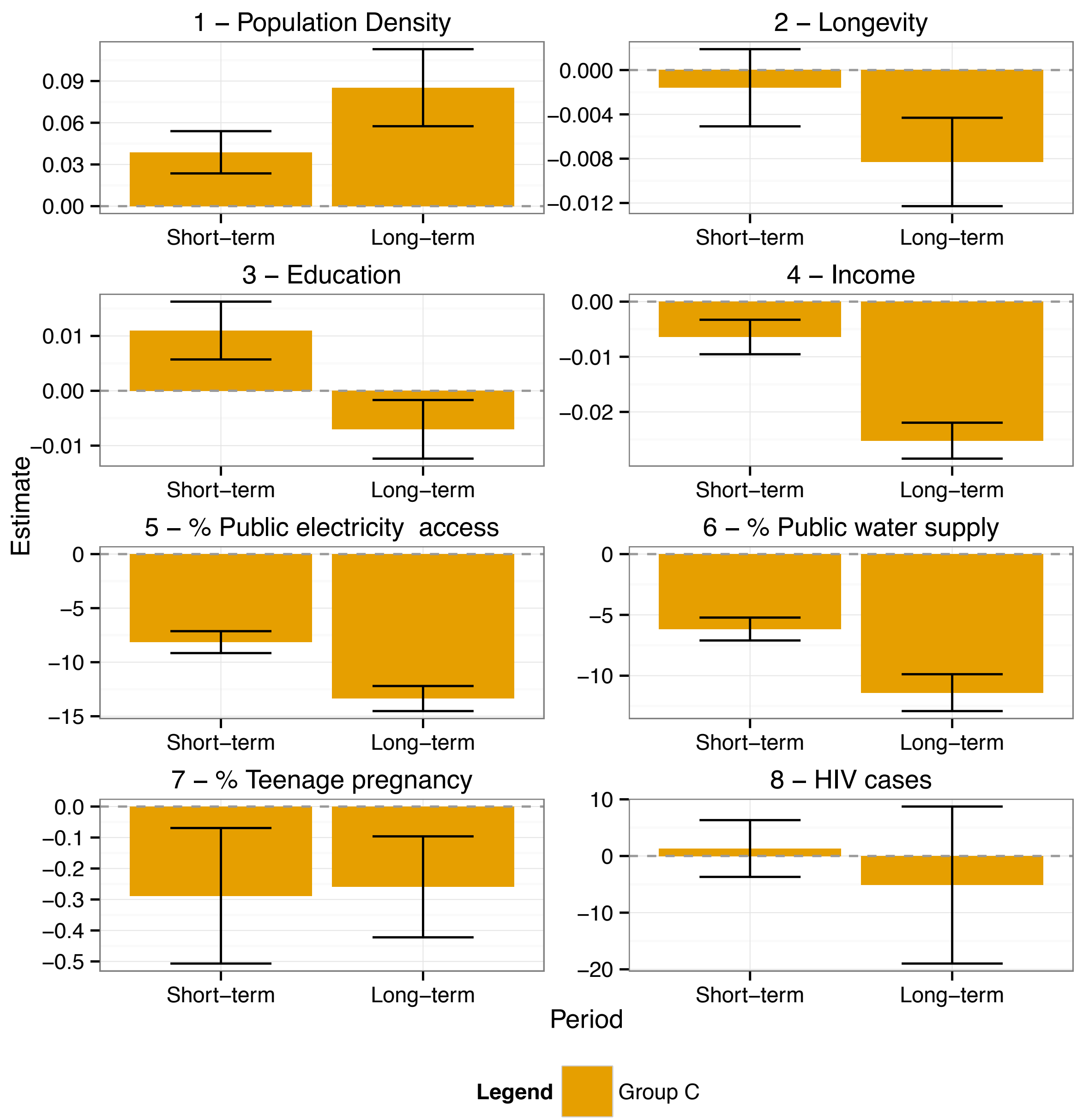

Figure S10: Difference-in-differences regression results for the human development indicators and other outcomes of interest in WRFC treated counties (Group C). Bars represent the average y_1 coefficients estimate from model 3 described in the methods section. Error bars represents the 95% confidence intervals defined as two times the standard errors (robust standard errors are clustered at the county level). Short term represents the first decade after hydropower development (1991-2000). Long term represents two decades after WRFC implementation (1991-2010).

The overall assessment from Figure S indicates that the WRFC policy had a short-term positive effect on the education indicator in the counties with hydropower plants built before

1991. However, the improved social conditions likely led to population migration to treated counties, increasing those counties' populations. In the long term, population growth might have outweighed the benefits obtained from the increased WRFC funds. As a result, the short-term positive education outcome disappeared in the long run. Similarly, the decrease in average income in treated counties might be explained by an increase in the labor supply (and thus a decrease in job vacancies and wages) as a result of population growth. The only observed positive effect is a reduction of the teenage pregnancy rates, which can be explained by better educational conditions observed in the short-term.

Long-term population growth should also explain the negative effects on the percentage of households with access to electricity and piped water. It seems that local governments are not capable of keeping the same levels of service when facing a demographic pressure. As for HIV cases, the outcomes are not significantly affected by the WRFC policy. Therefore, there is evidence that the WRFC policy is not contributing to improve socioeconomic conditions in the long term. Indeed, the policy seems to be the underlying force behind negative outcomes.

References

Angrist, JD & Pischke, J-S 2008, *Mostly Harmless Econometrics: An Empiricist's Companion*, pp. 1–290.

Cameron, AC & Miller, DL 2015, 'A practitioner's guide to cluster-robust inference', *Journal of Human Resources*.

Cameron, A.C., Gelbach, J.B. and Miller, D.L., 2008. Bootstrap-based improvements for inference with clustered errors. *The Review of Economics and Statistics*, *90*(3), pp.414-427.

ANEEL, 2015a, 'Sistema de informações georreferenciadas do setor elétrico - SIGEL', ANEEL, viewed <http://sigel.aneel.gov.br/sigel.html>.

ANEEL, 2015b, 'Water resources use financial compensation data', ANEEL, viewed <http://www.aneel.gov.br/aplicacoes/cmpf/gerencial/>.

Severnini, E. R. The Power of Hydroelectric Dams: Agglomeration Spillovers. *IZA (Institute for the Study of Labor)* 1–70 (2014).

Willmott JC, Matsuura K The Climate Data Guide: Global (land) precipitation and temperature: Willmott & Matsuura, University of Delaware. Available at: https://climatedataguide.ucar.edu/climate-data/global-land-precipitation-and-temperature-willmott-matsuura-university-delaware#NCDF4%20tutorial.

Wooldridge, JM 2004, *Econometric Analysis of Cross Section and Panel Data*, TM Press (ed.),, pp. 1–753.

ANNEX B1 – List of treated counties

IBGE Code	County	State	IBGE Code	County	State	IBGE Code	County	State
1703008	Babaçulândia	TO	3166808	Serra do Salitre	MG	4212601	Peritiba	SC
1703073	Barra do Ouro	TO	3167707	Sobrália	MG	4213104	Piratuba	SC
1703701	Brejinho de Nazaré	TO	3169703	Turmalina	MG	4216107	São Domingos	SC
1706506	Darcinópolis	TO	3170107	Uberaba	MG	4219853	Zortéa	SC
1707702	Filadélfia	TO	3170206	Uberlândia	MG	4300109	Agudo	RS
1709005	Goiatins	TO	3170404	Unaí	MG	4300505	Alpestre	RS
1709807	Ipueiras	TO	3502101	Andradina	SP	4300802	Antônio Prado	RS
1710904	Itapiratins	TO	3502804	Araçatuba	SP	4300901	Aratiba	RS
1712009	Lajeado	TO	3506508	Birigui	SP	4301206	Arroio do Tigre	RS
1713205	Miracema do Tocantins	TO	3507753	Brejo Alegre	SP	4301800	Barracão	RS
1713809	Palmeiras do Tocantins	TO	3508108	Buritama	SP	4302105	Bento Gonçalves	RS
1715705	Palmeirante	TO	3509106	Caiuá	SP	4302303	Bom Jesus	RS
1715754	Palmeirópolis	TO	3510005	Cândido Mota	SP	4305959	Cotiporã	RS
1716208	Paranã	TO	3511003	Castilho	SP	4307203	Erval Grande	RS
1716604	Peixe	TO	3511409	Cerqueira César	SP	4307401	Esmeralda	RS
1718204	Porto Nacional	TO	3518206	Guararapes	SP	4307815	Estrela Velha	RS
1720259	São Salvador do Tocantins	TO	3519501	Ibirarema	SP	4308052	Faxinalzinho	RS
1721000	Palmas	TO	3520103	Igarapava	SP	4308201	Flores da Cunha	RS
1721307	Tupiratins	TO	3524402	Jacareí	SP	4309753	Ibarama	RS
2102804	Carolina	MA	3524907	Jambeiro	SP	4310702	Itatiba do Sul	RS
2104057	Estreito	MA	3526506	Lavínia	SP	4311700	Machadinho	RS
2702405	Delmiro Gouveia	AL	3527256	Lourdes	SP	4311908	Marcelino Ramos	RS
2705804	Olho d'Água do Casado	AL	3528601	Manduri	SP	4312005	Mariano Moro	RS
2707107	Piranhas	AL	3530102	Mirandópolis	SP	4312203	Maximiliano de Almeida	RS
2801207	Canindé de São Francisco	SE	3534807	Ouro Verde	SP	4312708	Nonoai	RS
2901700	Antônio Cardoso	BA	3535309	Palmital	SP	4313086	Nova Pádua	RS
2904852	Cabaceiras do Paraguaçu	BA	3535408	Panorama	SP	4313102	Nova Palma	RS
2904902	Cachoeira	BA	3535606	Paraibuna	SP	4313359	Nova Roma do Sul	RS
2907301	Castro Alves	BA	3536406	Paulicéia	SP	4314464	Pinhal da Serra	RS
2908200	Conceição da Feira	BA	3537404	Pereira Barreto	SP	4314472	Pinhal Grande	RS

2910800	Feira de Santana	BA	3538808	Piraju	SP	4315552	Rio dos Índios	RS
2911600	Governador Mangabeira	BA	3541307	Presidente Epitácio	SP	4320602	Severiano de Almeida	RS
2915304	Itagimirim	BA	3541505	Presidente Venceslau	SP	4322509	Vacaria	RS
2916302	Itapebi	BA	3543600	Rifaina	SP	4322806	Veranópolis	RS
2916807	Itarantim	BA	3544251	Rosana	SP	5000807	Anaurilândia	MS
2924009	Paulo Afonso	BA	3545407	Salto Grande	SP	5001904	Bataguassu	MS
2925956	Rafael Jambeiro	BA	3546009	Santa Branca	SP	5002001	Batayporã	MS
2928802	Santo Estêvão	BA	3547106	Santa Mercedes	SP	5002308	Brasilândia	MS
2929305	São Gonçalo dos Campos	BA	3548054	Santo Antônio do Aracanguá	SP	5007554	Santa Rita do Pardo	MS
3100500	Açucena	MG	3552304	Sud Mennucci	SP	5007935	Sonora	MS
3101102	Aimorés	MG	3554300	Teodoro Sampaio	SP	5008305	Três Lagoas	MS
3101805	Alpercata	MG	3556305	Valparaíso	SP	5101258	Araputanga	MT
3103009	Antônio Dias	MG	4101101	Andirá	PR	5103007	Chapada dos Guimarães	MT
3103504	Araguari	MG	4103024	Boa Esperança do Iguaçu	PR	5104500	Indiavaí	MT
3106507	Berilo	MG	4103057	Boa Vista da Aparecida	PR	5104609	Itiquira	MT
3108008	Bom Sucesso	MG	4103602	Cambará	PR	5105002	Jauru	MT
3108503	Botumirim	MG	4104428	Candói	PR	5106208	Nova Brasilândia	MT
3108800	Braúnas	MG	4104600	Capitão Leônidas Marques	PR	5106752	Pontes e Lacerda	MT
3109451	Cabeceira Grande	MG	4106571	Cruzeiro do Iguaçu	PR	5108352	Vale de São Domingos	MT
3118205	Conquista	MG	4108452	Foz do Jordão	PR	5200100	Abadiânia	GO
3120300	Cristália	MG	4109401	Guarapuava	PR	5200308	Alexânia	GO
3120904	Curvelo	MG	4111001	Itambaracá	PR	5201504	Aporé	GO
3125804	Fernandes Tourinho	MG	4117255	Nova Prata do Iguaçu	PR	5203203	Barro Alto	GO
3127701	Governador Valadares	MG	4119301	Pinhão	PR	5204102	Cachoeira Alta	GO
3127800	Grão Mogol	MG	4120903	Quedas do Iguaçu	PR	5204300	Caçu	GO
3129301	Iapu	MG	4123006	Salto do Lontra	PR	5204508	Caldas Novas	GO
3130002	Ibituruna	MG	4125209	São Jorge d'Oeste	PR	5204656	Campinaçu	GO
3130408	Ijaci	MG	4127858	Três Barras do Paraná	PR	5204706	Campinorte	GO

3130705	Indianópolis	MG	4200051	Abdon Batista	SC	5204805	Campo Alegre de Goiás	GO
3131604	Iraí de Minas	MG	4200507	Águas de Chapecó	SC	5205109	Catalão	GO
3134103	Itueta	MG	4200754	Alto Bela Vista	SC	5205307	Cavalcante	GO
3134301	Itumirim	MG	4201000	Anita Garibaldi	SC	5205521	Colinas do Sul	GO
3136108	Joanésia	MG	4201257	Apiúna	SC	5205802	Corumbá de Goiás	GO
3136520	José Gonçalves de Minas	MG	4201273	Arabutã	SC	5205901	Corumbaíba	GO
3138203	Lavras	MG	4203253	Capão Alto	SC	5206206	Cristalina	GO
3138351	Leme do Prado	MG	4203402	Campo Belo do Sul	SC	5206909	Davinópolis	GO
3144706	Nova Era	MG	4203600	Campos Novos	SC	5208004	Formosa	GO
3145000	Nova Ponte	MG	4203907	Capinzal	SC	5210109	Ipameri	GO
3147006	Paracatu	MG	4204103	Caxambu do Sul	SC	5211305	Itarumã	GO
3148103	Patrocínio	MG	4204152	Celso Ramos	SC	5212501	Luziânia	GO
3149200	Pedrinópolis	MG	4204178	Cerro Negro	SC	5213087	Minaçu	GO
3149804	Perdizes	MG	4204202	Chapecó	SC	5214606	Niquelândia	GO
3149903	Perdões	MG	4204301	Concórdia	SC	5215231	Novo Gama	GO
3149952	Periquito	MG	4206652	Guatambú	SC	5217401	Pires do Rio	GO
3152006	Pompéu	MG	4206900	Ibirama	SC	5219209	Santa Cruz de Goiás	GO
3154309	Resplendor	MG	4207601	Ipira	SC	5219456	Santa Rita do Novo Destino	GO
3155009	Rio Doce	MG	4207684	Ipuaçu	SC	5219753	Santo Antônio do Descoberto	GO
3156908	Sacramento	MG	4208005	Itá	SC	5220504	Serranópolis	GO
3157104	Salto da Divisa	MG	4209300	Lages	SC	5220603	Silvânia	GO
3157401	Santa Cruz do Escalvado	MG	4209904	Lontras	SC	5221601	Uruaçu	GO
3157708	Santa Juliana	MG	4211876	Paial	SC			

ANNEX B2 – Residual Diagnostics

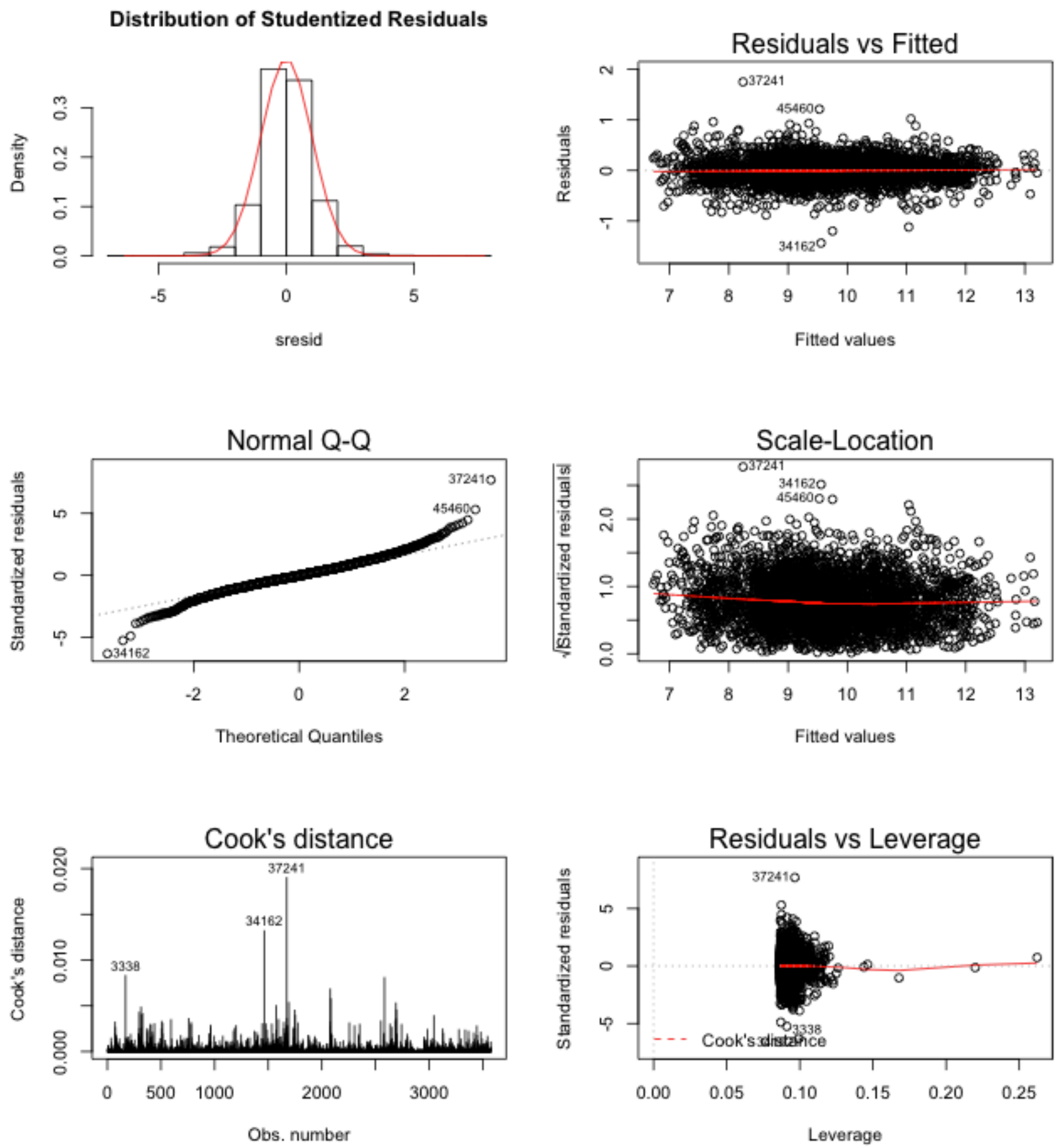

Figure S11: Agricultural GDP regression residuals diagnostics (Model 1)

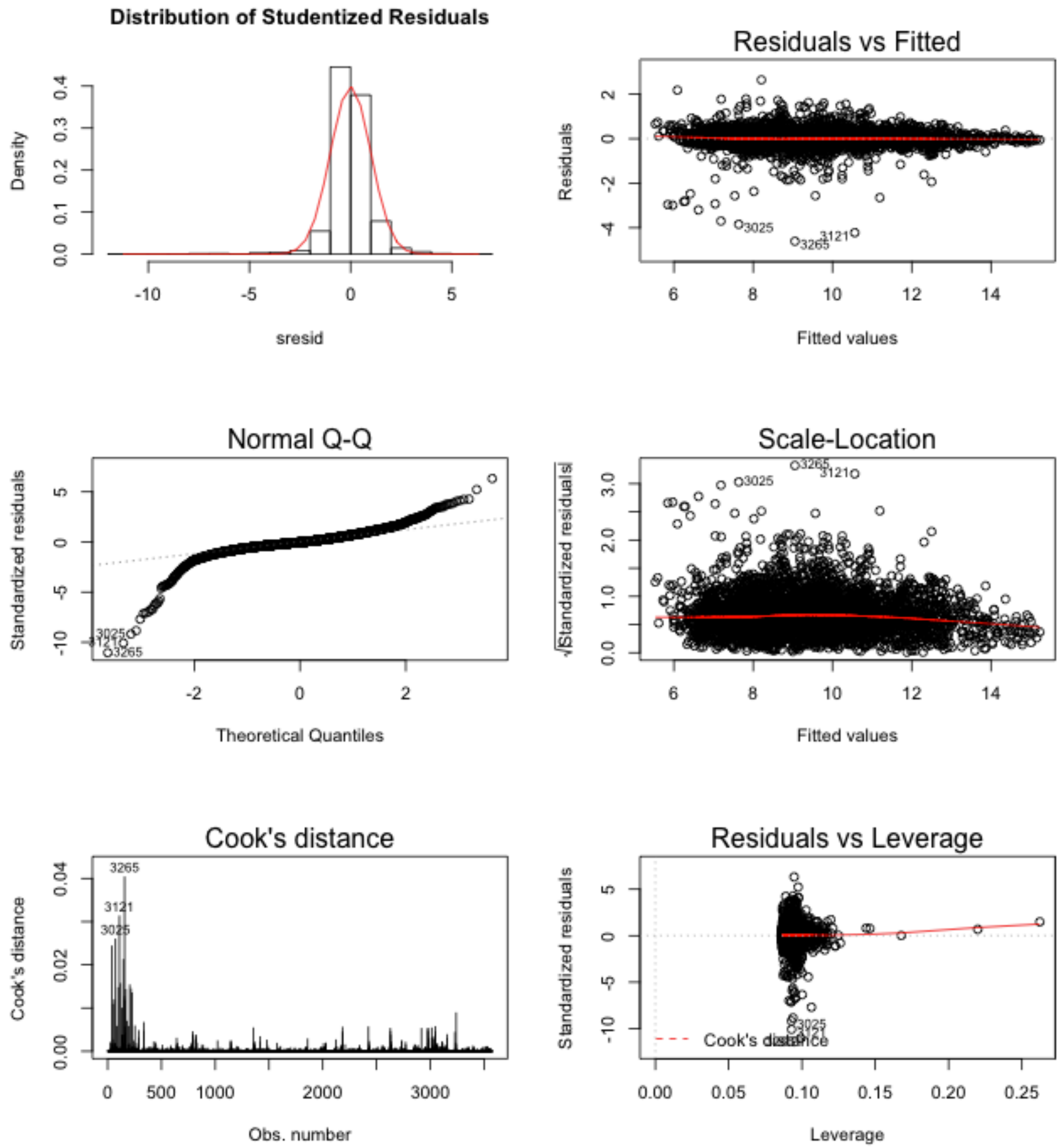

Figure S10: Industry GDP regression residuals diagnostics (Model 1)

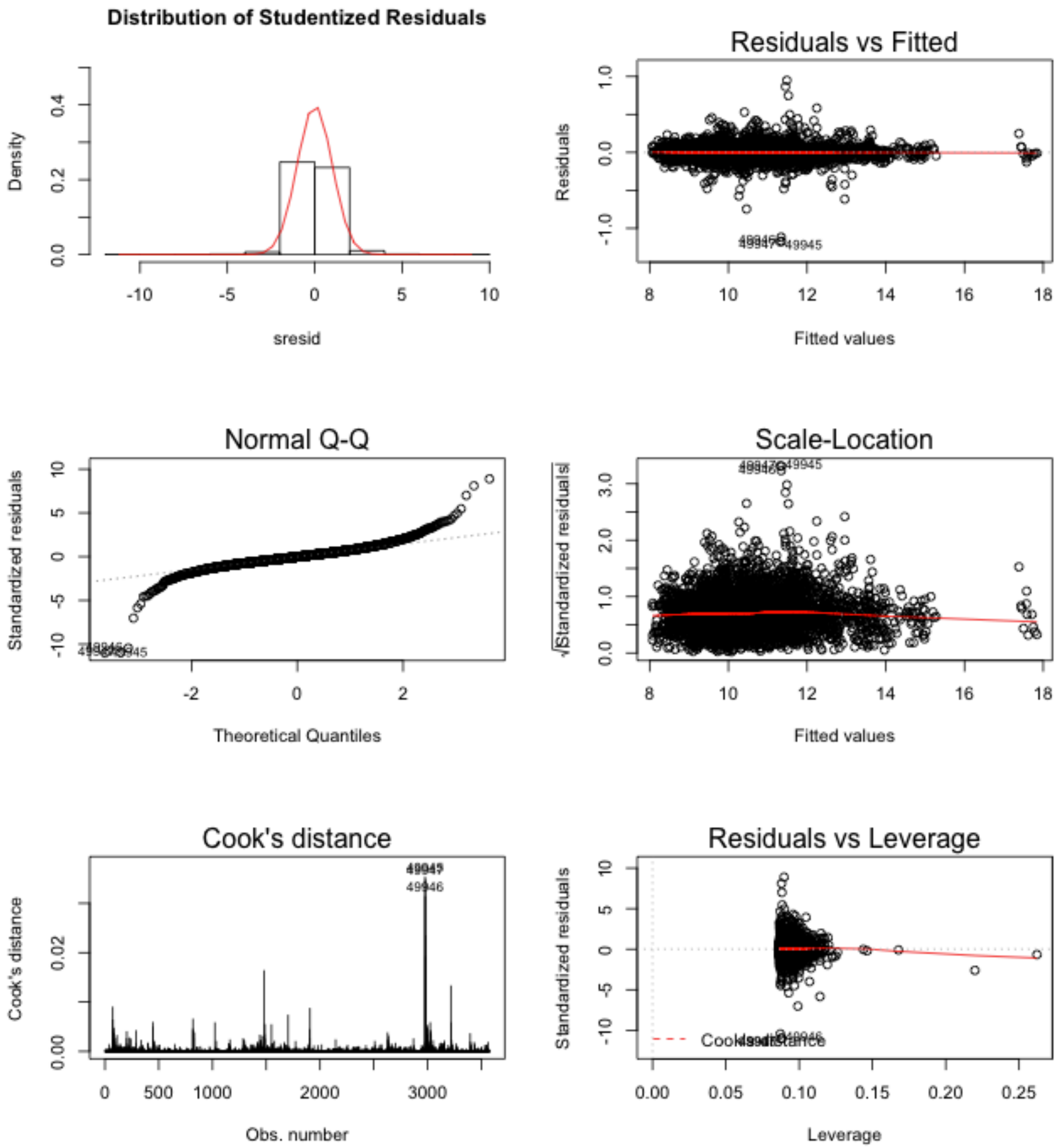

Figure S13: Services GDP regression residuals diagnostics (Model 1)

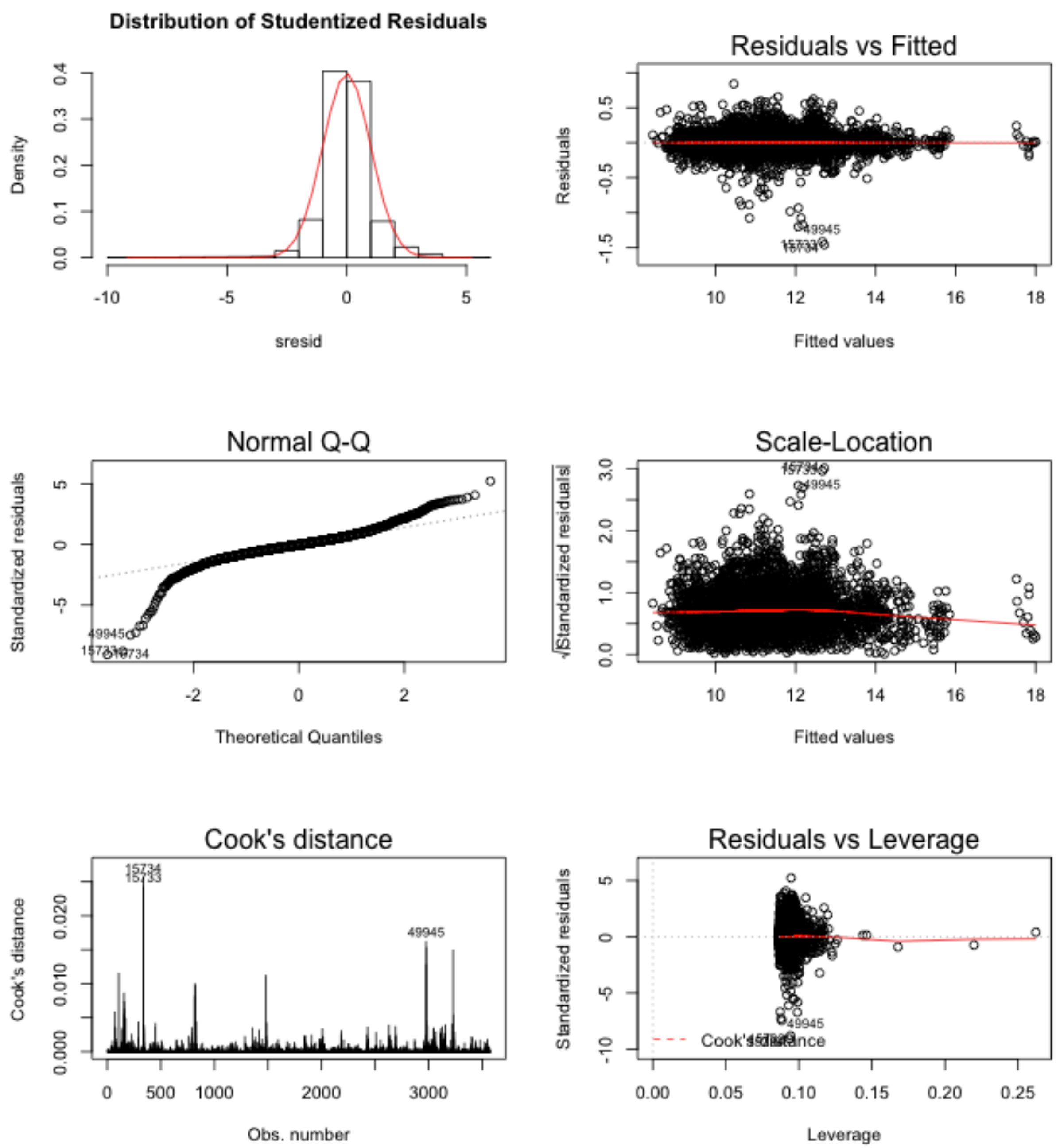

Figures S14: Total GDP regression residuals diagnostics (Model 1)

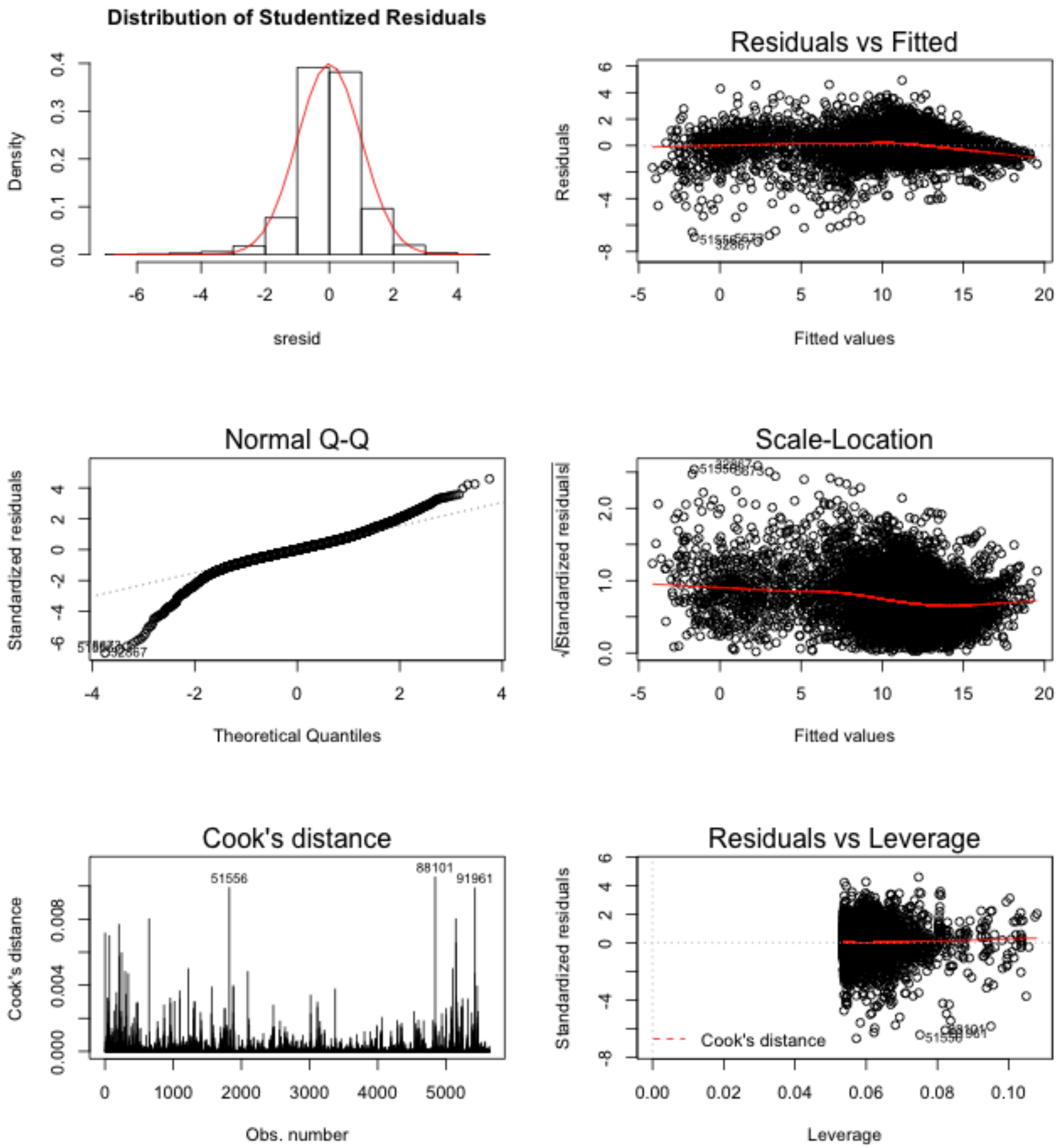

Figure S15: Services Tax (ISS) regression residuals diagnostics (Model 1)

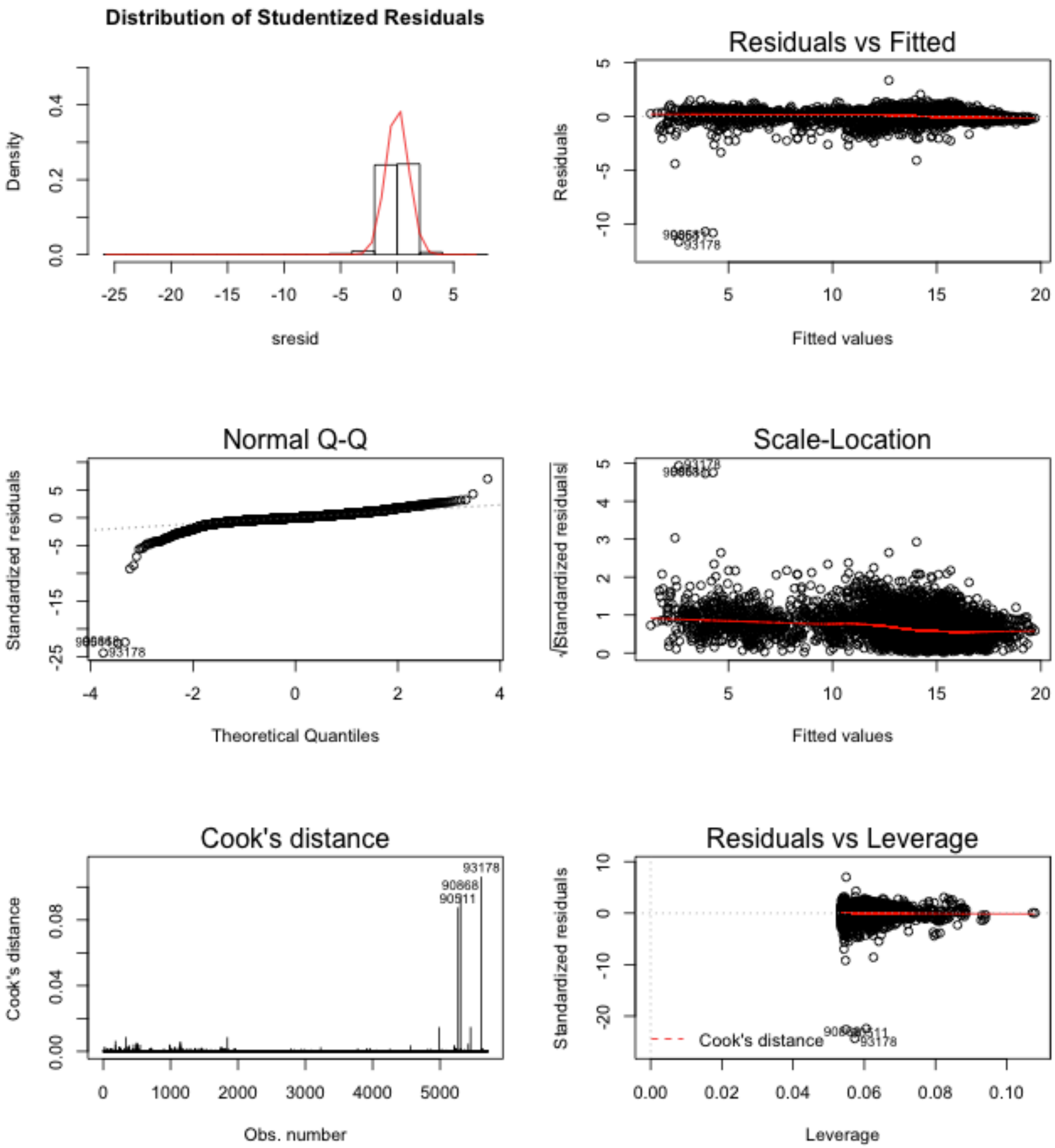

Figure S16: State Transfer (ICMS) regression residuals diagnostics (Model 1)

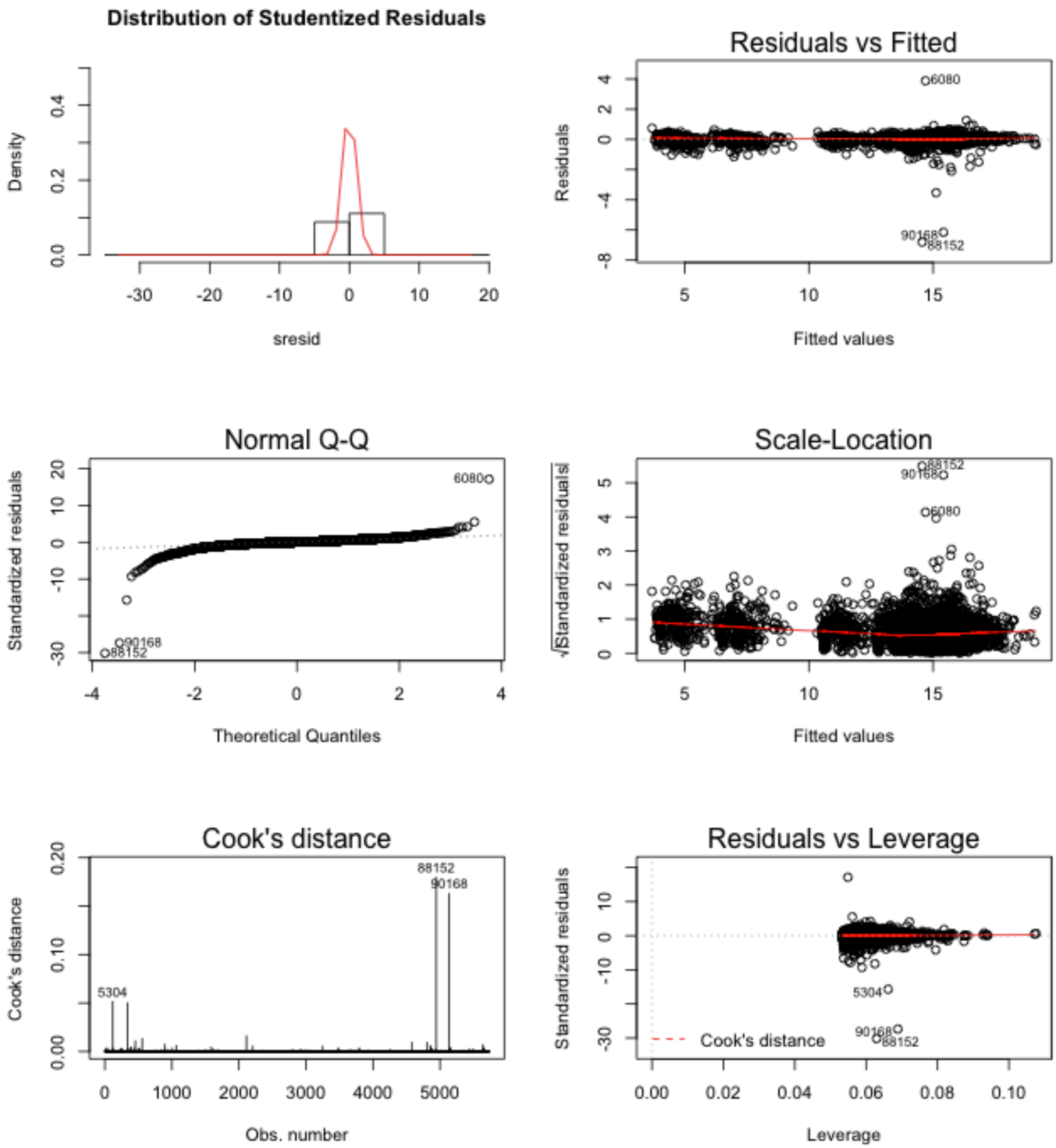

Figure S17: Federal Transfer (FPM) regression residuals diagnostics (Model 1)

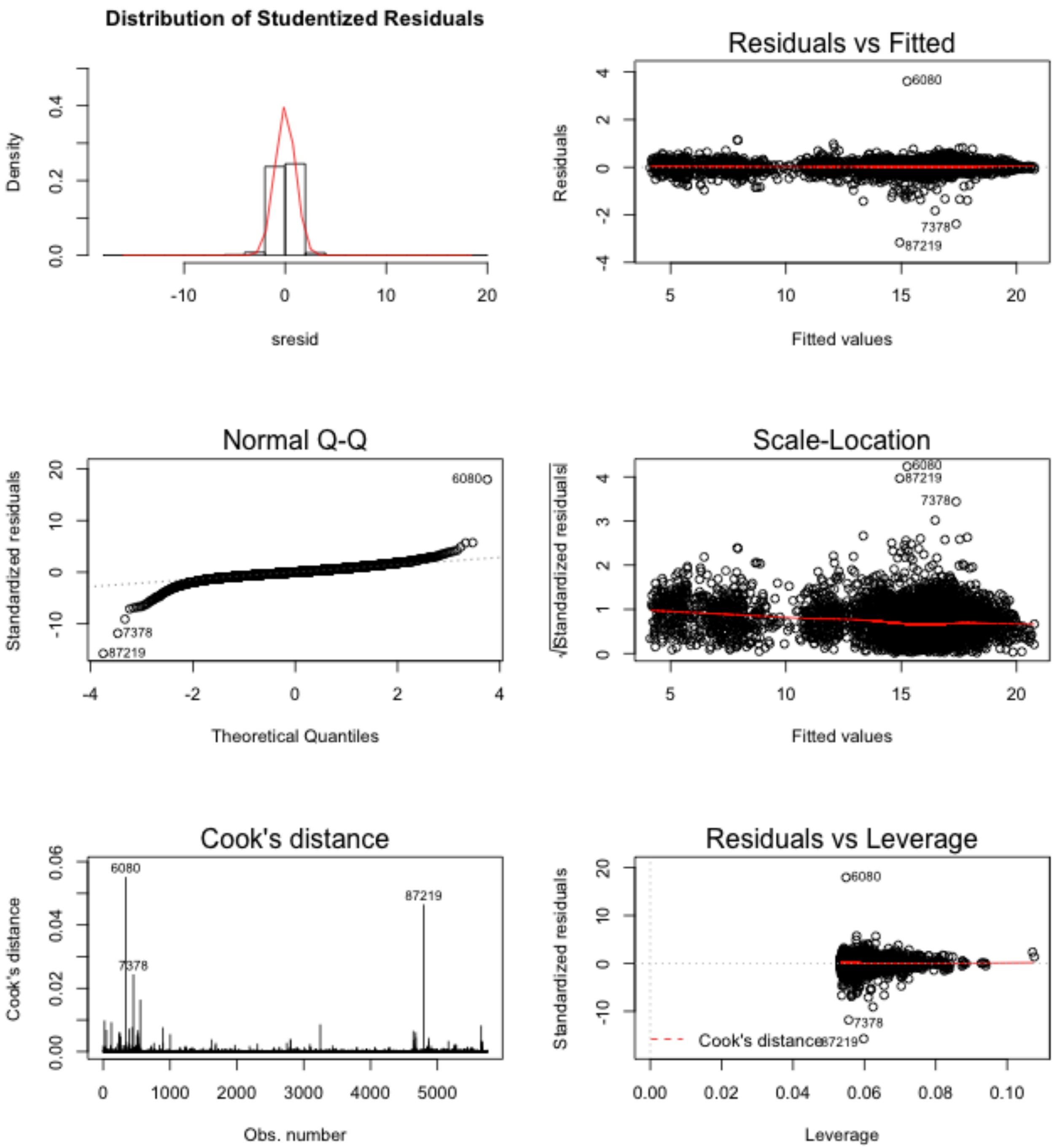

Figure S18: Public revenue regression residuals diagnostics (Model 1)

ANNEX B3 – Sensitivity Analysis – Socioeconomic Indicators

Table S22: Sensitivity Analysis – regression results (dependent variable: average income; short term; Group A)

	Clustering Alternatives			Specification alternatives		
	Main Model	*A*	*B*	*Relaxing the restriction of using only counties with unexplored hydropower potential as controls*	*Without covariates (temperature, precipitation, royalties and state GDP)*	*Adding a covariate (population)*
Standard errors clustered by county:	*Yes*	*Yes*	*No*	*Yes*	*Yes*	*Yes*
Standard errors clustered by hydropower plant:	*Yes*	*No*	*No*	*Yes*	*Yes*	*Yes*
County and Year Fixed Effects	*Yes*	*Yes*	*Yes*	*Yes*	*Yes*	*Yes*
Ψ (Group A/ Short-term)	0.001 (0.009)	0.001 (0.008)	0.001 (0.006)	0.005 (0.010)	0.005 (0.011)	0.001 (0.009)
T1 (Year 2000)	0.063*** (0.001)	0.063*** (0.004)	0.063*** (0.003)	0.062*** (0.000)	0.062*** (0.001)	0.064*** (0.001)
Group A	0.072*** (0.027)	0.072*** (0.026)	0.072** (0.029)	0.109*** (0.008)	0.129*** (0.006)	0.080*** (0.025)
Precipitation	-0.000 (0.000)	-0.000 (0.000)	-0.000 (0.000)	-0.000*** (0.000)		-0.000 (0.000)
Air Temperature	-0.018** (0.008)	-0.018** (0.008)	-0.018*** (0.006)	-0.007*** (0.002)		-0.017** (0.008)
Population						-0.000*** (0.000)

Notes: ***Significant at the 1 percent level;**Significant at the 5 percent level;*Significant at the 10 percent level.

Table S23: Sensitivity Analysis – regression results (dependent variable: average income; long term; Group A)

	Clustering Alternatives			Specification alternatives		
	Main Model	*A*	*B*	*Relaxing the restriction of using only counties with unexplored hydropower potential as controls*	*Without covariates (temperature, precipitation, royalties and state GDP)*	*Adding a covariate (population)*
Standard errors clustered by county:	*Yes*	*Yes*	*No*	*Yes*	*Yes*	*Yes*
Standard errors clustered by hydropower plant:	*Yes*	*No*	*No*	*Yes*	*Yes*	*Yes*
County and Year Fixed Effects	*Yes*	*Yes*	*Yes*	*Yes*	*Yes*	*Yes*
Ψ (Group A/ Long-term)	-0.002 (0.015)	-0.002 (0.011)	-0.002 (0.006)	0.002 (0.016)	-0.005 (0.017)	-0.003 (0.015)
T2 (Year 2010)	0.117*** (0.007)	0.117*** (0.007)	0.117*** (0.005)	0.123*** (0.001)	0.130*** (0.001)	0.120*** (0.007)
Group A	0.195*** (0.024)	0.195*** (0.021)	0.195*** (0.028)	0.166*** (0.008)	0.171*** (0.008)	0.205*** (0.023)
Precipitation	0.000** (0.000)	0.000*** (0.000)	0.000*** (0.000)	0.000* (0.000)		0.000*** (0.000)
Air Temperature	0.013 (0.009)	0.013* (0.007)	0.013*** (0.004)	0.000 (0.001)		0.013 (0.009)
Population						-0.000*** (0.000)

Notes: ***Significant at the 1 percent level;**Significant at the 5 percent level;*Significant at the 10 percent level.

Table S24: Sensitivity Analysis – regression results (dependent variable: average income; short term; Group B)

	Clustering Alternatives			Specification alternatives		
	Main Model	*A*	*B*	*Relaxing the restriction of using only counties with unexplored hydropower potential as controls*	*Without covariates (temperature, precipitation, royalties and state GDP)*	*Adding a covariate (population)*
Standard errors clustered by county:	*Yes*	*Yes*	*No*	*Yes*	*Yes*	*Yes*
Standard errors clustered by hydropower plant:	*Yes*	*No*	*No*	*Yes*	*Yes*	*Yes*
County and Year Fixed Effects	*Yes*	*Yes*	*Yes*	*Yes*	*Yes*	*Yes*
Ψ (Group B/ Short-term)	0.001 (0.006)	0.001 (0.006)	0.001 (0.004)	0.003 (0.006)	0.001 (0.006)	0.001 (0.006)
T2 (Year 2010)	0.062*** (0.003)	0.062*** (0.005)	0.062*** (0.004)	0.062*** (0.001)	0.068*** (0.001)	0.063*** (0.003)
Group B	0.205*** (0.024)	0.205*** (0.029)	0.205*** (0.033)	0.181*** (0.008)	0.156*** (0.003)	0.205*** (0.024)
Precipitation	-0.000 (0.000)	-0.000 (0.000)	-0.000 (0.000)	-0.000*** (0.000)		-0.000 (0.000)
Air Temperature	0.008** (0.004)	0.008* (0.005)	0.008** (0.003)	0.004*** (0.001)		0.007** (0.004)
Population						-0.000 (0.000)

Notes: ***Significant at the 1 percent level;**Significant at the 5 percent level;*Significant at the 10 percent level.

Table 25: Sensitivity Analysis – regression results (dependent variable: education; short term; Group A)

	Clustering Alternatives			Specification alternatives		
	Main Model	*A*	*B*	*Relaxing the restriction of using only counties with unexplored hydropower potential as controls*	*Without covariates (temperature, precipitation, royalties and state GDP)*	*Adding a covariate (population)*
Standard errors clustered by county:	*Yes*	*Yes*	*No*	*Yes*	*Yes*	*Yes*
Standard errors clustered by hydropower plant:	*Yes*	*No*	*No*	*Yes*	*Yes*	*Yes*
County and Year Fixed Effects	*Yes*	*Yes*	*Yes*	*Yes*	*Yes*	*Yes*
Ψ (Group A/ Short-term)	0.017 (0.015)	0.017 (0.012)	0.017** (0.008)	0.023 (0.020)	0.026 (0.022)	0.017 (0.015)
T1 (Year 2000)	0.200*** (0.004)	0.200*** (0.007)	0.200*** (0.004)	0.203*** (0.000)	0.195*** (0.003)	0.201*** (0.003)
Group A	-0.032 (0.073)	-0.032 (0.041)	-0.032 (0.039)	0.063*** (0.011)	0.124*** (0.011)	-0.026 (0.073)
Precipitation	-0.000 (0.000)	-0.000 (0.000)	-0.000 (0.000)	-0.000*** (0.000)		-0.000 (0.000)
Air Temperature	-0.051** (0.024)	-0.051*** (0.014)	-0.051*** (0.007)	-0.028*** (0.002)		-0.051** (0.024)
Population						-0.000 (0.000)

Notes: ***Significant at the 1 percent level;**Significant at the 5 percent level;*Significant at the 10 percent level.

Table S26: Sensitivity Analysis – regression results (dependent variable: education; long term; Group A)

	Clustering Alternatives			Specification alternatives		
	Main Model	*A*	*B*	*Relaxing the restriction of using only counties with unexplored hydropower potential as controls*	*Without covariates (temperature, precipitation, royalties and state GDP)*	*Adding a covariate (population)*
Standard errors clustered by county:	*Yes*	*Yes*	*No*	*Yes*	*Yes*	*Yes*
Standard errors clustered by hydropower plant:	*Yes*	*No*	*No*	*Yes*	*Yes*	*Yes*
County and Year Fixed Effects	*Yes*	*Yes*	*Yes*	*Yes*	*Yes*	*Yes*
Ψ (Group A/ Long-term)	0.007 (0.015)	0.007 (0.013)	0.007 (0.008)	0.017 (0.018)	0.007 (0.016)	0.007 (0.015)
T2 (Year 2010)	0.386*** (0.010)	0.386*** (0.009)	0.386*** (0.006)	0.372*** (0.001)	0.384*** (0.003)	0.386*** (0.011)
Group A	0.132*** (0.038)	0.132*** (0.026)	0.132*** (0.036)	0.169*** (0.009)	0.154*** (0.008)	0.135*** (0.036)
Precipitation	0.000 (0.000)	0.000 (0.000)	0.000** (0.000)	0.000 (0.000)		0.000 (0.000)
Air Temperature	-0.005 (0.012)	-0.005 (0.009)	-0.005 (0.005)	0.006*** (0.001)		-0.005 (0.012)
Population						-0.000 (0.000)

Notes: ***Significant at the 1 percent level;**Significant at the 5 percent level;*Significant at the 10 percent level.

Table 27: Sensitivity Analysis – regression results (dependent variable: education; short term; Group B)

	Clustering Alternatives			Specification alternatives		
	Main Model	*A*	*B*	*Relaxing the restriction of using only counties with unexplored hydropower potential as controls*	*Without covariates (temperature, precipitation, royalties and state GDP)*	*Adding a covariate (population)*
Standard errors clustered by county:	*Yes*	*Yes*	*No*	*Yes*	*Yes*	*Yes*
Standard errors clustered by hydropower plant:	*Yes*	*No*	*No*	*Yes*	*Yes*	*Yes*
County and Year Fixed Effects	*Yes*	*Yes*	*Yes*	*Yes*	*Yes*	*Yes*
Ψ (Group B/ Short-term)	0.010 (0.012)	0.010 (0.010)	0.010 (0.007)	0.016 (0.011)	0.014 (0.013)	0.010 (0.012)
T2 (Year 2010)	0.183*** (0.005)	0.183*** (0.007)	0.183*** (0.006)	0.183*** (0.001)	0.193*** (0.006)	0.181*** (0.005)
Group B	0.192*** (0.048)	0.192*** (0.048)	0.192*** (0.059)	0.136*** (0.015)	0.092*** (0.006)	0.192*** (0.049)
Precipitation	-0.000*** (0.000)	-0.000*** (0.000)	-0.000*** (0.000)	-0.000*** (0.000)		-0.000*** (0.000)
Air Temperature	0.015** (0.007)	0.015** (0.007)	0.015** (0.006)	0.007*** (0.002)		0.015** (0.007)
Population						0.000 (0.000)

Notes: ***Significant at the 1 percent level;**Significant at the 5 percent level;*Significant at the 10 percent level.

Table S28: Sensitivity Analysis – regression results (dependent variable: longevity; short term; Group A)

	Clustering Alternatives			Specification alternatives		
	Main Model	*A*	*B*	*Relaxing the restriction of using only counties with unexplored hydropower potential as controls*	*Without covariates (temperature, precipitation, royalties and state GDP)*	*Adding a covariate (population)*
Standard errors clustered by county:	*Yes*	*Yes*	*No*	*Yes*	*Yes*	*Yes*
Standard errors clustered by hydropower plant:	*Yes*	*No*	*No*	*Yes*	*Yes*	*Yes*
County and Year Fixed Effects	*Yes*	*Yes*	*Yes*	*Yes*	*Yes*	*Yes*
Ψ (Group A/ Short-term)	0.007 (0.006)	0.007 (0.005)	0.007* (0.004)	0.004 (0.007)	0.003 (0.009)	0.007 (0.006)
T1 (Year 2000)	0.070*** (0.001)	0.070*** (0.003)	0.070*** (0.002)	0.069*** (0.000)	0.071*** (0.001)	0.070*** (0.001)
Group A	0.116*** (0.019)	0.116*** (0.015)	0.116*** (0.018)	0.091*** (0.004)	0.051*** (0.005)	0.116*** (0.018)
Precipitation	-0.000 (0.000)	-0.000 (0.000)	-0.000 (0.000)	0.000*** (0.000)		-0.000 (0.000)
Air Temperature	0.020*** (0.006)	0.020*** (0.005)	0.020*** (0.003)	0.015*** (0.001)		0.020*** (0.006)
Population						0.000 (0.000)

Notes: ***Significant at the 1 percent level;**Significant at the 5 percent level;*Significant at the 10 percent level.

Table S29: Sensitivity Analysis – regression results (dependent variable: longevity; long term; Group A)

	Clustering Alternatives			Specification alternatives		
	Main Model	*A*	*B*	*Relaxing the restriction of using only counties with unexplored hydropower potential as controls*	*Without covariates (temperature, precipitation, royalties and state GDP)*	*Adding a covariate (population)*
Standard errors clustered by county:	*Yes*	*Yes*	*No*	*Yes*	*Yes*	*Yes*
Standard errors clustered by hydropower plant:	*Yes*	*No*	*No*	*Yes*	*Yes*	*Yes*
County and Year Fixed Effects	*Yes*	*Yes*	*Yes*	*Yes*	*Yes*	*Yes*
Ψ (Group A/ Long-term)	0.003 (0.018)	0.003 (0.010)	0.003 (0.006)	-0.005 (0.015)	0.001 (0.016)	0.003 (0.018)
T2 (Year 2010)	0.133*** (0.009)	0.133*** (0.006)	0.133*** (0.004)	0.145*** (0.001)	0.141*** (0.001)	0.133*** (0.009)
Group A	0.135*** (0.031)	0.135*** (0.018)	0.135*** (0.025)	0.114*** (0.007)	0.079*** (0.008)	0.138*** (0.031)
Precipitation	-0.000** (0.000)	-0.000** (0.000)	-0.000*** (0.000)	-0.000*** (0.000)		-0.000** (0.000)
Air Temperature	0.015 (0.011)	0.015** (0.007)	0.015*** (0.004)	0.007*** (0.002)		0.015 (0.011)
Population						-0.000 (0.000)

Notes: ***Significant at the 1 percent level;**Significant at the 5 percent level;*Significant at the 10 percent level.

Table S30: Sensitivity Analysis – regression results (dependent variable: longevity; short term; Group B)

	Clustering Alternatives			Specification alternatives		
	Main Model	*A*	*B*	*Relaxing the restriction of using only counties with unexplored hydropower potential as controls*	*Without covariates (temperature, precipitation,royalties and state GDP)*	*Adding a covariate (population)*
Standard errors clustered by county:	*Yes*	*Yes*	*No*	*Yes*	*Yes*	*Yes*
Standard errors clustered by hydropower plant:	*Yes*	*No*	*No*	*Yes*	*Yes*	*Yes*
County and Year Fixed Effects	*Yes*	*Yes*	*Yes*	*Yes*	*Yes*	*Yes*
Ψ (Group B/ Short-term)	-0.006 (0.008)	-0.006 (0.007)	-0.006 (0.004)	-0.009 (0.008)	-0.004 (0.009)	-0.006 (0.008)
T2 (Year 2010)	0.073*** (0.004)	0.073*** (0.005)	0.073*** (0.004)	0.074*** (0.000)	0.071*** (0.002)	0.073*** (0.004)
Group B	0.085** (0.034)	0.085** (0.034)	0.085** (0.036)	0.088*** (0.008)	0.095*** (0.004)	0.084** (0.034)
Precipitation	-0.000** (0.000)	0	-0.000** (0.000)	-0.000*** (0.000)		-0.000** (0.000)
Air Temperature	-0.002 (0.005)	-0.002 (0.005)	-0.002 (0.004)	-0.002** (0.001)		-0.002 (0.005)
Population						-0.000 (0.000)

Notes: ***Significant at the 1 percent level;**Significant at the 5 percent level;*Significant at the 10 percent level.

Table S31: Sensitivity Analysis – regression results (dependent variable: population density; short term; Group A)

	Clustering Alternatives			Specification alternatives		
	Main Model	*A*	*B*	*Relaxing the restriction of using only counties with unexplored hydropower potential as controls*	*Without covariates (temperature, precipitation, royalties and state GDP)*	*Adding a covariate (population)*
Standard errors clustered by county:	*Yes*	*Yes*	*No*	*Yes*	*Yes*	*Yes*
Standard errors clustered by hydropower plant:	*Yes*	*No*	*No*	*Yes*	*Yes*	*Yes*
County and Year Fixed Effects	*Yes*	*Yes*	*Yes*	*Yes*	*Yes*	*Yes*
Ψ (Group A/ Short-term)	0.023 (0.053)	0.023 (0.047)	0.023 (0.034)	-0.017 (0.052)	0.012 (0.054)	0.033 (0.050)
T1 (Year 2000)	0.035*** (0.010)	0.035 (0.041)	0.035* (0.019)	0.076*** (0.002)	0.035*** (0.002)	0.016 (0.012)
Group A	1.138*** (0.160)	1.138*** (0.146)	1.138*** (0.169)	1.175*** (0.028)	0.962*** (0.027)	0.965*** (0.132)
Precipitation	-0.000 (0.000)	-0.000 (0.000)	-0.000 (0.000)	-0.000*** (0.000)		-0.000 (0.000)
Air Temperature	0.051 (0.056)	0.051 (0.060)	0.051 (0.032)	0.053*** (0.003)		0.046 (0.051)
Population						0.000*** (0.000)

Notes: ***Significant at the 1 percent level;**Significant at the 5 percent level;*Significant at the 10 percent level.

Table S32: Sensitivity Analysis – regression results (dependent variable: population density; long term; Group A)

	Clustering Alternatives			Specification alternatives		
	Main Model	*A*	*B*	*Relaxing the restriction of using only counties with unexplored hydropower potential as controls*	*Without covariates (temperature, precipitation, royalties and state GDP)*	*Adding a covariate (population)*
Standard errors clustered by county:	*Yes*	*Yes*	*No*	*Yes*	*Yes*	*Yes*
Standard errors clustered by hydropower plant:	*Yes*	*No*	*No*	*Yes*	*Yes*	*Yes*
County and Year Fixed Effects	*Yes*	*Yes*	*Yes*	*Yes*	*Yes*	*Yes*
Ψ (Group A/ Long-term)	0.028 (0.078)	0.028 (0.069)	0.028 (0.049)	-0.015 (0.087)	0.042 (0.084)	0.048 (0.074)
T2 (Year 2010)	0.127*** (0.043)	0.127** (0.063)	0.127*** (0.035)	0.121*** (0.008)	0.077*** (0.003)	0.091** (0.041)
Group A	0.988*** (0.143)	0.988*** (0.129)	0.988*** (0.216)	1.127*** (0.044)	1.009*** (0.042)	0.850*** (0.140)
Precipitation	-0.000*** (0.000)	-0.000*** (0.000)	-0.000*** (0.000)	-0.000 (0.000)		-0.000*** (0.000)
Air Temperature	-0.036 (0.055)	-0.036 (0.048)	-0.036 (0.030)	0.025*** (0.005)		-0.035 (0.052)
Population						0.000*** (0.000)

Notes: ***Significant at the 1 percent level;**Significant at the 5 percent level;*Significant at the 10 percent level.

Table S33: Sensitivity Analysis – regression results (dependent variable: population density; short term; Group B)

	Clustering Alternatives			Specification alternatives		
	Main Model	*A*	*B*	*Relaxing the restriction of using only counties with unexplored hydropower potential as controls*	*Without covariates (temperature, precipitation, royalties and state GDP)*	*Adding a covariate (population)*
Standard errors clustered by county:	*Yes*	*Yes*	*No*	*Yes*	*Yes*	*Yes*
Standard errors clustered by hydropower plant:	*Yes*	*No*	*No*	*Yes*	*Yes*	*Yes*
County and Year Fixed Effects	*Yes*	*Yes*	*Yes*	*Yes*	*Yes*	*Yes*
Ψ (Group B/ Short-term)	0.008 (0.028)	0.008 (0.027)	0.008 (0.019)	0.005 (0.031)	0.014 (0.030)	0.000 (0.023)
T2 (Year 2010)	0.057** (0.023)	0.057** (0.024)	0.057*** (0.016)	0.062*** (0.002)	0.045*** (0.005)	0.039** (0.020)
Group B	0.018 (0.195)	0.018 (0.167)	0.018 (0.151)	0.064*** (0.025)	0.114*** (0.015)	0.027 (0.168)
Precipitation	-0.000*** (0.000)	0	-0.000** (0.000)	0.000*** (0.000)		-0.000** (0.000)
Air Temperature	-0.017 (0.031)	-0.017 (0.026)	-0.017 (0.016)	-0.008** (0.004)		-0.011 (0.026)
Population						0.000*** (0.000)

Notes: ***Significant at the 1 percent level;**Significant at the 5 percent level;*Significant at the 10 percent level.

Table S34: Sensitivity Analysis – regression results (dependent variable: access to piped water; short term; Group A)

	Clustering Alternatives			Specification alternatives		
	Main Model	*A*	*B*	*Relaxing the restriction of using only counties with unexplored hydropower potential as controls*	*Without covariates (temperature, precipitation, royalties and state GDP)*	*Adding a covariate (population)*
Standard errors clustered by county:	*Yes*	*Yes*	*No*	*Yes*	*Yes*	*Yes*
Standard errors clustered by hydropower plant:	*Yes*	*No*	*No*	*Yes*	*Yes*	*Yes*
County and Year Fixed Effects	*Yes*	*Yes*	*Yes*	*Yes*	*Yes*	*Yes*
Ψ (Group A/ Short-term)	-1.940 (3.814)	-1.940 (3.142)	-1.940 (2.016)	1.396 (4.054)	-2.889 (4.022)	-2.213 (3.757)
T1 (Year 2000)	16.111*** (0.516)	16.111*** (1.530)	16.111*** (1.121)	11.334*** (0.256)	15.104*** (0.286)	16.576*** (0.504)
Group A	62.317*** (10.308)	62.317*** (11.232)	62.317*** (9.965)	60.883*** (2.098)	48.028*** (2.011)	66.671*** (9.927)
Precipitation	-0.018*** (0.006)	-0.00018	-0.018*** (0.005)	0.003*** (0.001)		-0.017*** (0.006)
Air Temperature	2.742 (3.037)	2.742 (3.659)	2.742 (1.917)	4.837*** (0.244)		2.896 (2.952)
Population						-0.000*** (0.000)

Notes: ***Significant at the 1 percent level;**Significant at the 5 percent level;*Significant at the 10 percent level.

Table S35: Sensitivity Analysis – regression results (dependent variable: access to piped water; short term;Group A)

	Clustering Alternatives			Specification alternatives		
	Main Model	*A*	*B*	*Relaxing the restriction of using only counties with unexplored hydropower potential as controls*	*Without covariates (temperature, precipitation, royalties and state GDP)*	*Adding a covariate (population)*
Standard errors clustered by county:	*Yes*	*Yes*	*No*	*Yes*	*Yes*	*Yes*
Standard errors clustered by hydropower plant:	*Yes*	*No*	*No*	*Yes*	*Yes*	*Yes*
County and Year Fixed Effects	*Yes*	*Yes*	*Yes*	*Yes*	*Yes*	*Yes*
Ψ (Group A/ Long-term)	-5.855 (7.771)	-5.855 (4.263)	-18.531075	-5.768 (6.660)	-6.702 (7.343)	-6.064 (7.762)
T2 (Year 2010)	21.926*** (2.966)	21.926*** (2.589)	21.926*** (2.254)	25.112*** (0.353)	24.758*** (0.894)	22.297*** (2.939)
Group A	48.655*** (12.927)	48.655*** (9.007)	48.655*** (13.856)	30.973*** (3.774)	24.016*** (3.671)	50.088*** (12.927)
Precipitation	-0.020** (0.009)	-0.020*** (0.007)	-0.020*** (0.005)	-0.024*** (0.001)		-0.020** (0.009)
Air Temperature	6.138 (4.196)	6.138** (2.861)	6.138*** (1.956)	0.232 (0.806)		6.131 (4.215)
Population						-0.000*** (0.000)

Notes: ***Significant at the 1 percent level;**Significant at the 5 percent level;*Significant at the 10 percent level.

Table S36: Sensitivity Analysis – regression results (dependent variable: access to piped water; short term;Group B)

	Clustering Alternatives			Specification alternatives		
	Main Model	*A*	*B*	*Relaxing the restriction of using only counties with unexplored hydropower potential as controls*	*Without covariates (temperature, precipitation, royalties and state GDP)*	*Adding a covariate (population)*
Standard errors clustered by county:	*Yes*	*Yes*	*No*	*Yes*	*Yes*	*Yes*
Standard errors clustered by hydropower plant:	*Yes*	*No*	*No*	*Yes*	*Yes*	*Yes*
County and Year Fixed Effects	*Yes*	*Yes*	*Yes*	*Yes*	*Yes*	*Yes*
Ψ (Group B/ Short-term)	-0.232 (4.354)	-0.232 (3.221)	-0.232 (2.263)	0.023 (4.051)	1.661 (4.788)	-0.238 (4.390)
T2 (Year 2010)	11.175*** (2.083)	11.175*** (2.520)	11.175*** (1.959)	12.148*** (0.181)	11.456*** (1.471)	11.162*** (2.242)
Group B	45.384** (17.567)	45.384*** (15.209)	45.384** (18.196)	34.370*** (5.191)	39.905*** (2.394)	45.391** (17.634)
Precipitation	-0.030*** (0.005)	-0.030*** (0.006)	-0.030*** (0.005)	-0.031*** (0.001)		-0.030*** (0.006)
Air Temperature	0.362 (2.656)	0.362 (2.312)	0.362 (1.873)	-1.360** (0.691)		0.366 (2.679)
Population						0.000 (0.000)

Notes: ***Significant at the 1 percent level;**Significant at the 5 percent level;*Significant at the 10 percent level.

Table S37: Sensitivity Analysis – regression results (dependent variable: access to electricity; short term; Group A)

	Clustering Alternatives			Specification alternatives		
	Main Model	*A*	*B*	*Relaxing the restriction of using only counties with unexplored hydropower potential as controls*	*Without covariates (temperature, precipitation,royalties and state GDP)*	*Adding a covariate (population)*
Standard errors clustered by county:	*Yes*	*Yes*	*No*	*Yes*	*Yes*	*Yes*
Standard errors clustered by hydropower plant:	*Yes*	*No*	*No*	*Yes*	*Yes*	*Yes*
County and Year Fixed Effects	*Yes*	*Yes*	*Yes*	*Yes*	*Yes*	*Yes*
Ψ (Group A/ Short-term)	-3.067 (2.583)	-3.067 (2.244)	-3.067 (1.887)	-0.256 (3.859)	-4.781 (3.581)	-3.360 (2.548)
T1 (Year 2000)	15.368*** (0.441)	15.368*** (1.618)	15.368*** (1.049)	10.439*** (0.255)	15.296*** (0.379)	15.864*** (0.478)
Group A	80.625*** (7.835)	80.625*** (8.087)	80.625*** (9.360)	64.123*** (1.995)	49.347*** (1.790)	85.334*** (6.846)
Precipitation	-0.006 (0.005)	-0.006 (0.008)	-0.006 (0.005)	0.016*** (0.001)		-0.005 (0.005)
Air Temperature	9.127*** (2.255)	9.127*** (2.222)	9.127*** (1.819)	6.658*** (0.122)		9.313*** (2.123)
Population						-0.000*** (0.000)

Notes: ***Significant at the 1 percent level;**Significant at the 5 percent level;*Significant at the 10 percent level.

Table S38: Sensitivity Analysis – regression results (dependent variable: access to electricity; long term; Group A)

	Clustering Alternatives			Specification alternatives		
	Main Model	*A*	*B*	*Relaxing the restriction of using only counties with unexplored hydropower potential as controls*	*Without covariates (temperature, precipitation, royalties and state GDP)*	*Adding a covariate (population)*
Standard errors clustered by county:	*Yes*	*Yes*	*No*	*Yes*	*Yes*	*Yes*
Standard errors clustered by hydropower plant:	*Yes*	*No*	*No*	*Yes*	*Yes*	*Yes*
County and Year Fixed Effects	*Yes*	*Yes*	*Yes*	*Yes*	*Yes*	*Yes*
Ψ (Group A/ Long-term)	-5.783 (3.552)	-5.783* (3.422)	-5.783** (2.887)	-4.145 (3.580)	-7.044 (5.443)	-6.207* (3.571)
T2 (Year 2010)	18.085*** (1.956)	18.085*** (2.940)	18.085*** (2.056)	18.275*** (0.263)	22.243*** (0.625)	18.827*** (1.950)
Group A	66.449*** (6.383)	66.449*** (8.268)	66.449*** (12.625)	54.433*** (2.504)	41.196*** (2.721)	69.339*** (6.606)
Precipitation	-0.012*** (0.004)	-0.000072	-0.012** (0.005)	-0.012*** (0.001)		-0.012*** (0.004)
Air Temperature	7.077*** (2.342)	7.077*** (2.609)	7.077*** (1.779)	3.594*** (0.649)		7.073*** (2.394)
Population						-0.000*** (0.000)

Notes: ***Significant at the 1 percent level;**Significant at the 5 percent level;*Significant at the 10 percent level.

Table S39:Sensitivity Analysis – regression results (dependent variable: access to electricity; short term; Group B)

	Clustering Alternatives			Specification alternatives		
	Main Model	*A*	*B*	*Relaxing the restriction of using only counties with unexplored hydropower potential as controls*	*Without covariates (temperature, precipitation, royalties and state GDP)*	*Adding a covariate (population)*
Standard errors clustered by county:	*Yes*	*Yes*	*No*	*Yes*	*Yes*	*Yes*
Standard errors clustered by hydropower plant:	*Yes*	*No*	*No*	*Yes*	*Yes*	*Yes*
County and Year Fixed Effects	*Yes*	*Yes*	*Yes*	*Yes*	*Yes*	*Yes*
Ψ (Group B/ Short-term)	-0.319 (2.916)	-0.319 (2.077)	-0.319 (1.479)	0.862 (2.552)	0.408 (2.876)	-0.096 (2.927)
T2 (Year 2010)	7.277*** (1.051)	7.277*** (1.413)	7.277*** (1.280)	7.161*** (0.153)	8.620*** (1.630)	7.771*** (1.259)
Group B	35.251*** (9.557)	35.251*** (7.703)	35.251*** (11.889)	24.838*** (3.859)	22.229*** (1.438)	34.982*** (9.487)
Precipitation	-0.000066	-0.011*** (0.004)	-0.011*** (0.003)	-0.014*** (0.001)		-0.011* (0.006)
Air Temperature	1.862 (1.315)	1.862 (1.153)	1.862 (1.224)	0.285 (0.532)		1.695 (1.296)
Population						-0.000*** (0.000)

Notes: ***Significant at the 1 percent level;**Significant at the 5 percent level;*Significant at the 10 percent level.

Table S40: Sensitivity Analysis – regression results (dependent variable: teenage pregnancy; short term; Group A)

	Clustering Alternatives			Specification alternatives		
	Main Model	*A*	*B*	*Relaxing the restriction of using only counties with unexplored hydropower potential as controls*	*Without covariates (temperature, precipitation, royalties and state GDP)*	*Adding a covariate (population)*
Standard errors clustered by county:	*Yes*	*Yes*	*No*	*Yes*	*Yes*	*Yes*
Standard errors clustered by hydropower plant:	*Yes*	*No*	*No*	*Yes*	*Yes*	*Yes*
County and Year Fixed Effects	*Yes*	*Yes*	*Yes*	*Yes*	*Yes*	*Yes*
Ψ (Group A/ Short-term)	-0.433 (0.615)	-0.433 (0.726)	-0.433 (0.446)	-0.461 (0.652)	-0.522 (0.676)	-0.433 (0.614)
T1 (Year 2000)	1.040*** (0.075)	1.040*** (0.366)	1.040*** (0.248)	0.915*** (0.012)	0.965*** (0.047)	1.040*** (0.077)
Group A	-0.486 (1.575)	-0.486 (1.809)	-0.486 (2.205)	-1.195*** (0.338)	-2.022*** (0.338)	-0.484 (1.485)
Precipitation	-0.001 (0.001)	-0.001 (0.002)	-0.001 (0.001)	0.000*** (0.000)		-0.001 (0.001)
Air Temperature	0.352 (0.391)	0.352 (0.559)	0.352 (0.418)	0.292*** (0.024)		0.352 (0.389)
Population						-0.000 (0.000)

Notes: ***Significant at the 1 percent level;**Significant at the 5 percent level;*Significant at the 10 percent level.

Table S41: Sensitivity Analysis – regression results (dependent variable: teenage pregnancy; long term; Group A)

	Clustering Alternatives			Specification alternatives		
	Main Model	*A*	*B*	*Relaxing the restriction of using only counties with unexplored hydropower potential as controls*	*Without covariates (temperature, precipitation, royalties and state GDP)*	*Adding a covariate (population)*
Standard errors clustered by county:	*Yes*	*Yes*	*No*	*Yes*	*Yes*	*Yes*
Standard errors clustered by hydropower plant:	*Yes*	*No*	*No*	*Yes*	*Yes*	*Yes*
County and Year Fixed Effects	*Yes*	*Yes*	*Yes*	*Yes*	*Yes*	*Yes*
Ψ (Group A/ Long-term)	-1.001 (0.680)	-1.001 (0.616)	-1.001*** (0.355)	-1.214* (0.686)	-1.087 (0.660)	-1.013 (0.672)
T2 (Year 2010)	0.147 (0.185)	0.147 (0.302)	0.147 (0.253)	0.560*** (0.060)	0.426*** (0.039)	0.169 (0.173)
Group A	-1.745*** (0.392)	-1.614125	-1.745 (1.555)	-2.424*** (0.341)	-2.838*** (0.330)	-1.662*** (0.374)
Precipitation	0.000 (0.001)	0.000 (0.001)	0.000 (0.001)	-0.001*** (0.000)		0.000 (0.001)
Air Temperature	0.368** (0.143)	0.368 (0.282)	0.368* (0.217)	0.051 (0.042)		0.368** (0.144)
Population						-0.000 (0.000)

Notes: ***Significant at the 1 percent level;**Significant at the 5 percent level;*Significant at the 10 percent level.

Table S42: Sensitivity Analysis – regression results (dependent variable: teenage pregnancy; short term; Group B)

	Clustering Alternatives			Specification alternatives		
	Main Model	*A*	*B*	*Relaxing the restriction of using only counties with unexplored hydropower potential as controls*	*Without covariates (temperature, precipitation, royalties and state GDP)*	*Adding a covariate (population)*
Standard errors clustered by county:	*Yes*	*Yes*	*No*	*Yes*	*Yes*	*Yes*
Standard errors clustered by hydropower plant:	*Yes*	*No*	*No*	*Yes*	*Yes*	*Yes*
County and Year Fixed Effects	*Yes*	*Yes*	*Yes*	*Yes*	*Yes*	*Yes*
Ψ (Group B/ Short-term)	-0.015 (0.227)	-0.015 (0.411)	-0.015 (0.300)	-0.252 (0.281)	-0.020 (0.265)	-0.006 (0.226)
T2 (Year 2010)	-0.080592	-0.368 (0.411)	-0.368 (0.260)	-0.478*** (0.019)	-0.613*** (0.096)	-0.346 (0.226)
Group B	-4.987** (2.340)	-4.987** (2.405)	-4.987** (2.410)	-2.262*** (0.298)	-2.815*** (0.133)	-4.999** (2.371)
Precipitation	-0.000 (0.001)	-0.000 (0.001)	-0.000 (0.001)	-0.001*** (0.000)		-0.000 (0.001)
Air Temperature	-0.342 (0.356)	-0.342 (0.369)	-0.342 (0.248)	0.061 (0.039)		-0.349 (0.362)
Population						-0.000 (0.000)

Notes: ***Significant at the 1 percent level;**Significant at the 5 percent level;*Significant at the 10 percent level.

Table S43: Sensitivity Analysis – regression results (dependent variable: HIV cases; short term; Group A)

	Clustering Alternatives			Specification alternatives		
	Main Model	*A*	*B*	*Relaxing the restriction of using only counties with unexplored hydropower potential as controls*	*Without covariates (temperature, precipitation, royalties and state GDP)*	*Adding a covariate (population)*
Standard errors clustered by county:	*Yes*	*Yes*	*No*	*Yes*	*Yes*	*Yes*
Standard errors clustered by hydropower plant:	*Yes*	*No*	*No*	*Yes*	*Yes*	*Yes*
County and Year Fixed Effects	*Yes*	*Yes*	*Yes*	*Yes*	*Yes*	*Yes*
Ψ (Group A/ Short-term)	3.392 (9.061)	3.392 (9.557)	3.392 (4.860)	3.719 (7.813)	3.210 (7.896)	3.738 (9.129)
T1 (Year 2000)	4.533* (2.308)	4.533** (2.012)	4.533* (2.706)	4.335*** (0.373)	4.876*** (1.065)	3.921 (2.575)
Group A	-12.528 (21.308)	-12.528 (22.905)	-12.528 (24.012)	-16.980*** (3.436)	-15.605*** (3.948)	-18.240 (22.445)
Precipitation	0.004 (0.024)	0.004 (0.023)	0.004 (0.012)	0.000 (0.001)		0.003 (0.024)
Air Temperature	1.335 (6.063)	1.335 (6.885)	1.335 (4.553)	-0.328 (0.536)		1.168 (6.189)
Population						0.000** (0.000)

Notes: ***Significant at the 1 percent level;**Significant at the 5 percent level;*Significant at the 10 percent level.

Table S44: Sensitivity Analysis – regression results (dependent variable: HIV cases; long term; Group A)

	Clustering Alternatives			Specification alternatives		
	Main Model	*A*	*B*	*Relaxing the restriction of using only counties with unexplored hydropower potential as controls*	*Without covariates (temperature, precipitation, royalties and state GDP)*	*Adding a covariate (population)*
Standard errors clustered by county:	*Yes*	*Yes*	*No*	*Yes*	*Yes*	*Yes*
Standard errors clustered by hydropower plant:	*Yes*	*No*	*No*	*Yes*	*Yes*	*Yes*
County and Year Fixed Effects	*Yes*	*Yes*	*Yes*	*Yes*	*Yes*	*Yes*
Ψ (Group A/ Long-term)	9.160 (16.364)	9.160 (17.321)	9.160 (9.422)	10.569 (15.267)	7.510 (15.901)	9.600 (16.372)
T2 (Year 2010)	3.419 (5.737)	3.419 (5.009)	3.419 (6.720)	5.654*** (0.317)	8.826*** (3.259)	2.635 (5.810)
Group A	3.638 (21.169)	3.638 (24.141)	3.638 (41.223)	-15.402** (6.743)	-15.755** (7.950)	0.607 (22.079)
Precipitation	0.005 (0.022)	0.005 (0.027)	0.005 (0.016)	-0.001 (0.002)		0.005 (0.022)
Air Temperature	6.830 (7.369)	6.830 (7.961)	6.830 (5.766)	0.528 (0.711)		6.846 (7.409)
Population						0.000* (0.000)

Notes: ***Significant at the 1 percent level;**Significant at the 5 percent level;*Significant at the 10 percent level.

Table S45: Sensitivity Analysis – regression results (dependent variable: HIV cases; long term; Group B)

	Clustering Alternatives			Specification alternatives		
	Main Model	*A*	*B*	*Relaxing the restriction of using only counties with unexplored hydropower potential as controls*	*Without covariates (temperature, precipitation, royalties and state GDP)*	*Adding a covariate (population)*
Standard errors clustered by county:	*Yes*	*Yes*	*No*	*Yes*	*Yes*	*Yes*
Standard errors clustered by hydropower plant:	*Yes*	*No*	*No*	*Yes*	*Yes*	*Yes*
County and Year Fixed Effects	*Yes*	*Yes*	*Yes*	*Yes*	*Yes*	*Yes*
Ψ (Group B/ Short-term)	-3.307 (3.788)	-3.307 (3.305)	-3.307 (2.952)	-0.127 (1.515)	-3.701 (4.378)	-3.130 (3.754)
T2 (Year 2010)	4.832 (5.392)	4.832 (3.353)	4.832* (2.555)	1.862*** (0.100)	4.947 (3.945)	5.223 (5.575)
Group B	-17.795 (18.085)	-17.795 (16.075)	-17.795 (23.729)	-22.510*** (0.992)	-18.187*** (2.189)	-18.008 (18.372)
Precipitation	0.006 (0.011)	0.006 (0.009)	0.006 (0.006)	0		0.006 (0.011)
Air Temperature	0.166 (2.979)	0.166 (2.525)	0.166 (2.442)	-0.403** (0.177)		0.035 (3.101)
Population						-0.000 (0.000)

Notes: ***Significant at the 1 percent level;**Significant at the 5 percent level;*Significant at the 10 percent level.

8. APPENDIX C: CHAPTER 4

8.1. Introduction

This document includes details about the data and methods described in Chapter 4, as well as complementary results and discussion. We provide additional details about the government database used to model the Brazilian system and the method employed to build the baseline and alternative scenarios. We also describe in more details the hydrothermal scheduling issue and the SDDP algorithm applied to solve the electricity optimization problem. Further, we describe the method developed to produce wind time series from reanalysis data and its validity.

8.2 Detailed description of the baseline and alternative scenarios

To model the Brazilian electric system we used a database developed by *Empresa de Pesquisa Energetica* (EPE). EPE is the state company responsible for creating the long-term Brazilian energy plans. Every year, EPE issues an expansion plan (*Plano Decenal de Energia*) assessing the current and future energy infrastructure. One of the products from this plan is a set of files containing the characteristics of the Brazilian electric system, including demand projections, the major transmission lines, and the details about each power plant used to model the hydrothermal operation planning of the current and future system (EPE 2015). Those files are the inputs of the optimal operation model used by the government called *NEWAVE.* We downloaded the *NEWAVE* files from the EPE website and imported those files to SDDP.

Here, we present the main details about EPE's 2015 report files and the method applied to build the alternative scenarios. Note, however, that we are still summarizing part of the information. For example, we are not presenting the details about the hydrology of each flow gauge station associated with each hydropower plant. However, those details are available upon request to the paper authors.

8.2.1 Current System (May 2013)

The EPE's 2015 report files represent most of the current Brazilian interconnected electric system (SIN) as of May 2013, and contain 133 hydroelectric power plants (86 GW) and 99 thermal power plants (20 GW). Other renewables like wind, biomass, and small hydro account for less than 10 GW. Table S1 describes the hydropower plants in operation in May 2013 (initial system) and their major characteristics. Table S1 also includes 10 reservoirs and water structures without power capacity that are part of the system.

Table S1 - Hydropower plants in operation (May, 2013): major characteristics

ID	Name	Number of units	Installed Capacity (MW)	Average production coefficient ($MW/m^3/s$)	Max. Turbined flow (m3/s)	Volume (Hm^3)	Reservoir Area (km^2)	Subsystem
1	Camargos	2	46	0.18	220	792	54	pa
2	Itutinga	4	52	0.24	236	11	2	pa
3	Funil Grande	3	180	0.35	585	304	38	pa
4	Corumba III	2	96	0.36	278	972	65	pa
5	Furnas	8	1312	0.75	1692	22950	1048	pa
6	Masc. Moraes	10	478	0.32	1328	4040	204	pa
7	Estreito Gde	6	1104	0.56	2028	1423	47	pa
8	Jaguara	4	424	0.40	1076	450	34	pa
9	Igarapava	5	210	0.15	1480	480	52	pa
10	Volta Grande	4	380	0.25	1584	2244	202	pa
11	P. Colombia	4	328	0.20	1988	1524	144	pa
12	Caconde	2	80	0.78	94	555	21	pa
13	Euclid Cunha	4	109	0.75	148	14	1	pa
14	A.S.Oliveira	2	32	0.21	178	25	3	pa
15	Marimbondo	8	1488	0.47	2944	6150	305	pa
16	A. Vermelha	6	1396	0.46	2958	11025	526	pa

17	Serra Facao	2	213	0.61	324	5199	157	pa
18	B. Coqueiros	2	90	0.33	278	348	26	pa
19	Emborcacao	4	1192	1.04	1048	17725	319	pa
20	Nova Ponte	3	510	0.94	576	12792	297	pa
21	Miranda	3	408	0.61	675	1120	48	pa
22	Capim Branco 1	3	240	0.50	495	241	31	pa
23	Capim Branco 2	3	210	0.40	537	879	55	pa
24	Corumba IV	2	127	0.61	208	3708	153	pa
25	Corumba I	3	375	0.57	570	1500	44	pa
26	Itumbiara	6	2082	0.65	2940	17027	537	pa
27	Cach Dourada	10	658	0.28	2513	460	69	pa
28	Sao Simao	6	1710	0.61	2670	12540	534	pa
29	Barra Bonita	4	140	0.16	756	3135	231	pa
30	A.Souza Lima	3	144	0.19	771	544	63	pa
31	Ibitinga	3	131	0.19	702	985	115	pa
32	Promissao	3	264	0.20	1293	7408	496	pa
33	N.Avanhandav	3	347	0.26	1431	2720	212	pa
34	Ilha Solt Eq	25	4252	0.38	11604	34432	1803	pa
35	Jupia	14	1551	0.19	8344	3354	327	pa
36	P. Primavera	14	1540	0.17	8904	14400	1915	pa
37	A.A. Laydner	2	101	0.28	364	7008	388	pa
38	Piraju	2	80	0.23	362	84	13	pa
39	Chavantes	4	414	0.64	626	8795	350	pa
40	L. N. Garcez	4	74	0.15	580	45	12	pa
41	Canoas II	3	72	0.13	561	151	24	pa
42	Canoas I	3	83	0.15	567	212	29	pa
43	Cacu	2	65	0.24	280	232	15	pa
44	Capivara	4	618	0.35	1684	10540	454	pa
45	Taquarucu	5	525	0.22	2550	677	75	pa
46	Rosana	4	354	0.19	2468	1918	218	pa
47	Foz R Claro	2	68	0.25	298	95	8	pa
48	Salto	2	116	0.45	260	826	60	pa
49	Slt Verdinho	2	93	0.37	254	264	37	pa
50	Ourinhos	3	44	0.09	486	21	4	pa
51	Espora	3	32	0.39	72	209	25	pa
52	Retiro Baixo	2	84	0.32	262	242	21	se
53	Peixe Angica	3	499	0.24	2073	2741	264	se
54	Sao Salvador	2	243	0.20	1206	952	104	se
55	Billings*	0	0	0.00	0	1133	85	se
56	Henry Borden	14	889	5.65	152	1	1	se
57	Jaguari	2	28	0.48	64	1236	42	se
58	Paraibuna/Pa	2	87	0.67	127	4732	140	se
59	S.Branca Par	2	56	0.33	144	439	19	se
60	Funil	3	222	0.50	387	888	29	se
61	Lajes*	1	0	0.00	99999.9	445	30	se
62	Picada	2	50	1.10	44	7	1	se

63	Sobragi	3	60	0.63	90	1	0	se
64	Ilha Pombos	5	187	0.26	724	8	4	se
65	Nilo Pecanha	6	380	2.63	144	38	1	se
66	Fontes A	1	44	2.53	17	467	1	se
67	P. Passos	2	100	0.31	318	17	1	se
68	Salto Grande	4	102	0.78	132	78	6	se
69	P. Estrela	2	112	0.41	248	89	4	se
70	Baguari	4	140	0.17	872	38	13	se
71	Aimores	3	330	0.24	1296	186	31	se
72	Mascarenhas	4	198	0.18	1216	22	4	se
73	Irape	3	399	1.43	267	5964	100	se
74	Candonga	3	140	0.47	318	54	3	se
75	Tres Marias	6	396	0.40	924	19528	716	se
76	Queimado	3	105	1.58	72	557	34	se
77	Guilman-Amor	4	140	1.02	136	12	1	se
78	Sa Carvalho	4	78	0.94	83	1	0	se
79	Jauru	3	118	0.92	127	17	2	se
80	Guapore	3	120	1.41	84	21	4	se
81	Rosal	2	55	1.69	32	11	1	se
82	Serra da Mesa	3	1275	0.96	1191	54400	1190	se
83	Cana Brava	3	450	0.40	1155	2300	139	se
84	Lajeado	5	903	0.32	3400	4940	626	se
85	Manso	4	210	0.50	400	7337	331	se
86	Ponte Pedra	3	176	2.20	81	199	19	se
87	Sta Clara Mg	3	60	0.46	132	146	8	se
88	Itiquira 1	2	61	0.76	80	5	2	se
89	Itiquira 2	2	97	1.24	78	1	0	se
90	Dardanelos	5	261	0.87	306	0	0	se
91	Guarapiranga*	0	0	0.00	0	190	22	se
92	Calha-Cedae*	1	0	0.00	99999.9	0	0	se
93	Fontes BC	2	88	2.53	34	38	0	se
94	Vigario	1	0	0.00	144	38	0	se
95	Santana	1	89	0.45	190	12	0	se
96	Vertsanta*	1	0	0.00	99999.9	0	0	se
97	Sta. Cecilia	1	31	0.19	160	6	0	se
98	Tocos	1	0	0.00	25	2	0	se
99	Balbina	0	275	0.20	0	20006	2121	ma
100	Rondon 2	3	74	0.53	138	478	60	ar
101	Samuel	5	217	0.24	845	3493	408	ar
102	Sto Antonio	12	835	0.14	6816	2075	271	ar
103	Itaipu	20	14000	1.06	13260	29000	1350	it
104	Estreito Toc	8	1087	0.20	6280	5400	590	ne
105	Curua-Una	3	30	0.15	186	530	49	ne
106	Tucurui	25	8535	0.51	14626	50275	2090	ne
107	Itapebi	3	462	0.72	660	1634	62	no
108	Sobradinho	6	1050	0.22	4278	34116	2786	no

109	Itaparica	6	1480	0.44	3264	10782	717	no
110	Comp Paf-Mox	1	4280	1.02	4199	1226	213	no
111	Xingo	6	3162	1.08	2976	3800	60	no
112	B. Esperanca	4	237	0.36	624	5085	322	no
113	P. Cavalo	2	160	0.91	180	3072	110	no
114	Maua	3	352	1.02	339	2137	75	su
115	Jordao	1	0	0.00	173.5	110	1	su
116	G. B. Munhoz	4	1676	1.09	1376	5779	96	su
117	Segredo	4	1260	1.02	1268	2950	77	su
118	Slt.Santiago	4	1420	0.88	1516	6775	169	su
119	Salto Osorio	6	1078	0.63	1784	1124	56	su
120	Salto Caxias	4	1240	0.59	2100	3573	141	su
121	Sta Clara Pr	2	120	0.79	162	431	15	su
122	Fundao	2	120	0.83	152	35	2	su
123	Barra Grande	3	690	1.35	516	4904	74	su
124	Passo S Joao	2	77	0.26	326	102	21	su
125	Sao Jose	2	51	0.20	288	186	23	su
126	Campos Novos	3	880	1.62	558	1477	31	su
127	Machadinho	3	1140	0.90	1311	3340	71	su
128	Ita	5	1450	0.92	1590	5100	141	su
129	Passo Fundo	2	226	2.22	102	1589	112	su
130	Monjolinho	2	74	0.56	134	150	5	su
131	Quebra Queixo	3	120	1.04	114	137	5	su
132	Castro Alves	3	130	0.75	159	92	4	su
133	Monte Claro	2	130	0.36	372	11	1	su
134	14 De Julho	2	100	0.30	340	55	5	su
135	Foz Chapeco	4	855	0.45	1888	1502	79	su
136	Ernestina*	0	0	0.00	0	259	28	su
137	Passo Real	2	158	0.34	466	3646	152	su
138	Jacui	6	180	0.83	234	29	5	su
139	Itauba	4	500	0.83	620	620	17	su
140	D. Francisca	2	125	0.34	376	330	19	su
141	G. P. Souza	4	260	6.49	40	179	8	su
142	Salto Pilao*	2	192	1.78	110	0	0	su
143	Jordao Fico*	0	0	0.00	0	0	0	su

** Intermediate reservoirs or water systems without power capacity.*
Subsystems: se - Southeast, su - South, no - Northeast, ne - North, pa - Parana, ar - Acre/Roraima, ma - Manaus/Amapa/Boa Vista

The hydropower plants are organized according to the cascade structure. In other words, hydropower plants from the same watershed/water system are arranged from upstream to downstream. Figure S1 shows an example of cascading structure for the São Francisco watershed hydropower plants. The cascade structure is crucial information for hydrothermal electricity system modeling because the reservoirs with storage located upstream have the ability to regulate the water flow for the power plants downstream optimizing the energy production.

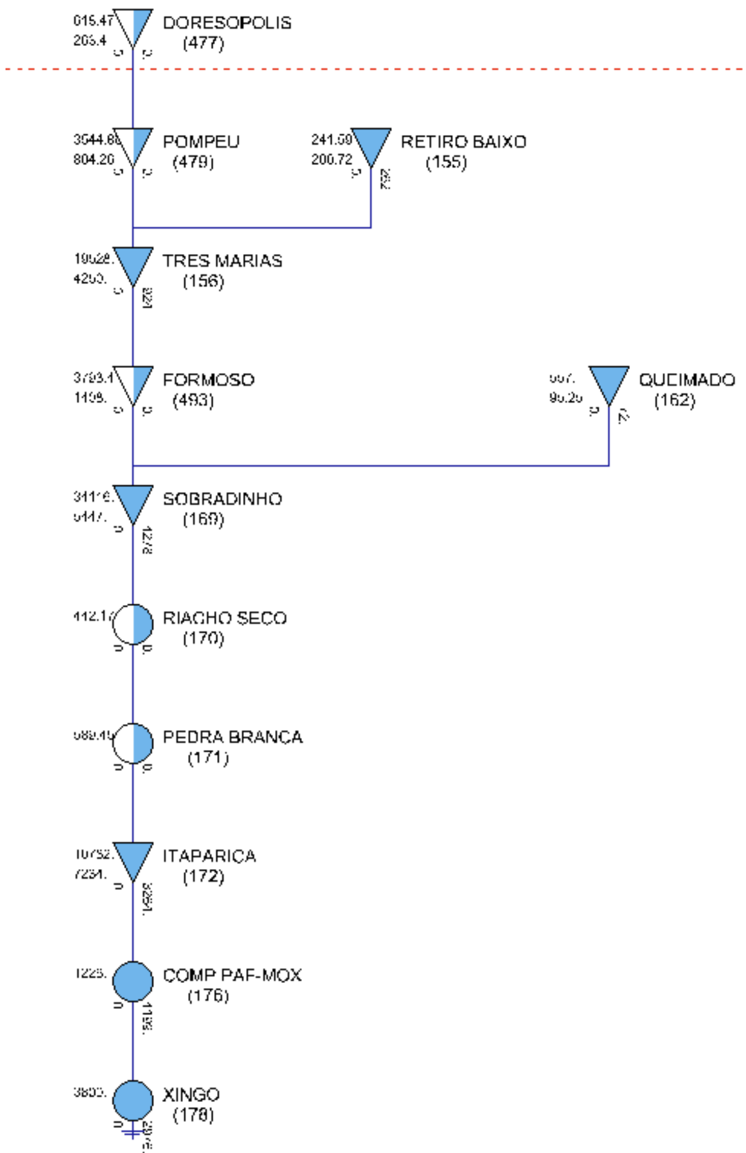

Figure S1 - Hydropower plants cascade structure of the São Francisco river. Circles represent run-of-river hydropower plants and triangles represent hydropower plant with storage capacity. Blue represents existing plants and white/blue represent future plants.

Table S2 describes the main characteristics of the 99 thermal power plants in system in May 2013, including the marginal operational costs and emission factors. The marginal cost of electricity is defined in the EPE's database based on the reports from the generators and it is used to define the dispatch order and thermal operation costs in the optimization.

Table S2 - Thermal plants in operation (May, 2013): major characteristics

ID	Nome	Installed Capacity (MW)	Type	Operational Marginal Costs (Reais/MWh)	Emissions (Mg CO2eq/MWh)	Subsystem
1	Angra 1	640	Nuclear	23	16	se
2	Igarapé	131	Oil	645	840	se
3	St.Cruz 34	400	Oil	310	840	se
4	Carioba	0	Oil	937	840	se
5	R.Silveira	30	Diesel	523	840	se
6	Cuiabá G CC	480	Natural Gas	512	470	se
7	Angra 2	1350	Nuclear	20	16	se
8	Linhares	204	Natural Gas	180	470	se
9	Ute Brasilia	0	Diesel	1047	840	se
10	Maranhão V	338	Natural Gas	111	470	ne
11	P.Médici A	110	Coal	116	1000	su
12	P. Médici B	288	Coal	116	1000	su
13	J.Lacerda C	363	Coal	138	1000	su
14	J.Lacerda B	262	Coal	167	1000	su
15	J.Lacerda A1	100	Coal	222	1000	su
16	J.Lacerda A2	132	Coal	168	1000	su
17	Figueira	17	Coal	373	1000	su
18	Charqueadas	72	Coal	181	1000	su
19	Nutepa	0	Oil	780	840	su
20	S.Jeronimo	18	Coal	248	1000	su
21	W.Arjona G	206	Natural Gas	198	470	se
22	Uruguaiana G	0	Natural Gas	740	470	su
23	Maranhão IV	338	Natural Gas	111	470	ne
24	Fortaleza	320	Natural Gas	111	470	no
25	Termobahia	159	Natural Gas	205	470	no
26	MC2 N Veneci	169	Natural Gas	161	470	ne
27	Termorio	1036	Natural Gas	166	470	se
28	Araucária	485	Natural Gas	696	470	su
29	Viana	175	Oil	617	840	se
30	Pirat.12g_Tc	0	Natural Gas	470	470	se
31	Campina Grande	169	Oil	617	840	no
32	Global 1	149	Oil	694	840	no

33	Juiz De Fora	87	Natural Gas	189	470	se
34	Global 2	149	Oil	694	840	no
35	Maracanau I	163	Oil	599	840	no
36	Termoceara	223	Natural Gas	236	470	no
37	Eletrobolt	386	Natural Gas	219	470	se
38	Ibiritermo	226	Natural Gas	260	470	se
39	Canoas	167	Natural Gas	675	470	su
40	Termonordeste	162	Oil	612	840	no
41	Tres Lagoas	350	Natural Gas	142	470	se
42	Termoparaiba	162	Oil	612	840	no
43	Geramar II	159	Oil	617	840	ne
44	Geramar I	159	Oil	617	840	ne
45	Fafen	137	Natural Gas	259	470	no
46	Vale Do Acu	310	Natural Gas	288	470	no
47	St.Cruz Nova	500	Natural Gas	119	470	se
48	Macae Mer	929	Natural Gas	385	470	se
49	Camacari D	316	Diesel	733	840	no
50	Termope	533	Natural Gas	70	470	no
51	Cubatão	216	Natural Gas	233	470	se
52	Cocal	28	Biomass	168	40	se
53	Pie-Rp	30	Biomass	178	40	se
54	Xavante	54	Diesel	1145	840	se
55	Altos	13	Diesel	725	840	no
56	Novapirat	555	Natural Gas	321	470	se
57	Aracati	11	Diesel	725	840	no
58	Bahia 1	31	Oil	743	840	no
59	Baturite	11	Diesel	725	840	no
60	Campo Maior	13	Diesel	725	840	no
61	Caucaia	15	Diesel	725	840	no
62	Crato	13	Diesel	725	840	no
63	Enguia Pecém	15	Diesel	725	840	no
64	Iguatu	15	Diesel	725	840	no
65	Juazeiro	15	Diesel	725	840	no
66	Marambaia	13	Diesel	725	840	no
67	Nazaria	13	Diesel	725	840	no
68	Maua B4	135	Oil	450	840	ma
69	Petrolina	136	Oil	926	840	no
70	Potiguar	53	Diesel	1022	840	no
71	Termocabo	49	Oil	609	840	no
72	Daia	38	Diesel	790	840	se
73	Goiania 2 BR	136	Diesel	859	840	se
74	Candiota 3	350	Coal	60	1000	su
75	Termomanaus	143	Diesel	1133	8840	no
76	Pau Ferro I	94	Diesel	1133	840	no
77	Potiguar III	55	Diesel	1022	840	no
78	P. Pecem 2	365	Coal	123	1000	no

79	Camacari MI	152	Oil	844	840	no
80	Camacari PI	150	Oil	844	840	no
81	P. Pecem 1	720	Coal	115	1000	no
82	Cisframa	4	Biomass	216	40	su
83	Suape Ii	381	Oil	629	840	no
84	Norteflu-1	400	Natural Gas	38	470	se
85	Norteflu-2	100	Natural Gas	59	470	se
86	Norteflu-3	200	Natural Gas	103	470	se
87	Norteflu-4	72	Natural Gas	287	470	se
88	Porto Itaqui	360	Coal	118	1000	ne
89	Palmeira Goi	140	Diesel	777	840	se
90	Do Atlântico	456	Natural Gas	134	470	se
91	T.Norte 2	340	Oil	551	840	ar
92	Ute Sol*	197	Natural Gas	0	470	se
93	Aparecida	166	Natural Gas	302	470	ma
94	Pie C Rocha	85	Natural Gas	0	470	ma
95	Pie Jaraqui *	66	Natural Gas	0	470	ma
96	Pie Manauara*	67	Natural Gas	0	470	ma
97	Maua B3	110	Natural Gas	412	470	ma
98	Pie P Negra *	66	Natural Gas	0	470	ma
99	Pie Tambaqui*	66	Natural Gas	0	470	ma

Subsystems: se - Southeast, su - South, no - Northeast, ne - North, pa - Parana, ar - Acre/Roraima, ma - Manaus/Amapa/Boa Vista.*Note that some projects have zero operation marginal costs because of special contract characteristics from those plants.

In the EPE model, hydro and thermal power plants are modelled individually. However, other renewables such as wind, small hydropower plants, and biomass are modelled as a group in each subsystem. Figure S2 projects the average renewable generation output by subsystem according to the EPE's report files. Thus, the renewable generation in May 2013 is represented by the output defined in the first month of Figure S2. Figure S2 also presents the renewable generation projection to 2028. The different renewable sources explain the distinct generation output profile over time in Figure S2. For instance, most of the renewable generation in the Southeast is from sugar cane bagasse so the harvest seasons explain the generation peaks and valleys. Similarly, wind generation occurs mainly in the South and Northeast subsystems, which have larger variability in output associated with seasonal wind speed profiles. The North, Acre-

Rondônia, and Tapajos-Teles Pires subsystems include some small hydropower plants but there is limited capacity expansion in these subsystems by 2028 in the baseline scenario.

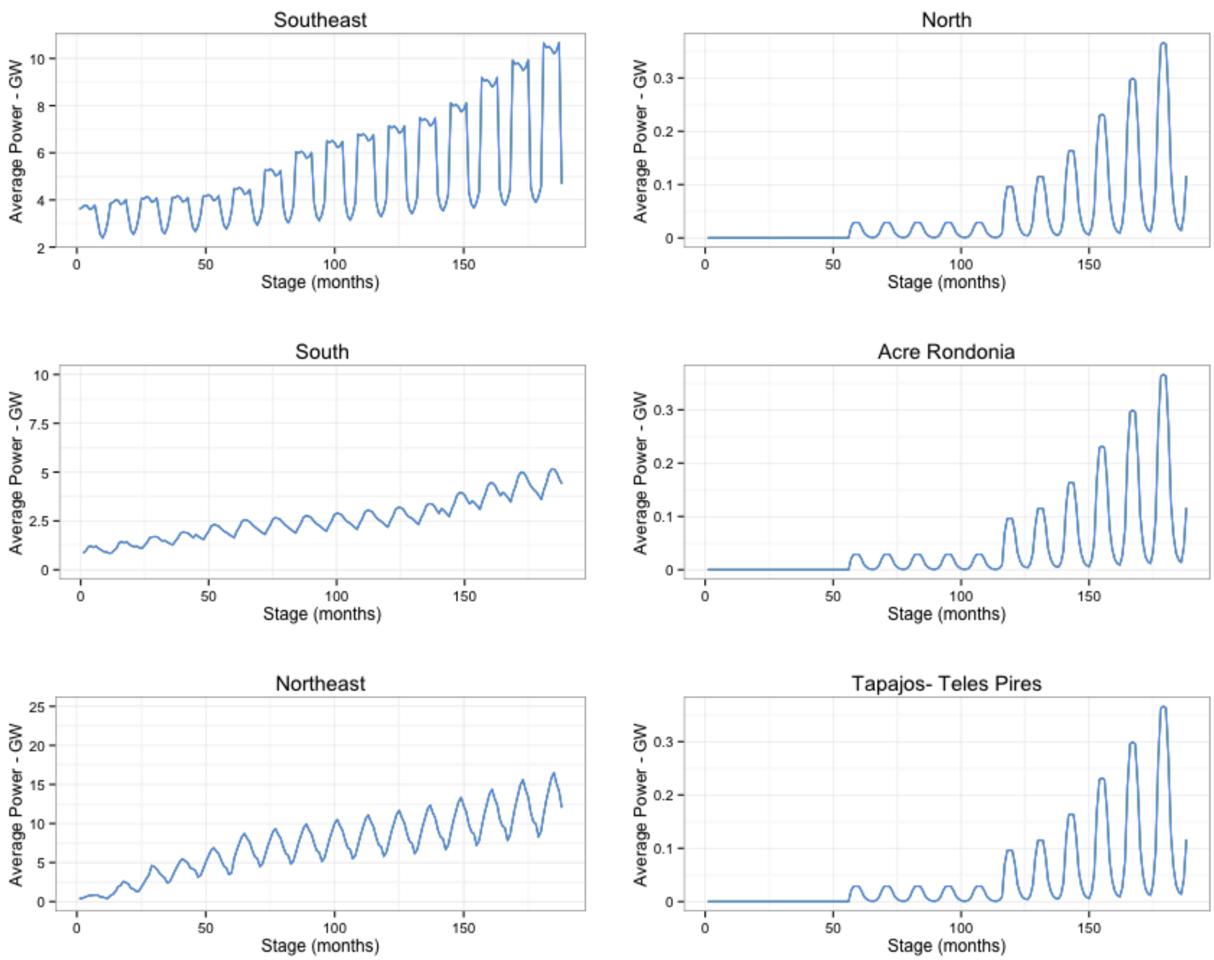

Figure S2 - Small renewables (Wind, small hydro, and biomass) expansion in the baseline scenario. Projected average output per month.

We improved EPE's modelling features for wind generation by replacing the fixed monthly output defined in the Northeast and South subsystem (Figure S2) by wind generation series created using wind speed data from the National Centers for Environmental Prediction (NCEP) Climate Forecast System Reanalysis (CFSR) (Saha et al. 2016) for the current and future wind parks.

Table S3 presents the major characteristics from wind parks in operation in December 2014. Although the system simulation starts in May 2013, we represented the system from May 2013 to December 2014 in the baseline using the parks defined in Table S3. We applied this simplification because we were not able to rebuild the schedule of the wind parks that enter in operation from May 2013 to December 2014. Therefore, the wind parks in operation in December of 2014 represent the system in the first 17 months of operation and no additional wind is included during this period for the baseline. We simulated wind parks listed in Table S3 using NCEP-CSFR wind speeds and creating 32 years of hourly generation series for each plant. We aggregate the results by subsystem and demand block to create the inputs to SDDP.

Table S3 - Wind parks in operation (2014): major characteristics

ID	Name	Installed Capacity (MW)	Longitude	Latitude	Number of generators	State	Subsystem
1	Agua Doce	9	-51.70	-26.59	15	SC	su
2	indios	50	-50.29	-30.00	25	RS	su
3	Albatroz	5	-34.97	-6.55	6	PB	no
4	Alegria I	51	-36.38	-5.11	31	RN	no
5	Alegria II	101	-36.41	-5.11	61	RN	no
6	Alhandra	6	-34.94	-7.27	3	PB	no
7	Alvorada	8	-42.59	-14.19	5	BA	no
8	Amparo	23	-51.61	-26.60	15	SC	su
9	Aquibata	30	-51.72	-26.61	20	SC	su
10	Aratua I	14	-36.34	-5.09	9	RN	no
11	Areia Branca	27	-36.90	-4.98	13	RN	no
12	Asa Branca IV	32	-35.98	-5.34	20	RN	no
13	Asa Branca V	32	-36.01	-5.39	20	RN	no
14	Asa Branca VI	32	-36.00	-5.36	20	RN	no
15	Asa Branca VII	32	-35.95	-5.26	20	RN	no
16	Asa Branca VIII	32	-35.98	-5.29	20	RN	no
17	Atlantica	5	-34.97	-6.55	6	PB	no
18	Atlantica I	30	-50.33	-30.32	10	RS	su
19	Atlantica II	30	-50.34	-30.33	10	RS	su
20	Atlantica IV	30	-50.33	-30.30	10	RS	su
21	Atlantica V	30	-50.31	-30.30	10	RS	su
22	Barra dos Coqueiros	35	-36.93	-10.81	23	SE	no
23	Beberibe	26	-38.08	-4.19	32	CE	no

24	Boca do Corrego	24	-39.66	-3.10	9	CE	no
25	Bom Jardim	31	-49.57	-28.44	21	SC	su
26	Bons Ventos	37	-37.76	-4.45	18	CE	no
27	Buriti	30	-39.98	-2.89	20	CE	no
28	Cabeτo Preto	20	-35.95	-5.43	11	RN	no
29	Cabeτo Preto IV	20	-35.97	-5.46	11	RN	no
30	Caetite 2	30	-42.50	-14.19	15	BA	no
31	Caetite 3	30	-42.51	-14.22	15	BA	no
32	Cajucoco	30	-39.96	-2.93	20	CE	no
33	Caminho da Praia	2	-35.01	-8.33	1	PE	no
34	Campo Belo	11	-51.75	-26.62	7	SC	su
35	Camurim	5	-34.97	-6.56	6	PB	no
36	Candiba	10	-42.62	-14.18	6	BA	no
37	Canoa Quebrada	57	-37.75	-4.48	28	CE	no
38	Caravela	5	-34.97	-6.56	6	PB	no
39	Carcara II	30	-37.00	-4.96	10	RN	no
40	Cascata	6	-51.73	-26.60	4	SC	su
41	Cerro Chato I	30	-55.73	-30.83	15	RS	no
42	Cerro Chato II	30	-55.70	-30.85	15	RS	no
43	Cerro Chato III	30	-55.71	-30.81	15	RS	su
44	Coelhos I	5	-34.97	-6.58	6	PB	no
45	Coelhos II	5	-34.97	-6.57	6	PB	no
46	Coelhos III	5	-34.98	-6.58	6	PB	no
47	Coelhos IV	5	-34.98	-6.59	6	PB	no
48	Col⌈nia	19	-38.88	-3.53	9	CE	no
49	Cruz Alta	30	-51.74	-26.63	20	SC	su
50	Da Prata	22	-42.64	-13.95	13	BA	no
51	de Palmas	3	-51.70	-26.58	5	PR	no
52	Delta do Parnaiba	30	-41.72	-2.83	15	PI	no
53	Dos Araτas	32	-42.55	-14.12	19	BA	no
54	Dunas de Paracuru	42	-38.99	-3.43	21	CE	no
55	Elebras Cidreira 1	70	-50.18	-30.07	31	RS	su
56	Enacel	32	-37.76	-4.51	15	CE	no
57	Eurus VI	8	-35.93	-5.23	4	RN	no
58	Fazenda Rosario	8	-50.39	-30.44	4	RS	no
59	Fazenda Rosario 2	20	-50.41	-30.45	10	RS	su
60	Fazenda Rosario 3	14	-50.42	-30.45	7	RS	su
61	Faisa I	29	-39.27	-3.32	14	CE	no
62	Faisa III	25	-39.27	-3.34	12	CE	no
63	Faisa IV	25	-39.26	-3.32	12	CE	no
64	Foz do Rio Choro	25	-38.15	-4.12	12	CE	no
65	Gargau	20	-41.08	-21.57	12	RJ	no
66	Gravata Fruitrade	5	-35.60	-8.27	3	PE	no
67	Guanambi	21	-42.62	-14.21	13	BA	no
68	Guirapa	29	-42.64	-14.22	18	BA	no

69	Icaraizinho	55	-39.67	-3.02	26	CE	no
70	Icarai	17	-39.63	-3.03	8	CE	no
71	Icarai I	27	-39.59	-3.08	13	CE	no
72	Icarai II	38	-39.60	-3.09	18	CE	no
73	Igapora	30	-42.66	-13.87	19	BA	no
74	Juremas	16	-35.85	-5.38	7	RN	no
75	Lagoa do Mato	3	-37.64	-4.59	2	CE	no
76	Licinio de Almeida	24	-42.65	-14.18	15	BA	no
77	Macaubas	35	-42.34	-12.34	21	BA	no
78	Mandacaru	5	-35.60	-8.28	3	PE	no
79	Mangue Seco 1	26	-36.31	-5.19	13	RN	no
80	Mangue Seco 2	26	-36.32	-5.16	13	RN	no
81	Mangue Seco 3	26	-36.35	-5.18	13	RN	no
82	Mangue Seco 5	26	-36.40	-5.15	13	RN	no
83	Mar e Terra	23	-36.92	-4.97	11	RN	no
84	Mataraca	5	-34.98	-6.58	6	PB	no
85	Mel 02	20	-36.97	-4.94	10	RN	no
86	Miassaba 3	68	-36.49	-5.14	41	RN	no
87	Miassaba II	14	-36.41	-5.08	9	RN	no
88	Millennium	10	-34.97	-6.50	13	PB	no
89	Morro dos Ventos I	29	-35.82	-5.36	18	RN	no
90	Morro dos Ventos III	29	-35.87	-5.39	18	RN	no
91	Morro dos Ventos IV	29	-35.88	-5.38	18	RN	no
92	Morro dos Ventos IX	30	-35.93	-5.31	19	RN	no
93	Morro dos Ventos VI	29	-35.88	-5.35	18	RN	no
94	Morrao	30	-42.68	-14.09	18	BA	no
95	Nossa Senhora da Conceiτao	29	-42.68	-13.90	18	BA	no
96	Novo Horizonte	30	-42.36	-12.31	18	BA	no
97	Osorio	50	-50.29	-29.97	25	RS	su
98	Pulpito	30	-49.61	-28.47	20	SC	su
99	Pajeu do Vento	26	-42.64	-14.01	16	BA	no
100	Paracuru	25	-38.96	-3.44	12	CE	no
101	Pedra Branca	30	-41.10	-9.88	12	BA	no
102	Pedra do Reino	30	-40.89	-9.52	10	BA	no
103	Pedra do Reino III	18	-40.88	-9.50	6	BA	no
104	Pedra do Sal	18	-41.71	-2.83	20	PI	no
105	Pindai	24	-42.66	-14.20	15	BA	no
106	Piraua	5	-35.49	-7.49	3	PE	no
107	Planaltina	27	-42.64	-13.98	17	BA	no
108	Porto das Barcas	20	-41.76	-2.83	10	PI	no
109	Porto Salgado	20	-41.73	-2.83	10	PI	no
110	Porto Seguro	6	-42.67	-13.87	4	BA	no
111	Praia do Morgado	20	-40.27	-2.81	13	CE	no
112	Praia Formosa	101	-41.04	-2.91	48	CE	no
113	Praias de Parajuru	29	-37.90	-4.36	19	CE	no
114	Prainha	10	-38.38	-3.87	20	CE	no

115	Presidente	5	-34.98	-6.58	6	PB	no
116	Quixaba	26	-37.69	-4.57	17	CE	no
117	Rei dos Ventos 1	58	-36.19	-5.10	35	RN	no
118	Rei dos Ventos 3	60	-36.17	-5.12	36	RN	no
119	Rio do Ouro	30	-49.61	-28.45	20	SC	su
120	Rio Verde	30	-42.60	-14.17	19	BA	no
121	RN 15 - Rio do Fogo	49	-35.38	-5.33	62	RN	no
122	Salto	30	-51.78	-26.60	20	SC	su
123	Sangradouro	50	-50.30	-29.93	25	RS	su
124	Sangradouro 2	26	-50.28	-29.93	13	RS	su
125	Sangradouro 3	24	-50.31	-29.95	12	RS	no
126	Santa Clara I	30	-35.90	-5.25	15	RN	no
127	Santa Clara II	30	-35.91	-5.26	15	RN	no
128	Santa Clara III	30	-35.91	-5.27	15	RN	no
129	Santa Clara IV	30	-35.91	-5.24	15	RN	no
130	Santa Clara VI	30	-35.92	-5.24	15	RN	no
131	Santa Maria	5	-35.59	-8.29	3	PE	no
132	Santo Ant⌠nio	3	-49.60	-28.45	2	SC	su
133	Seabra	31	-42.37	-12.27	18	BA	no
134	Seraima	30	-42.71	-14.13	18	BA	no
135	Serra do Salto	19	-42.64	-14.16	12	BA	no
136	Sete Gamelerias	30	-41.10	-9.86	15	BA	no
137	Sao Pedro do Lago	30	-41.10	-9.87	13	BA	no
138	Tanque	30	-42.61	-14.09	18	BA	no
139	Taiba	5	-38.94	-3.50	10	CE	no
140	Taiba Aguia	23	-38.89	-3.53	11	CE	no
141	Taiba Albatroz	17	-38.92	-3.51	8	CE	no
142	Taiba Andorinha	15	-38.90	-3.52	7	CE	no
143	Uniao dos Ventos 1	22	-35.84	-5.08	14	RN	no
144	Uniao dos Ventos 2	22	-35.82	-5.08	14	RN	no
145	Uniao dos Ventos 3	22	-35.81	-5.08	14	RN	no
146	Uniao dos Ventos 4	11	-35.80	-5.09	7	RN	no
147	Uniao dos Ventos 5	24	-35.78	-5.09	15	RN	no
148	Uniao dos Ventos 6	13	-35.77	-5.10	8	RN	no
149	Uniao dos Ventos 7	14	-35.75	-5.10	9	RN	no
150	Uniao dos Ventos 8	14	-35.89	-5.07	9	RN	no
151	Uniao dos Ventos 9	11	-35.89	-5.09	7	RN	no
152	Ventos do Nordeste	22	-42.61	-14.11	13	BA	no
153	Vitoria	5	-35.01	-6.57	3	PB	no
154	Volta do Rio	29	-39.97	-2.86	19	CE	no
155	Xavante	5	-35.40	-8.18	3	PE	no

Subsystems:, su - South, no - Northeast

8.2.2 Expansion scenarios

Table 4-3 in the Chapter 4 summarizes the additional power capacity in relation to the system in May 2013 for the baseline and alternative scenarios. The details about the baseline schedule for each hydroelectric and thermal power plant are described in the Annex C1. In the case of the future wind parks, they are represented by groups of 25 dummy parks with 30 MW of installed capacity each. Thus, each group contains 750 MW of installed capacity. To obtain the number of groups included per year, divide the power capacity per year described in Table 4-3 (Chapter 4) by 750. For instance, in 2028, the baseline scenario includes 2250 MW of additional wind capacity, divided in three groups of 750 MW. We defined the wind groups schedule by including one group per month in a given year. For example, if four groups are projected for the 2015 baseline agenda, the schedule will go from January to April (750 MW per month).

We created a total of 109 different wind groups to model the wind capacity in the baseline and alternative scenarios. The location of each power plant (with 30 MW) from this group was selected using a lottery with replacement based on the location sample of 1065 future wind parks. Figure S3 defines the location of the sample of 1065 wind parks. Furthermore, each group of 750 MW is subdivided in two subsystems: South and Northeast.

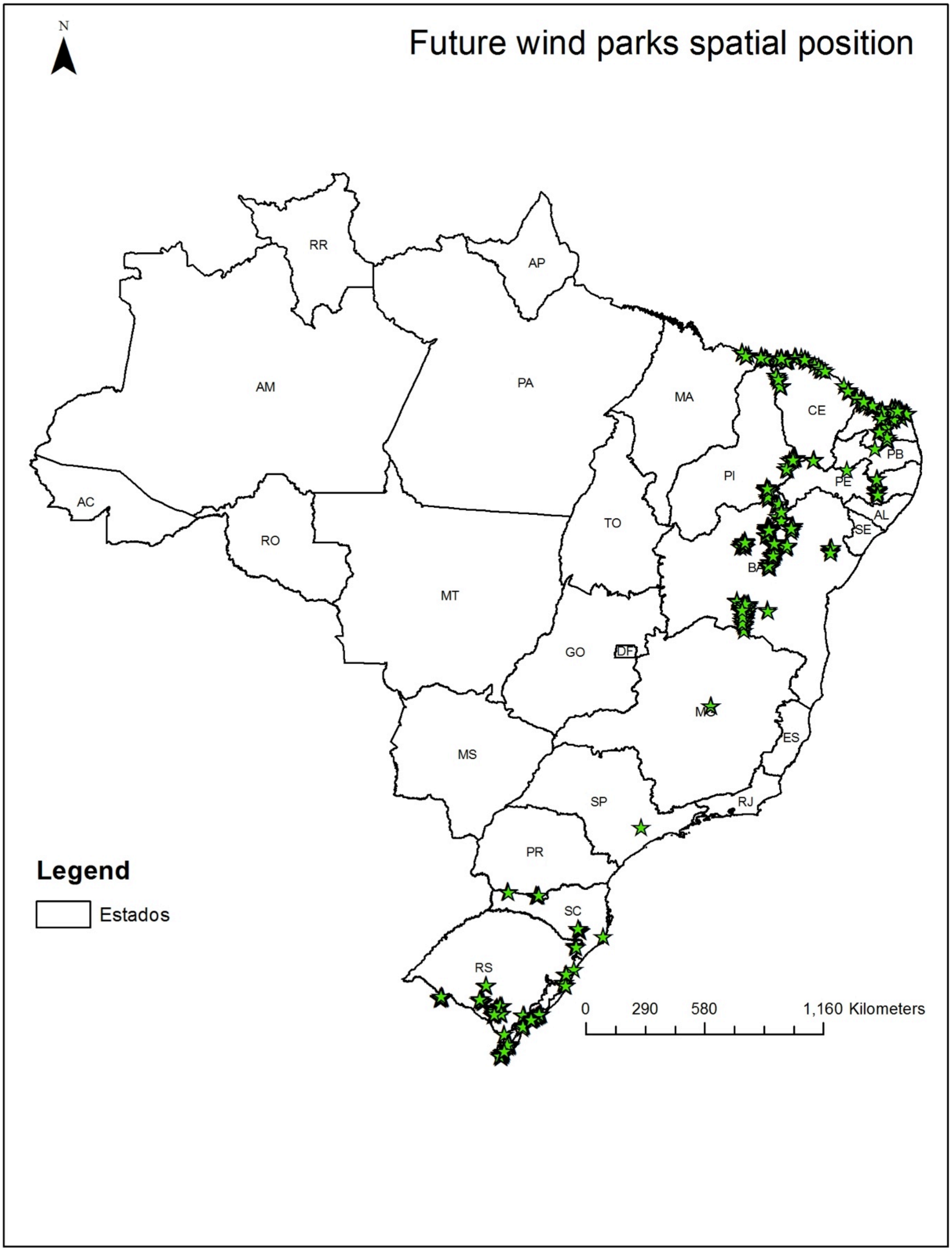

Figure S3 - Spatial distribution of wind parks under initial stages of development

8.3 Hydrothermal scheduling and SDDP characteristics

The objective of hydrothermal scheduling is to determine the sequence of hydroelectric dispatch, which minimizes the expected thermal operation cost (given by fuel cost plus penalties for rationing) along the planning horizon (PSR 2014) . A decision tree described in Figure S4 illustrates the stochastic hydrothermal scheduling problem. Figure S4 shows that the system operator has two options: use hydro today or save water in the storage hydroelectric reservoirs. The top branch indicates that if hydroelectricity is used today and future inflows are high, the system operation is efficient because reservoir storage can be recovered. In contrast, if a drought occurs in the future, it may be necessary to dispatch more expensive thermal generation, or even interrupt load supply. The bottom branch implies that if storage levels are kept high through a more intensive use of thermal generation today, and high inflows occur in the future, reservoirs may spill, wasting energy and resulting in higher operation costs. Lastly, if a dry period occurs in the bototm branch, the storage will displace expensive thermal or avoid rationing in the future (PSR 2014).

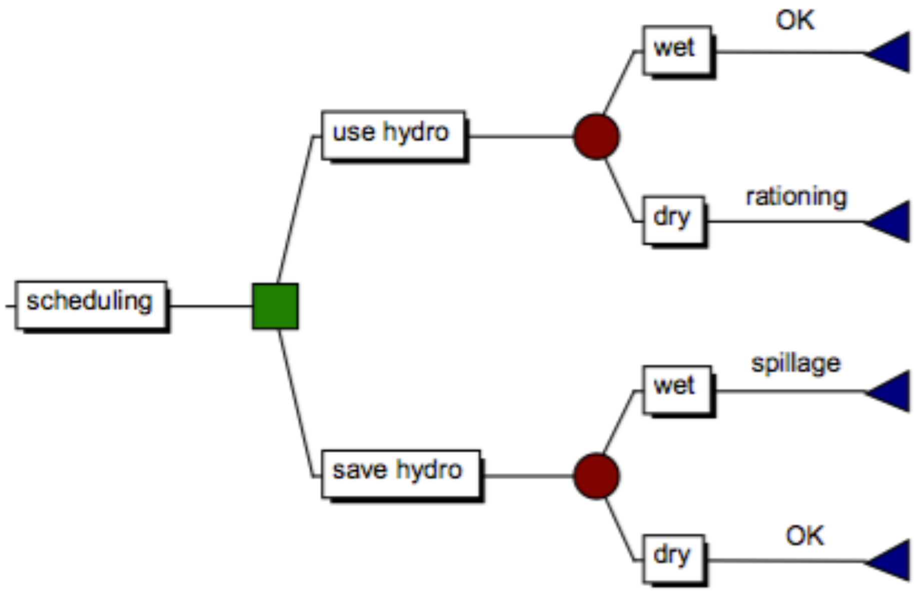

Figure S4 - Stochastic hydrothermal scheduling problem (Source: (PSR 2014))

Linear programming (LP) algorithms could, in principle, solve the system optimization problem described in Figure S2(PSR 2014). However, the actual scheduling problem involves several hydro plants and, like our case, a study horizon of several years. Due to the exponential increase of inflow branches with time and number of plants, the resulting stochastic optimization problem quickly becomes computationally infeasible ("curse of dimensionality") (Pereira & Pinto 1991).

We used the multi-stage stochastic optimization tool applied to energy planning called SDDP (stochastic dual dynamic programming) to support the analysis of the expansion plans (Pereira & Pinto 1991; PSR 2014). SDDP is also the name of the algorithm behind the software (Pereira & Pinto 1991). Power Systems Research (PSR), a Brazilian company, developed the optimization tool, and provided it for this study. SDDP simulates the future behavior of the system under several hydrological scenarios and calculates a policy that minimizes a risk-adjusted cost-based objective function (Pereira & Pinto 1991; Gorenstin et al. 2004; PSR 2014). The solution algorithm decomposes the multi-stage stochastic problem into several one-stage sub problems. Each sub problem corresponds to a linearized optimal power flow with additional constraints representing the hydro reservoir equations and a piecewise linear approximation of the expected future cost function (Pereira & Pinto 1991; Gorenstin et al. 2004; PSR 2014). Each sub problem is solved by a customized network flow/Dual Simplex algorithm (Gorenstin et al. 2004).

Figure S5 illustrates the one-stage optimization problem. The basic idea behind the optimization is to minimize the immediate cost (ICF) and the future cost (FCF) subject to the operating constraints through the study horizon. The ICF decreases as more hydroelectricity is used today (stage *t*), which means that more water is passing through the turbines and less water is available in the storage reservoirs. On the other hand, FCF increases as more hydropower is dispatched and less water will be stored to supply the future demand leading to the use of more expensive thermal generation in the future. The FCF reflects the expected thermal generation expenses from stage *t+1* to the end of the study horizon (PSR 2014).

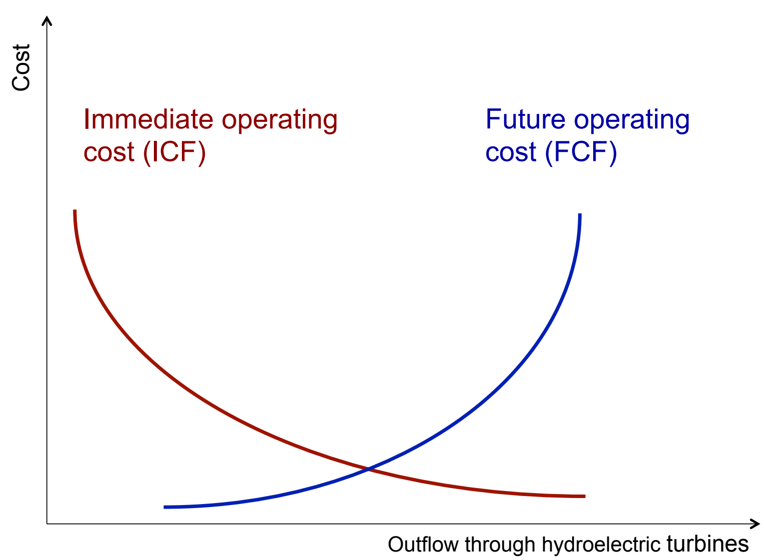

Figure S5 - Immediate and future cost functions versus outflow through hydroelectric turbines. The higher the outflow, the lower is the amount of water stored within hydroelectric reservoirs (Source: adapted from (PSR 2014)).

Formally, Equation S1 defines the objective function.

$$Min\ ICF + FCF \qquad \text{(S1)}$$

The FCI is given by the sum of the thermal costs c(j) x g_{tk}, in stage *t*, plus penalties for operating constraint violations (PSR 2014). Equation S2 defines the immediate cost function

$$ICF = \sum_{K=1}^{K} \sum_{j=1}^{J} c(j) \times g_{tk}(j) + c_{\delta} \times \delta_{gt} \qquad \text{(S2)}$$

where

k: indexes load block in the stage

K: number of load blocks

j: indexes thermal plants

J: number of thermal plants

$c(j)$: operating cost of plant j

$g_{tk}(j)$: energy production of plant j in stage t, block k

$c_{\delta:}$ generic representation of operating constraint violation cost

$\delta_{gt:}$ violation amount in stage t violation u

The solution of the FCF approximation is the main advance from the SDDP algorithm (Pereira & Pinto 1991). The future cost function, which depends on storage levels and past stream flows (Equation S3), is represented as a set of linear constraints, each one representing a segment of the piecewise linear function(PSR 2014).

$$FCF = \alpha_{t+1}(\upsilon_{t+1}, \alpha_t) \quad \text{(S3)}$$

where

$\upsilon_{(t+1)}$: final storage vector in stage t

α_t: lateral inflow vector in stage t

The SDDP solution of the FCF is essentially composed of two phases: backward and forward. The backwards pass derives its name from the fact that during its execution, the algorithm solves one-stage problems in reverse chronological order. The solution of a problem at stage *t* is used to generate a cut, i.e., a supporting hyper plane, providing an approximation to future costs associated with decisions taken at stage *t+1*(Rebennack, Flach & Pereira 2012; PSR 2014). Once the algorithm has progressed to the first stage, the forward phase performs a Monte Carlo simulation by solving one-stage problems taking into account the previously calculated cuts. The solution of the backward phase results in a lower bound of the future cost function. In contrast, the sum of the costs along the horizon given by the problems solved during the forward simulation results in an upper bound estimate (Rebennack, Flach & Pereira 2012; PSR 2014). All the details about SDDP algorithm are presented in the SDDP method manual (PSR 2014)

The optimization also takes into account all system constraints, such as water balance (inflows and outflows from each reservoirs), storage limits, loads (electricity demand), minimum and maximum outflow restrictions (e.g. for navigation or environmental purposes) and the thermal generation limits (PSR 2014). We follow the system constraints defined by in the EPE's 2015 report files. The use of optimization tools, like SDDP, is a key factor to represent, study and plan any electric system with hydropower reservoirs.

8.4 Using reanalysis data to create wind electricity output scenarios

The EPE modeling approach defines wind generation as "must-run" power plants that follow an electricity output projection that represent the average wind seasonal variability (South and Northeast subsystems in Figure S2). The wind park representation adopted by EPE to characterize the wind electricity output in the 2023 expansion plan is very basic, and a key model limitation because it disregards the stochastic features of wind, as well as daily variability. To overcome this limitation, we created wind generation series for current and future wind parks.

The SDDP interface allows the incorporation of renewables variability in the optimal dispatch optimization through the inclusion historical records or data produced by an external model ("renewables scenarios"). SDDP assumes that the energy production in renewable plants is variable, but independent from one stage to the next. In other words, there is zero serial correlation. Before the iterative process of operating policy calculation starts, SDDP determines the scenarios to be used as follows: for each stage *t* and for each conditioned inflow ("opening" in the backward recursion), a renewable energy production scenario is randomly sampled from the renewable scenarios. Those scenarios are then used in the backward phase. The forward simulation phase use the same scenarios sampled in the backward phase. If the number of forward series is higher than the number of openings, a "carrousel" scheme is applied(PSR 2014).

We created wind generation series using wind speed data from the National Centers for Environmental Prediction (NCEP) Climate Forecast System Reanalysis (CFSR) (Saha et al. 2016) for the current and future wind parks. CFSR is an atmospheric reanalysis product available at an hourly time resolution from 1979 to the present and a horizontal resolution of 0.5° latitude

× 0.5° longitude. Several studies assessed the characteristics, uncertainty and biases of using reanalysis CSFR to wind-power simulation but they are restricted to the United States(Rose & Apt 2015; 2016), Portugal (Carvalho, Rocha, Gómez-Gesteira & Santos 2014b), United Kingdom (Sharp et al. 2015), off-shore of the Iberian Peninsula Coast (Carvalho, Rocha, Gómez-Gesteira & Santos 2014a), and the Tibetan Plateau(Bao & Zhang 2013). Table S5 summarizes the main characteristics of those studies and their main findings.

Table S4 - References about the use of wind speed NCEP-CSFR reanalysis

Study	Studied region	Study characteristics	Major results related to CSFR
Rose and Apt, 2015	United States Great Plains	The authors developed a model that quantifies the uncertainties across many sites and corrects for biases of the reanalysis data. They applied this model to 32 years of reanalysis data for 1002 plausible wind-plant sites to estimate variability of wind energy generation and the smoothing effect of aggregating distant wind plants	The authors find that coefficient of variation (COV) of annual energy generation of individual wind plants in the Great Plains is 5-12%, but the COV of all those plants aggregated together is 3.0%.
Rose and Apt, 2016	United States Great Plains	The authors develop a model of the bias and uncertainty of CFS reanalysis wind speeds.	The authors found that the CFS reanalysis data underestimate wind speeds at high elevations, at high measurement heights, and in unstable atmospheric conditions. For example, at a site with an elevation of 500 m and hub height of 80 m, a CFS reanalysis wind speed of 8 m/ s is 0.2 m/s higher to 1.3 m/s lower than the measured wind speed
Carvalho et. al, 2014	Portugal	The authors compared wind simulation and wind energy production using several reanalysis dataset (including the NCEP-CSFR) and compared with observed data.	The comparison between NCEP-CSFR wind speeds and empirical data indicates root mean squared error of 2.19 m/s and correlation coefficient of 0.78.
Carvalho et. al, 2014	Iberian Peninsula coast	The authors compared off-shore wind simulation using several reanalysis datasets (including the NCEP-CSFR) and compared with buoy observed data.	The comparison between NCEP-CSFR wind speeds and empirical data indicates root mean squared error of 1.85 m/s and correlation coefficient of 0.86.
Sharp et al.,2015	United Kingdom	The authors evaluated the NCEP CFSR reanalysis model for hourly wind speeds by comparing the data against 264 onshore and 12 offshore weather	The comparison between NCEP-CSFR wind speeds and empirical data indicates a root mean squared error that vary from 1 to 8 m/s depending on the measuring station but most of the results fall between 1 and 4m/s. The correlation coefficient varies from 0.57 to

		stations, over a period of 30 years.	0.92, but most of the results fall 0.75 and 0.85.
Bao et al., 2014	Tibetan Plateau	The authors compared NCEP-CSFR reanalysis wind speed data against data from 11 stations	The mean biases of U and V wind components for each dataset are small and mostly within 1 m/s throughout the vertical column. CFSR root mean square error actually results in 21% at 500 hPa and 32% at 200 and 150 hPa). The correlation coefficient between each reanalysis and the sounding observations for both U and V wind components is generally high at upper levels but drops to no higher than 0.70 at 500 hPa for all reanalyzes

Table S4 indicates that NCEP-CSFR reanalysis wind data quality have been discussed in several studies, however, we did not find any reference that focused on Brazil or South America. Although the main objective of this is study is not to assess the quality of using NCEP-CSFR reanalysis wind data in Brazil, we obtained wind generation data from 31 wind parks in Brazil, and we compared the real generation output from those wind parks against wind generation simulated using NCEP-CSFR wind speeds.

8.4.1 Simulating wind electricity output using NCEP-CSFR wind speeds

We obtained wind generation data from 31 wind parks owned by *CPFL Renováveis*, a company that develops and operates a renewable portfolio in Brazil. The data corresponds to hourly generation outputs from October 2014 to October 2015. We used the CPFL data to evaluate the application of NCEP-CSFR wind speeds as inputs to wind generation model (wind power function). Table S5 describes the main characteristics of CPFL wind parks.

Table S5 - Major characteristics of the CPFL wind parks

Nome	Longitude (W)	Latitude (S)	Installed Capacity (MW)	Rotor diameter (m)	Generators Capacity (MW)	Number of generators	Subsystem
Atlântica I	50°18'57"	30°19'08"	30	116	3.0	10	South
Atlântica II	50°19'24"	30°19'36"	30	116	3.0	10	South
Atlântica IV	50°20'06"	30°17'31"	30	116	3.0	10	South
Atlântica V	50°18'18"	30°17'30"	30	116	3.0	10	South
Bons Ventos	37°45'34"	04°26'49"	50.0	88	2.1	24	Northeast
Canoa Quebrada	37°45'28"	04°28'01"	57.0	88	2.0	28	Northeast
Canoa Quebrada RDV	37°41'43"	04°32'09"	10.5	82.5	1.5	7	Northeast
Costa Branca	35°51'09"	05°25'17"	20.7	101	2.3	5	Northeast
Costa Branca	35°51'09"	05°25'18"	20.7	101	2.3	4	Northeast
Enacel	37°45'39"	04°30'35"	31.5	88	2.1	15	Northeast
Eurus I	35°51'29"	05°22'07"	30.0	82.5	1.5	20	Northeast
Eurus III	35°52'34"	05°24'14"	30.0	82.5	1.5	20	Northeast
Foz do Rio Choró	38°09'01"	04°07'32"	25.2	88	2.1	12	Northeast
Icaraizinho	39°40'26"	03°01'04"	54.6	88	2.1	26	Northeast
Juremas	35°50'47"	05°23'23"	16.1	82	2.3	3	Northeast
Juremas	35°50'47"	05°23'23"	16.1	82	2.3	4	Northeast
Macacos	35°50'54"	05°24'43"	20.7	101	2.3	4	Northeast
Macacos	35°50'54"	05°24'43"	20.7	101	2.3	4	Northeast
Morro dos Ventos I	35°49'08"	05°21'46"	28.8	82	1.6	18	Northeast
Morro dos Ventos III	35°52'06"	05°22'28"	28.8	82	1.6	18	Northeast
Morro dos Ventos IV	35°52'42"	05°20'37"	28.8	82	1.6	18	Northeast
Morro dos Ventos IX	35°54'47"	05°18'19"	30.0	82	1.6	19	Northeast
Morro dos Ventos VI	35°52'51"	05°22'55"	28.8	82	1.6	18	Northeast
Paracuru	38°57'43"	03°25'53"	25.2	88	2.1	12	Northeast
Pedra Preta - A	35°51'12"	05°25'37"	20.7	101	2.3	6	Northeast
Pedra Preta - B	35°51'12"	05°25'37"	20.7	101	2.3	4	Northeast
Santa Clara I - A	35°53'55"	05°14'35"	30.0	89.5	2.0	6	Northeast
Santa Clara I -B	35°53'55"	05°14'35"	30.0	89.5	2.0	7	Northeast
Santa Clara II - A	35°54'38"	05°16'03"	16.0	82	2.0	6	Northeast
Santa Clara II - B	35°54'38"	05°16'03"	14.0	82	2.0	7	Northeast
Santa Clara III - A	35°54'12"	05°16'08"	16.0	89	2.0	8	Northeast
Santa Clara III - B	35°54'12"	05°16'08"	14.0	89	2.0	7	Northeast
Santa Clara V - A	35°55'18"	05°15'35"	16.0	89.5	2.0	8	Northeast
Santa Clara V - B	35°55'18"	05°15'35"	14.0	89.5	2.0	7	Northeast
Santa Clara VI - A	35°55'37"	05°14'25"	16.0	89.5	2.0	8	Northeast
Santa Clara VI - B	35°55'37"	05°14'25"	14.0	89.5	2.0	7	Northeast
Taíba Albatroz	38°54'59"	03°30'37"	16.5	88	2.1	8	Northeast

First, we simulated wind generation for each wind park listed in Table S5 using NCEP-CSFR wind speeds from October 2014 to October 2015 (period of the real data). Specifically, we used the u and v components of the wind speeds at the layer between two "level at specified pressure differences from ground to level"(0,30 mbar). This layer corresponds to an average over the atmosphere up to the level where pressure is 30 mbar lower than at the surface (about 300 m up), which is approximately the height where the turbine rotors are located (roughly 150m up the ground depending on the wind structure).

Using the NCEP-CSFR wind speeds as inputs, we assessed four different wind generation models. The first two models are based on theoretical wind power functions: a cubic and an exponential. The power curves are defined in equation S4 and S5:

$$q\ (v) = \frac{1}{2}\rho A C_p v^3 \qquad \text{- Cubic} \qquad \text{(S4)}$$

$$q\ (v) = \frac{1}{2}\rho A K_p (v^\beta - v_{ci}^\beta) \qquad \text{- Exponential} \qquad \text{(S5)}$$

Where q is the energy output in Watts, A is the rotor area (m^2), ρ is the air density (kg/m^3); assumed 1.23), C_p is the power coefficients (assumed 0.4), v is the wind speed in (m/s) from NCEP-CFSR, v_{ci} is the cut-in wind speed in (assumed 5 m/s) and K_p and β are coefficients of exponential approximation (assumed 0.899 and 2.706, respectively) (Carrillo et al. 2013).

The other two models represent the wind power functions numerically. A wind power function has three key points: (i) cut-in speed below which the turbine will not produce power, (ii) rated speed at which the rated power of the turbine is produced, and (iii) cut-off speed beyond which the turbine is not allowed to deliver power(M. Brower: AWS Truewind, LLC & Albany 2009). The first non-parametric power function is a hyperbolic tangent (tanh) shaped curve built with a cut-in speed (c1, 3.5 m/s), a rated speed (c2, 11 m/s), and a cut-off speed (c3, 25 m/s). The second numerical representation of the wind power curves is based on three different composite power curves for each wind class developed by the Renewable National Energy Laboratory - NREL (M. Brower: AWS Truewind, LLC & Albany 2009). Table S7 defines the NREL composite power curves for a 2 MW turbines. For each site, we developed a code in R that choses the best composite power curve based on the wind speed averages of each site. When the generator capacity does not correspond to 2MW, we the figures in Table S6 scale up or down based on the wind park generator capacity. For example, Atlantica I wind park has 3MW generators, and, thus, we multiplied the composite power curve by 1.5 (3MW/2MW).

Table S6- NREL composite power curves (source: (M. Brower: AWS Truewind, LLC & Albany 2009)).

Wind speed	Power (kW)		
m/s	IEC Class 1	IEC Class 2	IEC Class 3
0	0	0	0
1	0	0	0
2	0	0	0
3	0	0	12.6
4	39	65.6	82.4
5	136.2	176.8	204
6	280.2	347.8	378
7	474.2	574.6	621.4
8	732.6	867.8	943
9	1,046.6	1,213.2	1,325.8
10	1,404.2	1,553.6	1,676.6
11	1,712.8	1,810	1,892.8
12	1,911.2	1,943.4	1,974.2
13	1,974.8	1,985.2	1,995.2
14	1,989	1,995.8	1,999
15	1,996.4	1,999.6	1,999.8
16	1,998	2,000	2,000
17	2,000	2,000	2,000
18	2,000	2,000	2,000
19	2,000	2,000	2,000
20	2,000	2,000	2,000
21	2,000	2,000	2,000
21.01	2,000	2,000	0
22	2,000	2,000	0
23	2,000	2,000	0
24	2,000	2,000	0
25	2,000	2,000	0
25.01	0	0	0
100	0	0	0

We evaluated the four wind generation models against the real data from CPFL wind parks calculating the Pearson correlation, the coefficient of determination (R^2) and the root mean square error (RMSE). The four-model comparison indicated that NREL composite power curves represent the most flexible and accurate model to transform wind speeds to electricity generation in Brazil without having the manufacturing details from the turbines. Thus, we assumed the NREL composite wind power curves as our reference to generate electricity outputs as a function of the NCEP-CSFR wind speeds.

Table S8 presents the correlation, R^2, and RMSE between the real data (CPFL wind parks) and model (NREL composite curves). The results are presented by hour, but we also aggregated the results by load block. As explained in Chapter 4, three load blocks represent the daily demand variability: high (6 p.m.-9 p.m.), medium (7 a.m-6 p.m., and 9 p.m. - 12 p.m.), and low (0 a.m. - 7 a.m.).

Table S8 - Real data (from 31 CPFL Renováveis wind parks) versus model statistics: Pearson correlation, coefficient of determination, and root mean squared error (RMSE)

Wind Park	Pearson Correlation		Coefficient of determination (R2)		RMSE (kWh)		RMSE (% of the maximum generation in the period)	
	By hour	By block	By hour	By block	By hour	By block	By hour	By block
Atlântica I	0.64	0.83	0.41	0.69	8,541	53,520	28%	7%
Atlântica II	0.63	0.83	0.40	0.69	8,193	49,867	27%	7%
Atlântica IV	0.62	0.82	0.39	0.68	8,580	52,544	29%	7%
Atlântica V	0.61	0.80	0.37	0.64	8,835	56,725	29%	8%
Bons Ventos	0.67	0.89	0.44	0.80	10,592	64,768	21%	5%
Canoa Quebrada	0.66	0.89	0.43	0.80	12,670	70,036	22%	5%
Canoa Quebrada RDV	0.62	0.88	0.39	0.77	2,955	20,672	28%	8%
Costa Branca	0.65	0.92	0.43	0.84	2,416	14,867	12%	3%
Costa Branca	0.62	0.92	0.38	0.84	2,002	11,689	10%	2%
Enacel	0.55	0.85	0.30	0.71	7,789	46,662	25%	6%
Eurus I	0.60	0.92	0.36	0.85	5,688	31,441	19%	4%
Eurus III	0.64	0.91	0.41	0.83	6,047	35,898	20%	5%
Foz do Rio Choró	0.69	0.92	0.48	0.85	5,386	35,823	21%	6%
Icaraizinho	0.75	0.94	0.56	0.89	11,843	75,440	22%	6%
Juremas	0.59	0.91	0.35	0.83	1,604	9,405	10%	2%
Juremas	0.60	0.92	0.36	0.84	2,094	12,246	13%	3%
Macacos	0.65	0.93	0.43	0.86	1,892	10,658	9%	2%
Macacos	0.62	0.92	0.39	0.84	2,175	12,553	11%	3%
Morro dos Ventos I	0.60	0.92	0.36	0.85	6,111	35,274	21%	5%
Morro dos Ventos III	0.62	0.91	0.38	0.83	6,201	38,094	22%	6%
Morro dos Ventos IV	0.60	0.91	0.36	0.83	6,596	41,525	23%	6%
Morro dos Ventos IX	0.54	0.91	0.29	0.83	5,955	34,351	20%	5%
Morro dos Ventos VI	0.64	0.93	0.41	0.86	6,084	36,613	21%	5%
Paracuru	0.71	0.94	0.51	0.89	5,262	28,472	21%	5%
Pedra Preta	0.69	0.93	0.48	0.87	1,849	11,150	9%	2%
Pedra Preta	0.65	0.92	0.43	0.85	2,415	13,661	12%	3%
Santa Clara I	0.54	0.92	0.29	0.85	3,271	19,264	11%	3%
Santa Clara I	0.57	0.93	0.33	0.86	3,781	22,881	13%	3%
Santa Clara II	0.59	0.92	0.34	0.85	2,790	16,072	17%	4%
Santa Clara II	0.61	0.92	0.37	0.85	3,185	18,655	23%	6%
Santa Clara III	0.61	0.92	0.38	0.84	3,555	21,804	22%	6%
	0.61	0.92	0.37	0.85	3,404	22,006	24%	7%
Santa Clara V	0.63	0.91	0.40	0.83	4,022	28,302	25%	7%
	0.63	0.92	0.40	0.84	4,022	21,244	29%	6%
Santa Clara VI	0.50	0.91	0.25	0.82	6,353	97,612	40%	25%
	0.50	0.91	0.25	0.82	4,862	67,992	35%	20%
Taíba Albatroz	0.64	0.92	0.41	0.84	4,188	24,778	25%	6%

Statistics:

Minimum	0.50	0.80	0.25	0.64	1,604	9,405	9%	2%
Maximum	0.75	0.94	0.56	0.89	12,670	97,612	40%	25%
Average	0.62	0.90	0.39	0.82	5,222	34,177	21%	6%

Table S8 shows that average hourly correlation between the real data and model varies from 0.5 to 0.75, which is within the same range found by the literature described in Table S5. The hourly R^2 results vary from 0.25 to 0.56 indicating that the model goodness of fit is modest. The RMSE results also indicate that difference between model and real data is significant (9% to 40% of the total generation capacity for one hour) for hourly predictions. However, when we aggregate the hourly results within the daily blocks and compare model and real data, the correlation, R^2, and RMSE improve significantly. The aggregation by block increases the average correlation from 0.62 to 0.90. Similarly, the average R^2 improves from 0.39 to 0.82, and the average RMSE (as a proportion of the total generation) decreases from 21% to 6%. Therefore, the use of NCEP-CSFR wind speeds as inputs to the NREL power function model represents real data reasonably when generation is aggregated by block within the day.

The large improvement happens because although the model does not represent very well the hourly time series, it describes very well the hourly generation distributions. Figure S6 illustrates this idea. The top plot in Figure S6 shows the hourly time series comparison between model and real data for Morro dos Ventos III wind park. While it is possible to see some periods of good fit, other periods standout with noteworthy errors. The bottom plot shows a general hourly generation agreement between the real data and model histograms. Thus, the model describes very well the hourly data probability distributions such that when we aggregate the daily hours by three blocks, the errors between real data and model decrease significantly as shown by the statistics described in Table S8.

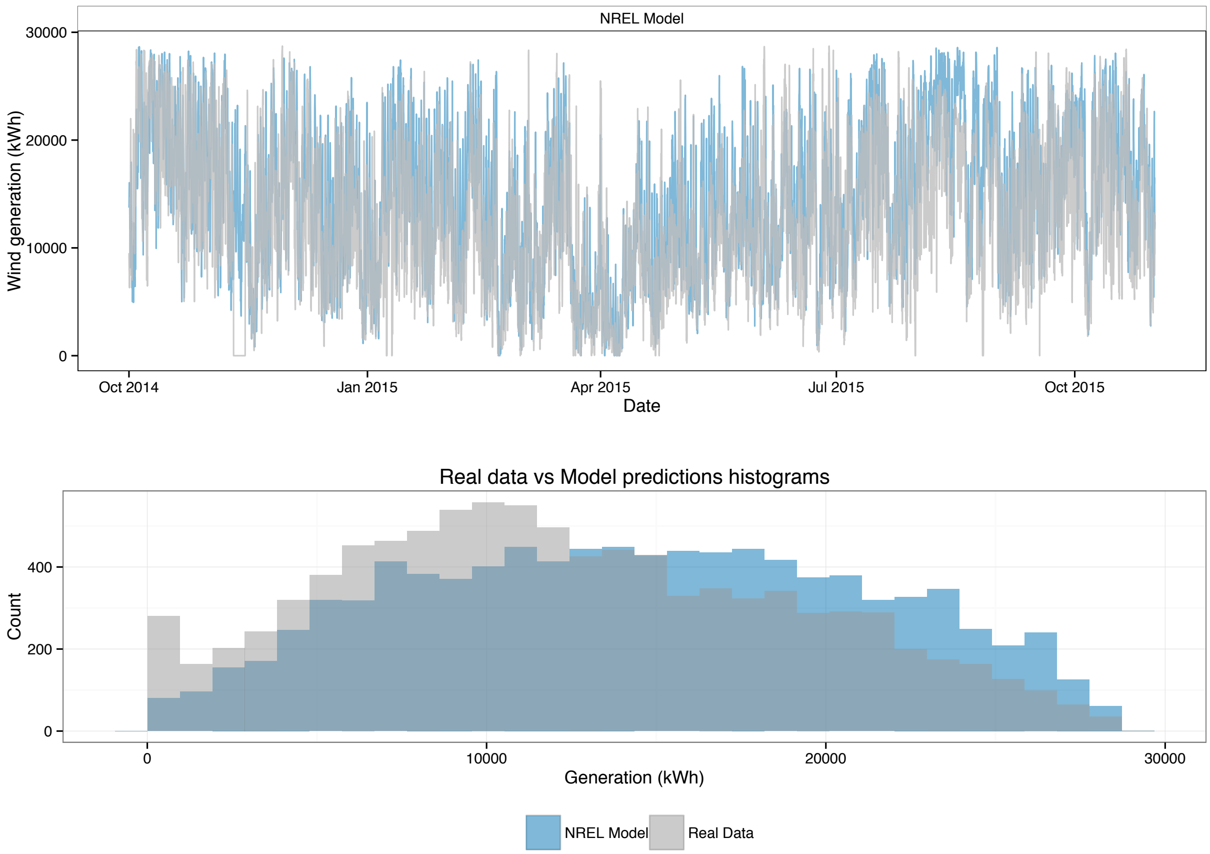

Figure S6 - Comparison between model vs. real data wind power output. Example for Morro dosVentos III Wind park. Top: Hourly generation time series. Bottom: Hourly histograms.

8.5 Costs

The Chamber of Electric Energy Trading (*Câmara de Comercialização de Energia - CCEE*, in Portuguese), which is the Brazilian electricity market operator, provides a dataset of all new power plants that sold energy in public auction since 2005 (CCEE 2015). This database contains the installed capacity and the forecasted capital costs for 826 power plants built from 2005 to 2015. Figure S7 contains the cost per unit of power histograms by fuel type.

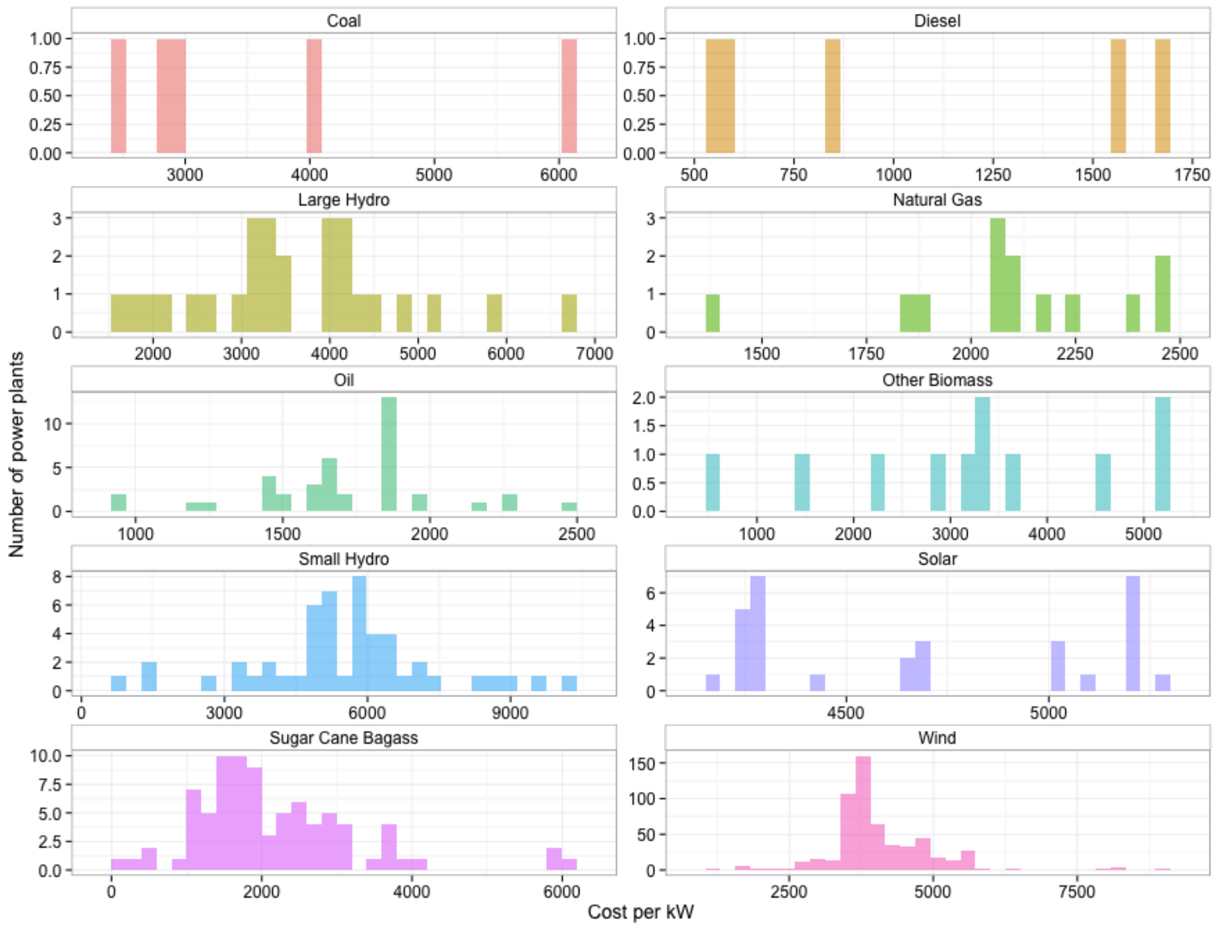

Figure S7 - Power plant cost per unit of power (reais/kW) by source: histograms

We used the power plant construction costs from Figure S7 to estimate the capital costs for the baseline and alternative scenarios. Some power plants that are in the baseline scenario were already auctioned by the time of this study; thus, we applied the capital costs reported by the project itself. In the case of the future projects that did not go into auction yet, we estimated the capital costs according to the following assumptions:

Coal: 2,440 reais/kW (auction value for Pecem 1 project)

Diesel: 1,040 reais/kW (Diesel Projects average)

Large Hydro: based on installed capacity and calculated using the linear regressions described in Figure S8

Natural Gas: 2,100 reais/kW (NG Projects average)

Oil: 1,710 reais/kW (Oil Projects average)

Wind: 4,000 reais/kW (Wind Projects average)

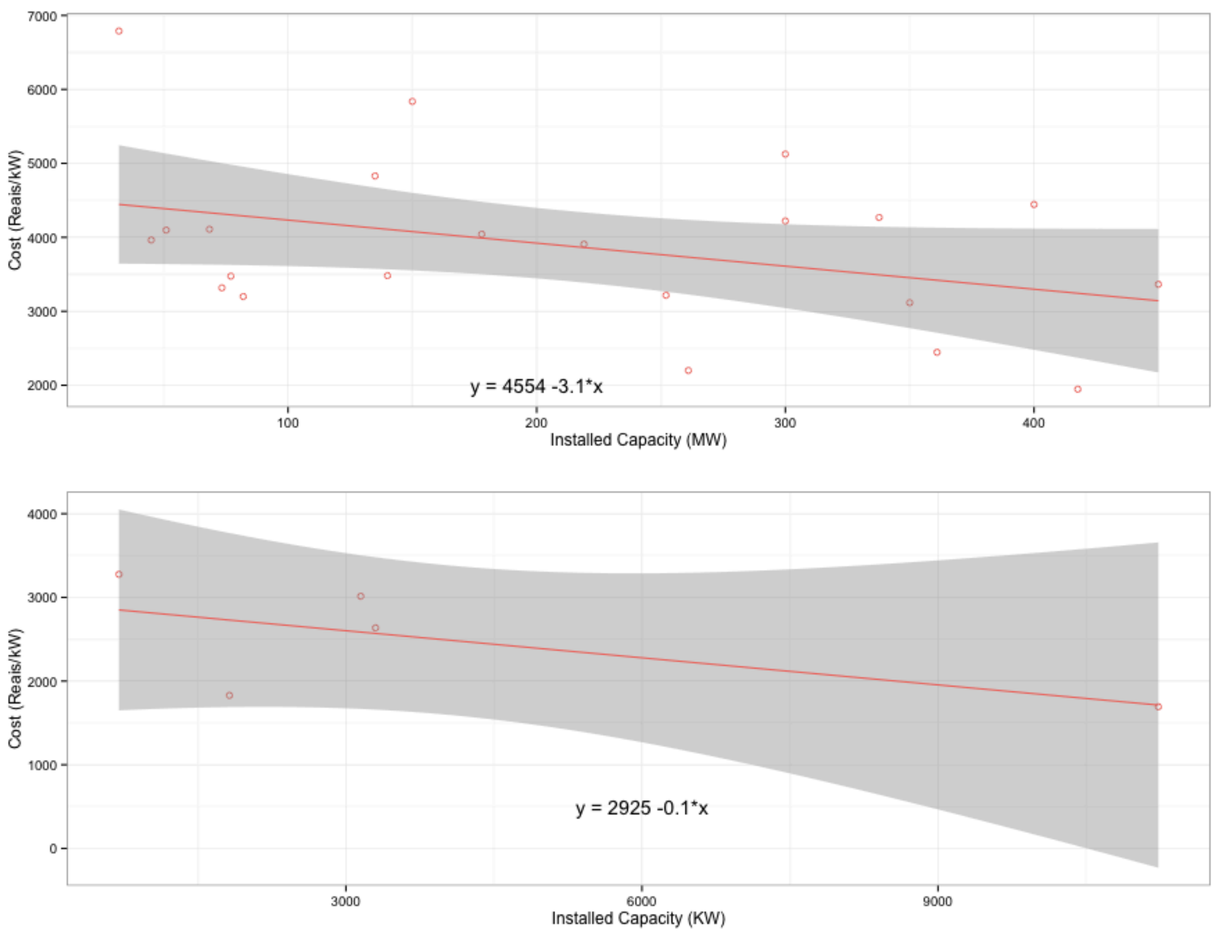

Figure S8 - Capital Costs per kW versus installed capacity. Top: hydropower plants between 30 and 500 MW. Bottom: hydropower plants with more than 500 MW.

Tables S9 and S10 describe the estimated capital costs and maintenance costs. Annual operation and maintenance costs are estimated as 2% of the capital costs, which does not include the marginal fuel costs from thermal power plants (defined in Appendix A, table AS2). We annualized the capital costs assuming a power plant lifetime of 50 years and internal rate of return of 12%.

Table S9 - Hydroelectric power plants costs

Scenario	*Name*	*Installed Capacity (MW)*	*Estimated construction cost (Reais/kW)*	*Total Construction Cost (million reais)*	*Annual O&M (million reais)*	*Annualized cost (million reais)*
Hydropower plants replaced in scenarios Wind27 and Natural Gas	Bem Querer	708	2,847	2,017	40	283
	Castanheira	192	3,949	758	15	106
	Cachoeira do Caí	802	2,837	2,275	46	319
	Cachoeira dos Patos	528	2,867	1,514	30	213
	Carecuru	240	3,799	913	18	128
	Jamanxim	881	2,828	2,492	50	350
	Jardim de Ouro	227	3,840	872	17	122
	Jatobá	2,338	2,668	6,237	125	876
	Marabá	1,708	2,737	4,674	93	656
	Paradão A	199	3,926	782	16	110
	São Luís do Tapajós*	300	2,074	622	12	87
	São Luís do Tapajós	7,740	2,074	16,050	321	2,254
	Serra Quebrada	1,328	2,779	3,690	74	518
	São Simão Alto	3,509	2,539	8,909	178	1,251
	Santa Isabel	1,087	2,805	3,050	61	428
	Salto Augusto de Baixo	1,461	2,764	4,039	81	567
	Tucuma	453	3,139	1,423	28	200
	Tabajara	350	3,459	1,211	24	170
	Total replaced capacity: scenarios A and C	**24,052**		**61,527**	**1,231**	**8,640**
Hydropower plants replaced in scenarios Wind39 and Coal/Oil/diesel retirement"	Belo Monte*	233	1,693	395	8	55
	Belo Monte	11,000	1,693	18,623	372	2,615
	Cachoeira do Caldeirão	219	3,908	856	17	120
	Colíder	300	4,221	1,266	25	178
	Ferreira Gomes	252	3,217	811	16	114
	Jirau	3,750	2,636	9,885	198	1,388
	São Manoel	700	3,276	2,293	46	322
	Sinop	400	4,444	1,778	36	250
	Santo Antônio do Jari	370	4,762	1,762	35	247
	Santo Antônio	3,151	1,947	6,135	123	861
	Teles Pires	1,820	1,829	3,329	67	467
	Replaced capacity before 2020	22,195		**47,132**	**943**	**6,618**
	Total replaced capacity: scenarios B	**46,247**		**108,658**	**2,173**	**15,258**
Non-Amazon reservoirs baseline	Água Limpa	380	3,366	1,279	26	180
	Apertados	277	4,113	1,139	23	160
	Arraias	70	4,327	303	6	43
	Baixo Iguaçu	584	3,458	2,018	40	283

Batalha	53	4,381	230	5	32
Biboca	57	4,367	249	5	35
Buriti Queimado	142	4,104	583	12	82
Comissário	280	4,110	1,152	23	162
Davinópolis	74	4,315	319	6	45
Doresópolis	60	4,358	261	5	37
Ercilândia	174	4,274	744	15	104
Formoso	342	3,484	1,191	24	167
Foz do Piquiri	192	4,246	815	16	114
Garibaldi	175	4,001	700	14	98
Iraí	330	3,521	1,162	23	163
Itaocara I	145	4,095	594	12	83
Itapiranga	725	2,845	2,062	41	290
Maranhão Baixo	125	4,157	520	10	73
Mirador	80	4,296	344	7	48
Murta	120	4,172	501	10	70
Pai Querê	292	3,639	1,063	21	149
Paranhos	94	4,350	408	8	57
Pedra Branca	320	3,552	1,137	23	160
Pompéu	209	3,896	815	16	114
Porteiras 2	86	4,277	368	7	52
Prainha	796	2,837	2,260	45	317
Riacho Seco	276	3,688	1,018	20	143
Santa Branca	58	4,364	253	5	36
São Jerônimo	330	3,521	1,161.93	23	163
São Roque	135	4,126	557	11	78
Salto Apiacás	45	3,946	178	4	25
Sumauma	458	3,124	1,431	29	201
Simplicio	305				
Telemaco Borba	109	4,206	458	9	64
Tijuco Alto	193	4,145	800	16	112
Toricoejo	76	4,308	327	7	46
Torixoreu	408	3,279	1,338	27	188
Vila Grande Chopin	82	3,139	258	5	36
Total Non-Amazon hydroelectric plants	**8,657**		**29,995**	**600**	**4,212**

Table S10- Thermal power plants costs (Fuel costs are detailed in Annex C1)

Name	Type	Installed Capacity (MW)	Cost per kW (reais)	*Total Construction Cost (million reais)*	*Annual O&M (million reais)*	*Annualized cost (million reais)*
Angra 3	nuclear	1,405	11,000	15,455	309	309
Aparecida	NG	166	2,100	349	7	7
Baixada Fluminense	NG	530	1,861	986	20	20
Camacari G	NG	316	2,100	663	13	13
Campo Grande	biomass	150	3,309	496	10	10
Canto Buriti	biomass	150	3,129	469	9	9
ERB candeias	biomass	17	2,287	38	1	1
Maranhao III	NG	519	2,226	1,155	23	23
Maranhao IV	NG	338	2,226	751	15	15
Maua 3	NG	583	2,112	1,231	25	25
Maua B3	NG	110	2,112	232	5	5
Maua B4	oil	135	1,712	231	5	5
MC2 N Veneci	oil	176	1,859	328	7	7
P. Pecem 1	coal	720	2,441	1,758	35	35
P. Pecem 2	coal	365	2,441	891	18	18
Parnaiba IV	NG	56	2,100	118	2	2
Pernambuco 3	oil	201	1,640	329	7	7
PIE C Rocha	NG	85	2,100	179	4	4
PIE jaraqui	NG	66	2,100	138	3	3
PIE manauara	NG	67	2,100	140	3	3
PIE P Negra	NG	66	2,100	139	3	3
PIE Tambaqui	NG	66	2,100	138	3	3
Porto Itaqui	coal	360	2,441	879	18	18
Santana 1 w	diesel	58	1,036	60	1	1
Santana 2 ge	diesel	50	1,036	52	1	1
Suape II	oil	381	1,659	633	13	13
Suzano ma	biomass	255	3,239	825	17	17
UTE Ind Gas1	NG	1,300	2,100	2,730	55	55
UTE Ind Gas2	NG	8,900	2,100	18,690	374	374
UTE Ind Gas3	NG	1,400	2,100	2,940	59	59
UTE Ind Nuc	nuclear	1,000	5,000	5,000	100	100
Total Baseline		**19,990**		**58,025**	**1,160**	**23**
Scenario C - NG	gas	14,431	2,100	30,309	606	606
Total Scenario C		**34,423**		**88,334**	**1,767**	**629**

References

Bao, X & Zhang, F 2013, 'Evaluation of NCEP–CFSR, NCEP–NCAR, ERA-Interim, and ERA-40 Reanalysis Datasets against Independent Sounding Observations over the Tibetan Plateau', *JOURNAL OF CLIMATE*, vol. 26, no. 1, pp. 206–214.

Carrillo, C, Montaño, AFO, Cidrás, J & Díaz-Dorado, E 2013, 'Review of power curve modelling for wind turbines', *Renewable and Sustainable Energy Reviews*, vol. 21, no. C, Elsevier, pp. 572–581.

Carvalho, D, Rocha, A, Gómez-Gesteira, M & Santos, CS 2014a, 'Comparison of reanalyzed, analyzed, satellite-retrieved and NWP modelled winds with buoy data along the Iberian Peninsula coast', *Remote Sensing of Environment*, vol. 152, no. C, Elsevier Inc., pp. 480–492.

Carvalho, D, Rocha, A, Gómez-Gesteira, M & Santos, CS 2014b, 'WRF wind simulation and wind energy production estimates forced by different reanalyses: Comparison with observed data for Portugal', *Applied Energy*, vol. 117, no. C, Elsevier Ltd, pp. 116–126.

EPE 2015, 'Newave input files', EPE (ed.),, 2015th ed, Empresa de Pesquisa Energetica (EPE), viewed <http://www.epe.gov.br/Estudos/Paginas/Plano%20Decenal%20de%20Energia%20%E2%80%93%20PDE/EPEpublicaarquivosdoprogramaNewavedoPDE2023.aspx?CategoriaID=345>.

Gorenstin, BG, M, CN, da Costa, JP & Pereira, M 2004, 'Sthocastic optimization of a hydro-thermal system including network constraints', *IEEE Transactions Power Systems*, pp. 1–7.

M. Brower: AWS Truewind, LLC & Albany, NY 2009, *Development of Eastern Regional Wind Resource and Wind Plant Output Datasets*, National Renewable Energy Laboratory (ed.),, National Renewable Energy Laboratory, pp. 1–66.

Pereira, M & Pinto, L 1991, 'Multi-stage stochastic optimization applied to energy planning', *Mathematical Programming*.

PSR 2014, *SDDP Methodology Manual*, Power Systems Research (PSR), pp. 1–88.

Rebennack, S, Flach, B & Pereira, M 2012, 'Stochastic hydro-thermal scheduling under emissions constraints', *Power Systems*.

Rose, S & Apt, J 2016, 'Quantifying sources of uncertainty in reanalysis derived wind speed', *Renewable Energy*, vol. 94, no. C, Elsevier Ltd, pp. 157–165.

Rose, S & Apt, J 2015, 'What can reanalysis data tell us about wind power?', *Renewable Energy*, vol. 83, no. C, Elsevier Ltd, pp. 963–969.

Saha, S, Moorthi, S, Pan, H-L, Wu, X, Wang, J, Nadiga, S, Tripp, P, Kistler, R, Woollen, J, Behringer, D, Liu, H, Stokes, D, Grumbine, R, Gayno, G, Wang, J, Hou, Y-T, Chuang, H-Y, Juang, H-MH, Sela, J, Iredell, M, Treadon, R, Kleist, D, Van Delst, P, Keyser, D, Derber, J, Ek, M, Meng, J, Wei, H, Yang, R, Lord, S, Van Den Dool, H, Kumar, A, Wang, W, Long, C, Chelliah, M, Xue, Y, Huang, B, Schemm, J-K, Ebisuzaki, W, Lin, R, Xie, P, Chen, M, Zhou, S, Higgins, W, Zou, C-Z, Liu, Q, Chen, Y, Han, Y, Cucurull, L, Reynolds, RW, Rutledge, G & Goldberg, M 2016, 'NCEP Climate Forecast System Reanalysis (CFSR) Selected Hourly Time-Series Products, January 1979 to December 2010', Research Data Archive at the National Center for Atmospheric Research, Computational & IS Laboratory (eds),, Research Data Archive at the National Center for Atmospheric Research, Computational and Information Systems Laboratory.

Sharp, E, Dodds, P, Barrett, M & Spataru, C 2015, 'Evaluating the accuracy of CFSR reanalysis hourly wind speed forecasts for the UK, using in situ measurements and geographical information', *Renewable Energy*, vol. 77, no. c, Elsevier Ltd, pp. 527–538.

ANNEX C1 - Hydropower and thermal power plants schedule: Baseline scenario

Table AS1 - Detailed schedule and characteristics for hydropower plants in the baseline

SDDP - ID	Date (d/m/y)	Name	Number of generators	Installed Capacity (MW)	Additional Installed Capacity (MW)	Production coefficient (MWh/m^3)	Maximum flow (m^3/s)	Maximum reservoir volume (hm^3)	Subsystem
258	1/10/23	Agua Limpa	0	0	0	0.00	0	43	se
258	1/1/24	Agua Limpa	1	190	190	0.92	199	43	se
258	1/4/24	Agua Limpa	2	380	190	0.92	398	43	se
578	1/5/20	Apertados	0	0	0	0.00	0	207	su
578	1/8/20	Apertados	1	46.3	46.3	0.23	208	207	su
578	1/10/20	Apertados	2	92.6	46.3	0.23	416	207	su
578	1/12/20	Apertados	3	138.9	46.3	0.23	624	207	su
444	1/11/21	Arraias	0	0	0	0.00	0	566	se
444	1/2/22	Arraias	1	35	35	0.18	190	566	se
444	1/4/22	Arraias	2	70	35	0.18	380	566	se
314	1/1/15	B.Monte Comp	0	0	0	0.00	0	4802	ne
314	1/3/15	B.Monte Comp	1	38.8	38.8	0.12	411	4802	ne
314	1/5/15	B.Monte Comp	2	77.6	38.8	0.12	822	4802	ne
314	1/7/15	B.Monte Comp	3	116.4	38.8	0.12	1233	4802	ne
314	1/9/15	B.Monte Comp	4	155.2	38.8	0.12	1644	4802	ne
314	1/11/15	B.Monte Comp	5	194	38.8	0.12	2055	4802	ne
314	1/1/16	B.Monte Comp	6	233.1	39.1	0.12	2466	4802	ne
83	1/3/16	Baixo Iguacu	0	0	0	0.00	0	212	su
83	1/6/16	Baixo Iguacu	1	116.7	116.7	0.16	834	212	su
83	1/8/16	Baixo Iguacu	2	233.4	116.7	0.16	1668	212	su
83	1/10/16	Baixo Iguacu	3	350.2	116.8	0.16	2502	212	su
20	1/2/14	Batalha	0	0	0	0.00	0	1782	pa
20	1/5/14	Batalha	2	52.5	52.5	0.33	154	1782	pa
288	1/1/15	Belo Monte	0	0	0	0.00	0	4802	bm
288	1/4/16	Belo Monte	1	611.1	611.1	0.80	775	4802	bm
288	1/6/16	Belo Monte	2	1222.2	611.1	0.80	1550	4802	bm
288	1/8/16	Belo Monte	3	1833.3	611.1	0.80	2325	4802	bm
288	1/10/16	Belo Monte	4	2444.4	611.1	0.80	3100	4802	bm
288	1/12/16	Belo Monte	5	3055.5	611.1	0.80	3875	4802	bm
288	1/2/17	Belo Monte	6	3666.6	611.1	0.80	4650	4802	bm
288	1/4/17	Belo Monte	7	4277.7	611.1	0.80	5425	4802	bm
288	1/6/17	Belo Monte	8	4888.8	611.1	0.80	6200	4802	bm
288	1/8/17	Belo Monte	9	5499.9	611.1	0.80	6975	4802	bm
288	1/10/17	Belo Monte	10	6111	611.1	0.80	7750	4802	bm
288	1/12/17	Belo Monte	11	6722.1	611.1	0.80	8525	4802	bm

288	1/2/18	Belo Monte	12	7333.2	611.1	0.80	9300	4802	bm
288	1/4/18	Belo Monte	13	7944.3	611.1	0.80	10075	4802	bm
288	1/6/18	Belo Monte	14	8555.4	611.1	0.80	10850	4802	bm
288	1/8/18	Belo Monte	15	9166.5	611.1	0.80	11625	4802	bm
288	1/10/18	Belo Monte	16	9777.6	611.1	0.80	12400	4802	bm
288	1/12/18	Belo Monte	17	10388.8	611.2	0.80	13175	4802	bm
288	1/2/19	Belo Monte	18	11000	611.2	0.80	13950	4802	bm
339	1/4/22	Bem Querer	0	0	0	0.00	0	2530	ma
339	1/7/22	Bem Querer	1	54.5	54.5	0.14	381	2530	ma
339	1/9/22	Bem Querer	2	109	54.5	0.14	762	2530	ma
339	1/11/22	Bem Querer	3	163.5	54.5	0.14	1143	2530	ma
339	1/1/23	Bem Querer	4	218	54.5	0.14	1524	2530	ma
339	1/3/23	Bem Querer	5	272.5	54.5	0.14	1905	2530	ma
339	1/5/23	Bem Querer	6	327	54.5	0.14	2286	2530	ma
339	1/5/23	Bem Querer	7	381.5	54.5	0.14	2667	2530	ma
339	1/9/23	Bem Querer	8	436	54.5	0.14	3048	2530	ma
339	1/11/23	Bem Querer	9	490.5	54.5	0.14	3429	2530	ma
339	1/1/24	Bem Querer	10	545	54.5	0.14	3810	2530	ma
339	1/3/24	Bem Querer	11	599.5	54.5	0.14	4191	2530	ma
339	1/5/24	Bem Querer	12	654	54.5	0.14	4572	2530	ma
339	1/7/24	Bem Querer	13	708.4	54.4	0.14	4953	2530	ma
531	1/1/28	Biboca	0	0	0	0.00	0	225	se
531	1/4/28	Biboca	1	19	19	0.27	88	225	se
531	1/6/28	Biboca	2	38	19	0.27	176	225	se
531	1/8/28	Biboca	3	57	19	0.27	264	225	se
430	1/10/26	Buriti Queim	0	0	0	0.00	0	2481	se
430	1/1/27	Buriti Queim	1	35.5	35.5	0.36	84	2481	se
430	1/3/27	Buriti Queim	2	71	35.5	0.36	168	2481	se
430	1/5/27	Buriti Queim	3	106.5	35.5	0.36	252	2481	se
430	1/7/27	Buriti Queim	4	142	35.5	0.36	336	2481	se
204	1/11/16	Cach Caldeir	0	0	0	0.00	0	231	ma
204	1/1/17	Cach Caldeir	1	73	73	0.14	547	231	ma
204	1/3/17	Cach Caldeir	2	146	73	0.14	1094	231	ma
204	1/5/17	Cach Caldeir	3	219	73	0.14	1641	231	ma
237	1/5/24	Cach Do Cai	0	0	0	0.00	0	3418	tt
237	1/8/24	Cach Do Cai	1	160.4	160.4	0.29	532	3418	tt
237	1/11/24	Cach Do Cai	2	320.8	160.4	0.29	1064	3418	tt
237	1/2/25	Cach Do Cai	3	481.2	160.4	0.29	1596	3418	tt
237	1/5/25	Cach Do Cai	4	641.6	160.4	0.29	2128	3418	tt
237	1/8/25	Cach Do Cai	5	802	160.4	0.29	2660	3418	tt
235	1/1/23	Cach Patos	0	0	0	0.00	0	697	tt
235	1/4/24	Cach Patos	1	176	176	0.27	611	697	tt
235	1/7/24	Cach Patos	2	352	176	0.27	1222	697	tt

235	1/10/24	Cach Patos	3	528	176	0.27	1833	697	tt
422	1/2/28	Carecuru	0	0	0	0.00	0	1309	ma
422	1/5/28	Carecuru	1	80	80	0.16	469	1309	ma
422	1/7/28	Carecuru	2	160.1	80.1	0.16	938	1309	ma
422	1/9/28	Carecuru	3	240.2	80.1	0.16	1407	1309	ma
409	1/1/21	Castanheira	0	0	0	0.00	0	768	tt
409	1/4/21	Castanheira	1	64	64	0.13	486	768	tt
409	1/6/21	Castanheira	2	128	64	0.13	972	768	tt
409	1/8/21	Castanheira	3	192	64	0.13	1458	768	tt
228	1/4/15	Colider	0	0	0	0.00	0	1525	tt
228	1/7/15	Colider	1	100	100	0.21	527	1525	tt
228	1/9/15	Colider	2	200	100	0.21	1054	1525	tt
228	1/11/15	Colider	3	300	100	0.21	1581	1525	tt
577	1/12/19	Comissario	0	0	0	0.00	0	970	su
577	1/3/20	Comissario	1	46.7	46.7	0.31	153	970	su
577	1/5/20	Comissario	2	93.4	46.7	0.31	306	970	su
577	1/7/20	Comissario	3	140.1	46.7	0.31	459	970	su
23	1/9/18	Davinopolis	0	0	0	0.00	0	506	pa
23	1/1/19	Davinopolis	1	24.7	24.7	0.32	78	506	pa
23	1/3/19	Davinopolis	2	49.4	24.7	0.32	156	506	pa
23	1/5/19	Davinopolis	3	74	24.6	0.32	234	506	pa
477	1/11/27	Doresopolis	0	0	0	0.00	0	618	se
477	1/2/28	Doresopolis	1	30	30	0.42	70	618	se
477	1/4/28	Doresopolis	2	60	30	0.42	140	618	se
579	1/5/20	Ercilandia	0	0	0	0.00	0	167	su
579	1/8/20	Ercilandia	1	29	29	0.14	227	167	su
579	1/10/20	Ercilandia	2	58	29	0.14	454	167	su
579	1/12/20	Ercilandia	3	87	29	0.14	681	167	su
284	1/10/14	Ferreira Gom	0	0	0	0.00	0	137	ma
284	1/1/15	Ferreira Gom	1	84	84	0.16	574	137	ma
284	1/3/15	Ferreira Gom	2	168	84	0.16	1148	137	ma
284	1/5/15	Ferreira Gom	3	252	84	0.16	1722	137	ma
493	1/8/27	Formoso	0	0	0	0.00	0	3793	se
493	1/11/27	Formoso	1	114	114	0.22	430	3793	se
493	1/2/28	Formoso	2	228	114	0.22	860	3793	se
493	1/5/28	Formoso	3	342	114	0.22	1290	3793	se
580	1/1/20	Foz Piquiri	0	0	0	0.00	0	189	su
580	1/4/20	Foz Piquiri	1	32	32	0.14	254	189	su
580	1/6/20	Foz Piquiri	2	64	32	0.14	508	189	su
580	1/8/20	Foz Piquiri	3	96	32	0.14	762	189	su
89	1/7/13	Garibaldi	0	0	0	0.00	0	296	su
89	1/10/13	Garibaldi	1	58.3	58.3	0.39	160	296	su
89	1/11/13	Garibaldi	2	116.6	58.3	0.39	320	296	su

89	1/1/14	Garibaldi	3	175	58.4	0.39	480	296	su
104	1/5/25	Irai	0	0	0	0.00	0	229	su
104	1/7/25	Irai	1	66	66	0.13	502	229	su
104	1/9/25	Irai	2	132	66	0.13	1004	229	su
104	1/11/25	Irai	3	198	66	0.13	1506	229	su
104	1/1/26	Irai	4	264	66	0.13	2008	229	su
104	1/3/26	Irai	5	330	66	0.13	2510	229	su
186	1/10/18	Itaocara I	0	0	0	0.00	0	413	se
186	1/1/19	Itaocara I	1	72.5	72.5	0.23	334	413	se
186	1/3/19	Itaocara I	2	145	72.5	0.23	668	413	se
100	1/7/21	Itapiranga	0	0	0	0.00	0	722	su
100	1/8/21	Itapiranga	1	144.9	144.9	0.25	583	722	su
100	1/11/21	Itapiranga	2	289.8	144.9	0.25	1166	722	su
100	1/2/22	Itapiranga	3	434.7	144.9	0.25	1749	722	su
100	1/5/22	Itapiranga	4	579.6	144.9	0.25	2332	722	su
100	1/8/22	Itapiranga	5	724.6	145	0.25	2915	722	su
236	1/2/24	Jamanxim	0	0	0	0.00	0	1005	tt
236	1/5/24	Jamanxim	1	293.6	293.6	0.49	576	1005	tt
236	1/8/24	Jamanxim	2	587.3	293.7	0.49	1152	1005	tt
236	1/11/24	Jamanxim	3	881	293.7	0.49	1728	1005	tt
234	1/1/25	Jardim Ouro	0	0	0	0.00	0	1978	tt
234	1/4/25	Jardim Ouro	1	56.7	56.7	0.10	443	1978	tt
234	1/6/25	Jardim Ouro	2	113.4	56.7	0.10	886	1978	tt
234	1/8/25	Jardim Ouro	3	170.2	56.8	0.10	1329	1978	tt
234	1/10/25	Jardim Ouro	4	227	56.8	0.10	1772	1978	tt
233	1/10/20	Jatoba	0	0	0	0.00	0	4014	tt
233	1/1/21	Jatoba	1	58.4	58.4	0.14	423	4014	tt
233	1/2/21	Jatoba	2	116.8	58.4	0.14	846	4014	tt
233	1/3/21	Jatoba	3	175.2	58.4	0.14	1269	4014	tt
233	1/4/21	Jatoba	4	233.6	58.4	0.14	1692	4014	tt
233	1/5/21	Jatoba	5	292	58.4	0.14	2115	4014	tt
233	1/6/21	Jatoba	6	350.4	58.4	0.14	2538	4014	tt
233	1/7/21	Jatoba	7	408.8	58.4	0.14	2961	4014	tt
233	1/8/21	Jatoba	8	467.2	58.4	0.14	3384	4014	tt
233	1/9/21	Jatoba	9	525.6	58.4	0.14	3807	4014	tt
233	1/10/21	Jatoba	10	584	58.4	0.14	4230	4014	tt
233	1/11/21	Jatoba	11	642.4	58.4	0.14	4653	4014	tt
233	1/12/21	Jatoba	12	700.8	58.4	0.14	5076	4014	tt
233	1/1/22	Jatoba	13	759.2	58.4	0.14	5499	4014	tt
233	1/2/22	Jatoba	14	817.6	58.4	0.14	5922	4014	tt
233	1/3/22	Jatoba	15	876	58.4	0.14	6345	4014	tt
233	1/4/22	Jatoba	16	934.4	58.4	0.14	6768	4014	tt
233	1/5/22	Jatoba	17	992.8	58.4	0.14	7191	4014	tt

233	1/6/22	Jatoba	18	1051.2	58.4	0.14	7614	4014	tt
233	1/7/22	Jatoba	19	1109.6	58.4	0.14	8037	4014	tt
233	1/8/22	Jatoba	20	1168	58.4	0.14	8460	4014	tt
233	1/9/22	Jatoba	21	1226.5	58.5	0.14	8883	4014	tt
233	1/10/22	Jatoba	22	1285	58.5	0.14	9306	4014	tt
233	1/11/22	Jatoba	23	1343.5	58.5	0.14	9729	4014	tt
233	1/12/22	Jatoba	24	1402	58.5	0.14	10152	4014	tt
233	1/1/23	Jatoba	25	1460.5	58.5	0.14	10575	4014	tt
233	1/2/23	Jatoba	26	1519	58.5	0.14	10998	4014	tt
233	1/3/23	Jatoba	27	1577.5	58.5	0.14	11421	4014	tt
233	1/4/23	Jatoba	28	1636	58.5	0.14	11844	4014	tt
233	1/5/23	Jatoba	29	1694.5	58.5	0.14	12267	4014	tt
233	1/6/23	Jatoba	30	1753	58.5	0.14	12690	4014	tt
233	1/7/23	Jatoba	31	1811.5	58.5	0.14	13113	4014	tt
233	1/8/23	Jatoba	32	1870	58.5	0.14	13536	4014	tt
233	1/9/23	Jatoba	33	1928.5	58.5	0.14	13959	4014	tt
233	1/10/23	Jatoba	34	1987	58.5	0.14	14382	4014	tt
233	1/11/23	Jatoba	35	2045.5	58.5	0.14	14805	4014	tt
233	1/12/23	Jatoba	36	2104	58.5	0.14	15228	4014	tt
233	1/1/24	Jatoba	37	2162.5	58.5	0.14	15651	4014	tt
233	1/2/24	Jatoba	38	2221	58.5	0.14	16074	4014	tt
233	1/3/24	Jatoba	39	2279.5	58.5	0.14	16497	4014	tt
233	1/4/24	Jatoba	40	2338	58.5	0.14	16920	4014	tt
285	1/7/13	Jirau	0	0	0	0.00	0	2747	ar
285	1/10/13	Jirau	1	75	75	0.16	538	2747	ar
285	1/3/14	Jirau	4	300	225	0.16	2152	2747	ar
285	1/4/14	Jirau	6	450	150	0.16	3228	2747	ar
285	1/5/14	Jirau	7	525	75	0.16	3766	2747	ar
285	1/6/14	Jirau	9	675	150	0.16	4842	2747	ar
285	1/7/14	Jirau	11	825	150	0.16	5918	2747	ar
285	1/9/14	Jirau	13	975	150	0.16	6994	2747	ar
285	1/10/14	Jirau	15	1125	150	0.16	8070	2747	ar
285	1/11/14	Jirau	16	1200	75	0.16	8608	2747	ar
285	1/12/14	Jirau	17	1275	75	0.16	9146	2747	ar
285	1/1/15	Jirau	18	1350	75	0.16	9684	2747	ar
285	1/2/15	Jirau	23	1725	375	0.16	12374	2747	ar
285	1/3/15	Jirau	24	1800	75	0.16	12912	2747	ar
285	1/4/15	Jirau	26	1950	150	0.16	13988	2747	ar
285	1/5/15	Jirau	28	2100	150	0.16	15064	2747	ar
285	1/6/15	Jirau	31	2325	225	0.16	16678	2747	ar
285	1/7/15	Jirau	33	2475	150	0.16	17754	2747	ar
285	1/8/15	Jirau	35	2625	150	0.16	18830	2747	ar
285	1/9/15	Jirau	37	2775	150	0.16	19906	2747	ar

285	1/10/15	Jirau	39	2925	150	0.16	20982	2747	ar
285	1/11/15	Jirau	40	3000	75	0.16	21520	2747	ar
285	1/1/16	Jirau	41	3075	75	0.16	22058	2747	ar
285	1/2/16	Jirau	42	3150	75	0.16	22596	2747	ar
285	1/5/16	Jirau	43	3225	75	0.16	23134	2747	ar
285	1/6/16	Jirau	44	3300	75	0.16	23672	2747	ar
285	1/7/16	Jirau	45	3375	75	0.16	24210	2747	ar
285	1/8/16	Jirau	46	3450	75	0.16	24748	2747	ar
285	1/8/16	Jirau	47	3525	75	0.16	25286	2747	ar
285	1/10/16	Jirau	48	3600	75	0.16	25824	2747	ar
285	1/11/16	Jirau	50	3750	150	0.16	26900	2747	ar
274	1/11/24	Maraba	0	0	0	0.00	0	5346	ne
274	1/2/25	Maraba	1	71.1	71.1	0.16	579	5346	ne
274	1/4/25	Maraba	2	142.2	71.1	0.16	1158	5346	ne
274	1/6/25	Maraba	3	213.3	71.1	0.16	1737	5346	ne
274	1/8/25	Maraba	4	284.4	71.1	0.16	2316	5346	ne
274	1/10/25	Maraba	5	355.5	71.1	0.16	2895	5346	ne
274	1/12/25	Maraba	6	426.6	71.1	0.16	3474	5346	ne
274	1/2/26	Maraba	7	497.7	71.1	0.16	4053	5346	ne
274	1/4/26	Maraba	8	568.8	71.1	0.16	4632	5346	ne
274	1/6/26	Maraba	9	639.9	71.1	0.16	5211	5346	ne
274	1/8/26	Maraba	10	711	71.1	0.16	5790	5346	ne
274	1/10/26	Maraba	11	782.1	71.1	0.16	6369	5346	ne
274	1/12/26	Maraba	12	853.2	71.1	0.16	6948	5346	ne
274	1/2/27	Maraba	13	924.4	71.2	0.16	7527	5346	ne
274	1/4/27	Maraba	14	995.6	71.2	0.16	8106	5346	ne
274	1/6/27	Maraba	15	1066.8	71.2	0.16	8685	5346	ne
274	1/8/27	Maraba	16	1138	71.2	0.16	9264	5346	ne
274	1/10/27	Maraba	17	1209.2	71.2	0.16	9843	5346	ne
274	1/12/27	Maraba	18	1280.4	71.2	0.16	10422	5346	ne
274	1/2/28	Maraba	19	1351.6	71.2	0.16	11001	5346	ne
274	1/4/28	Maraba	20	1422.8	71.2	0.16	11580	5346	ne
274	1/6/28	Maraba	21	1494	71.2	0.16	12159	5346	ne
274	1/8/28	Maraba	22	1565.2	71.2	0.16	12738	5346	ne
274	1/10/28	Maraba	23	1636.4	71.2	0.16	13317	5346	ne
274	1/12/28	Maraba	24	1707.6	71.2	0.16	13896	5346	ne
426	1/10/26	Maranhao Bai	0	0	0	0.00	0	3626	se
426	1/1/27	Maranhao Bai	1	41.6	41.6	0.55	65	3626	se
426	1/3/27	Maranhao Bai	2	83.3	41.7	0.55	130	3626	se
426	1/5/27	Maranhao Bai	3	125	41.7	0.55	195	3626	se
250	1/11/23	Mirador	0	0	0	0.00	0	1505	se
250	1/2/24	Mirador	1	40	40	1.14	34	1505	se
250	1/4/24	Mirador	2	80	40	1.14	68	1505	se

149	1/7/27	Murta	0	0	0	0.00	0	340	se
149	1/10/27	Murta	1	40	40	0.36	111	340	se
149	1/1/28	Murta	2	80	40	0.36	222	340	se
149	1/4/28	Murta	3	120	40	0.36	333	340	se
85	1/6/26	Pai Quere	0	0	0	0.00	0	2588	su
85	1/9/26	Pai Quere	1	97.4	97.4	1.15	80	2588	su
85	1/12/26	Pai Quere	2	194.7	97.3	1.15	160	2588	su
85	1/3/27	Pai Quere	3	292	97.3	1.15	240	2588	su
584	1/6/20	Paranhos	0	0	0	0.00	0	169	su
584	1/7/20	Paranhos	1	31.2	31.2	0.27	118	169	su
584	1/9/20	Paranhos	2	62.5	31.3	0.27	236	169	su
337	1/7/23	Paredao A	0	0	0	0.00	0	106	ma
337	1/10/23	Paredao A	1	99.6	99.6	0.32	312	106	ma
337	1/1/24	Paredao A	2	199.3	99.7	0.32	624	106	ma
171	1/7/25	Pedra Branca	0	0	0	0.00	0	589	no
171	1/10/25	Pedra Branca	1	40	40	0.08	404	589	no
171	1/12/25	Pedra Branca	2	80	40	0.08	808	589	no
171	1/1/26	Pedra Branca	3	120	40	0.08	1212	589	no
171	1/3/26	Pedra Branca	4	160	40	0.08	1616	589	no
171	1/5/26	Pedra Branca	5	200	40	0.08	2020	589	no
171	1/7/26	Pedra Branca	6	240	40	0.08	2424	589	no
171	1/9/26	Pedra Branca	7	280	40	0.08	2828	589	no
171	1/11/26	Pedra Branca	8	320	40	0.08	3232	589	no
479	1/10/23	Pompeu	0	0	0	0.00	0	3545	se
479	1/1/24	Pompeu	1	69.7	69.7	0.32	216	3545	se
479	1/3/24	Pompeu	2	139.4	69.7	0.32	432	3545	se
479	1/5/24	Pompeu	3	209.1	69.7	0.32	648	3545	se
428	1/2/24	Porteiras 2	0	0	0	0.00	0	1969	se
428	1/3/24	Porteiras 2	1	21.5	21.5	0.29	62	1969	se
428	1/5/24	Porteiras 2	2	43	21.5	0.29	124	1969	se
428	1/7/24	Porteiras 2	3	64.5	21.5	0.29	186	1969	se
428	1/9/24	Porteiras 2	4	86	21.5	0.29	248	1969	se
365	1/9/21	Prainha	0	0	0	0.00	0	1836	se
365	1/12/22	Prainha	1	113.8	113.8	0.17	611	1836	se
365	1/2/23	Prainha	2	227.6	113.8	0.17	1222	1836	se
365	1/4/23	Prainha	3	341.4	113.8	0.17	1833	1836	se
365	1/6/23	Prainha	4	455.2	113.8	0.17	2444	1836	se
365	1/8/23	Prainha	5	569	113.8	0.17	3055	1836	se
365	1/10/23	Prainha	6	682.8	113.8	0.17	3666	1836	se
365	1/12/23	Prainha	7	796.4	113.6	0.17	4277	1836	se
170	1/12/23	Riacho Seco	0	0	0	0.00	0	442	no
170	1/1/24	Riacho Seco	1	34.5	34.5	0.09	495	442	no
170	1/3/24	Riacho Seco	2	69	34.5	0.09	990	442	no

170	1/5/24	Riacho Seco	3	103.5	34.5	0.09	1485	442	no
170	1/7/24	Riacho Seco	4	138	34.5	0.09	1980	442	no
170	1/9/24	Riacho Seco	5	172.5	34.5	0.09	2475	442	no
170	1/11/24	Riacho Seco	6	207	34.5	0.09	2970	442	no
170	1/1/25	Riacho Seco	7	241.5	34.5	0.09	3465	442	no
170	1/3/25	Riacho Seco	8	276	34.5	0.09	3960	442	no
239	1/5/20	S L Tap Comp	0	0	0	0.00	0	7766	tt
239	1/8/20	S L Tap Comp	1	150	150	0.25	630	7766	tt
239	1/10/20	S L Tap Comp	2	300	150	0.25	1260	7766	tt
238	1/8/20	S Luiz Tapaj	1	215	215	0.32	741	7766	tt
238	1/10/20	S Luiz Tapaj	2	430	215	0.32	1482	7766	tt
238	1/12/20	S Luiz Tapaj	3	645	215	0.32	2223	7766	tt
238	1/2/21	S Luiz Tapaj	4	860	215	0.32	2964	7766	tt
238	1/4/21	S Luiz Tapaj	5	1075	215	0.32	3705	7766	tt
238	1/6/21	S Luiz Tapaj	6	1290	215	0.32	4446	7766	tt
238	1/8/21	S Luiz Tapaj	7	1505	215	0.32	5187	7766	tt
238	1/10/21	S Luiz Tapaj	8	1720	215	0.32	5928	7766	tt
238	1/12/21	S Luiz Tapaj	9	1935	215	0.32	6669	7766	tt
238	1/2/22	S Luiz Tapaj	10	2150	215	0.32	7410	7766	tt
238	1/4/22	S Luiz Tapaj	11	2365	215	0.32	8151	7766	tt
238	1/6/22	S Luiz Tapaj	12	2580	215	0.32	8892	7766	tt
238	1/8/22	S Luiz Tapaj	13	2795	215	0.32	9633	7766	tt
238	1/10/22	S Luiz Tapaj	14	3010	215	0.32	10374	7766	tt
238	1/12/22	S Luiz Tapaj	15	3225	215	0.32	11115	7766	tt
238	1/2/23	S Luiz Tapaj	16	3440	215	0.32	11856	7766	tt
238	1/4/23	S Luiz Tapaj	17	3655	215	0.32	12597	7766	tt
238	1/6/23	S Luiz Tapaj	18	3870	215	0.32	13338	7766	tt
238	1/8/23	S Luiz Tapaj	19	4085	215	0.32	14079	7766	tt
238	1/10/23	S Luiz Tapaj	20	4300	215	0.32	14820	7766	tt
238	1/12/23	S Luiz Tapaj	21	4515	215	0.32	15561	7766	tt
238	1/2/24	S Luiz Tapaj	22	4730	215	0.32	16302	7766	tt
238	1/2/24	S Luiz Tapaj	23	4945	215	0.32	17043	7766	tt
238	1/6/24	S Luiz Tapaj	24	5160	215	0.32	17784	7766	tt
238	1/6/24	S Luiz Tapaj	25	5375	215	0.32	18525	7766	tt
238	1/10/24	S Luiz Tapaj	26	5590	215	0.32	19266	7766	tt
238	1/12/24	S Luiz Tapaj	27	5805	215	0.32	20007	7766	tt
238	1/2/25	S Luiz Tapaj	28	6020	215	0.32	20748	7766	tt
238	1/4/25	S Luiz Tapaj	29	6235	215	0.32	21489	7766	tt
238	1/6/25	S Luiz Tapaj	30	6450	215	0.32	22230	7766	tt
238	1/8/25	S Luiz Tapaj	31	6665	215	0.32	22971	7766	tt
238	1/10/25	S Luiz Tapaj	32	6880	215	0.32	23712	7766	tt
238	1/12/25	S Luiz Tapaj	33	7095	215	0.32	24453	7766	tt
238	1/2/26	S Luiz Tapaj	34	7310	215	0.32	25194	7766	tt

238	1/4/26	S Luiz Tapaj	35	7525	215	0.32	25935	7766	tt
238	1/6/26	S Luiz Tapaj	36	7740	215	0.32	26676	7766	tt
268	1/11/23	S. Quebrada	0	0	0	0.00	0	4000	ne
268	1/2/24	S. Quebrada	1	166	166	0.24	654	4000	ne
268	1/5/24	S. Quebrada	2	332	166	0.24	1308	4000	ne
268	1/8/24	S. Quebrada	3	498	166	0.24	1962	4000	ne
268	1/11/24	S. Quebrada	4	664	166	0.24	2616	4000	ne
268	1/2/25	S. Quebrada	5	830	166	0.24	3270	4000	ne
268	1/5/25	S. Quebrada	6	996	166	0.24	3924	4000	ne
268	1/8/25	S. Quebrada	7	1162	166	0.24	4578	4000	ne
268	1/11/25	S. Quebrada	8	1328	166	0.24	5232	4000	ne
414	1/10/24	S.Simao Alto	0	0	0	0.00	0	3832	tt
414	1/1/25	S.Simao Alto	1	269.9	269.9	0.46	587	3832	tt
414	1/4/25	S.Simao Alto	2	539.8	269.9	0.46	1174	3832	tt
414	1/7/25	S.Simao Alto	3	809.7	269.9	0.46	1761	3832	tt
414	1/10/25	S.Simao Alto	4	1079.6	269.9	0.46	2348	3832	tt
414	1/1/26	S.Simao Alto	5	1349.5	269.9	0.46	2935	3832	tt
414	1/1/26	S.Simao Alto	6	1619.4	269.9	0.46	3522	3832	tt
414	1/7/26	S.Simao Alto	7	1889.3	269.9	0.46	4109	3832	tt
414	1/10/26	S.Simao Alto	8	2159.2	269.9	0.46	4696	3832	tt
414	1/1/27	S.Simao Alto	9	2429.1	269.9	0.46	5283	3832	tt
414	1/4/27	S.Simao Alto	10	2699	269.9	0.46	5870	3832	tt
414	1/7/27	S.Simao Alto	11	2969	270	0.46	6457	3832	tt
414	1/10/27	S.Simao Alto	12	3239	270	0.46	7044	3832	tt
414	1/1/28	S.Simao Alto	13	3509	270	0.46	7631	3832	tt
566	1/2/24	Santa Branca	0	0	0	0.00	0	147	su
566	1/5/24	Santa Branca	1	29	29	0.39	70	147	su
566	1/7/24	Santa Branca	2	58	29	0.39	140	147	su
273	1/10/26	Santa Isabel	0	0	0	0.00	0	1850	ne
273	1/1/27	Santa Isabel	1	135.9	135.9	0.22	723	1850	ne
273	1/4/27	Santa Isabel	2	271.8	135.9	0.22	1446	1850	ne
273	1/7/27	Santa Isabel	3	407.7	135.9	0.22	2169	1850	ne
273	1/10/27	Santa Isabel	4	543.6	135.9	0.22	2892	1850	ne
273	1/1/28	Santa Isabel	5	679.5	135.9	0.22	3615	1850	ne
273	1/4/28	Santa Isabel	6	815.4	135.9	0.22	4338	1850	ne
273	1/7/28	Santa Isabel	7	951.2	135.8	0.22	5061	1850	ne
273	1/10/28	Santa Isabel	8	1087	135.8	0.22	5784	1850	ne
58	1/6/28	Sao Jeronimo	0	0	0	0.00	0	2045	su
58	1/9/28	Sao Jeronimo	1	165	165	0.75	227	2045	su
58	1/12/28	Sao Jeronimo	2	330	165	0.75	454	2045	su
230	1/10/17	Sao Manoel	0	0	0	0.00	0	577	tt
230	1/1/18	Sao Manoel	1	140	140	0.22	761	577	tt
230	1/3/18	Sao Manoel	2	280	140	0.22	1522	577	tt

230	1/5/18	Sao Manoel	3	420	140	0.22	2283	577	tt
230	1/7/18	Sao Manoel	4	560	140	0.22	3044	577	tt
230	1/9/18	Sao Manoel	5	700	140	0.22	3805	577	tt
88	1/8/16	Sao Roque	0	0	0	0.00	0	796	su
88	1/10/16	Sao Roque	1	45	45	0.42	103	796	su
88	1/12/16	Sao Roque	2	90	45	0.42	206	796	su
88	1/2/17	Sao Roque	3	135	45	0.42	309	796	su
129	1/6/13	Simplicio	0	0	0	0.00	0	127	se
129	1/7/13	Simplicio	3	305.7	305.7	0.93	309	127	se
227	1/10/17	Sinop	0	0	0	0.00	0	3071	tt
227	1/1/18	Sinop	1	133.3	133.3	0.22	600	3071	tt
227	1/3/18	Sinop	2	266.6	133.3	0.22	1200	3071	tt
227	1/5/18	Sinop	3	400	133.4	0.22	1800	3071	tt
225	1/12/17	Slt Apiacas	0	0	0	0.00	0	2	tt
225	1/1/18	Slt Apiacas	3	45	45	0.22	204	2	tt
412	1/10/24	Slt Aug Baix	0	0	0	0.00	0	366	tt
412	1/1/25	Slt Aug Baix	1	162.3	162.3	0.21	776	366	tt
412	1/4/25	Slt Aug Baix	2	324.6	162.3	0.21	1552	366	tt
412	1/7/25	Slt Aug Baix	3	486.9	162.3	0.21	2328	366	tt
412	1/10/25	Slt Aug Baix	4	649.2	162.3	0.21	3104	366	tt
412	1/1/26	Slt Aug Baix	5	811.5	162.3	0.21	3880	366	tt
412	1/4/26	Slt Aug Baix	6	973.8	162.3	0.21	4656	366	tt
412	1/7/26	Slt Aug Baix	7	1136.2	162.4	0.21	5432	366	tt
412	1/10/26	Slt Aug Baix	8	1298.6	162.4	0.21	6208	366	tt
412	1/1/27	Slt Aug Baix	9	1461	162.4	0.21	6984	366	tt
286	1/8/14	Sto Ant Jari	0	0	0	0.00	0	133	ma
286	1/11/14	Sto Ant Jari	1	123.3	123.3	0.23	556	133	ma
286	1/12/14	Sto Ant Jari	2	246.6	123.3	0.23	1112	133	ma
286	1/1/15	Sto Ant Jari	3	370	123.4	0.23	1668	133	ma
287	1/7/13	Sto Antonio	14	981.68	981.68	0.14	8014	2075	ar
287	1/9/13	Sto Antonio	16	1128.28	146.6	0.14	9212	2075	ar
287	1/2/14	Sto Antonio	17	1201.58	73.3	0.14	9811	2075	ar
287	1/3/14	Sto Antonio	20	1414.08	212.5	0.14	11546	2075	ar
287	1/5/14	Sto Antonio	24	1707.28	293.2	0.14	13942	2075	ar
287	1/6/14	Sto Antonio	26	1853.88	146.6	0.14	15140	2075	ar
287	1/7/14	Sto Antonio	28	2000.48	146.6	0.14	16338	2075	ar
287	1/8/14	Sto Antonio	30	2147.08	146.6	0.14	17536	2075	ar
287	1/9/14	Sto Antonio	32	2286.28	139.2	0.14	18672	2075	ar
287	1/12/15	Sto Antonio	34	2425.48	139.2	0.14	19808	2075	ar
287	1/1/16	Sto Antonio	35	2495.08	69.6	0.14	20376	2075	ar
287	1/3/16	Sto Antonio	37	2637.98	142.9	0.14	21543	2075	ar
287	1/4/16	Sto Antonio	38	2711.28	73.3	0.14	22142	2075	ar
287	1/5/16	Sto Antonio	40	2857.88	146.6	0.14	23340	2075	ar

287	1/6/16	Sto Antonio	41	2931.18	73.3	0.14	23939	2075	ar
287	1/7/16	Sto Antonio	43	3077.58	146.4	0.14	25137	2075	ar
287	1/8/16	Sto Antonio	44	3150.78	73.2	0.14	25736	2075	ar
347	1/1/27	Sumauma	0	0	0	0.00	0	2847	se
347	1/4/27	Sumauma	1	152.7	152.7	0.25	614	2847	se
347	1/7/27	Sumauma	2	305.4	152.7	0.25	1228	2847	se
347	1/10/27	Sumauma	3	458.2	152.8	0.25	1842	2847	se
340	1/10/20	Tabajara	0	0	0	0.00	0	851	ar
340	1/1/21	Tabajara	1	116.7	116.7	0.22	517	851	ar
340	1/4/21	Tabajara	2	233.4	116.7	0.22	1034	851	ar
340	1/7/21	Tabajara	3	350	116.6	0.22	1551	851	ar
56	1/5/19	Telem Borba	0	0	0	0.00	0	210	su
56	1/7/19	Telem Borba	1	54.5	54.5	0.43	126	210	su
56	1/10/19	Telem Borba	2	109	54.5	0.43	252	210	su
229	1/2/15	Teles Pires	0	0	0	0.00	0	897	tt
229	1/4/15	Teles Pires	2	728	728	0.50	1544	897	tt
229	1/5/15	Teles Pires	3	1092	364	0.50	2316	897	tt
229	1/7/15	Teles Pires	4	1456	364	0.50	3088	897	tt
229	1/8/15	Teles Pires	5	1820	364	0.50	3860	897	tt
116	1/12/27	Tijuco Alto	0	0	0	0.00	0	2044	su
116	1/3/28	Tijuco Alto	1	64.4	64.4	1.07	60	2044	su
116	1/6/28	Tijuco Alto	2	128.7	64.3	1.07	120	2044	su
259	1/11/26	Toricoejo	0	0	0	0.00	0	274	se
259	1/2/27	Toricoejo	1	38	38	0.18	212	274	se
259	1/4/27	Toricoejo	2	76	38	0.18	424	274	se
270	1/9/23	Torixoreu	0	0	0	0.00	0	1836	se
270	1/12/23	Torixoreu	1	136	136	0.91	147	1836	se
270	1/3/24	Torixoreu	2	272	136	0.91	294	1836	se
270	1/6/24	Torixoreu	3	408	136	0.91	441	1836	se
407	1/7/27	Tucuma	0	0	0	0.00	0	1087	tt
407	1/10/27	Tucuma	1	56.6	56.6	0.14	389	1087	tt
407	1/12/27	Tucuma	2	113.2	56.6	0.14	778	1087	tt
407	1/2/28	Tucuma	3	169.8	56.6	0.14	1167	1087	tt
407	1/4/28	Tucuma	4	226.5	56.7	0.14	1556	1087	tt
407	1/6/28	Tucuma	5	283.2	56.7	0.14	1945	1087	tt
407	1/8/28	Tucuma	6	339.9	56.7	0.14	2334	1087	tt
407	1/10/28	Tucuma	7	396.6	56.7	0.14	2723	1087	tt
407	1/12/28	Tucuma	8	453.3	56.7	0.14	3112	1087	tt
583	1/7/27	V. Gde Chopi	0	0	0	0.00	0	19	su
583	1/10/27	V. Gde Chopi	1	27.4	27.4	0.25	112	19	su
583	1/12/27	V. Gde Chopi	2	54.8	27.4	0.25	224	19	su

Table AS2 - Detailed schedule and characteristics for thermal power plants in the baseline (NG= natural gas)

Num	Name	Date	Installed Capacity (MW)	Type	System Id	Marginal operational costs (reais/MWh)	GHG Emissions
44	Angra 3	01/06/2018	1405	nuclear	se	25	16
46	Mc2 N Veneci	01/03/2014	176	NG	ne	161	470
84	Camacari G	01/01/2017	316	NG	no	733	470
93	Camacari D	01/01/2017	0	diesel	no	733	840
94	Santana 2 Ge	01/07/2014	50	diesel	ma	744	840
94	Santana 2 Ge	01/01/2015	0	diesel	ma	744	840
98	Pernambuco 3	01/01/2014	201	oil	no	456	840
106	Erb Candeias	01/06/2014	17	biomass	no	60	40
116	Parnaiba Iv	01/01/2014	56	natural NG	ne	69	470
128	Canto Buriti	01/01/2018	150	biomass	no	90	40
129	Campo Grande	01/01/2018	150	biomass	no	84	40
136	Suzano Ma	01/05/2014	255	biomass	ne	0	40
140	Maua 3	01/09/2014	375	NG	ma	0	470
140	Maua 3	01/04/2015	583	NG	ma	0	470
141	Maua B4	01/09/2014	0	oil	ma	450	840
201	Aparecida	01/09/2014	0	NG	ma	302	470
206	Maua B3	01/09/2014	0	NG	ma	412	470
208	Santana 1 W	01/07/2014	58	diesel	ma	539	840
208	Santana 1 W	01/01/2015	0	diesel	ma	539	840
211	Baixada Flu	01/12/2014	530	NG	se	86	470
211	Baixada Flu	01/03/2014	344	NG	se	86	470
212	Maranhao Iii	01/01/2015	519	NG	ne	59	470
303	Ute Ind Nuc	01/01/2025	1000	nuclear	su	20	16
304	Ute Ind Gas2	01/01/2020	1500	NG	se	250	470
304	Ute Ind Gas2	01/01/2021	3000	NG	se	250	470
304	Ute Ind Gas2	01/01/2022	4500	NG	se	250	470
304	Ute Ind Gas2	01/01/2023	7000	NG	se	250	470
304	Ute Ind Gas2	01/01/2027	8400	NG	se	250	470
304	Ute Ind Gas2	01/01/2028	8900	NG	se	250	470
305	Ute Ind Gas1	01/01/2027	1300	NG	se	250	470
307	Ute Ind Gas3	01/01/2019	500	NG	su	250	470
307	Ute Ind Gas3	01/01/2027	900	NG	su	250	470
307	Ute Ind Gas3	01/01/2028	1400	NG	su	250	470